

DOCTORAL THESIS

Biodiversity and Niche Partitioning of the Siphonophora (Cnidaria) off south-eastern Japan



Mary Matilda Grossmann

December, 2013

**Department of Genome System Science
Graduate School of Nanobiosciences
Yokohama City University
Yokohama, Japan**

DOCTORAL THESIS

Biodiversity and Niche Partitioning of the Siphonophora (Cnidaria) off south-eastern Japan

Mary Matilda Grossmann
December, 2013

Department of Genome System Science
Graduate School of Nanobiosciences
Yokohama City University

Members of the Doctoral Judging Committee

Prof. Dhugal John Lindsay (Supervisor)
Prof. Yuichi Nogi (Chairman)
Prof. Yasuhiro Ozeki (Japan)

Table of Contents

List of Figures	3
List of Tables.....	7
Glossary.....	9
General Introduction	11
1. Biodiversity.....	13
2. Paradox of the Plankton (Hutchinson, 1941).....	14
3. Siphonophora.....	17
4. Study plan	22
CHAPTER I.....	23
Study location and hydrography	23
I. Study location.....	27
II. Sampling.....	29
III. Hydrography	31
CHAPTER II	39
I. Study of Sagami Bay	47
1. Siphonophore diversity and vertical distribution.....	47
2. Community structure analysis.....	55
II. Generalization to all stations	69
1. Siphonophore diversity	69
2. Vertical distribution	73
3. Community structure.....	75
CHAPTER III.....	81
Trophic partitioning and taxonomic spread of the Siphonophora	81
I. Quantification of the potential prey field of the Siphonophora.....	85
1. Abundance.....	89
2. Copepoda size spectra.....	93
3. Predation pressure	95
4. Siphonophore nematocysts.....	99
II. Estimation of the trophic niche of eudoxid vs. polygastric stages through stable isotopes: a case study on <i>Dimophyes arctica</i> (Chun, 1897).....	103

1. Origin of <i>Dimophyes arctica</i>	109
2. Trophic position	111
III. Genetic divergence	113
General Discussion	129
General Conclusion.....	135
1. Study location and hydrography	137
2. Diversity, distribution and spatio-temporal niche partitioning of the Siphonophora.	137
3. Trophic partitioning and taxonomic spread	138
4. Conclusions.....	139
5. Further Research.....	140
References	141
Acknowledgements	157
Appendices	159
Appendix 1.....	161
1. Establishment and validation of a learning set adapted to the waters off south-eastern Japan	165
2. Estimation of copepod prosome length from pixel-based measurements derived from the ZooScan and ZooProcess systems.....	172
Appendix 2.....	181
1. <i>Eudoxia macra</i> Totton, 1954, is the eudoxid stage of <i>Lensia cossack</i> Totton, 1941 (Siphonophora, Cnidaria).....	185
2. Re-description of <i>Lensia leloupi</i> Totton, 1954.....	197
3. Description of the eudoxid stage of <i>Lensia havock</i> Totton, 1941	205
4. <i>Lensia</i> sp. A, a new species of five-ridged <i>Lensia</i>	209
Appendix 3.....	215
1. Description of eudoxid stages.....	219
2. Taxonomic notes on some multistriate <i>Lensia</i> species.....	225

List of Figures

- Figure 1: Life cycle of the calycophoran siphonophore *Chelophyses appendiculata* (Eschscholtz, 1829) (Siphonophora: Calycophorae: Diphyidae) ... p. 16
- Figure 2: Schematic diagrams of three siphonophore life stages showing orientation terminology ... p. 18
- Figure 3: Examples of fishing position and sampling of siphonophore colonies ... p. 20
- Figure 4: Bathymetric map of the sampling area showing the 3 stations (Kamogawa, Oshima and Sagami Bay), and the 2 supplementary sampling points (DF15 and DF28) ... p. 26
- Figure 5: Temperature (°C) and salinity profiles at the 3 stations ... p.30
- Figure 6: Dissolved oxygen concentration (mL.L^{-1}) and combined nitrites and nitrates, phosphates and silica concentration ($\mu\text{mol.L}^{-1}$) profiles at the 3 stations, and the corresponding temperature and salinity characteristics ... p. 32
- Figure 7: Map representing the flow of the Kuroshio Current and schematic diagram of Sagami Bay at the time of sampling ... p. 35
- Figure 8: Methodological flow-chart for the identification of siphonophore colonies from plankton net samples ... p. 42
- Figure 9: Form richness, total abundance, diversity and evenness over the water column in Sagami Bay ... p. 48
- Figure 10: Length of the bract of the eudoxid and anterior nectophore of the polygastric stages of *Dimophyes arctica* ... p. 52

Figure 11: Siphonophore community structure in Sagami Bay ...	p. 54
Figure 12: Multi-Dimensional Scaling (MDS) results for the Siphonophora present in Sagami Bay ...	p. 56
Figure 13: Form richness, total abundance, diversity and evenness over the water column at the 3 stations ...	p. 70
Figure 14: Maximum vertical range and mean depth (weighted by abundance) during the day and night of all forms having been sampled during both day and nighttimes; all stations combined ...	p. 72
Figure 15: Community structure analysis dendrogram, graphical representation of the inter-nest clusters obtained, and forms contributing the most to the dissimilarity between clusters, for Siphonophora sampled at all 3 stations ...	p. 74
Figure 16: Multi-Dimensional Scaling (MDS) results for the Siphonophora sampled at the 3 stations ...	p. 76
Figure 17: Total particle, plankton and copepod abundance over the water column at night at the 3 stations ...	p. 88
Figure 18: Relative abundance of the 5 considered copepod categories over the water column at the 3 sampling stations ...	p. 90
Figure 19: Copepod prosome length profiles over the water column at night at the 3 sampling stations ...	p. 92
Figure 20: Calycophoran siphonophore feeding rates as a function of prey density and number of gastrozooids per siphonophore colony ...	p. 94
Figure 21: Siphonophore cnidoband and nematocyst types ...	p. 98
Figure 22: Bayesian consensus tree based on the mitochondrial 16S gene ...	p. 118

- Figure 23: Neighbour-Joining and Maximum Likelihood trees based on the mitochondrial 16S gene ... p. 120
- Figure 24: Genetic distance between individuals of different families, genera, species and geographic origin ... p. 122
- Figure 25: Maximum vertical range and mean depth of diphid forms belonging to the two genetically defined *Lensia* groups, and those tentatively assigned to group 1 ... p. 124
- Figure 26: Illustration of the morphological characteristics associated with the two phylogenetically defined *Lensia* groups ... p. 126
- Figure 27: Graphical representation of the three parameters used to test the efficiency of automatic recognition ... p. 166
- Figure 28: Examples of scanned images from the categories “Ostracoda” and “Poecilostomatoida” ... p. 170
- Figure 29: Illustration of the prosome length measurement ... p. 174
- Figure 30: Relationships between prosome length and area, diameter, maximum Feret’s diameter and equivalent spherical diameter ... p. 176
- Figure 31: Guide to the taxonomic terms employed for the description of polygastric and eudoxid stages of diphid-type calycophoran siphonophores ... p. 182
- Figure 32: Illustration of the eudoxid stage *Eudoxia macra* Totton, 1954 and its polygastric stage *Lensia cossack* Totton, 1941 ... p. 188
- Figure 33: Genetic distance between species, between individuals of the same species from different geographic locations, and between individuals of the same species from the same geographic location ... p. 190

Figure 34: Bayesian consensus tree based on the mitochondrial 16S gene ... p. 192

Figure 35: Illustrations and photographs of the eudoxid and polygastric stages of *Lensia leloupi* Totton, 1954 and some related species ... p. 200

Figure 36: Illustrations and photographs of the eudoxid and polygastric stages of *Lensia havock* Totton, 1941 ... p. 206

Figure 37: Illustration and photographs of the polygastric stage of *Lensia* sp. A ... p. 211

Figure 38 Illustrations and photographs of *Eodoxia cf. galathea* Moser, 1925 ... p. 218

Figure 39: Photographs of the eudoxid stage ‘Eudoxid B’ ... p. 220

Figure 40: Illustration and photographs of the eudoxid stage ‘Bract I’ ... p. 222

Figure 41: Illustrations and photographs of *Lensia ajax* Totton, 1941; *L. ajax* sensu Margulis and Alekseev, 1985; *L. hostile* Totton, 1941 and *L. zenkevitchi* Margulis, 1970 ... p. 224

List of Tables

Table 1: Characteristics of the MULTI-SPLASH IONESS tows performed in March 2006 off south-eastern Japan ...	p. 28
Table 2: Estimated number of zooids comprising a single physonect, prayid or hippopodiid colony in the present study ...	p. 44
Table 3: Species known to be present in Sagami Bay ...	p.46
Table 4: Most abundant form per depth stratum and sampling time in Sagami Bay ...	p. 50
Table 5: Forms contributing at least 5% to the total abundance of a given net sample, and the assemblages obtained at 20% similarity cut-off from the inter-form cluster analysis ...	p. 58
Table 6: Depth range and mean depth of the siphonophore forms collected in Sagami Bay during the March 2006 MULTI-SPLASH cruise, with literature-based information on their known geographic ranges ...	p. 61
Table 7: Depth range and mean depth of the siphonophore forms collected at all stations during the March 2006 MULTI-SPLASH cruise ...	p. 66
Table 8: Categories of organisms used for the study of the potential prey field of Siphonophora ...	p. 86
Table 9: Estimated minimum predation pressure of the siphonophore community at the surface and at the depth of maximum abundance of <i>Dimophyes arctica</i> ...	p. 96
Table 10: Characteristics of the 5 <i>Dimophyes arctica</i> samples, their isotopic $\delta^{15}\text{N}$ ratio of phenylalanine, and estimated trophic position relative to that of the eudoxid stages ...	p. 108

Table 11: Characteristics of the samples sequenced for the present work ...	p. 114
Table 12: Calycophoran sequences obtained from GenBank ...	p. 116
Table 13: Composition of the leaning set ...	p. 164
Table 14: Efficiency of the automatic identification of the Kamogawa 700 to 400 m plankton samples ...	p. 168
Table 15: Regression equation of copepod prosome length against equivalent spherical diameter ...	p. 178
Table 16: Characteristics of the samples sequenced for the present work ...	p. 186

Glossary

Bract (保護葉): asexual zooid of variable shape, primarily used for protection of the gastro- and gonozooids; found on the siphosome or as part of the free eudoxid stage.

Cnidoband (刺胞叢): alignments of large numbers of nematocysts; on the tentilla of the tentacles.

Epipelagic (表層): pertaining to the upper 200 m of the water column.

Eudoxid stage (有性生殖世代): specific sexual life stage produced by some calyphoran siphonophore families; composed of a single cormidium (usually one bract, one gonophore, one stomach and associated tentacle).

Gastrozooid (栄養体): with an associated tentacle, siphonophore zooid specialized in the capture and digestion of prey.

Gonozooid (生殖体): siphonophore zooid specialized in the production and maturation of the gonads; each gonozooid is of a single sex, but colonies may be dioecious or monoecious depending on species.

Gyre (環流): large, circular, homogeneous zone found in the northern and southern parts of the Atlantic and Pacific Oceans and in the Indian Ocean, delimited by rotating currents, the direction of which is determined by the Coriolis effect.

Hydroecium (幹室): cavity or slit present on many zooids, often surrounded by mesogloal extensions, in which passes the stem.

Left (左): the side of a zooid visible when the upper side is to the right of the page.

Lower (下): side of a zooid on which the hydroecium is found (ventral in older literature).

Mesh Size (目合): distance between the fibers of the material making up a plankton net. The larger the distance between fibers, the larger the minimum size of the animals a net can collect.

Mesopelagic (中・深層): pertaining to the area of the ocean found between 200 and 1000 m depth.

Nectophore (泳鐘): zooid serving for the propulsion of physonect and calycophoran siphonophores; composed of a muscular bag-like structure which contracts rhythmically, also often containing lipidic reserves stored in modified canals.

Nematocyst (刺胞), ‘stinging cell’: cell composed of a trigger-released spine or filament contained in a capsule which, when released, will ensnarl prey items.

Niche (ニッチ): position or function of an organism in a community or ecosystem.

Ostium (泳囊開口部): name of the opening of the nectosac of nectophores and gonophores.

Plankton (浮遊生物): set of motile aquatic organisms incapable of swimming against currents due to their size or other intrinsic parameters.

Polygastric stage (無性生殖世代): largest, and most long-lived life stage of a siphonophore; asexual stage composed of an association of zooids with specific functions on a common stem.

Prosome (頭胸部): anterior part of crustaceans, composed of all segments carrying legs or head parts.

Ridge (稜): stiff mesogloal line, more or less prominent, often of diagnostic importance.

Right (右): the side of a zooid visible when the upper side is to the left of the page.

Siphonophora (管クラゲ): order of hydrozoan jellyfish, characterized by their pelagic, colonial life stages.

Somatocyst (体囊): specific part of the gastrovascular canal system in which lipidic reserves are stored.

Stem (幹): central chord from which the zooids of a colony are budded.

Tentillum, tentilla (側糸): secondary tentacle branching from the primary tentacle; carries a cnidoband.

Thermocline (水温躍層): physical boundary layer, separating the mixed surface layer from the deeper more stable layers.

Upper (上): side of a zooid opposite the hydroecium (dorsal in older literature).

Velum (縁膜): thin skirt of tissue surrounding the ostium, helping in swimming.

Zooid (個虫): elemental unit of a siphonophore colony, of polyp or medusa origin, specialized in specific physiological functions: nectophores for swimming, gastrozooids for digesting food, gonozooids to produce gonads, etc.

General Introduction

1. Biodiversity

Biodiversity represents the specific richness of the environment (number of different species present), and the composition and structure of the different communities (relative abundance of the different species, inter-specific interactions, etc...). The mechanisms controlling biodiversity are described in the main evolutionary theories, such as the Competitive Exclusion Principle (Gause, 1935; Levin, 1970), which states that species with similar ecological niches cannot coexist in time and space. If they do, then competition for resources will cause a decrease in biodiversity, favouring the “fittest” of species for any given environment. A high biodiversity may be maintained in the presence of spatio-temporal disturbances, physico-chemical barriers, or selective ecological niches of the considered species.

An ecological niche is the specific environment in which a species lives. Ecological niches are of two types: the potential niche, representing the habitat suitable, physiologically, to the survival of a species, and the realized niche, representing the area a species truly inhabits. Indeed, parameters extrinsic to the animals also influence on the geographic repartition of species. These parameters can be physical and chemical geographical barriers (e.g. high mountains, large rivers, arid lands, etc...) that prevent species from reaching certain favourable areas, or biological constraints linked to competition for resources and to predation.

The study of biodiversity and ecological niches is important to the understanding of life on Earth: why do the species we see today exist and how do they interact with their environment; and for the protection of this life against ever-increasing anthropogenic pressure. A high biodiversity has been shown to increase the resilience of ecosystems (e.g. Fisher *et al.*, 2006). Indeed, if many different species with similar ecological positions and roles exist together, they will show different responses to environmental or anthropogenic disturbances, thereby allowing the persistence of the ecosystem, despite a loss or shift in species. A quantification of biodiversity is therefore important to discover where areas of high biodiversity, and therefore high resilience, are found, and which areas show a seemingly low biodiversity, and may represent fragile environments in need of protection from anthropogenic stresses.

2. Paradox of the Plankton (Hutchinson, 1941)

The marine environment is, apart from the extremely small volume of water in direct contact with land, extremely large, and generally homogeneous. The Pacific Ocean, for example, is 4 km deep on average, and spans more than 10^8 km². Additionally, apart from the landlocked Aral, Caspian and Dead Seas, all seas and oceans communicate with each other through at least shallow isthmuses, and temperature gradients are low compared to terrestrial ecosystems. At 500 m depth in the Pacific Ocean, for example, the temperature gradient is less than 20°C, from the cold deep waters of the Japan Sea (0.5°C) to the warmest core of the Kuroshio current (15°C), and does not show large seasonal variability. The main physico-chemical gradients influencing the open ocean are pressure, which increases from 1 to more than 500 atmospheres, and oceanic currents. These are large, fast-moving bodies of water with specific physico-chemical characteristics. They greatly influence the dispersal of small planktonic organisms, which are unable to swim against or across such currents. Biological interactions such as competition for resources and predation are extremely difficult to estimate in the 3 dimensional space of the open ocean, and little information is, at present, available on these constraints.

In 1941, Hutchinson found, in the surface waters of the North Pacific Gyre, an ecosystem with an extremely high biodiversity of autotrophic planktonic organisms, in what appeared to be a stable, homogeneous environment (Hutchinson, 1941). This being contrary to the laws established by the Competitive Exclusion Principle, he named this observation the Paradox of the Plankton. Twenty years later, he discovered the high biodiversity of plankton could be maintained by irregular, weather-driven disturbances (Hutchinson, 1961). However, the open ocean is, on average, 4000 m deep, and while wind may play an important role in maintaining the diversity of Hutchinson's photosynthetic, surface-dwelling plankters, these phenomena are not known to extend more than a couple hundred metres in depth.

How, then, do the evolutionary theories apply to the entire open ocean?

Does the Paradox of the Plankton exist at depth?

Previous studies investigating the Paradox of the Plankton and niche partitioning in the open ocean have included works on the crustacean orders Copepoda (Kuriyama and Nishida, 2006; Mc Gowan and Walker, 1979; 1985; 1993), and Amphipoda (Shulenberger, 1979). These studies observed the same type of paradox, where a great many species with seemingly similar distributional and ecological niches coexisted. However, in-depth studies of these organisms and the inter-specific relationships they had revealed the presence of small-scale differences in depth distribution, migration patterns, trophic ecology or reproductive timing, helping to maintain a high biodiversity.

In order to study the universal validity of these characters and their application to all planktonic groups which seemingly violate the Competitive Exclusion Principle, the factors influencing niche partitioning were studied in a planktonic group which greatly differed from the previous biological models: the Siphonophora.

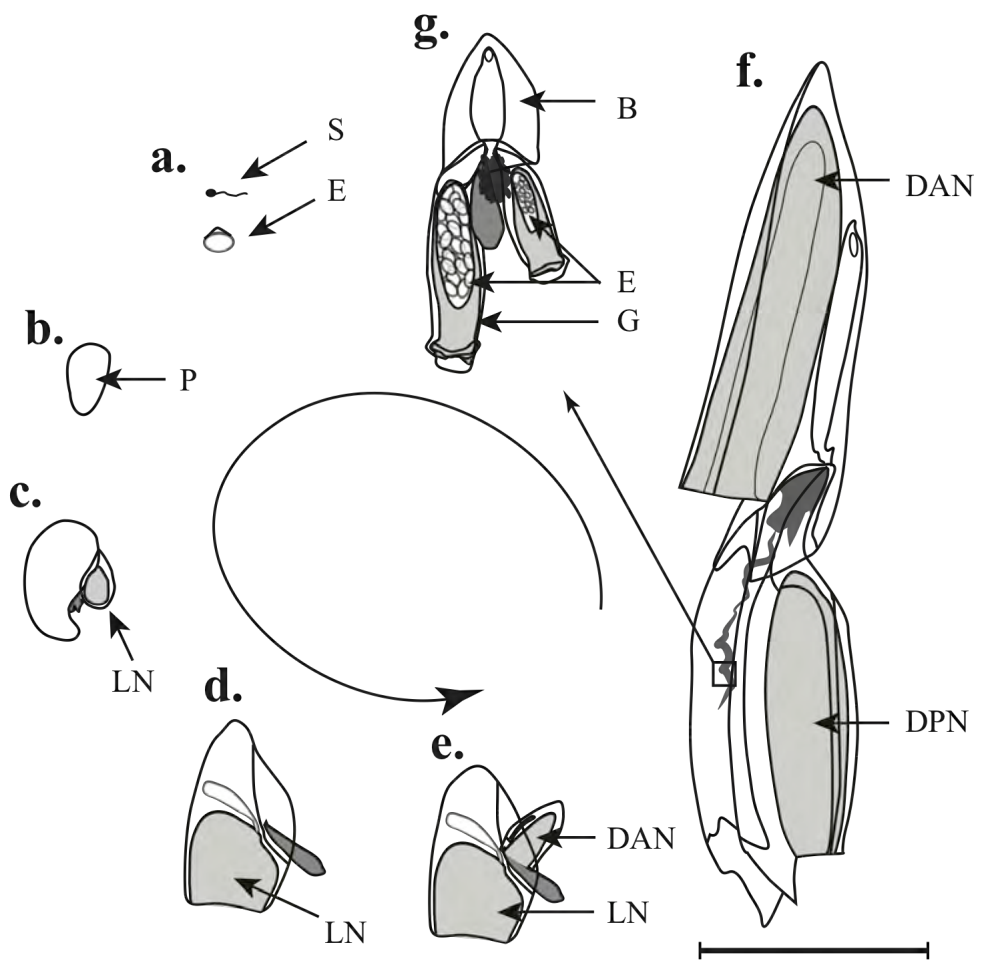


Figure 1: Life cycle of the calycophoran siphonophore *Chelophyses appendiculata* (Eschscholtz, 1829) (Siphonophora: Calycophorae: Diphyidae): a. Gametes; b. Planula stage; c. Calyconula stage; d. Larval stage; e. Post-larval stage; f. Polygastric stage; g. Eudoxid stage. Terminology: B: bract; DAN: definitive anterior nectophore; DPN: definitive posterior nectophore; E: egg; G: gonophore; LN: larval nectophore; P: planula; S: spermatozoid. (b. and c. redrawn after Carré and Carré, 1995). Scale bar = 1 mm.

3. Siphonophora

Both of the heterotrophic biological models chosen for the previous studies on the Paradox of the Plankton were pelagic crustaceans, with sizes generally in the millimetre to centimetre scale. Copepods, especially, are an extremely species-rich group, and the studies were therefore mostly performed at genus or family levels. Furthermore, the studied animals showed a wide range of trophic types, including carnivores, herbivores, detritivores, omnivores, parasites, etc... It is possible the complexity of inter-specific interactions, and the diversity of the trophic niches present within these groups, may have facilitated the coexistence of these pelagic crustaceans.

In order to simplify the study, and test its application to a wider range of planktonic organisms, a less species-rich group of entirely carnivorous planktonic animals was chosen: the Siphonophora.

Siphonophora are an order of Cnidaria, of the class Hydrozoa and subclass Hydroidolina. There are, to date, 191 valid species of siphonophore species (World Register of Marine Species). However, as seen below, they are still a relatively understudied group, and the number of known species will increase as further geographical areas are explored, and genetic studies unveil cryptic species (*cf.* Appendix 2.1; Pontin and Cruickshank, 2011).

Siphonophora usually represent an important part of the cnidarian plankton, and are common throughout all the oceans of the world, and present at all oceanic depths. As with the other Hydroidolina, a siphonophore individual will go through several different life stages (Fig.1), and these, apart from the planula stage (Fig. 1, b), are all colonial in nature. The eudoxid stage (Fig. 1.g.) exists only in the Abylidae, Amphicaryoninae, all Clausophyidae except the Clausophyinae, all Diphyidae except the Sulculeolariinae, the Nectopyramidinae, and Sphaeronectidae (Mapstone, 2009), other siphonophores releasing their gametes directly from the gonophores on the stem of the polygastric stage. The colonial structure of the Siphonophora explains many of their specific features. Siphonophore individuals can measure from less than 5 mm to more than 40 m in length, a unique characteristic shared only by the Nemertea. This variation in size is attained by addition of successive zooids to the stem (e.g. more than 40 nectophores, over 100 gastrozooids, etc...) rather than by variations in the size of individual zooids.

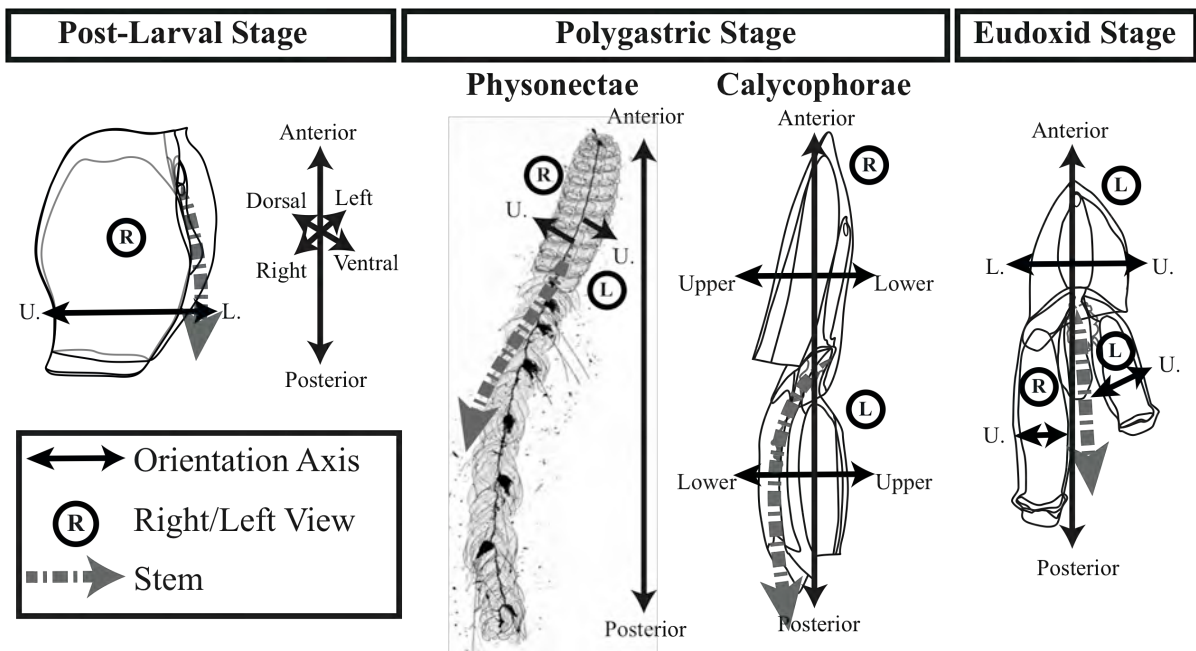


Figure 2: Schematic diagram of three siphonophore life stages showing orientation terminology, based on Haddock *et al.* (2005). Post-larval stage based on *Mica micula* Margulies, 1982 (*modified after* Grossmann *et al.*, 2013b); Polygastric stages: *Agalma elegans* (Sars, 1846) and *Chelophyses appendiculata* (Eschscholtz, 1829); Eudoxid stage: *Chelophyses appendiculata* (Eschscholtz, 1829). U.: upper; L.: lower. Colonies not to scale.

Zooids are extremely specialized buds, either of polyp or medusa origin, serving different physiological functions (e.g. nectophores for swimming, gastrozooids for digesting food, gonozooids to produce gonads, etc...). The vascular system and neural network of all buds of a colony communicate via the stem. Specific terminology is applied to each zooid of a siphonophore colony, which reflects its positioning with regard to the main axis of the animal, and to the direction in which it would normally swim (Fig 2). Although many siphonophores have a well-developed swimming capacity, they are primarily passive predators. The swimming motions of the nectophores and contractility of the stem allow for the deployment of the tentacles and tentilla into a fishing position (Fig. 3.a) and the colony then remains immobile while prey swim or drift into contact with the net of tentilla produced.

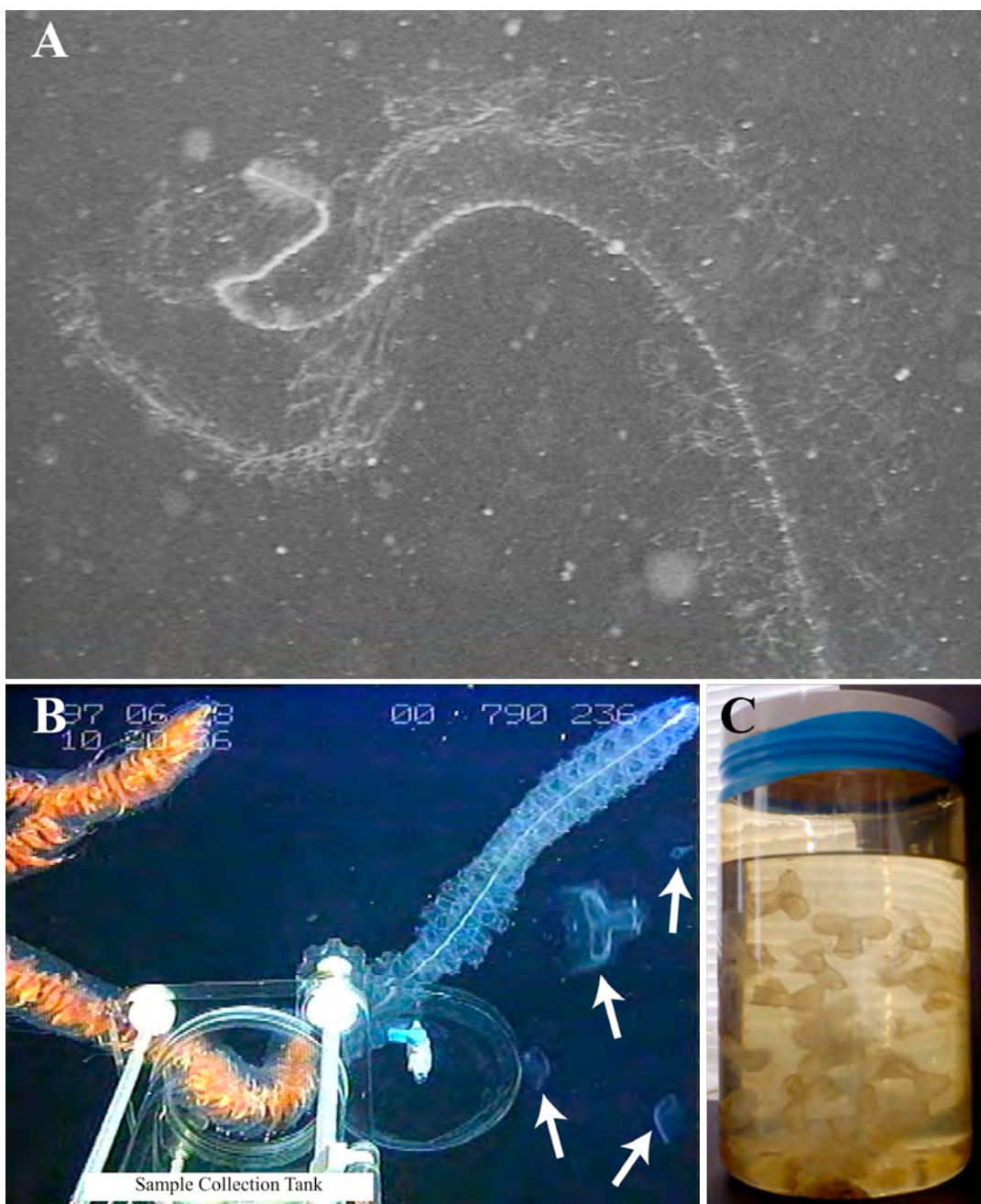


Figure 3: A: *Apolemia* sp. colony in fishing position; B: *Stephanomia amphytridis* (Lesueur and Petit, 1807) during sampling with the R.O.V. *DOLPHIN 3K*; C: same colony after preservation. In B, arrows mark portions of the colony being lost during sampling.

The colonial structure of siphonophores, however, is also their weakest point, both literally and figuratively. Most siphonophores are extremely sensitive to mechanical and photic stress (despite the lack of eye-cells), and sampling by plankton nets, or even the strong white lights of underwater survey vehicles, will often cause the individual zooids to separate from the stem, thereby effectively killing the animal (Fig. 3. b, c). This near-systematic destruction of the colonies during sampling renders identification of siphonophores difficult.

For the great majority of species, identification is based on the morphology of the nectophores of the polygastric stage alone, this often being the largest stage of a given species (Fig. 1. f), although for some species, the morphology of other zooids, or the presence of specific types of zooids has also been shown to be of taxonomic importance (e.g. Pugh, 2005). The eudoxid stages are often either undescribed (e.g. in the genus *Lensia*), or have not been linked with certainty to any known polygastric stage (e.g. *Eudoxia macra* Totton, 1954 – cf. Appendix 2). Little information is available on the other developmental stages, especially those of midwater siphonophore species, which cannot easily be caught and maintained under laboratory conditions.

The methodology applied to siphonophore analyses varies greatly amongst authors. Indeed, one siphonophore individual can be represented by the approximate number of zooids comprising a colony (e.g. Pugh, 1984), which requires some previous knowledge of the considered species, either by in-situ observations or by the rare capture of entire colonies. More commonly, only the anterior nectophores of a species are counted, physonects and hippopodiids being accounted for as numbers of nectophores, and no other life stage besides the polygastric one being taken into account (e.g. Kitamura *et al.*, 2003). This minimalist approach stems from the fact that for a large number of siphonophore species, only the polygastric stage is known and that it is impossible, from loose siphonophore parts alone, to estimate the number of parts comprising a single individual. This discrepancy in methodology leads to some important problems when comparing literature-based results of siphonophore numbers and abundances. Additionally, the largest siphonophore life stage, the polygastric stage, being the pelagic equivalent of the sessile polyp stage of other Hydroidolina (it produces sexual medusae stages, the eudoxids, by asexual budding at the extremity of the stem), while other planktonic organisms are recorded as numbers of sexual stages (e.g. Copepoda, Chaetognatha, non-siphonophore Cnidara), the Siphonophora are recorded as number of asexual, polyp, stages.

4. Study plan

The study of the biodiversity and niche partitioning of the Siphonophora off south-eastern Japan was carried out primarily through the analysis of plankton-net-collected samples. Sampling method and protocol having been shown to highly influence the measure of biodiversity and abundance (Skjoldal *et al.*, 2013), this allowed the present results to be put into perspective with those of the previous plankton-net-based studies of niche partitioning amongst planktonic animals (Kuriyama and Nishida, 2006; Mc Gowan and Walker, 1979; 1985; 1993; Shulenberger, 1979). The Siphonophora were identified to the lowest taxonomic level possible, and their biodiversity and vertical distributions were studied, and put into context with the physico-chemical characteristics of the water column they were collected in (Chapters I and II, p. 23 and p. 39). Vertical segregation alone being insufficient to explain the lack of competitive exclusion amongst many of the closely-related species within a given siphonophore community, the trophic and phylogenetic positions of the dominant species, and the inter-specific and inter-generic interactions existing between them were studied (Chapter III, p. 81). Finally, the biodiversity of the Siphonophora off south-eastern Japan, one of the most species-rich areas of Japanese waters, could be assessed, and the temporal, distributional and physiological processes helping to maintain this high biodiversity were reviewed.

CHAPTER I

Study location and hydrography

Introduction

Sagami Bay is one of the most well-studied areas of Japanese waters. Indeed, as well as being of easy access from the larger Tokyo area, it houses a great diversity of different ecosystems, inducing a large faunal richness (Fujikura *et al.*, 2012). In March 2006, a multi-platform survey was performed in Sagami Bay and the adjacent waters, in order to study the planktonic and bacterial community, and the interactions they had with their environment. This study included the measurement of physico-chemical environmental parameters as well as the collection and *in-situ* observation of planktonic organisms of various sizes, ranging from sub-micrometre bacteria to tens of centimetre-long fish. As part of this vast project, siphonophore cnidarians sampled by plankton net were studied, with a focus on their biodiversity and on the mechanisms controlling niche partitioning in these pelagic cnidarians.

The first studies of niche partitioning amongst heterotrophic planktonic Copepoda and Amphipoda (McGowan and Walker, 1979; 1985; Shulenberger, 1979), were performed in the North Pacific Gyre, an area characterized by its low spatial and temporal variability. However, outside these stable gyres, the transport of large volumes of water over great distances by the large-scale ocean circulation plays an important role in determining the physico-chemical characteristics, as well as the faunal composition of any given area. Indeed, in their study of niche partitioning within a family of planktonic copepods from Sagami Bay, Kuriyama and Nishida (2006) showed the presence of a mixture of sub-arctic and sub-tropical copepod species in the temperate bay, due to the influence of the Kuroshio and Oyashio Currents. The influence of these currents, and the hydrographic complexity they create in Sagami Bay is both a motor for biodiversity, and a handicap for the study of it.

In order for the studied biological signals to be comparable with previous results, both from Sagami Bay and other locations, a detailed examination of the structure of the water column at the time of sampling was performed.

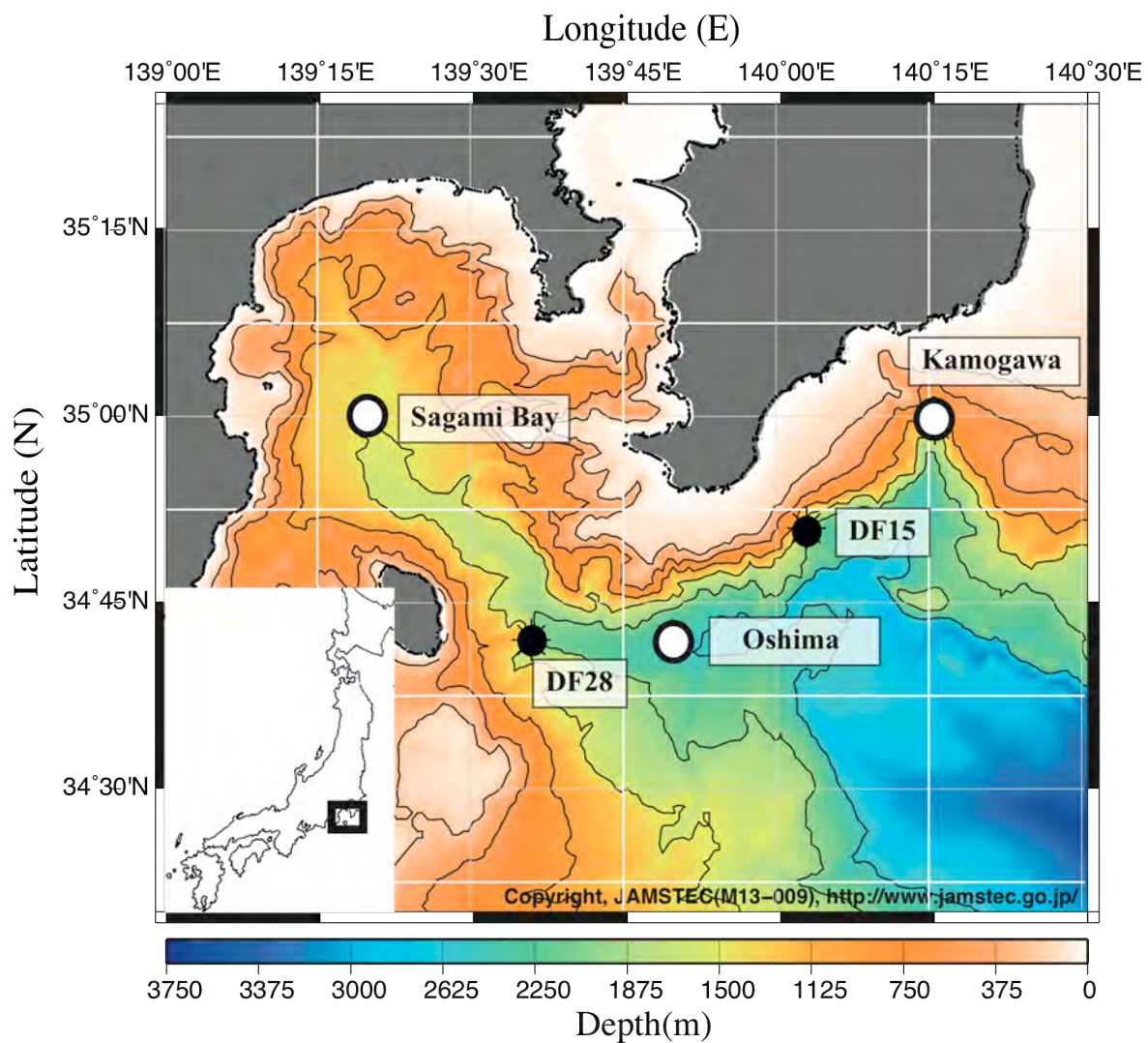


Figure 4: Bathymetric map of the sampling area showing the 3 stations (Kamogawa, Oshima and Sagami Bay), and the 2 supplementary sampling points (DF15 and DF28).

I. Study location

The MULTI-SPLASH cruise took place aboard the *R/V Kaiyo* (KY06-03) between the 14th and 25th of March, 2006. Plankton was collected in Sagami Bay ($35^{\circ}0.25'N$, $139^{\circ}20'E$), east of Oshima Island ($34^{\circ}42'N$, $139^{\circ}50'E$), and off of Kamogawa ($34^{\circ}59.43'N$, $140^{\circ}15.54'E$), from 1000 m to the surface (Fig. 4). Two additional points, DF15 ($34^{\circ}51.07'N$, $140^{\circ}02.97'E$) and DF28 ($34^{\circ}42.04'N$, $139^{\circ}35.89'E$) served as mid-point measurement locations for some physical water parameters.

The surface waters along the southern and eastern coasts of Japan are highly influenced by two large oceanic currents: the Oyashio, formed north of Japan and flowing southwards along the eastern coast, and the Kuroshio, flowing north-eastwards along the southern coast of Japan from its origin in the western equatorial Pacific. These two currents, the cold and warm western boundary currents of the Pacific subarctic and subtropical gyres, respectively, have characteristic physico-chemical characteristics, and are known to have water mass-specific associated planktonic fauna of copepods, chaetognaths and appendicularians (Hidaka, 2008; Kâ and Hwang, 2011; Kidachi and Ito, 1979; Kobari *et al.*, 2008; Miyamoto *et al.*, 2012; Oh *et al.*, 1991; Shimode *et al.*, 2006). Although the main body of these currents heads eastwards across the Pacific as part of the North Pacific Oceanic Gyre, when the two currents meet off eastern Japan, part of the Oyashio gets subducted, creating the Intermediate Oyashio Water, and flows south-westwards along the south-eastern coast of Japan, between 300 and 500 m-depth (Yang *et al.*, 1993a).

Sagami Bay, a semi-circular bay off south-eastern Japan, is one of the most well-studied bays in Japan, and several studies have been made on the cnidarians present in the bay, using various sampling methods (Hunt and Lindsay, 1999; Kawamura, 1954; Kitamura, 1997; 2000; 2009; Kitamura *et al.*, 2003; Lindsay and Hunt, 2005; Toyokawa *et al.*, 1998). However, it is also one of the most complex bays, hydrographically speaking. Indeed, as well as seasonal stratification events, waters in the bay can be periodically influenced at the surface by runoff water from the surrounding land and from Tokyo Bay, by branches of the Kuroshio Current and, in the mesopelagic zone, by mixtures of North Pacific Intermediate Water, and, at times, by intrusions of Oyashio Intermediate Water (Sekine and Uchiyama, 2002; Senju *et al.*, 1998; Yang *et al.*, 1993b), as well as by periodic passages of typhoons in the summer and autumn months.

Sagami Bay							
Day				Night			
Depth stratum (m)	Date	Start Time	Filtered Volume (m³)	Depth stratum (m)	Date	Start Time	Filtered Volume (m³)
0-50	3/19/06	16:32	815.3	0-78	3/19/06	23:44	869.00
50-100	3/19/06	16:22	1007.99	78-200	3/19/06	23:28	1465.88
100-200	3/19/06	16:11	1245.35	200-250	3/19/06	23:15	584.57
200-300	3/19/06	15:55	1343.16	250-300	3/19/06	23:05	473.38
300-350	3/19/06	15:44	905.91	300-350	—	—	—
350-400	3/19/06	15:30	1111.97	350-400	3/19/06	22:36	737.24
400-450	3/23/06	17:12	1487.64	400-450	3/15/06	4:12	1640.83
450-500	3/23/06	17:01	1228.81	450-500	3/15/06	4:00	1573.09
500-550	3/23/06	16:49	1166.63	500-550	3/15/06	3:49	1482.16
550-600	3/23/06	16:38	1114.69	550-600	3/15/06	3:38	1331.26
600-650	3/23/06	16:23	1566.04	600-650	3/15/06	3:25	1614.65
650-700	3/23/06	16:09	1349.32	650-700	3/15/06	3:15	1268.47
700-750	—	—	—	700-750	3/14/06	23:59	1675.30
750-800	3/19/06	12:39	758.37	750-820	3/14/06	23:42	2005.38
800-850	3/19/06	12:27	580.36	820-850	3/14/06	23:33	960.29
850-900	3/19/06	12:15	480.71	850-900	3/14/06	23:17	1743.52
900-950	3/19/06	12:05	536.93	900-950	3/14/06	23:08	971.84
950-1000	3/19/06	11:53	447.59	950-980	3/14/06	22:59	1001.00
Oshima							
Day				Night			
Depth stratum (m)	Date	Start Time	Filtered Volume (m³)	Depth stratum (m)	Date	Start Time	Filtered Volume (m³)
0-50	3/24/06	15:28	1954.40	0-50	3/25/06	2:01	620.20
50-100	3/24/06	15:20	799.74	50-100	3/25/06	1:49	1403.27
100-200	3/24/06	15:09	1324.73	100-200	3/25/06	1:37	1339.78
200-300	3/24/06	14:55	1652.95	200-300	3/25/06	1:24	1463.54
300-350	3/24/06	14:45	1141.85	300-350	3/25/06	1:13	1036.88
350-400	3/24/06	14:33	1230.00	350-400	3/25/06	1:05	735.79
400-450	3/25/06	14:50	1588.55	400-450	3/24/06	21:58	1271.65
450-500	3/25/06	14:40	799.54	450-500	3/24/06	21:49	755.01
500-550	3/25/06	14:28	980.66	500-550	3/24/06	21:38	993.84
550-600	3/25/06	14:18	915.64	550-600	3/24/06	21:21	1653.60
600-650	3/25/06	14:07	937.48	600-650	3/24/06	21:07	1412.84
650-700	3/25/06	13:54	1222.99	650-700	3/24/06	20:55	1337.71
700-750	3/15/06	15:21	1448.80	700-750	3/15/06	22:05	787.21
750-800	3/15/06	15:07	1241.19	750-800	3/15/06	21:53	1004.55
800-850	3/15/06	14:54	1394.79	800-850	3/15/06	21:39	892.67
850-900	3/15/06	14:40	1008.66	850-900	3/15/06	21:23	550.18
900-950	3/15/06	14:27	1132.22	900-950	3/15/06	21:14	568.06
950-1000	3/15/06	14:15	941.61	950-1000	3/15/06	21:00	436.36
Kamogawa							
Day				Night			
Depth stratum (m)	Date	Start Time	Filtered Volume (m³)	Depth stratum (m)	Date	Start Time	Filtered Volume (m³)
0-50	3/20/06	16:13	1038.00	0-82	3/21/06	1:27	550.10
50-100	3/20/06	15:54	1139.16	82-100	3/21/06	1:19	829.60
100-200	3/20/06	15:37	966.02	86-200	3/21/06	1:14	726.32
200-300	3/20/06	15:22	834.97	200-300	3/21/06	1:05	1148.01
300-350	3/20/06	15:01	841.39	300-350	3/21/06	0:55	1151.70
350-400	3/20/06	14:45	570.52	350-400	3/21/06	0:45	1188.19
400-450	3/21/06	16:17	1269.11	400-450	3/20/06	21:57	839.94
450-500	3/21/06	16:04	1180.87	450-500	3/20/06	21:46	904.91
500-550	3/21/06	15:54	1240.85	500-550	3/20/06	21:38	750.64
550-600	3/21/06	15:43	1307.64	550-600	3/20/06	21:29	724.54
600-650	3/21/06	15:30	1461.01	600-650	3/20/06	21:18	851.30
650-700	3/21/06	15:21	1116.92	650-700	3/20/06	21:06	884.32
700-750	3/22/06	16:20	1535.70	700-750	3/25/06	22:21	997.67
750-800	3/22/06	16:11	1112.94	750-800	3/25/06	22:10	1073.36
800-850	3/22/06	15:59	1378.10	800-850	3/25/06	22:01	924.06
850-900	3/22/06	15:48	1284.14	850-900	3/25/06	21:53	900.65
900-950	3/22/06	15:35	1567.47	900-950	3/25/06	21:40	1401.84
950-1000	3/22/06	15:23	1481.59	950-1000	3/25/06	21:27	1318.64

Table 1: Characteristics of the MULTI-SPLASH IONESS tows performed in March 2006 off south-eastern Japan.

II. Sampling

Plankton sampling was carried out with an IONESS (Intelligent Operated Net Environmental Sampling System) plankton net (Kitamura *et al.*, 2001) equipped with 9 nets. The first, open during the descent, was not analyzed. The 6 following nets were opened successively, during the ascent, in order to sample depth strata of 50- to 100 m in vertical extent. Net tows were performed in 6 segments at each of the 3 stations: 3 during the day (labelled ‘Day’) and 3 during the night (‘Night’), approximately from 1000 to 700 m, 700 to 400 m and 400 m to the surface (Table 1). The nighttime net towed in Sagami Bay between 300 and 350 m was removed from the analysis due to contamination by surface plankton, and the daytime net towed in Sagami Bay between 700 and 750 m was removed due to the low filtered volume (239.55 m^3). The mouth of the IONESS measured 173 by 123 cm and the tow angle was 51.5° on average, resulting in an effective mouth area of 1.67 m^2 . The nylon mesh size was $330\text{ }\mu\text{m}$, and the nets were towed at speeds of 1.1 to 2.7 knots vs. water. The volume of water filtered by each net was estimated by a flow-meter situated just above the mouth of the net. The bulk samples were preserved in 5% seawater-buffered formalin, after removal of some specimens destined for DNA extraction and sequencing.

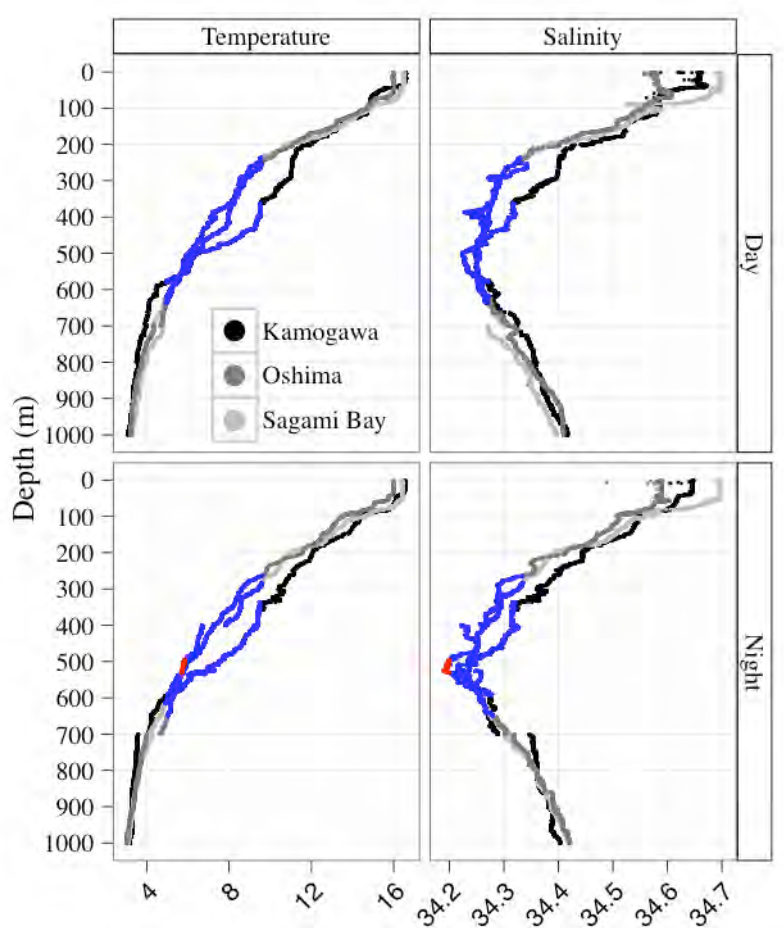


Figure 5: Temperature ($^{\circ}\text{C}$) and salinity profiles at the 3 stations during night and daytime. Blue colour indicates the extent of the Low Salinity Water (Senju *et al.*, 1998: density between 26.5 and 27.1), red indicates the extent of the Oyashio Intermediate Water (Sekine and Uchiyama, 2002; Senju *et al.*, 1998: salinity < 34.2 , temperature $< 7.0^{\circ}\text{C}$).

III. Hydrography

Material and Methods

The hydrographic characteristics of the water column were recorded *in-situ* by a Sea-Bird MicroCAT CTD (SBE-37SIP) attached to the IONESS frame, recording pressure, temperature and conductivity, from which depth, salinity and density were calculated. Sampling was performed at the 3 stations: Sagami Bay, Oshima, and Kamogawa, during both day and night time. The net tows of a given sampling station and time were performed in 3 segments: from 1000 to 700 m, 700 to 400 m and 400 m to the surface, on different days (Table 1). Dissolved oxygen was measured using a Sea-Bird SBE9+ CTD profiler at Kamogawa, Oshima and Sagami Bay on March 22nd, 26th and 19th, respectively, and at the 2 supplementary sampling points DF15 and DF28, on March 26th. Seawater was collected at the 3 stations on March 18th, at fixed depths, using Niskin bottles attached in a rosette. The concentrations of combined nitrates and nitrogen dioxide ($\text{NO}_2\text{-NO}_3$), phosphorus (PO_4) and silica (SiO_2) in the seawater were obtained by titration analyses.

Results

The water column was characterized by a marked thermocline, occupying about a 5 m stratum around 85 and 80 m in Sagami Bay during the day and night respectively, around 60 and 71 m off Oshima during the day and night respectively, and around 40 and 86 m off Kamogawa during the day and night respectively. Off Oshima, and during the daytime tow off Kamogawa, the thermocline was associated with a rapid increase in salinity of up to 0.04 units, over about 10 m. On the contrary, in Sagami Bay, the salinity showed a rapid decrease of about 0.05 units over a 10 m range. At night off Kamogawa, there was no marked change in salinity associated with the thermocline (Fig. 5).

Above the thermocline could be found a warm water mass with constant physico-chemical features. The surface mixed layer was characterized by the highest temperatures ($\geq 16^\circ\text{C}$) and the highest salinities (≥ 34.6) of the water column. At Oshima, the salinity increased from 34.58 to the maximum salinity (34.61) at the thermocline.

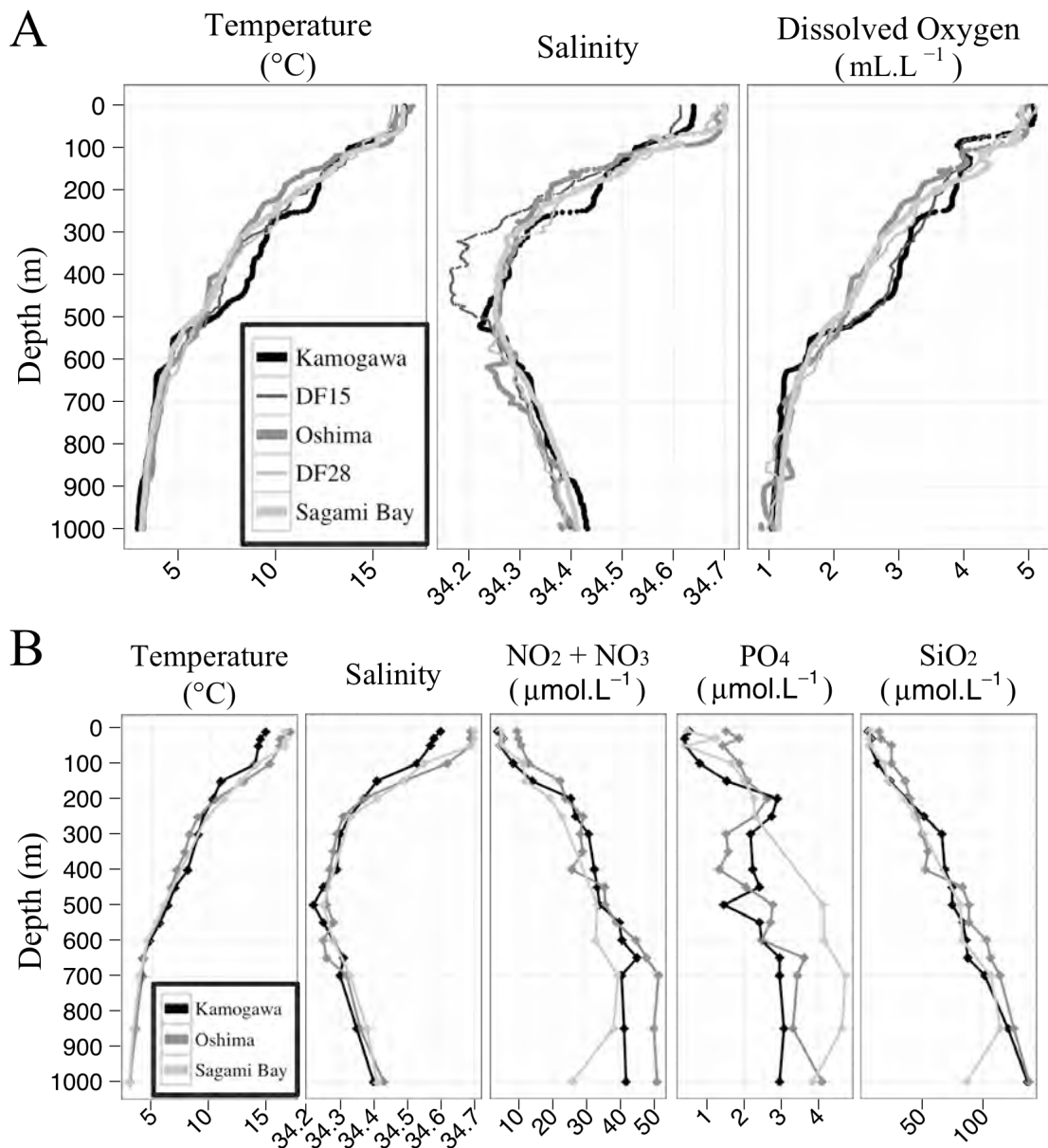


Figure 6: A: Dissolved oxygen concentration (mL.L^{-1}) profiles at the 3 stations and 2 supplementary sampling points, and the corresponding temperature and salinity characteristics; B: combined nitrites and nitrates, phosphates and silica concentration ($\mu\text{mol.L}^{-1}$) profiles at the 3 stations, and the corresponding temperature and salinity characteristics.

Below the thermocline, the temperature decreased steadily at all times in Sagami Bay and Oshima, while there was a small patch of warmer water off Kamogawa between 200 and 500 m, both during the day and nighttime (water 1 to 2°C warmer than at the other stations at the same depth). This warmer and more saline water mass could be due to mixing with Kuroshio waters. Off Kamogawa, the salinity decreased, sometimes rapidly, sometimes not at all, suggesting a mixture of water masses. Salinity reached a minimum of 34.22 at 500.5 m (temperature: 6.43°C, σt: 26.89) during the day, and a minimum of 34.21 at 520.9 m (temperature 7.1°C, σt: 26.78) during the night. At the other stations, the salinity decreased rapidly to around 200 m, before decreasing more slowly. There was no sharp low salinity minimum in Sagami Bay, a single minimum at 386.9 m off Oshima during the day (salinity: 34.23, temperature: 7.18°C, σt: 26.79), and two marked minima during the night, at 400.3 m (salinity: 34.22, temperature: 6.7°C, σt: 26.85), and at 524.4 m (salinity: 34.19, temperature: 5.71°C, σt: 26.95). Below the low-salinity zones, the salinity increased steadily, to reach values around 34.4 (temperature: 3.2°C, σt: 27.39) at 1000 m.

Dissolved oxygen concentrations were measured on March 26th at the 3 stations and 2 supplementary sampling points (Fig. 6. A). Dissolved oxygen concentrations over depth showed 2 main profiles: at Kamogawa and DF15, dissolved oxygen concentrations from the surface to the thermocline averaged 5 mL.L⁻¹. At the thermocline, the concentration decreased rapidly to around 4 mL.L⁻¹. At Kamogawa, rapid decreases in dissolved oxygen concentrations could also be found around 250 m (from 3.8 to 3.4 mL.L⁻¹), between 520 and 550 m (from 2.25 to 1.67 mL.L⁻¹) and around 615 m (from 1.55 to 1.3 mL.L⁻¹). At DF15, dissolved oxygen concentrations decreased steadily except between 470 and 530 m, and around 610 m, where concentrations decreased rapidly from 2.75 to 1.9 mL.L⁻¹ and from 1.8 to 1.48 mL.L⁻¹, respectively. At Oshima, DF28 and Sagami Bay, dissolved oxygen concentrations decreased steadily from the base of the thermocline to 1000 m, where they averaged 1.1 mL.L⁻¹. The temperature and salinity profiles at the 3 stations on March 26th being similar to those observed during the IONESS sampling, it is possible the higher temperatures and salinities observed between 200 and 500 m off Kamogawa were associated with higher dissolved oxygen concentrations.

Nutrient concentrations were measured a week before the IONESS sampling was performed, and the temperature and salinity profiles at all 3 stations resembled those found in Sagami Bay and Oshima during the IONESS sampling (Fig 6. B), without any midwater increased temperature and salinity as could be observed at Kamogawa station during the IONESS tows. The combined nitrites and nitrates increased steadily from the surface or subsurface ($3.4 \mu\text{mol.L}^{-1}$ at the surface off Kamogawa, 9.74 and $4.82 \mu\text{mol.L}^{-1}$ at 10 m off Oshima and Sagami Bay, respectively) to reach maxima around 700 m ($45.18 \mu\text{mol.L}^{-1}$ at 650 m off Kamogawa, 51.54 and $39.6 \mu\text{mol.L}^{-1}$ at 700 m off Kamogawa and Sagami Bay), where they became stable off Kamogawa and Oshima stations, and decreased to reach values of $26.16 \mu\text{mol.L}^{-1}$ at 1000 m in Sagami Bay. At Kamogawa and Oshima stations, phosphate concentrations were globally high below 200 m, except for a marked decrease at 500 m off Kamogawa ($1.44 \mu\text{mol.L}^{-1}$) and at 400 m off Oshima ($1.32 \mu\text{mol.L}^{-1}$). No measurements were taken between 250 and 500 m in Sagami Bay. However, the deeper waters of Sagami Bay contained the highest concentrations of phosphate, with a maximaum at 700 m of $4.71 \mu\text{mol.L}^{-1}$. Concentrations of silica increased steadily from the surface (6.32 , 16.15 and $8 \mu\text{mol.L}^{-1}$ at Kamogawa, Oshima and Sagami Bay stations, respectively) to 1000 m off Kamogawa and Oshima (137.76 and $138.9 \mu\text{mol.L}^{-1}$, respectively) and to 850 m in Sagami Bay ($115.74 \mu\text{mol.L}^{-1}$), with a decrease to $87.78 \mu\text{mol.L}^{-1}$ at 1000 m.

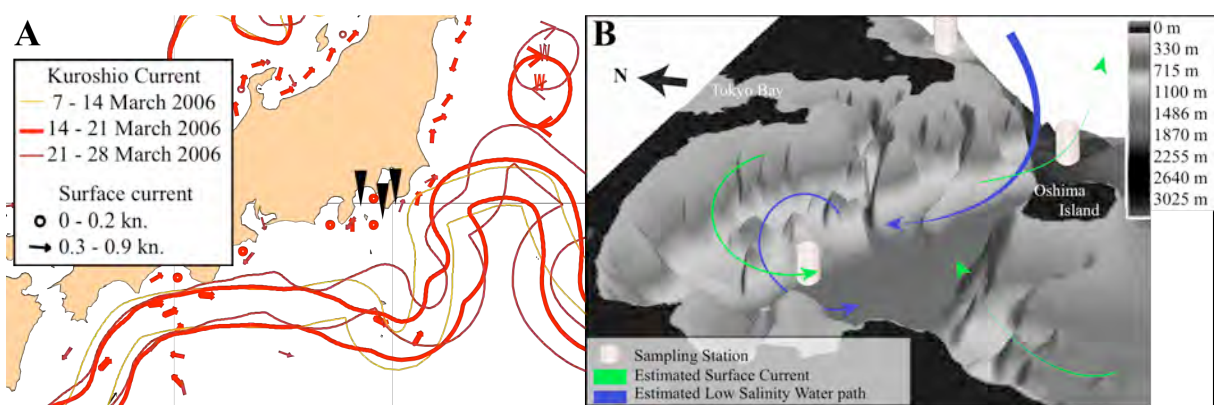


Figure 7: A: Map representing the flow of the Kuroshio Current between the 7th and 28th of March 2006 (Japan Coast Guard), black arrows indicating the position of the 3 sampling stations; B: Schematic diagram of Sagami Bay with, in green, the estimated path of the surface currents and, in blue, the estimated path of the midwater Low Salinity Water at the time of sampling with, in white, the position of the 3 sampling stations. (*modified after Grossmann and Lindsay, 2013b*)

Discussion

Despite having been measured over a period of 11 days, the water characteristics at each station were found to be relatively consistent. Until the 14th of March, the main body of the Kuroshio Current flowed close to the south-eastern shore of the Boso Peninsula, but did not approach Oshima Island or Sagami Bay (Fig. 7). At later dates, the Kuroshio Current made a large eddy towards the South of the sampling area, following an offshore non-large meander phase (Kawabe, 1995). None of the sampling stations were directly influenced by Kuroshio water (Fig. 7), and the surface currents were less than 0.3 knots until the 21st of March, when a stronger surface current could be observed flowing southwards out of Sagami Bay and influencing the surface waters of Oshima station. A marked thermocline separated the warm, homogeneous surface waters from the deeper waters at all stations. Unfortunately, apart from the nighttime samples in Sagami Bay and Kamogawa, the IONESS net sampled both above and below the thermocline.

The midwater low salinity zones greatly resembled that presented by Senju *et al.* (1998) as the Low Salinity Water (LSW: density between 26.5 and 27.1) intrusion sometimes observed in the Oshima East Channel and Sagami Bay. The LSW has been associated with Oyashio Intermediate Water (OIW) (Sekine and Uchiyama, 2002; Senju *et al.*, 1998; Yang *et al.*, 1993a), but in the present data set, the salinity was generally higher than the 34.2 indicative of that water mass (Sekine and Uchiyama, 2002; Senju *et al.*, 1998: salinity < 34.2, temperature < 7.0°C), except between 495 and 530 m at night off Oshima (minimum salinity = 34.19, and temperature = 5.71°C). The LSW observed therefore possibly represented a mixture of waters of northern origin. Contrary to that reported by Senju *et al.* (1998), the low salinity waters between 300 and 450 m did not correspond to waters enriched in phosphorous, but much the opposite (Fig. 6 B), pointing to a mixture of different water masses.

Chapter I Summary

Sampling was performed at 3 stations off south-eastern Japan: in Sagami Bay ($35^{\circ}0.25'N$, $139^{\circ}20'E$), east of Oshima Island ($34^{\circ}42'N$, $139^{\circ}50'E$), and off of Kamogawa ($34^{\circ}59.43'N$, $140^{\circ}15.54'E$). Because of the known hydrographic complexity and rapid variability of the sampling area, the physico-chemical characters of the water column were measured concurrently with the plankton sampling so as to be comparable. Two supplementary points, in between the 3 stations, allowed for an estimation of the horizontal variability of the physico-chemical parameters observed. During the sampling period, the Kuroshio Current did not directly influence any of the stations but a change in the location of the meander created, on the last sampling days, a surface current flowing out from Sagami and Tokyo Bays and bringing about a decrease in salinity in the surface waters of Oshima station at the time of sampling (March 25th). A marked sub-polar influence, associated with low salinities, could be seen at all 3 stations around 450 m. Additionally, the presence of several different water masses could be observed in the upper 400 to 200 m of the water column: the eastern-most station (Kamogawa) had warmer, more saline and more oxygenated waters than that found at the same depths in Sagami Bay and east of Oshima Island.

CHAPTER II

**Diversity and distribution of the Siphonophora and their
association with the main water masses**

Introduction

The oceans around Japan have been shown to house an extremely high biodiversity of benthic and pelagic organisms (Fujikura *et al.*, 2012). This could be explained by the wide variety of chemical and physical environments present. This diversity is uneven, however, waters off south-eastern Japan housing a much higher diversity than those on the Japan Sea side (e.g. Lindsay and Hunt, 2005).

The surface waters along the southern and eastern coasts of Japan are highly influenced by two large oceanic currents: the Oyashio and Kuroshio, that present specific physico-chemical characteristics, and are known to have water mass-specific associated planktonic fauna. Indeed, copepod, chaetognath (Kâ and Hwang, 2011) and appendicularian (Hidaka, 2008) species are known to be transported from the South China Sea into waters off northern Taiwan and southern Honshu (Kidachi and Ito, 1979) by association with the Kuroshio Current, and copepod and chaetognath species specific to Oyashio and polar waters have been recorded in the mesopelagic layers of Sagami Bay (Miyamoto *et al.*, 2012; Oh *et al.*, 1991; Shimode *et al.*, 2006) and off south-eastern Japan (Kobari *et al.*, 2008). However, no studies have yet been made on the possible extent of the lateral transport of pelagic cnidarians, a major predator group, into Sagami Bay and the surrounding waters by these current systems.

Sagami Bay, a semi-circular bay off south-eastern Japan, is one of the most studied bays in Japan, and several studies have been made on the cnidarians present in the bay, using various sampling methods (Hunt and Lindsay, 1999; Kawamura, 1954; Kitamura, 1997; 2000; 2009; Kitamura *et al.*, 2003; Lindsay and Hunt, 2005; Lindsay *et al.*, 1998; Toyokawa *et al.*, 1998). However, it is also one of the most complex bays, hydrographically speaking. Indeed, during the sampling period, a mixture of waters of different origins and physico-chemical parameters could be found in and around the Bay.

The abundance, diversity and community structure of cnidarians of the order Siphonophora, collected during the March 2006 MULTI-SPLASH cruise were studied, firstly in Sagami Bay, and then at the other two sampling stations. The structure of the water column at the time of sampling, characterized during the tows by a net-mounted CTD (*cf.* Chapter I. 3, p. 31), allowed the observed biological results to be placed into an environmental context and compared with the distributions of the tropical and subarctic waters present in the sampling area.

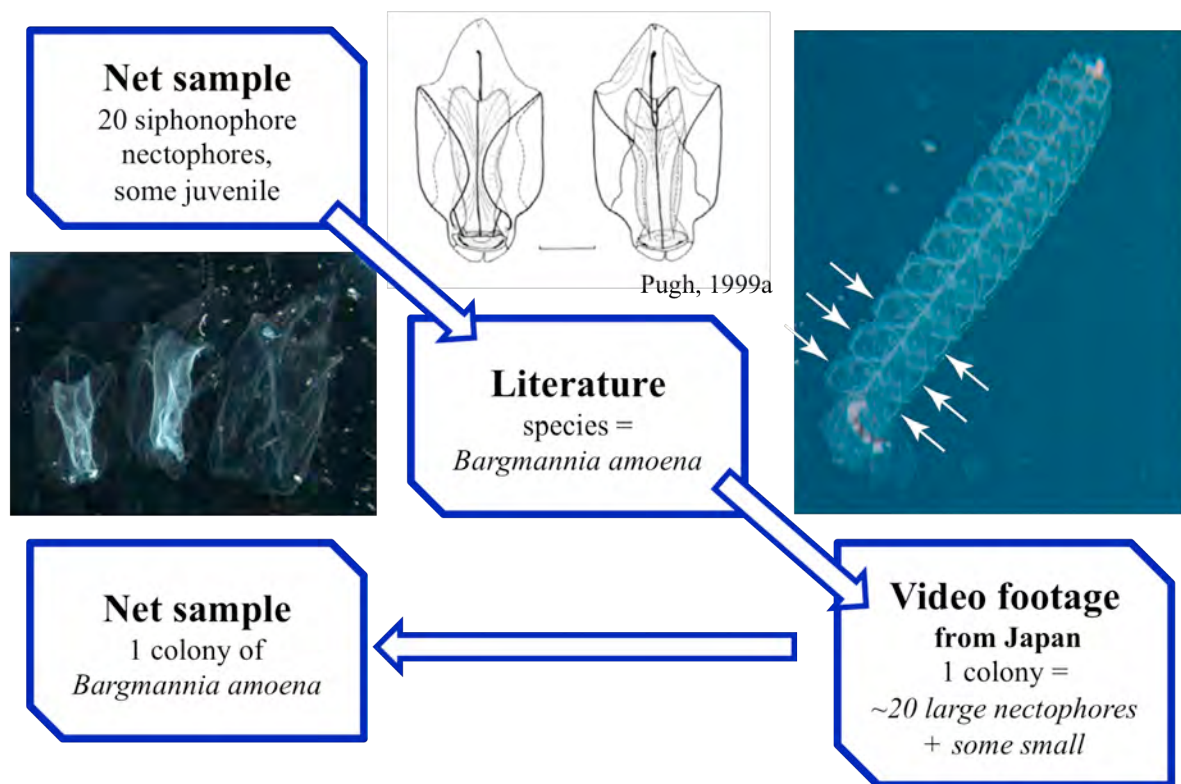


Figure 8: Methodological flow-chart for the identification of siphonophores from net samples.

Materials and Methods

All Siphonophora were sorted out of the 5% seawater-buffered formalin-preserved IONESS samples, and identified to the lowest taxonomic level possible using the most recent taxonomic guides to each group (Bouillon *et al.*, 2004; Grossmann *et al.*, 2012; Mapstone, 2009; Pugh, 1992; 1999a; 1999b; 2001; 2003; 2005; 2006; Totton, 1965a) and/or the original descriptions, especially for species of the genus *Lensia* Totton, 1932. DNA barcoding techniques were performed in order to identify previously undescribed species and life stages (*cf.* Appendix 2, p. 181). Siphonophore terminology follows Mapstone (2009), with ‘polygastric stage’ referring to the adult asexual colony, be it cystonect, physonect or calycophoran, and ‘eudoxid’ referring to the free eudoxid stage produced by the Abylidae, Amphicaryoninae, all Clausophyidae except the Clausophyinae, all Diphyidae except the Sulculeolariinae, the Nectopyramidinae and the Sphaeronectidae (Mapstone, 2009). The maximum number of zooids comprising a single physonect, hippopodiid or prayid individual was estimated from submersible-caught samples or video footage from Japanese waters (Fig. 8, Table 2). Calycophoran polygastric stages were counted as the number of complete colonies plus the highest number of either anterior or posterior nectophores. For those species producing free eudoxid stages, these were estimated to be the number of entire eudoxids plus the highest number of either bracts or gonophores, except in the family Abylidae, where it was estimated there were 2 gonophores for every bract (personal observation). This methodology was preferred over the counting of bracts alone, due to the large number of *Chuniphyes* spp. eodoxids, for which the bracts were not big enough to be reliably sampled by the 330 µm mesh of the net. Eodoxids of the genera *Chelophyes*, *Chuniphyes* and *Kephyses* could not be identified to species level and were considered a single form in each case. This may represent an underestimate of the number of forms present, as polygastric stages of 2 species of each of these genera were collected. Despite not being linked to any polygastric stage, 2 types of eudoxid stage and 10 other types of bract, to which gonophores could not be reliably linked, were identified. Five types of gonophores could be recognized, but were not included in the study, as it was considered probable their associated bracts were accounted for under a separate name. Because of the presence and considerable abundance of these eudoxid stages that could not be linked to a single, known polygastric stage, it was not possible to study species, but rather each developmental stage of a species was considered separately, and these entities were called forms.

Species	n	Maximum No. nectophores	Maximum No. bracts	References	Reference Locality
<i>Agalma clausi</i>	3	26	n/a	Bedot, 1888 BISMaL data portal; Lindsay and Miyake 2009	Mediterranean Sea
<i>Apolemiidae</i> spp.	8	10	n/a	Lindsay and Miyake 2009	Sagami Bay
<i>Bargmannia amoena</i>	8	22	n/a	BISMaL data portal; Lindsay and Miyake 2009	Sagami Bay
<i>Bargmannia lata</i>	1	18	n/a	BISMaL data portal; Lindsay and Miyake 2009	Kurose Hole, Japan (33°24.71'N, 139°40.48'E)
<i>Erenna richardi</i>	2	45	30+	Pugh, 2001	Caribbean
<i>Forskalia formosa</i>	4	14	n/a	BISMaL data portal; Lindsay and Miyake 2009	Sagami Bay
<i>Frillagalma vityazi</i>	5	8	n/a	BISMaL data portal; Lindsay and Miyake 2009	Sagami Bay
<i>Halistemma rubrum</i> †	n/a	30	n/a	Totton, 1965a	Mediterranean Sea
<i>Halistemma transliratum</i>	n/a	15	n/a	Pugh and Youngbluth, 1988	western Atlantic (26°13.5'N, 77°41.8'W)
<i>Marrus orthocanna</i>	6	40+	n/a	BISMaL data portal; Lindsay and Miyake 2009	Sagami Bay
<i>Nanomia bijuga</i>	10	20	n/a	BISMaL data portal; Lindsay and Miyake 2009	Sagami Bay
<i>Physophora gilmeri</i>	1	5	12	MULTI-SPLASH, intact colony	Oshima
<i>Amphicaryon</i> spp.	0	1 N1 + 1 N2			
<i>Maresearsia praecleara</i>	0	1 N1 + 1 N2			
<i>Desmophyes annectens</i>	2	2	30+	BISMaL data portal; Lindsay and Miyake 2009	Sagami Bay
<i>D. aff. villafrancae</i>	0	2*	n/a*		
<i>Lilyopsis rosea</i>	0	2*	n/a*		
<i>Rosacea plicata</i>	1	1 N1 + 1 N2	30+	BISMaL data portal; Lindsay and Miyake 2009	Japan Trench (38°56.10'N, 143°05.60'E), Okinawa (24°51.15'N, 23°49.94'E)
<i>Hippopodiidae</i> spp.	1	10	n/a	BISMaL data portal; Lindsay and Miyake 2009	Sagami Bay

†: *Halistemma rubrum* sensu Totton, 1965a

* Estimated from other Prayidae species; bracts unknown

Table 2: Estimated number of zooids composing a single physonect, prayid or hippopodiid colony in the present study (*modified after* Grossmann and Lindsay, 2013b)

Although conspecific, the different forms of a given species will have different swimming behaviours and predation mechanisms inherent to their size and morphology (Mackie *et al.*, 1987), and presumably, therefore, different ecological niches.

Abundance was estimated in numbers of individuals. 1000 m^{-3} , the filtered volume being estimated by a flow-meter situated just above the mouth of the net (Table 1). Shannon's diversity (H') and Pielou's evenness (J') indices were calculated in natural logarithm base using the R package "BiodiversityR" (Kindt, 2013). Analyses of similarity (ANOSIM) were conducted on square-root transformed abundance data to test the effect of sampling time and station on form distribution using the R package "vegan" (Oksanen *et al.*, 2013).

Multivariate analysis of the data was performed using the PRIMER v.6 software (Clarke and Warwick, 2001). Hierarchical cluster analyses were performed on square-root transformed abundance data with an average linkage and Bray Curtis similarity index. SIMilarity PERcentage (SIMPER) routines were carried out on the groups obtained in order to determine the forms contributing most to the Bray-Curtis dissimilarity between clusters, and 2-dimensional Multi-Dimensional Scaling (MDS) analyses were performed. Inter-form interactions were studied in Sagami Bay by performing a hierarchical cluster analysis with a Bray-Curtis similarity and average linkage on the forms contributing at least 5% to the total abundance of a given net sample, after standardization of the abundance of each form by the total abundance of the considered form (R-mode analysis).

Cystonectae	<i>Bassia bassensis</i>	<i>Lensia fowleri</i>
<i>Bathyphysa japonica</i> °	<i>Ceratocymba dentata</i> °	<i>Lensia grimaldii</i>
<i>Rhizophysa eysenhardtii</i> °	<i>Ceratocymba leuckartii</i> °	<i>Lensia hardy</i>
<i>Rhizophysa filiformis</i> °	<i>Ceratocymba sagittata</i> °	<i>Lensia havock</i>
Physonectae	<i>Chelophyes appendiculata</i>	<i>Lensia hostile</i>
<i>Agalma elegans</i> °	<i>Chelophyes contorta</i>	<i>Lensia hotspur</i>
<i>Agalma okeni</i> °	<i>Chuniphyes moserae</i>	<i>Lensia leloupi</i>
<i>Apolemia vityazi</i> °	<i>Chuniphyes multidentata</i>	<i>Lensia lelouveteau</i>
Apolemiidae A	<i>Clausophyes galeata</i>	<i>Lensia meteori</i>
Apolemiidae B	<i>Clausophyes laetmata</i>†	<i>Lensia multicristata</i>
<i>Athorybia rosacea</i> °	<i>Clausophyes moserae</i>	<i>Lensia panikkari</i>†
<i>Bargmannia amoena</i>	<i>Desmophyes annectens</i>	<i>Lensia quadriculata</i>
<i>Bargmannia elongata</i> °	<i>Desmophyes sp. aff. villafrancae</i>	<i>Lensia subtilis</i>
<i>Cordagalma cordiforme</i> °	<i>Dimophyes arctica</i>	<i>Lensia subtiloides</i> °
<i>Cordagalma</i> sp 1°	<i>Diphyes bojani</i>	<i>Lensia zenkevitchi</i>*
<i>Erenna laciniata</i> °	<i>Diphyes chamissonis</i> °	<i>Maresearsia praecleara</i> °
<i>Erenna richardi</i>	<i>Diphyes dispar</i>	<i>Muggiae atlantica</i>
<i>Forskalia asymmetrica</i> °	<i>Enneagonum hyalinum</i> °	<i>Muggiae bargmannae</i>
<i>Forskalia formosa</i> °	<i>Eodoxia cf. galathea</i>†	<i>Muggiae delsmani</i>
<i>Forskalia tholoides</i> °	<i>Eodoxoides mitra</i>	<i>Nectadamas diomedae</i> °
<i>Frillagalma vityazi</i>	<i>Eodoxoides spiralis</i>	<i>Nectadamas richardi</i>
<i>Halistemma rubrum</i>	<i>Gilia reticulata</i>	<i>Nectopyramis natans</i> °
<i>Lynchagalma utricularia</i> °	<i>Heteropyramis crystallina</i>	<i>Praya dubia</i> °
<i>Marrus orthocanna</i>	<i>Hippopodius hippopus</i> °	<i>Rosacea cymbiformis</i> °
<i>Nanomia bijuga</i>	<i>Kephyes ovata</i>	<i>Rosacea plicata</i>
<i>Physophora hydrostatica</i> °	<i>Kephyes</i> sp. A*	<i>Sphaeronectes fragilis</i> °
<i>Resomia</i> sp.°	<i>Lensia achilles</i>	<i>Sphaeronectes gamulini</i> °
<i>Sagamalia hinomaru</i> °	<i>Lensia ajax</i>*	<i>Sphaeronectes koellikeri</i> °
<i>Stephanomia amphytritis</i> °	<i>Lensia asymmetrica</i>	<i>Sphaeronectes pagesi</i> °
Calycophorae	<i>Lensia campanella</i>	<i>Stephanophyes superba</i> °
<i>Abyla haeckeli</i> °	<i>Lensia challengerii</i> °	<i>Sulculeolaria chuni</i> °
<i>Abyla trigona</i> °	<i>Lensia conoidea</i>	<i>Sulculeolaria monoica</i> °
<i>Abylopsis eschscholtzi</i>	<i>Lensia cordata</i>*	<i>Sulculeolaria turgida</i> °
<i>Abylopsis tetragona</i>	<i>Lensia cossack</i>	<i>Sulculeolaria quadrivalvis</i> °
<i>Amphicaryon acaule</i>	<i>Lensia exeter</i>	<i>Vogtia glabra</i>
<i>Amphicaryon ernestii</i> °		<i>Vogtia pentacantha</i>
<i>Amphicaryon peltifera</i> °		<i>Vogtia serrata</i>

Table 3: Species recorded from Sagami Bay (Alvariño, 1971; Bigelow, 1913; Hunt and Lindsay, 1999; Kawamura, 1954; Kitamura, 1997; 2000; 2009; Kitamura *et al.*, 2003; Lindsay and Hunt, 2005; Lindsay and Miyake, 2009; Lindsay *et al.*, 2011; Moser, 1913; 1925; Pagès *et al.*, 2006). In bold: first-time record from Sagami Bay; *: first- record from Japanese waters; †: first-time record from the Pacific Ocean; °: not collected in the present study.

I. Study of Sagami Bay

After **Mary M. Grossmann**, Dhugal J. Lindsay (2013b) Diversity and distribution of the Siphonophora (Cnidaria) in Sagami Bay, Japan, and their association with tropical and subarctic water masses. *J. Oceanogr.* **69**(4): 395–411.

1. Siphonophore diversity and vertical distribution

Fifty-nine species were identified in the MULTI-SPLASH IONESS samples from Sagami Bay (Table 3): 8 physonects and 51 calycophorans, of which 32 were of the family Diphyidae Quoy and Gaimard, 1827, and 21 of those were of the genus *Lensia* Totton, 1932. *Eudoxia cf. galathea* Moser, 1925 and seven previously undescribed eudoxid stages were recorded. These records have been added to the Ocean Biogeographic Information System via the Biological Information System for Marine Life (BISMaL) portal (Grossmann and Lindsay, 2013a). Eleven species and the eudoxid stage *E. cf. galathea* (Table 3, in bold) were recorded for the first time from Sagami Bay. Of these, *Heteropyramis crystallina* (Moser, 1925), *Kephyses* sp. A, *Lensia ajax* Totton, 1941, *L. cordata* Totton, 1965b and *L. zenkevitchi* Margulis, 1970 represent first-time records from Japanese waters (Table 3, *), while *Clausophyes laetmata* Pugh and Pagès, 1993, *Lensia panikkari* Daniel, 1970 and *E. cf. galathea* were recorded for the first time not only from Japan but from the entire Pacific Ocean (Table 3, †). Other calycophoran genera, such as *Abyla*, *Praya*, *Sphaeronectes*, *Sulculeolaria*, the physonects *Agalma*, *Cordagalma*, *Forskalia*, *Lychnagalma* and *Physophora*, and all cystonect genera are known to be present in the sampling area (Bigelow, 1913; Hunt and Lindsay, 1999; Kawamura, 1954; Kitamura, 1997; 2000; 2009; Kitamura *et al.*, 2003; Lindsay and Hunt, 2005; Lindsay and Miyake, 2009; Moser, 1925), but were not found in the present IONESS samples (Table 3, °). While most of the species recorded for the first time from Sagami Bay have previously been found in neighbouring areas such as Suruga Bay or the Ogasawara Islands (e.g. Kitamura, 2009; Pagès *et al.*, 2006), the bipolar species *Muggiaeae bargmannae* Totton, 1954 was collected twice in Sagami Bay, at night, between 400 and 450 m and between 550 and 600 m, while the only previous records from Japanese waters were from the Japan Sea (Park and Won, 2004).

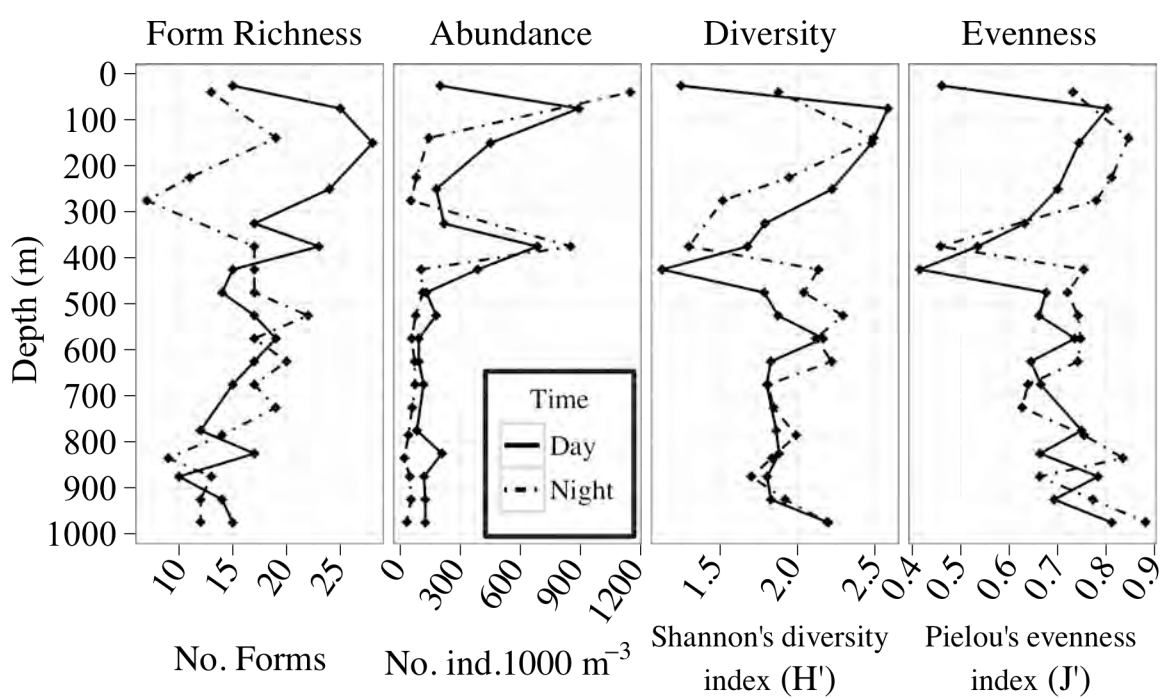


Figure 9: A: Form richness, B: Total abundance, C: Diversity, D: Evenness over the water column in each sampling series. Marks represent the mean sampling depth for each net. (Grossmann and Lindsay, 2013b, Fig. 3)

There were on average 17 forms per depth stratum, but form numbers varied greatly, both between samples and sampling times, from a minimum of 7 (Night, 250 to 300 m) to a maximum of 28 (Day, 950 to 1000 m) (Fig 9).

Total siphonophore abundance per net was relatively low, with a mean value of 240 individuals. 1000 m^{-3} , and a maximum of only 1148.5 individuals. 1000 m^{-3} (Night, 0 to 78 m). There were 2 marked peaks in abundance over the water column (Fig 9): between 50 and 100 m during the day and 0 to 78 m at night, and between 350 and 400 m at both sampling times. A smaller peak in abundance could be observed between 800 and 850 m during the day. At the upper peak in abundance, *Eudoxoides spiralis* (Bigelow, 1911) eudoxids were the most abundant form during the day (Table 4), while *Muggiae a atlantica* Cunningham, 1892 polygastric stages dominated the uppermost net at night. This difference could be due to the differences in sampling strata performed during the day and night (200-100-50-0 m during the day, 200-78-0 m at night) which could influence the estimation of abundance of animals present in only a 5- or 10 m stratum of the sampled depth. Indeed, while the uppermost daytime net spent about 13 seconds sampling each meter of the water column (50 to 0 m in 11 minutes), the nighttime net spent only half that amount of time (78 to 0 m in 8 minutes, or about 6.4 seconds. m^{-1}). Between 350 and 400 m, where the second peak of abundance could be observed, *Dimophyes arctica* (Chun, 1897) polygastric stages dominated, and it was at these depths that the maximum abundance of this species in any given sampling series could be found. Between 800 and 850 m during the day, at the smaller peak in abundance, the dominant form was the eudoxid stage of *Lensia havock* (Table 4).

Of the 44 forms collected both during the day and nighttime, the physonect *Nanomia bijuga* was the only one to display clear diel vertical migration patterns, the peak of abundance found between 100 and 200 m during the day being found between 0 and 78 m at night. However, because the upper 300 m of the water column was sampled in different depth strata during the day and night (Table 1), patterns of diel vertical migration may have been difficult to distinguish. In the mesopelagic zone, all species showed relatively stable patterns of both abundance and vertical distribution between day and nighttime, despite the sampling having been performed on different days (not shown).

Day	Night
0-50 m	<i>Muggiaea atlantica</i> e. (142.3)
50-100 m	<i>Eudoxoides spiralis</i> e. (210.3)
100-200 m	<i>Lensia leloupi</i> e. (128.5)
200-300 m	<i>Dimophyes arctica</i> p. (67.7)
300-350 m	<i>D. arctica</i> p. (89.4)
350-400 m	<i>D. arctica</i> p. (301.3)
400-450 m	<i>D. arctica</i> p. (266.2)
450-500 m	<i>D. arctica</i> p. (52.1)
500-550 m	<i>D. arctica</i> p. (75.4)
550-600 m	<i>D. arctica</i> e. (37.7)
600-650 m	<i>D. arctica</i> e. (49.2)
650-700 m	<i>Lensia havock</i> e. (46.7)
700-750 m	—
750-800 m	<i>D. arctica</i> e. (36.9)
800-850 m	<i>L. havock</i> e. (81.0)
850-900 m	<i>D. arctica</i> e. (41.6)
900-950 m	<i>D. arctica</i> e. (52.2)
950-1000 m	<i>D. arctica</i> e. (35.7)
0-78 m	<i>M. atlantica</i> p. (359.0)
78-200 m	<i>E. spiralis</i> p. (24.6)
200-250 m	Eudoxid B e. (22.2)
250-300 m	Eudoxid B e. (25.3)
300-350 m	—
350-400 m	<i>D. arctica</i> p. (558.9)
400-450 m	<i>D. arctica</i> p. (21.9)
450-500 m	<i>D. arctica</i> e. (31.1)
500-550 m	<i>D. arctica</i> e. (28.3)
550-600 m	<i>D. arctica</i> e. (19.5)
600-650 m	<i>L. havock</i> e. (21.1)
650-700 m	<i>L. havock</i> e. (33.1)
700-750 m	<i>L. havock</i> e. (29.8)
750-820 m	<i>L. havock</i> e. (16.0)
820-850 m	<i>L. havock</i> e. (8.3)
850-900 m	<i>L. havock</i> e. (25.8)
900-950 m	<i>L. havock</i> e. (22.6)
950-980 m	<i>Gilia reticulata</i> p. (7.0)

Table 4: Most abundant form per depth stratum and sampling time. In parentheses, abundance in number of individuals.1000 m⁻³; e: eudoxid, p: polygastric stage. (*modified after* Grossmann and Lindsay, 2013b, Table 4)

Both diversity and evenness indices were globally high over the whole water column, except for the uppermost daytime net, and for the 400 to 450 m stratum during the day and the 350 to 400 m stratum at night (Fig. 9). Shannon's diversity index (H') varied between 1.1 and 2.6 and Pielou's evenness index (J') had an average value of 0.7. The highest diversity was found in the daytime nets towed between 50 and 300 m and in the nighttime nets towed between 78 and 300 m. The uppermost daytime net, the only one to have sampled exclusively above the thermocline, showed very low diversity and evenness indices ($H'=1.25$, $J'=0.46$). The low diversity and evenness values around 400 m corresponded to the relative increase in abundance of *Dimophyes arctica*, associated, at night, with the midwater peak in total abundance. During the daytime, the decrease in diversity and evenness was found between 400 and 450 m, depths at which *D. arctica* represented 75.8% of the total siphonophore abundance, rather than at the midwater peak in total abundance, between 350 and 400 m, where *D. arctica* represented only 53.5% of the total siphonophore abundance.

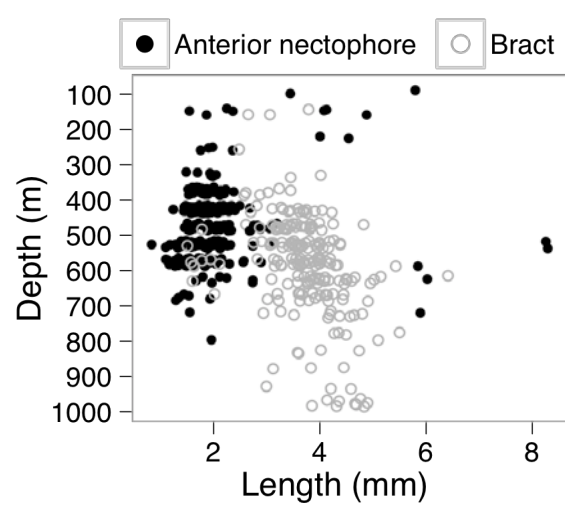


Figure 10: Length (mm) of the bract of the eudoxid (grey) and anterior nectophore of the polygastric (black) stages of *Dimophyes arctica*. (Grossmann and Lindsay, 2013b, Fig. 4)

Random measurements of 271 *Dimophyes arctica* anterior nectophores (from apex to ostium) and 217 bracts (from apex of the headpiece to end of neckshield) present in 27 of the nets, showed the bracts to measure 3.7 mm on average (Fig. 10), with the complete eudoxids being up to 50% longer (personal observation). Apart from a few large anterior nectophores more than 8 mm long, the median length of the anterior nectophores was 1.8 mm. No posterior nectophores of a size suitable for the small anterior nectophores were found, and it may be possible *D. arctica* polygastric stages do not produce posterior nectophores until they attain a certain size, as was described for the diphyid species *Chelophyes appendiculata* (Patriiti, 1964). However, even with these approximations, the eudoxids measured at least twice the length of the polygastric stages, pointing to the presence of different generations within the *D. arctica* population, since the large eudoxids could not be carried by such small polygastric colonies.

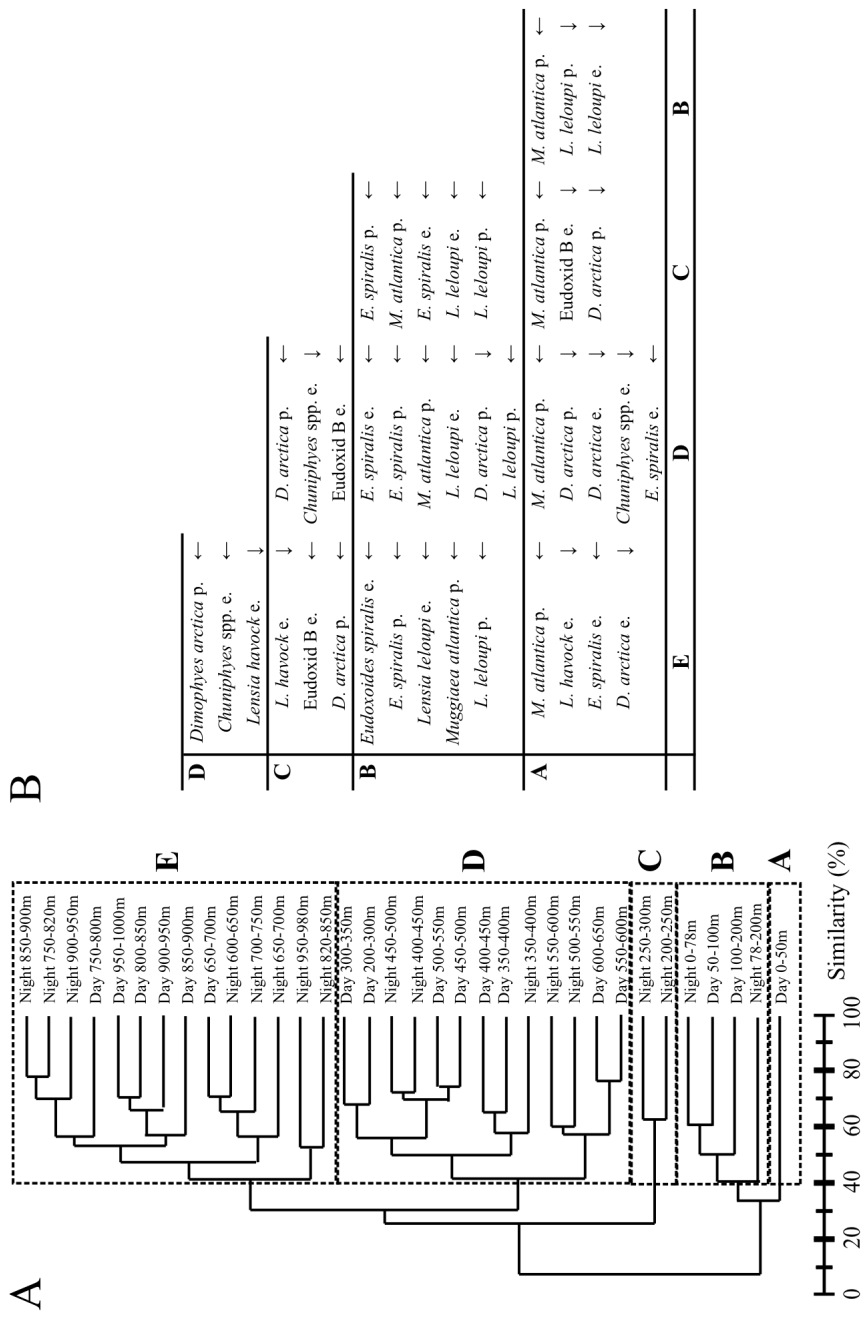


Figure 11: A: Community structure analysis dendrogram (clustering performed on square-root transformed abundance data, with an average linkage and Bray-Curtis similarity); B: Forms contributing the most to the dissimilarity between clusters (average dissimilarity ≥ 5 in terms of percentage abundance for each pair of clusters). e: eudoxid, p: polygastric stage; arrows indicate which, of columns or rows, a form contributes the most to. (modified after Grossmann and Lindsay, 2013b, Fig. 5 and Table 5)

2. Community structure analysis

The multivariate cluster analysis performed on square-root transformed abundance data produced 5 clusters at a 40% cut-off (Fig. 11. A), with between 1 and 19 net samples per group. Cluster A contained the daytime 0 – 50 m net sample, the only one to have sampled exclusively above the thermocline. This net sample was dominated by *Muggiae atlantica* polygastric stages. Cluster B contained the nets having sampled through the thermocline and down to 200 m depth. *Eudoxoides spiralis* eudoxids and polygastric stages gave the highest discrimination with the other clusters (Fig. 11. B). Cluster C contained the nighttime nets towed between 200 and 300 m. The nets in this cluster corresponded to the warmer, more saline waters found at these depths during the night, and Eudoxid B was the form giving the highest discrimination with the deeper nets, while the absence of *Chuniphyes* spp. eudoxids differentiated it from the daytime nets in the 200 to 300 m stratum. In cluster D, which contained all nets towed between 300 and 600 m, as well as the daytime nets towed between 200 and 300 m and between 600 and 650 m, *Dimophyes arctica* polygastric stages contributed the most to the dissimilarity of this cluster with Cluster E, which contained all the remaining nets.

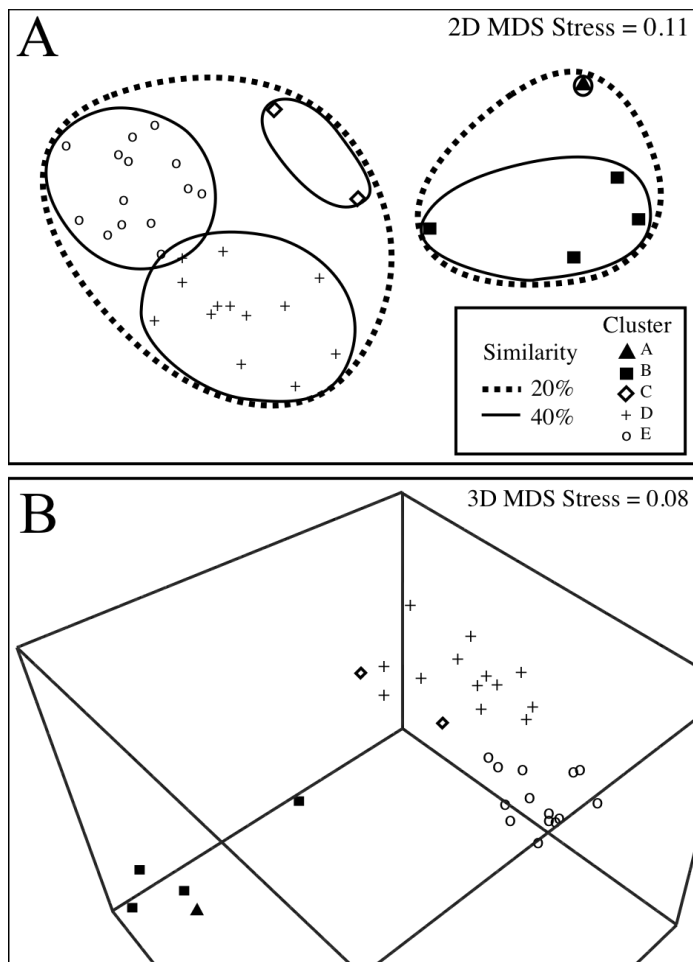


Figure 12: A: 2-dimensional Multi-Dimensional Scaling (2D MDS) diagram of the inter-net clustering, with 20% (dotted line) and 40% (solid line) similarity levels; B: 3-dimensional MDS diagram of the inter-net clustering. Each mark representing one net sample, shapes refer to the clusters observed in Fig. 11. (*modified after Grossmann and Lindsay, 2013b, Fig. 6*)

The 2D MDS (Fig. 12. A), with a stress value of 0.11, showed clusters A, B and C to be well defined, while clusters D and E showed very small distances in the area corresponding to the daytime sampling depths around 650 m (cluster D: 600 to 650 m; cluster E: 650 to 700 m). The 3D MDS analysis (stress = 0.08) showed a clear separation of these latter 2 clusters (Fig. 12. B).

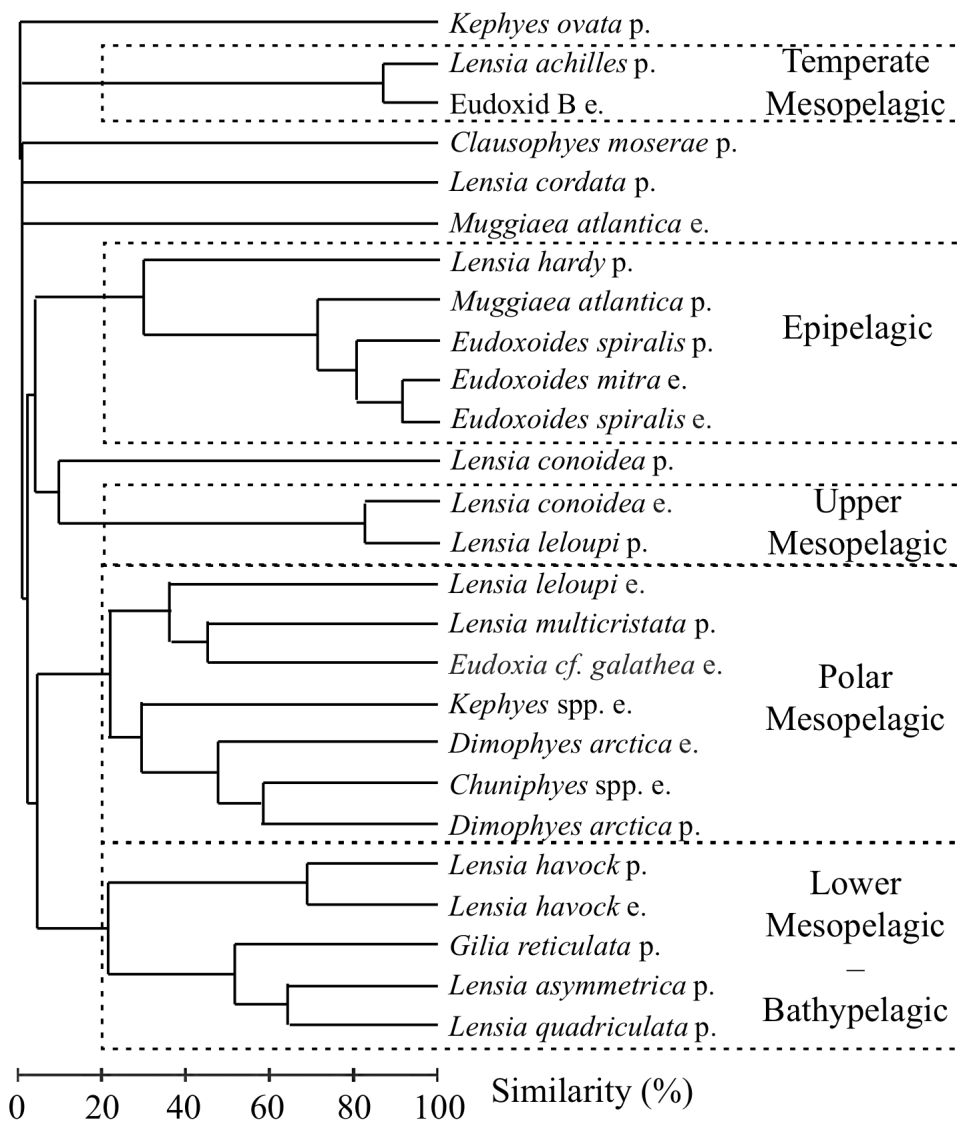


Table 5: Inter-species cluster analysis dendrogram (R-mode analysis: forms contributing at least 5% to the total abundance of a given net sample, abundance standardized by total, average linkage and Bray-Curtis similarity), and the assemblages obtained at a 20% similarity cut-off. e: eudoxid, p: polygastric stage. (modified after Grossmann and Lindsay, 2013b, Fig. 7)

The inter-species cluster analysis produced 5 main groups at a 20% similarity cut-off, and 5 forms did not cluster (*Clausophyes moserae*, *Kephyses ovata*, *Lensia conoidea* and *L. cordata* polygastric stages, and *Muggiae atlantica* eudoxids). The 5 assemblages could be linked with the depth distribution and origin of the different forms they contained (Table 5). The 2 distinct mesopelagic clusters could be differentiated by the origin of the forms they contained. Indeed, the first, composed of *Lensia achilles* and Eudoxid B, represented temperate mesopelagic species, as opposed to the second group, containing *Dimophyes arctica*, *Lensia multicristata* and the eudoxids of the genera *Chuniphyes* and *Kephyses*, forms that are generally more abundant in polar regions, and extremely rare in the mesopelagic zone of warm seas such as the Mediterranean (Alvariño, 1971; Mapstone, 2001) and Sulu Seas (D.J. Lindsay, personal observation).

		Depth Range	Mean Depth (m)	Known Depth Range	Depth References	Atlantic Ocean	Other Oceans	Location References
Physonectae								
Agalmatidae	<i>Halistenmma rubrum</i> ^a	p 100 - 200m	150	0 - 500m	Pugh 1999b	60°N-42°S	I. M. P. Alvariño 1971; Pugh 1999b	
	<i>Nanomia bijuga</i>	p 0 - 1000m	262.58	0 - 400m	Pugh 1999b	55°N - 59°S	I. M. P. Alvariño 1971; Pugh 1999b	
Apolemidae	<i>Apolemidae A</i>	p 650 - 850m	773.31	—	—	—	—	—
	<i>Apolemidae B</i>	p 450 - 950m	712.06	—	—	—	—	—
Erennidae	<i>Erema richardi</i>	p 850 - 950m	898.62	700 - 1000m	Pugh 1999b	35°N - 31°S	I. P. Alvariño 1971; Daniel 1985; Pugh 1999b	
Pyrostephidae	<i>Bargmannia amoena</i>	p 350 - 1000m	666.55	200 - 910m	Pugh 1999a	37°N - 45°S	I. P. Alvariño 1971; Pugh 1999a	
Incertae sedis	<i>Frillagalma vitvazi</i>	p 350 - 820m	503.84	0 - 2000m	Mapstone 2009	36 - 0°N	I. P. Mapstone 2009	
	<i>Marrus orthocanna</i>	p 600 - 1000m	796	0 - 700m	Mapstone 2009	60 - 35°N	I. M. P. Mapstone 2009	
Calyptophorae								
Abylidae	<i>Abylopsis eschscholtzi</i>	p 0 - 100m	48.09	0 - 200m	Pugh 1999b	40°N - 40°S	I. M. P. Alvariño 1971; Pugh 1999b	
		e 0 - 100m	63.31	—	—	—	—	—
	<i>A. tetragona</i>	p 0 - 200m	88.15	0 - 200m	Pugh 1999b	57°N - 45°S	I. M. P. Alvariño 1971; Pugh 1999b	
		e 0 - 400m	170.37	—	—	—	—	—
	<i>Bassia bassensis</i>	p 0 - 100m	46.32	0 - 200m	Pugh 1999b	60°N - 49°S	I. M. P. Alvariño 1971; Pugh 1999b	
Clausophyidae	<i>Chuniphyes moserae</i>	p 600 - 850m	766	> 1000m	Pugh 1999b	50°N - 67°S	I. M. P. Alvariño 1971; Pugh 1999b	
	<i>Ch. multidentata</i>	p 200 - 700m	427.51	300 - 800+	Pugh 1999b	60°N - 63°S	I. M. P. Alvariño 1971; Pugh 1999b	
	<i>Ch. spp.</i>	e 78 - 998m	446.73	—	—	—	—	—
	<i>Clausophyes galeata</i>	p 450 - 950m	727.7	> 1000m	Pugh 1999b	47°N - 67°S	P. Alvariño 1971; Pugh 1999b	
	<i>Cl. laetmata</i> [†]	p 550 - 850m	780.93	1800m	Pugh 1999b	59 - 62°S	—	—
	<i>Cl. moserae</i>	p 500 - 900m	665.58	500 - 1000+	Pugh 1999b	60°N - 65°S	I. M. P. Alvariño 1971; Mapstone 2009; Pugh 1999b	
	<i>Heteronormpis crystallina</i> [*]	c 500 - 700m	576.26	400 - 1000m	Pugh 1999b	60°N - 67°S	I. P. Mapstone 2009; Pugh 1999b	
	<i>Kephives ovata</i>	p 78 - 1000m	613.7	0 - 700m	Mapstone 2009	50°S - 46°N	I. M. P. Alvariño 1971; Mapstone 2009	
	<i>K. sp. nov.</i> [*]	p 450 - 1000m	776.89	—	—	—	—	—
	<i>Chelophyes appendiculata</i>	e 350 - 1000m	596.83	—	—	—	—	—
Diphyidae	<i>C. contorta</i>	p 78 - 200m	146.72	0 - 300m	Pugh 1999b	55°N - 56°S	I. M. P. Alvariño 1971; Pugh 1999b	
	<i>Dimophyses arctica</i>	p 78 - 1000m	403.66	0 - 600m	Pugh 1999b	74°N - 67°S	I. M. P. Alvariño 1971; Pugh 1999b	
	<i>Diphyses bojani</i>	p 0 - 50m	25.5	0 - 100m	Pugh 1999b	44°N - 40°S	I. M. P. Alvariño 1971; Pugh 1999b	
	<i>Dip. dispar</i>	e 0 - 200m	87.4	—	—	—	—	—
	<i>Eudoxoides mitra</i>	c 50 - 100m	75	0 - 200m	Pugh 1999b	47°N - 45°S	I. M. P. Alvariño 1971; Pugh 1999b	
	<i>E. spiralis</i>	p 0 - 700m	88.85	0 - 200m	Pugh 1999b	44°N - 40°S	I. M. P. Alvariño 1971; Pugh 1999b	
	<i>Gilia reticulata</i>	p 250 - 1000m	895.96	700 - 1100m	Pugh 1999b	60°N - 60°S	I. M. P. Alvariño 1971; Pugh 1999b	
	<i>Lensia achilles</i>	p 200 - 950m	473.18	500 - 900m	Pugh 1999b	60°N - 65°S	I. P. Alvariño 1971; Pugh 1999b	
	<i>L. atax</i> [*]	p 200 - 998m	492.65	200 - 1000m	Pugh 1999b	44°N - 33°S	I. P. Alvariño 1971; Pugh 1999b	
	<i>L. asymmetrica</i>	p 400 - 1000m	862.31	200 - 1000m	Pugh and Pagès 1997	—	P. Pugh and Pagès 1997	
	<i>L. campanella</i>	e 500 - 750m	600.57	—	—	—	—	—
	<i>L. conoidea</i>	p 0 - 100m	63.31	0 - 100m	Pugh 1999b	54°N - 38°S	I. M. P. Alvariño 1971; Pugh 1999b	
	<i>L. cordata</i> [*]	p 50 - 650m	111.61	0 - 300m	Pugh 1999b	69°N - 59°S	I. M. P. Alvariño 1971; Pugh 1999b	
	<i>L. exenter</i>	p 500 - 700m	602.01	500 - 1250m	Zhang 2005	—	I. P. Mapstone 2009; Zhang 2005	
	<i>L. fowleri</i>	p 350 - 400m	375	400 - 600m	Pugh 1999b	60°N - 33°S	Pugh 1999b	
	<i>L. grimaldii</i>	p 100 - 700m	332.81	0 - 300m	Pugh 1999b	61°N - 45°S	I. M. P. Alvariño 1971; Pugh 1999b	
	<i>L. hardy</i>	p 50 - 200m	150	200 - 500m	Pugh 1999b	53°N - 43°S	P. Alvariño 1971; Pugh 1999b	
	<i>L. havock</i>	p 250 - 1000m	754.26	1200 - 1600m	Pugh 1999b	18°N - 57°S	I. P. Alvariño 1971; Pugh 1999b	
	<i>L. hostile</i>	p 350 - 400m	375	500 - 1500m	Pugh 1999b	60°N - 66°S	I. M. P. Alvariño 1971; Pugh 1999b	
	<i>L. leloupi</i>	p 0 - 750m	110.68	0 - 200m	Pugh 1999b	44°N - 2°S	I.P. Daniel 1985; Kitamura, 1997; Pugh 1999b	
	<i>L. leloupeteaum</i>	p 200 - 1000m	548.85	600 - 1000m	Pugh 1999b	60°N - 33°S	I. P. Alvariño 1971; Pugh 1999b	
	<i>L. meteori</i>	p 100 - 200m	150	200 - 500m	Pugh 1999b	55°N - 39°S	I. M. P. Alvariño 1971; Pugh 1999b	
	<i>L. multicirrata</i>	p 100 - 1000m	417.51	100 - 500m	Pugh 1999b	60°N - 57°S	I. M. P. Alvariño 1971; Pugh 1999b	
	<i>L. panikkari</i> [†]	p 200 - 400m	277.54	0 - 200m	Daniel 1985	—	I. Daniel 1985	
	<i>L. quadruplicata</i>	p 500 - 1000m	876.73	678 - 1049m	Paués et al. 2006	42°N	P. Paués et al. 2006	
	<i>L. subtilis</i>	p 50 - 200m	93.34	0 - 200m	Pugh 1999b	55°N - 39°S	I. M. P. Alvariño 1971; Pugh 1999b	
	<i>L. zenkevitchi</i> [*]	p 350 - 650m	527.83	0 - 2540m	Margulis 1970	10°S	P. Margulis 1970; Mapstone 2009	
	<i>Muggiae atlantica</i>	p 0 - 1000m	50.93	0 - 100m	Pugh 1999b	55°N - 37°S	I. M. P. Alvariño 1971; Pugh 1999b	
	<i>M. bargmannae</i>	e 0 - 998	100.95	—	—	—	—	—
Hippopodiidae	<i>M. delsmani</i>	p 400 - 600m	507.83	200 - 500m	Pugh 1999b	42 - 67° N / S	I. P. Alvariño 1971; Park and Won 2004; Pugh 1999b	
	<i>Vogta glabra</i>	p 50 - 100m	75	—	—	—	I. P. Alvariño 1971	
	<i>V. pentacantha</i>	p 50 - 250m	163.71	100 - 500m	Pugh 1999b	62°N - 56°S	I. M. P. Alvariño 1971; Pugh 1999b	
	<i>V. serrata</i>	p 200 - 300m	250	—	Alvariño 1971	46°N - 32°S	I. M. P. Alvariño 1971	
Pravidae	<i>Amphicyaron acacae</i>	p 300 - 950m	504.62	400 - 800m	Pugh 1999b	66°N - 65°S	I. M. P. Alvariño 1971; Pugh 1999b	
	<i>Nectadamas richardii</i>	p 350 - 400m	375	0 - 100m	Pugh 1999b	60°N - 37°S	I. M. P. Alvariño 1971; Pugh 1999b	
	<i>Desmophyes annectens</i>	p 550 - 750m	575	0 - 1000m	Mapstone 2009	60°N - 0°N	P. Mapstone 2009	
	<i>D. aff. villalfrancae</i>	p 500 - 550m	484.67	0 - 200m	Zhang 2005	North Atlantic	I. M. P. Zhang 2005	
	<i>Rosacea plicata</i>	p 200 - 950m	441.99	200 - 500m	Pugh 1999b	60°N - 65°S	I. M. P. Alvariño 1971; Pugh 1999b	
	<i>Eudoxia macra</i>	e 50 - 200m	81.89	0 - 200m	Zhang 2005	34°S - 11°N	I. P. Alvariño 1971; Zhang 2005	
	<i>Eudoxia cf. galatheae</i> [†]	p 78 - 1000m	434.59	0 - 3000m	Moser 1925	15°N - 64°S	Moser 1925	
	<i>Eudoxia B</i>	e 0 - 700m	335.38	—	—	—	—	—
	<i>Bract D</i>	e 50 - 600m	209.49	—	—	—	—	—
	<i>Bract E</i>	e 700 - 750m	725	—	—	—	—	—
	<i>Bract F</i>	e 500 - 650m	568.21	—	—	—	—	—
	<i>Bract G</i>	e 100 - 200m	150	—	—	—	—	—
	<i>Bract H</i>	e 100 - 350m	174.73	—	—	—	—	—
	<i>Bract I</i>	e 100 - 700m	563.44	—	—	—	—	—

^a *Halistenmma rubrum* sensu Totton 1965a
^b as *Lensa hostile* (based on Fig. 51)

Table 6: Depth range and mean depth (weighted by abundance) of the siphonophore forms collected in Sagami Bay during the March 2006 MULTI-SPLASH cruise, with literature-based information on their known geographic ranges. Species in bold indicate first-time records from Sagami Bay; *: first-time records from Japanese waters; †: first-time records from the Pacific Ocean; e: eudoxid, p: polygastric stage; I: Indian Ocean, M: Mediterranean, P: Pacific Ocean. (modified after Grossmann and Lindsay, 2013b, Table 3)

Discussion

With 58 species of siphonophore recorded from the March 2006 MULTI-SPLASH IONESS samples, the species richness of Sagami Bay was found to be much higher than the 37 species collected by Mapstone (2009) in the Canadian Pacific from similar depth strata and using similar sampling gear. However, that study dealt with water masses around 48.5°N, while Sagami Bay is at 35°N and, moreover, a zone of important heterogeneity when considering the temporal variability of the waters present in the Bay. Indeed, waters in the Bay can be influenced at the surface by runoff water from the surrounding land and from Tokyo Bay, by sub-branches of the Kuroshio Current, and, in the mesopelagic zone, by a mixture of waters of northern origin, the Low Salinity Water (LSW), and, at times, by intrusions of Oyashio Intermediate Water (OIW) (Senju *et al.*, 1998).

The CTD profile and surface oceanographic maps (Japan Coast Guard, 2006) of the present sampling times showed no direct influence of either Kuroshio (offshore non-large meander type) (Fig. 7) or OIW at the sampling station, and the hydrographic characteristics in the Bay remained relatively constant during the 9-day sampling, the main differences being found at night, between 200 and 351 m, and, during the day, around 700 m. The cluster and Multi-Dimensional Scaling analyses showed a clear separation of the siphonophore communities based on the depth and origin of the different water masses of the Bay.

The epipelagic community, composed of clusters A and B, and spanning from 200 m to the surface, was dominated by *Muggiae atlantica*, an epipelagic species known to undergo seasonal blooms in spring and autumn (Kitamura, 2009; Mapstone, 2009), and by warm-water species of the genera *Abylopsis*, *Bassia* and *Eudoxoides*, absent in the Canadian Pacific (Mapstone, 2009), but recorded up to 60°N in the Atlantic (Table 6), an area influenced by a similar current system - the North Atlantic Drift. *Muggiae delsmani* Totton, 1954, an Indian Ocean species whose Pacific records include the Fiji and South China Seas, and other tropical waters of south-east Asia (Gao *et al.*, 2002; Rengarajan, 1973), was collected in the 50 to 100 m net during the day, possibly above the thermocline that was present between 82 and 88 m.

Another primarily tropical, neritic, species, *Lensia subtiloides* (Lens and van Riemsdijk, 1908), was completely absent from the present data set. It was previously found to be present from June to November, and absent in February from the upper 200 m of Sagami Bay (Kitamura, 2009), so perhaps season, rather than the effect of the Kuroshio Current, may play a greater role in determining its distribution in south-eastern Japan. Additionally, it is

possible the two morphologically similar species *Lensia leloupi* Totton, 1954 and *L. subtiloides* might compete for the same resources and be mutually exclusive. Indeed, in March, *L. leloupi* was one of the most abundant forms in the upper 200 m, and was one of the forms contributing the most to cluster B (Fig. 11), while the only previous records of this species from Sagami Bay were of a single individual in February and a single individual in June, from 0-150 m vertical NORPAC net tows (Kitamura, 1997).

However, the influence of the surface Kuroshio Current was not enough to explain the presence of all warm-water species. Indeed, the presence of *Lensia cordata* between 500 and 700 m, a species only previously recorded from the Indian Ocean (Totton, 1965b) and the South China Sea (Gao *et al.*, 2002; Zhang, 2005; Zhang and Lin, 1997), might point to a transport of waters in the mesopelagic zone from the tropical Pacific to Sagami Bay, possibly following a similar path to that of the Kuroshio Current. Similarly, *Lensia panikkari*, found between 200 and 400 m, has only previously been recorded in the Indian (Daniel, 1985; Gibbons and Thibault-Botha, 2002; Thibault-Botha and Gibbons, 2005) and Atlantic Oceans (Pugh, 1984).

The diversity of the Siphonophora matched that of a study of the scolecitrichid copepods of Sagami Bay (Kuriyama and Nishida, 2006) obtained using similar sampling methods, and of the calanoid copepod community sampled at the same station in Sagami Bay using smaller stratified net systems (Shimode *et al.*, 2006), both in terms of Shannon-Wiener (H') index values and of the profile of this index over the water column, except for the important decrease observed around 400 m in the present study. This decrease in diversity could be directly linked to the decrease in evenness caused by the single species *Dimophyses arctica*, the large increase in abundance of which coincided with the lowest salinity values. Although this species has a worldwide distribution, it is primarily found in cold, polar waters, and is believed to spawn only in such water masses (Stepanjants *et al.*, 2006). Indeed, the small *D. arctica* polygastric stages were concentrated within the LSW, associated with the much larger eudoxid stages, while larger polygastric stages were collected both in the LSW and the warmer upper-mesopelagic layers (Fig. 10). The numerical dominance of the polygastric stage over the eudoxid one, and the extremely small size of the anterior nectophores would indicate the generation succession occurring in May in the waters of British Columbia (Mapstone, 2009; Mills, 1982) and in Norwegian fjords (Hosia and Båmstedt, 2008) happened earlier, possibly at the start of March, in the present study area. This difference in timing between latitudes of 50 to 60°N and Sagami Bay might be due to the Oyashio origin of the LSW. The Oyashio Current flows at up to 0.4 m.s^{-1} southwards along

the north-eastern coast of Japan (Ohshima *et al.*, 2005), and the observed animals were probably produced in northern waters and transported into the mesopelagic depths of Sagami Bay by subduction of Oyashio waters at the Oyashio-Kuroshio convergence zone. Indeed, the maximum abundance of both eudoxid and polygastric stages of *D. arctica* were found around 400 m, much deeper than the upper-mesopelagic records of this species from Canadian (Mapstone, 2009; Mills, 1982) and Norwegian (Hosia and Båmstedt, 2008) waters. The presence of large numbers of eudoxids and very small, young, polygastric stages at depths greater than they are normally found in more northern waters (Table 6), could therefore resemble the pathway described for *Neocalanus cristatus* copepodite V stages by Oh *et al.* (1991). And similarly, it is not known whether the physico-chemical parameters of the bay would allow active reproduction of the polar *D. arctica*.

The presence of midwater, subarctic-derived water intrusion events in the Bay could also be confirmed by the presence of *Muggiaeae bargmannae*, a species found exclusively in Arctic and Antarctic waters. Margulis (1978) notes that in the western North Atlantic, mixing with ‘tropical water’ (the North Atlantic Drift) did not appear to affect the distribution of *M. bargmannae*. A similar phenomenon could be observed in Sagami Bay, where the water temperatures at the sampling area approximated 6°C, 2°C more than the upper temperature limit reported for this species by Stepanjants (1967).

Also found in the LSW waters were the eudoxid forms herein referred to as *Eudoxia cf. galathea* Moser, 1925. Although their vertical distribution ranged from 78 m at night to 1000 m during the day in Sagami Bay, their peak of maximum abundance was found between 350 and 450 m during the day, and between 400 and 450 m at Night. This is in agreement with the 300- to 500 m-depth distribution of this eudoxid recorded by Leloup and Hentschel (1935) in the Southern Atlantic. The samples described by Moser (1925) from the Southern and Atlantic Oceans were collected in non-closing vertical nets, but the majority of the samples were collected in nets towed from 400 m to the surface. The bracts of these eudoxids did show some similarity with the bracts of *Muggiaeae bargmannae* illustrated in Stepanjants (1967) and Zhang and Lin (2001) (see description of eudoxid stage in Appendix 3, p. 215). However, this species is primarily bipolar and appeared only twice in the present data series, in contrast to *E. cf. galathea*, one of the most abundant forms in the lower 600 m (not shown). This eudoxid stage, the eudoxids of *Dimophyes arctica*, *Eudoxoides spiralis*, *Lensia cossack*, *L. havock* and *Muggiaeae atlantica*, those of the genera *Chuniphyes* and *Kephyses*, as well as one other of unknown polygastric stage (‘Eudoxid B’), were found to contribute greatly to the community structure (Fig. 11), and eudoxid stages were the most abundant form in 65% of the net samples.

The lower mesopelagic cluster was characterized by deep-water species such as *Gilia reticulata*, *Lensia asymmetrica*, *L. havock* and *L. quadriculata*. These species are commonly found below 700 m at all latitudes and in all oceanic basins, and may represent a cold-, deep-water signature, as they have yet to be recorded from warm deep seas such as the Mediterranean (Table 6) or the Sulu Seas (D.J. Lindsay, personal observation). However, it is not known whether the high temperatures at depth, or the shallow sills controlling the water flow to these seas limit the access of these species, which are rarely recorded shallower than 200 m.

Despite the wide or worldwide distribution of most siphonophore species (Alvariño, 1971; Mapstone, 2009; Margulis, 1980), the stratified IONESS samples collected in Sagami Bay in March 2006 showed water mass-specific community structure within the Siphonophora. The presence of lateral transport of some key siphonophore species into Sagami Bay following both the Kuroshio and Oyashio paths could be confirmed. Eudoxid stages, although omitted from many siphonophore studies, were found to play important roles in the community structure.

Although it is one of the most well studied bays in Japan, the complex oceanographic structure of Sagami Bay means the biodiversity it houses has yet to be fully assessed. Indeed, eleven siphonophore species and two eudoxids of unknown parentage were recorded for the first time from the bay in this study, bringing the total number of siphonophores species known from Sagami Bay to 118, more than 60% of the total 191 valid siphonophore species (World Register of Marine Species).

			Depth range (m)	Mean depth (m)
Physonectae Haeckel 1888				
Agalmatidae Brandt 1835	<i>Agalmatidae</i> sp. (larval)		45 - 1000	251.3
<i>Agalma</i> Eschscholtz 1825	<i>A. clausi</i> (Bedot, 1888)		200 - 300	250
<i>Halistemma</i> Huxley 1895	<i>H. rubrum</i> (Vogt, 1852)		50 - 800	496.76
<i>Nanomia</i> Agassiz 1865	<i>H. transliratum</i> Pugh & Youngbluth 1988		45 - 100	72.76
Apolemiidae Huxley 1859	<i>N. bijuga</i> (Chiaja 1841)		0 - 1000	214.83
	<i>Apolemiidae A</i>		650 - 850	825
	<i>Apolemiidae B</i>		700 - 750	725
	<i>Apolemiidae C</i>		450 - 950	742.5
Erennidae Pugh, 2001				
<i>Erema</i> Bedot 1904	<i>E. richardi</i> Bedot 1904		850 - 950	898.62
Forskaliidae Haeckel 1888				
<i>Forskalia</i> Kölliker 1853	<i>F. formosa</i> Keferstein & Ehlers 1860*		200 - 300	250
Physophoridae Eschscholtz 1829				
<i>Physophora</i> Forskal 1775	<i>P. gilmeri</i> Pugh 2005*		200 - 300	250
Pyrostephidae Moser, 1925				
<i>Bargmannia</i> Totton 1954	<i>B. amoena</i> Pugh 1999		350 - 1000	664.55
	<i>B. lata</i> Mapstone 1998		700 - 850	767.01
Incertae sedis				
<i>Frillagalma</i> Daniel 1966	<i>F. vityazi</i> Daniel 1966		200 - 950	551.89
<i>Marrus</i> Totton 1954	<i>M. orthocanna</i> (Kramp 1942)		200 - 1000	760.4
Calycophorae Leuckart 1854				
Abylidiae Agassiz 1862				
<i>Abyla</i> Quoy & Gaimard 1827	<i>A. haeckeli</i> Lens & van Riemsdijk*	e.	0 - 45	23
<i>Abylopsis</i> Chun 1888	<i>A. eschscholtzi</i> (Huxley 1859)	e.	0 - 800	70.23
		p.	0 - 700	84.24
	<i>A. tetragona</i> (Otto 1823)	e.	0 - 700	80.87
		p.	0 - 600	60.46
<i>Bassia</i> Agassiz 1862	<i>B. bassensis</i> (Quoy & Gaimard 1834)	e.	0 - 700	46.96
		p.	0 - 750	50.64
<i>Ceratocymba</i> Chun 1888	<i>C. leuckartii</i> (Huxley 1859)*	e.	50 - 100	75
	<i>C. dentata</i> (Bigelow 1918)*	e.	500 - 550	525
<i>Enneagonum</i> Quoy & Gaimard 1827	<i>E. hyalinum</i> Quoy & Gaimard 1827*	p.	600 - 650	625
Clausophyidae Totton 1965				
<i>Chuniphyes</i> Lens & van Riemsdijk 1908	<i>Ch. spp.</i>	e.	78 - 1000	440.37
	<i>Ch. moserae</i> Totton 1954	p.	350 - 850	646.87
	<i>Ch. multidentata</i> Lens & van Riemsdijk 1908	p.	200 - 1000	423.77
<i>Clausophyes</i> Lens & van Riemsdijk 1908	<i>Cl. galeata</i> Lens & van Riemsdijk 1908	p.	450 - 950	747.46
	<i>Cl. laetmata</i> Pugh & Pagès 1993†	p.	550 - 850	775.51
	<i>Cl. moserae</i> (Margulis 1988)	p.	450 - 1000	675.64
<i>Heteropyramis</i> Moser 1925	<i>H. crystallina</i> (Moser 1925)*	e.	500 - 950	711.07
		p.	500 - 850	717.2
	<i>H. maculata</i> Moser 1925*	e.	350 - 400	375
<i>Kephyses</i> Pugh 2006	<i>K. spp.</i>	e.	300 - 1000	632.46
	<i>K. ovata</i> (Keferstein & Ehlers 1860)	p.	0 - 1000	553.69
	<i>K. sp. nov.</i>	p.	0 - 1000	643.16
Diphyidae Moser 1925				
<i>Chelophyes</i> Totton 1932	<i>C. spp.</i>	e.	0 - 450	43.04
	<i>C. appendiculata</i> (Eschscholtz 1829)	p.	45 - 300	169.26
<i>Dimophyes</i> Moser 1913	<i>C. contorta</i> (Lens & van Riemsdijk 1908)	p.	0 - 600	69.57
	<i>D. arctica</i> (Chun 1897)	e.	78 - 1000	622.43
		p.	78 - 1000	391.56
<i>Diphyes</i> Cuvier 1817	<i>D. bojani</i> (Eschscholtz 1829)	e.	0 - 200	58.29
		p.	0 - 50	25.5
	<i>D. dispar</i> Chamisso & Eysenhardt 1821	e.	0 - 350	77.27
<i>Eudoxoides</i> Huxley 1859	<i>E. mitra</i> (Huxley 1859)	e.	0 - 650	76.01
		p.	0 - 900	97.57
	<i>E. spiralis</i> (Bigelow 1911)	e.	0 - 900	80.37
		p.	0 - 950	103.9
<i>Gilia</i> Pugh & Pagès 1995	<i>G. reticulata</i> (Totton 1954)	e.	700 - 1000	856.22
		p.	250 - 1000	884.89
<i>Lensia</i> Totton 1932	<i>L. achilles</i> Totton 1941	e.	200 - 1000	692.48
		p.	100 - 1000	487.14
	<i>L. ajax</i> Totton 1941*	p.	200 - 1000	591.88
	<i>L. asymmetrica</i> Stepanjants 1970	e.	350 - 1000	741.83
		p.	400 - 1000	844.63

Table 7: Depth range and mean depth (weighted by abundance) of the siphonophore forms collected at all stations during the March 2006 MULTI-SPLASH cruise. *: first-time record from Japanese waters; †: first-time record from the Pacific Ocean; e: eudoxid, p: polygastric stage.

<i>L. campanella</i> (Moser 1925)	p.	0 - 100	60.95
<i>L. conoidea</i> (Keferstein & Ehlers 1860)	e.	0 - 700	105.09
	p.	0 - 600	123.14
<i>L. cossack</i> Totton 1941	e.	0 - 550	143.13
<i>L. cordata</i> Totton 1965*	p.	400 - 900	620.2
<i>L. exeter</i> Totton 1941	p.	300 - 400	368.03
<i>L. fowleri</i> (Bigelow 1911)	e.	100 - 200	150
	p.	0 - 700	199.24
<i>L. grimaldii</i> Leloup 1933	p.	200 - 350	256.56
<i>L. hardy</i> Totton 1941	p.	0 - 200	79.54
<i>L. havock</i> Totton 1941	e.	50 - 1000	619.82
	p.	250 - 1000	735.23
<i>L. hostile</i> Totton 1941	p.	350 - 850	509.68
<i>L. leloupi</i> Totton 1954	e.	0 - 1000	153.18
	p.	0 - 850	85.09
<i>L. lelouvetteau</i> Totton 1941	p.	200 - 1000	589.79
<i>L. meteori</i> (Leloup 1934)	e.	450 - 500	475
	p.	45 - 200	132.33
<i>L. multicristata</i> (Moser 1925)	p.	100 - 1000	413.14
<i>L. panikkari</i> Daniel 1970†	p.	50 - 400	241.1
<i>L. quadrivalvata</i> Pagès, Flood & Youngbluth 2006	p.	500 - 1000	850.59
<i>L. subtilis</i> (Chun 1886)	p.	0 - 350	84.98
<i>L. zenkevitchi</i> Margulis 1970*	p.	350 - 650	549.03
<i>M. atlantica</i> Cunningham 1892	e.	0 - 1000	28.59
<i>M. bargmannae</i> Totton 1954	p.	0 - 1000	36.57
<i>M. delsmani</i> Totton 1954	p.	400 - 600	507.83
<i>M. kochi</i>	p.	50 - 100	75
	p.	800 - 850	825
Incertae sedis (aff. Diphyidae)			
<i>Eudoxia cf. galathea</i> †	e.	78 - 1000	425.5
<i>Bract D</i>	e.	45 - 600	162.1
<i>Bract E</i>	e.	700 - 750	725
<i>Bract F</i>	e.	500 - 650	579.37
<i>Bract G</i>	e.	100 - 200	150
<i>Bract H</i>	e.	100 - 350	174.73
<i>Bract I</i>	e.	100 - 750	545.83
<i>Bract J</i>	e.	450 - 900	875
<i>Bract K</i>	e.	400 - 1000	709.48
<i>Bract L</i>	e.	100 - 200	150
<i>Bract M</i>	e.	500 - 950	525
<i>Eudoxid B</i>	e.	0 - 950	391.33
Hippopodiidae Kölliker 1853			
<i>Hippopodius</i> Quoy & Gaimard 1827			
<i>Vogtia</i> Kölliker 1853			
<i>H. hippopus</i> (Forskål 1776)		300 - 700	452.89
<i>V. glabra</i> Bigelow 1918		50 - 300	186.27
<i>V. pentacantha</i> Kölliker 1853*		200 - 750	471.67
<i>V. serrata</i> (Moser 1925)		100 - 950	484.2
Prayidae Kölliker 1853			
<i>Amphicaryoninae</i> Chun 1888			
<i>Amphicaryon</i> Chun 1888			
<i>A. acaule</i> Chun 1888	e.	450 - 500	100.84
<i>M. praecleara</i> Totton 1954	p.	0 - 450	251.3
	e.	50 - 400	
	e.	100 - 900	453.41
	p.	50 - 100	75
<i>Nectopyramidinae</i> Bigelow 1911a			
<i>Nectadamas</i> Pugh 1992			
<i>N. diomedae</i> (Bigelow 1911b)*	e.	400 - 450	425
<i>N. richardi</i> Pugh 1992	e.	350 - 850	572.75
	p.	350 - 800	528.74
<i>N. natans</i> (Bigelow 1911b)*	p.	450 - 950	925
<i>N. thetis</i> Bigelow 1911b	p.	600 - 650	625
<i>Prayinae</i> Chun 1897			
<i>Desmophyes</i> Haeckel 1888			
<i>D. annectens</i> Haeckel 1888		100 - 750	317.12
<i>D. haematogaster</i> Pugh 1992b		500 - 600	543.78
<i>D. aff. villafrancae</i> (Carré 1969)*		500 - 550	525
<i>L. rosea</i> Chun 1885		550 - 600	575
<i>R. plicata</i> Bigelow 1911a		200 - 950	458.46
<i>Sphaeronectidae</i> Huxley 1859			
<i>Sphaeronectes</i> Huxley 1859			
<i>S. fragilis</i> Carré 1968*	p.	350 - 550	413.66
<i>S. irregularis</i> (Claus 1873)	p.	450 - 500	475
<i>S. koellikeri</i> Huxley 1859	p.	0 - 100	35.99
<i>S. pagesi</i> Lindsay, Grossmann & Minemizu 2011	p.	0 - 300	57.15

Table 7 (cont.): Depth range and mean depth (weighted by abundance) of the siphonophore forms collected at all stations during the March, 2006 MULTI-SPLASH cruise. *: first-time record from Japanese waters; †: first-time record from the Pacific Ocean; e: eudoxid, p: polygastric stage.

II. Generalization to all stations

In part after: **Mary M. Grossmann**, Dhugal J. Lindsay: Structure and temporal variability of planktonic communities off south-eastern Japan (in preparation)

1. Siphonophore diversity

Eighty-three species of siphonophore could be identified from the IONESS net samples: 14 Physonectae and 69 Calycophorae (Table 7), of which 24 were not collected in Sagami Bay. Additionally, one type of physonect larval stage (Agalmatidae sp.), and 12 calycophoran eudoxids of unknown polygastric stage were recorded.

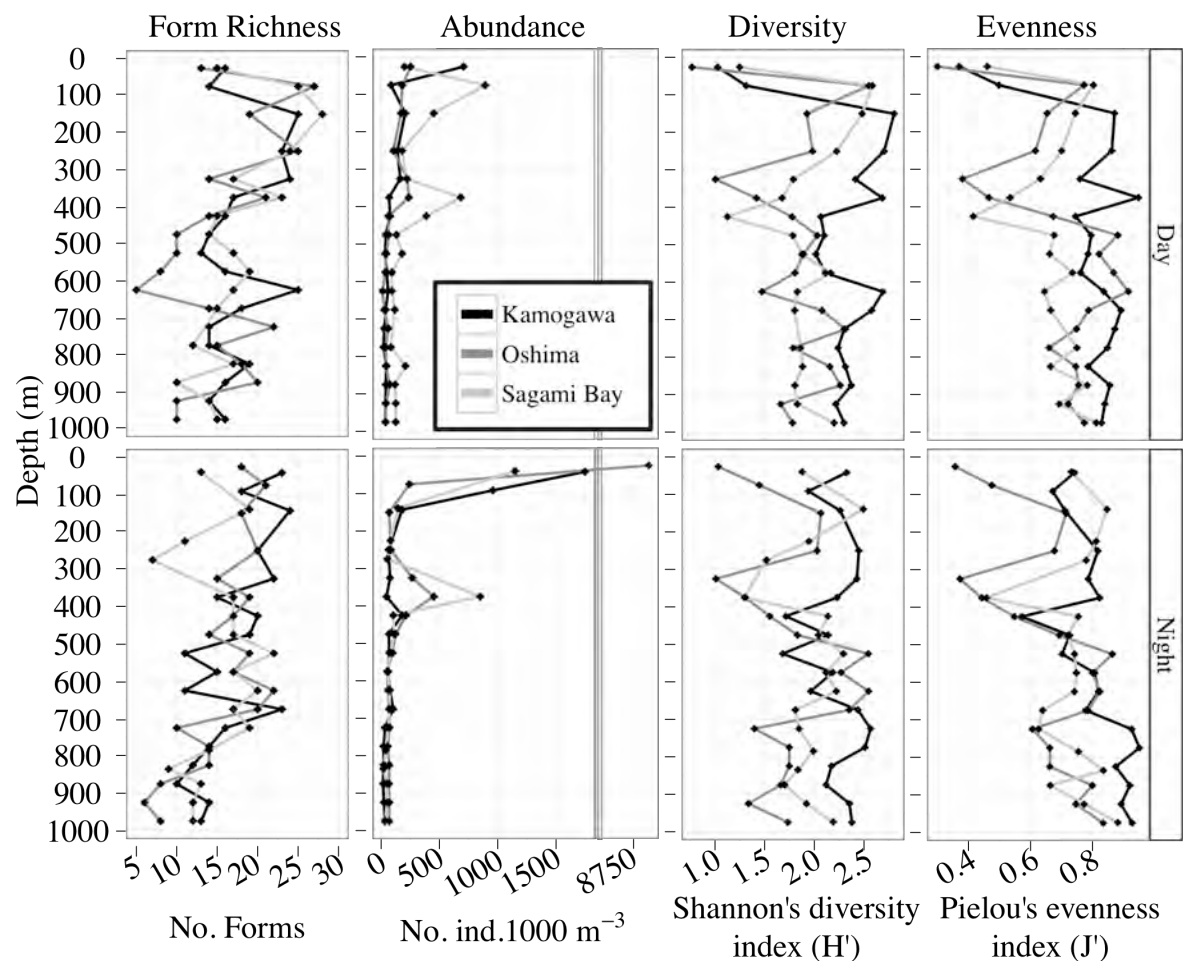


Figure 13: A: Form richness, B: Total abundance, C: Diversity, D: Evenness over the water column in each sampling series. Marks represent the mean sampling depth for each net.

There were on average 17.65 forms per net sample, with a minimum of 5 between 600 and 650 m during the day off Oshima, and a maximum of 28 forms, collected between 100 and 200 m during the day in Sagami Bay (Fig. 13). On average, only 2 or 3 individuals of each form occurred in any given net sample, and less than 5% of occurrences corresponded to the presence of more than 36 individuals in any given net sample. The 10 occurrences with the most individuals in a single net sample were of either *Muggiae atlantica* or *Dimophyes arctica*, with a maximum of 3712 *M. atlantica* eudoxids in the 50- to 0 m nighttime net off Oshima.

Abundance was highest at the Oshima station, with a maximum total abundance of nearly 9500 individuals. 1000 m^{-3} in the 50- to 0 m nighttime net. A similar peak in total abundance could be found in the upper 100 m of the water column at the other sampling locations and times, but this was an order of magnitude smaller, varying from 252.8 individuals. 1000 m^{-3} during the day east of Oshima, to 1747.0 individuals. 1000 m^{-3} during the night off Kamogawa. A second peak in abundance could be found around 350 m in Sagami Bay and off Oshima and around 450 m at night at the Kamogawa station. The deeper peak in abundance found between 800 and 850 m in Sagami Bay was not present at the other stations.

Diversity and evenness were globally high over the whole water column except for the uppermost sampling layer during the day at the 3 stations, and during the night at Oshima. A marked decrease in diversity and evenness was found between 300 and 350 m off Oshima and between 400 and 450 m in Sagami Bay, while off Kamogawa, Shannon's diversity (H') and Pielou's evenness (J') indices showed a slight decrease between 400 and 600 m.

Shannon's diversity and Pielou's evenness indices showed similar trends off Oshima and in Sagami Bay, but the sharp decrease in both indices found around 400 m in Sagami Bay was found at 300 – 400 m off Oshima during both the day and nighttime. The highest overall diversity and evenness profiles in the mesopelagic layer of the 3 sampling stations at Kamogawa station. There was a limited midwater decrease in diversity, between 400 and 600 m, and this was not accompanied by a statistically significant decrease in evenness.

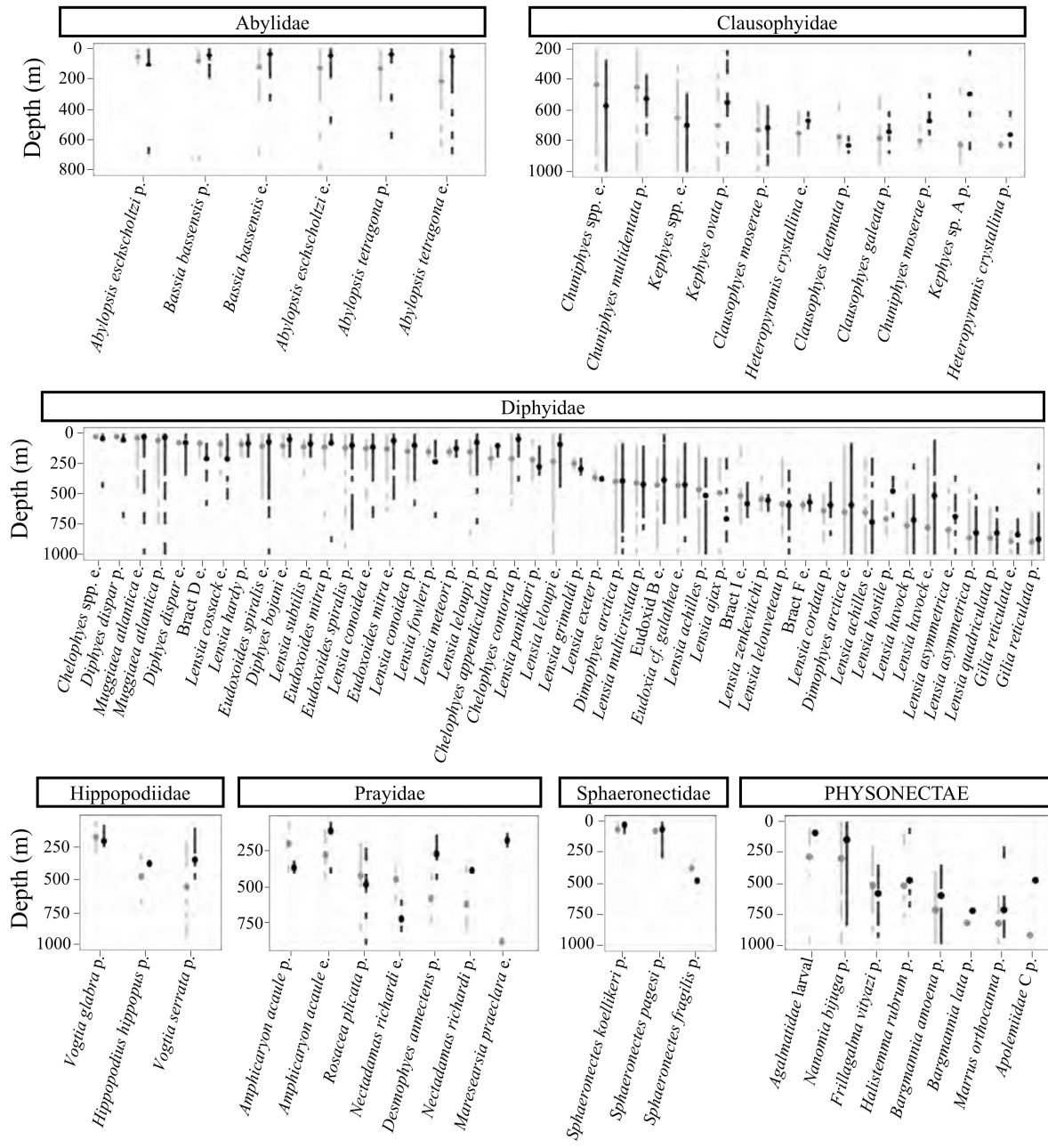


Figure 14: Maximum vertical range and mean depth (weighted by abundance) during the day (grey) and night (black) of all forms having been sampled during both day and nighttimes, ordered by weighted mean depth of daytime abundance; all stations combined. e: eudoxid, p: polygastric stage.

2. Vertical distribution

Similarity analyses (ANOSIM) showed neither station nor sampling time had a significant influence on form distributions ($R = 0.01$, $p = 0.77$ and $R = 0.01$, $p = 0.15$, respectively). Depth had a higher influence, with $R = 0.09$ and $p = 0.06$. The vertical extent and the depth of the abundance maxima of the different species clearly delimited an epi-and upper mesopelagic, a mesopelagic and a bathypelagic group of species. In the upper-mesopelagic group, in addition to the diel vertical migration (DVM) patterns of *Nanomia bijuga* observed in Sagami Bay, the combined data from the 3 sampling stations allowed DVM patterns to be observed in all but one form (*Abylopsis eschscholtzi* polygastric stages) of the family *Abylidiae*, in the diphyid genera *Chelophyes* and *Eudoxoides*, in *Diphyes bojani*, *Lensia leloupi* and *L. subtilis* (Fig. 14). Other epipelagic and mesopelagic species such as *Chuniphyes* spp., *Dimophyes arctica*, *Lensia achilles*, *L. multicristata* and *Muggiae atlantica* did not show clear DVM patterns, or were found deeper at night than during the day. All physonects appeared to perform DVM, except for *Frillagalma vityazi*, found to occur deeper at night than during the day. The lower mesopelagic species (e.g. *Gilia reticulata*, *Lensia asymmetrica*, *L. havock*, *L. quadriculata*) also appeared to perform DVM. For most species producing free eudoxids, and for which the eudoxids are known, the presence or absence of diel vertical migration was a character that appeared in both life stages and, apart from in the genus *Lensia*, appeared to be a generic characteristic.

Within the physonects and the calycophore families Hippopodiidae and Prayidae, species of the same family did not have similar vertical distributions, or showed abundance maxima at different depths. In the family Clausophyidae, the vertical ranges of congeneric species overlapped, but there was found to be a clear separation of their mean depth distribution. In the families Abylidiae and Diphyidae, however, many of the species of a given genus had overlapping vertical ranges and showed a similar mean depth distribution, as did two of the *Sphaeronectes* species.

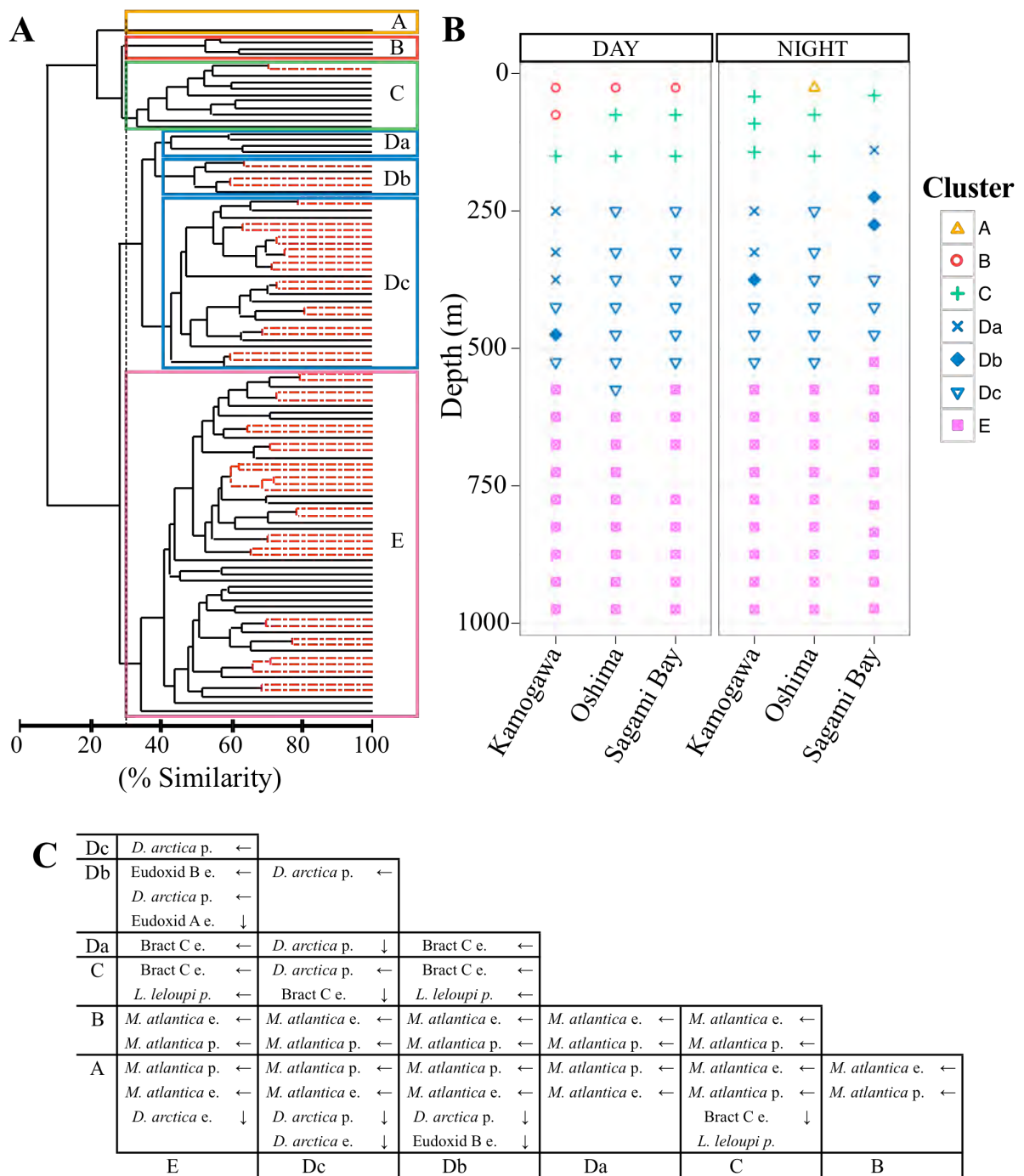


Figure 15: A: Community structure analysis dendrogram (clustering performed on square-root transformed abundance data, with an average linkage and Bray-Curtis similarity), red dotted lines indicate nodes unsupported by the SIMPROF analysis (Bray-Curtis similarity $\leq 95\%$); B: Graphical representation of the inter-net clusters obtained. Marks represent the mean sampling depth of each net; C: Forms contributing the most to the dissimilarity between clusters (average dissimilarity ≥ 5 in terms of percentage abundance for each pair of clusters). e: eudoxid, p: polygastric stage; arrows indicate which, of columns or rows, a form contributes the most to.

3. Community structure

Five groups were obtained by hierarchical cluster analysis at a 30% cut-off (Fig. 15. A). Three clusters described the upper 200 m of the water column (Fig. 15. B): cluster C contained the majority of the nets sampled above 200 m, while cluster B contained all the daytime surface net tows, as well as that towed from 100 to 50 m during the day off Kamogawa, and cluster A contained only the 50- to 0 m net collected at night off Oshima. Clusters A and B were dominated by *Muggiaea atlantica*, the eudoxid stages contributing more to cluster A, while the polygastric stages contributed more to cluster B (Fig. 15. C). Fifty-five forms, including upper-mesopelagic species that undergo DVM such as *Lensia leloupi*, *L. subtilis* and *Nanomia bijuga* contributed to cluster C. Cluster D corresponded to the 200- to 550 m-depth stratum, and cluster E contained the deeper nets. This latter had the highest richness, with 83 forms, representing 70 species, contributing to it, and it notably contained bathypelagic species such as *Gilia reticulata*, *Lensia asymmetrica* and *L. quadriculata*. Cluster D could be subdivided into 3 subgroups at a 40% similarity cut-off: cluster Da containing the nets collected between 200 and 400 m at night off Kamogawa, and during the day, between 200 and 300 m off Kamogawa, and between 78 and 200 m in Sagami Bay; cluster Db, containing the nets sampled between 100 and 300 m at night in Sagami Bay, between 350 and 400 m at night off Kamogawa, and from 450 to 500 m during the day off Kamogawa; cluster Dc, containing the remaining nets.

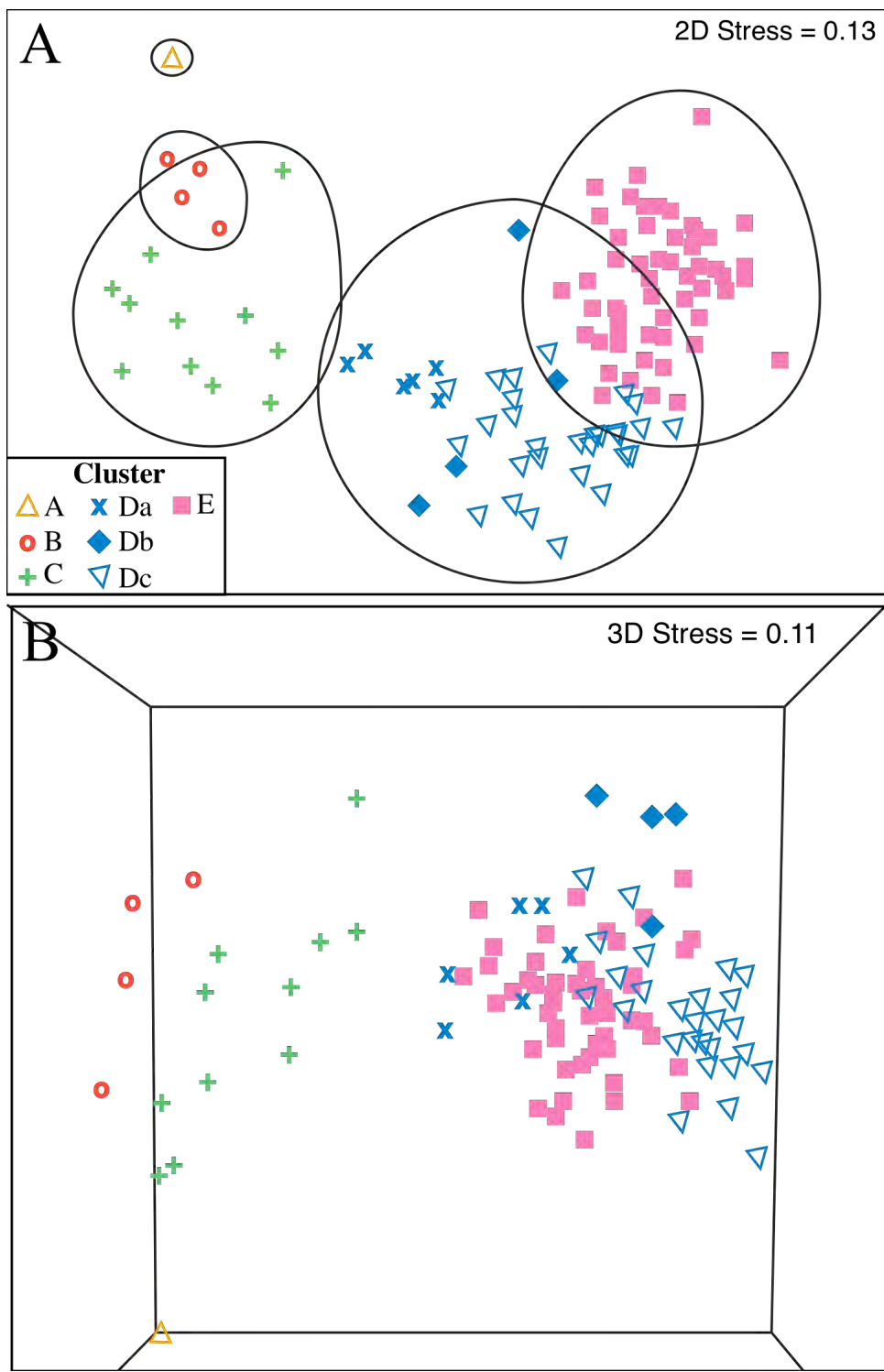


Figure 16: A: 2-dimensional Multi-Dimensional Scaling (2D MDS) diagram of the inter-net clustering, with 30% (solid line) similarity levels; B: 3-dimensional MDS diagram of the inter-net clustering. Each mark representing on net sample, shapes refer to the clusters observed in Fig. 15.

The 2-Dimensional Scaling Analysis (MDS) had a stress value of 0.13 (Fig. 16. A). Cluster A could be clearly differentiated, while clusters B and C appeared to overlap due to the positioning of the nighttime 50- to 100 m net from off Oshima. However, these clusters could be clearly differentiated in the 3-dimensional MDS (Fig. 16. B). Clusters D and E overlapped in the area corresponding to the nets sampled around 550 m, both in the 2D and 3D MDS.

Discussion

The community structure of the Siphonophora off south-eastern Japan during the March 2006 MULTI-SPLASH cruise was influenced by both the structure of the water column and by diel vertical migration (DVM) patterns of some of the dominant species. During the day, the surface community showed low diversity and evenness, being dominated by the eudoxid and polygastric stages of *Muggiae a atlantica* (Fig. 13). Below this, and down to 200 m, was an abundant community characterized by some of the highest richness and diversity values observed. This community was dominated by forms that undergo DVM, such as *Eudoxoides mitra* and *E. spiralis*, *Lensia leloupi* and *L. subtilis*, and was therefore found at the surface during the nighttime sampling.

A distinct siphonophore community was found in the upper 50 m at night at Oshima station, showing an extremely high total abundance, primarily due to *Muggiae a atlantica* eudoxids (75.7% of total siphonophore abundance) and polygastric stages (19.8% of total siphonophore abundance), and presenting low diversity and evenness indices. Associated with a lower salinity than was found at the other sampling locations and times (Fig. 5), this distinct community could be linked with a surface outflow of water from Tokyo Bay and the northern, coastal part of Sagami Bay, due to the modification of the structure of the Kuroshio Current near the end of the sampling period (Fig. 7) inducing an outflow of water at Oshima station. Indeed, the waters in the northern part of Sagami Bay were found to house extremely high concentrations of *M. atlantica* in June 1998 (Kitamura *et al.*, 2003), and large blooms of this species have also been recorded from Tokyo Bay in October (Toyokawa and Terasaki, 1994). With the predominance of *M. atlantica* and the absence of migrating upper-mesopelagic forms such as *Lensia leloupi* eudoxids or *Eudoxoides mitra* polygastric stages, this community more closely resembled the daytime surface community than the more mesopelagic community found at the surface at night in Sagami Bay and at Kamogawa station.

The deeper limit of the upper-mesopelagic cluster (Cluster C) was dictated by the increase in abundance of the polar *Dimophyes arctica*, the determinant species for the mesopelagic cluster. However, smaller-scale structures could also be observed within this cluster: cluster Da, found between 78 and 200 m at night in Sagami Bay, between 200 and 350 m at night off Kamogawa, and between 200 and 400 m off Kamogawa station during the day, could be related to the warmer, more saline and more oxygenated waters observable at

these depths, which did not have the characteristics of the Low Salinity Water, but rather of Kuroshio waters (Figs. 5, 6). Representing a mixture of deeper, more polar mesopelagic forms (*Chuniphyes* spp. eudoxids, *D. arctica*, *Lensia achilles*) and upper-mesopelagic forms, possibly associated with Kuroshio waters (*Lensia leloupi*, *L. panikkari*), this community was characterized by a high diversity and evenness. The main part of the mesopelagic cluster (Cluster Dc) corresponded to the Low Salinity Water signal. In this water mass were found the abundance maxima of several species that, at polar latitudes, have upper-mesopelagic to epipelagic distributions: e.g. *Chuniphyes* spp., *D. arctica*. Cluster Db, although similar to cluster Dc, was characterized by a very low contribution of *D. arctica* eudoxid stages.

Below the LSW, between 550 and 1000 m, although *Dimophyes arctica* was still abundant, only the eudoxid stage showed an important contribution to the cluster analysis, along with other lower-mesopelagic and bathypelagic species such as *Gilia reticulata*, *Lensia asymmetrica*, *L. havock* and *L. quadriculata*.

A complex community structure, highly influenced by the hydrography of the sampling area, could be found off south-eastern Japan in March 2006. Each community was composed of species sharing specific depth ranges, geographic origins and physiological mechanisms such as diel vertical migration (DVM). As observed in hyperiid amphipods from the North Pacific Gyre (Shulenberger, 1979) each community contained many congeneric species. Shulenberger (1979) established a list of seven factors helping to discriminate specific ecological niches: vertical range, DVM patterns, feeding periodicity, reproductive habits, diet, patchiness and co-occurrence with other hyperiid species. For the physonect siphonophores and the calycophoran families Clausophyidae, Hippopodiidae and Prayidae, although little is known of their diets, feeding patterns or reproduction, congeneric species showed vertical segregation of their depth of mean abundance, although they often had overlapping vertical ranges. However, for the families Abylidiae and Sphaeronectidae, and for the extremely species-rich Diphyidae, a large number of congeneric species appeared to coexist, both in time and space. Indeed, the presence or absence of DVM, at the scales investigated, except for the diphyid genus *Lensia*, appeared to be a generic characteristic within the Siphonophora. As these species corresponded to some of the most abundant present in the sampling area, trophic or reproductive segregation may play a more important role in niche partitioning.

Chapter II Summary

The biodiversity of Siphonophora off south-eastern Japan was found to be exceptional, with the collection of 82 species during the MULTI-SPLASH cruise, of which 16 were first-time records from Japanese waters, and 3 were first-time records not only from Japanese waters, but from the whole Pacific Ocean, bringing the total number of siphonophore species recorded from Japanese waters to 121, or more than 63% of the world siphonophore biodiversity. The first-time record of 11 species in Sagami Bay, one of the most well studied areas of Japan, showed the biodiversity of Siphonophora in this Bay has yet to be fully assessed.

Seven siphonophore communities could be found in the sampling zone. These were characterized by the origin (tropical, temperate, sub-polar...) and depth distribution of the species that composed them. The important hydrographic dynamism of the sampling area showed a clear influence on the community structure, with the presence of lateral transport of planktonic organisms from surrounding areas, both at the surface (waters from Tokyo Bay or coastal waters of Sagami Bay being washed offshore), and at depth (presence of Oyashio-derived waters and some of their associated fauna, and of a deep Kuroshio influence). The timing, intensity and vertical delimitation of this lateral transport is highly dependent on the course of the Kuroshio Current, the main hydrographic motor in the sampling area.

Diel vertical migration (DVM) patterns influenced a subset of the seven siphonophore communities. However, these migratory patterns appeared to be a generic or family specificity, as opposed to that observed in planktonic amphipods (Schulenberger, 1979) and, when present, appeared to be performed by both the eudoxid and polygastric stages. For the families Abylidae, Diphyidae and Sphaeronectidae, within a given community, many, if not all congeneric species were found to have overlapping areas of distribution and similar mean depths. For these species, corresponding to some of the most abundant in the sampling area, niche partitioning must therefore be controlled by factors other than vertical segregation. Following the criteria influencing niche partitioning established by Shulenberger (1979: vertical range, DVM patterns, feeding periodicity, reproductive habits, diet, patchiness and co-occurrence with other species), the potential trophic pressure and feeding habits of the siphonophore community were studied. Additionally, a phylogenetic analysis of the families contributing the most to the different communities was performed, in order to assess the genetic relatedness of the species showing similar vertical distributions, since organisms more closely related genetically are thought to be physiologically more similar.

CHAPTER III

**Trophic partitioning and taxonomic
spread of the Siphonophora**

Introduction

As in the previous studies of Copepoda and Amphipoda (Kuriyama and Nishida, 2006; Mc Gowan and Walker, 1979; 1985; 1993; Shulenberger, 1979), vertical segregation was found to play an important role in the niche partitioning of closely-related species. However, in two of the families containing some of the most abundant siphonophores collected, the Abylidiae and Diphyidae, congeneric species were often found to have overlapping vertical ranges, and similar mean depths. Furthermore, Siphonophora are believed to be exclusively carnivorous, which might enhance the competition existing between species present in a given area at the same time, and limit the extent of differences in feeding habit and diet in closely-related species.

Unfortunately, because of their fragile, colonial structure, entire siphonophore colonies are rarely sampled complete, and diet studies based on the identification of stomach contents are often impossible. In order to estimate the level of trophic competition present in the studied siphonophore communities, the potential predation pressure these siphonophores exerted on the copepod population present in the sampling area was studied. Additionally, the stable isotope technique was used to determine whether the eudoxids of a species, which were found to have similar depth distributions and diel vertical migration (DVM) patterns as the polygastric stages also had the same trophic position as the polygastric stages.

Finally, the phylogenetic relationships between species of the families Abylidiae, Clausophyidae, Diphyidae and Sphaeronectidae were established, to test whether genetic distance could help explain the overlapping areas of distribution and similar DVM patters observed in many congeneric species.

I. Quantification of the potential prey field of the Siphonophora.

Introduction

In-situ observations by SCUBA divers have enabled the global feeding mechanisms of siphonophores to be described. Passive predators, the number of prey caught by a given individual is directly correlated to the number of prey encountering the tentacles of an individual, and therefore dependant on prey densities and number of tentacles, rather than on the size of the stomachs (Mackie *et al.*, 1987). Indeed, siphonophores have been known to feed on prey much larger than their stomachs, by wrapping several consecutive stomachs around a single prey item, or inserting only as much of the prey as will fit into the gastrozooid (Mackie *et al.*, 1987; Pagès and Madin, 2010). The nematocyst types and morphology of the cnidobands carrying them being relatively constant features within the 3 siphonophore sub-orders, the size of the captured prey depends primarily on the distance between tentacles, and this is known to increase along the length of the stem, as the cormidia mature, while the nature of the prey captured appears to depend on the manner in which the tentacles are deployed (Mackie *et al.*, 1987). In polygastric stages, the number of tentacles and their associated stomach increases as the colony grows, while free eudoxids, produced by the liberation of a single cormidium from the posterior end of the stem of the polygastric stage, are composed of a single tentacle and associated stomach.

Because of their fragility and their capacity for burst swimming, siphonophores are difficult to maintain in laboratory conditions. The few studies of their diets and predation methods have therefore only been performed on species found in large numbers in surface waters (Mackie *et al.*, 1987) and that can be followed and studied *in situ* by SCUBA divers. There have been no studies on species living primarily below diving depths, 98% of the water column sampled during the MULTI-SPLASH cruise. The waters of south-eastern Japan housing such a large siphonophore and prey diversity, it was therefore not possible, with the little data available on siphonophore feeding rates and predation, to make accurate assumptions of the predation pressure the siphonophores of the present data set may represent.

What is studied hereafter is the potential predation pressure of the siphonophore population, and, more accurately, the minimum predation pressure.

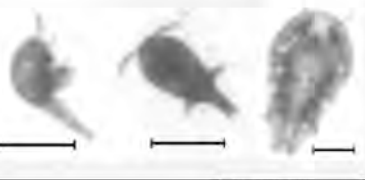
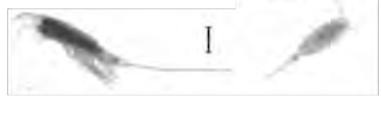
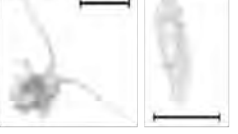
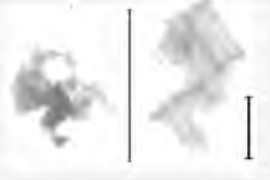
Calanoida		Copepods of the order Calanoida (except family Eucalanidae)
Eucalanidae		Copepods of the Calanoida family Eucalanidae
Poecilostomatoida		Copepods of the order Poecilostomatoida
Other Copepoda		Copepods of other orders
Other Plankton		All non-coopepod plankton
deadCope		Crustacean body parts (Copepoda, Ostracoda, Euphausia, ...)
Particles : <i>'Fiber'</i> , <i>'ParticleBig'</i> , <i>'ParticleSmall'</i>		Non-living organic and inorganic particles (different shapes)

Table 8: Categories of organisms used for the study of the potential prey field of the Siphonophora.

Material and methods

Siphonophores are believed to feed preferentially at night (Mackie *et al.*, 1987) and so the nighttime MULTI-SPLASH IONESS net tows performed at the 3 stations were analyzed (Table 1). After removal of all gelatinous plankton and after being filtered through a 5 mm mesh, the remaining sample was split using a Motoda Box Splitter, in order to obtain aliquots containing about 4000 individuals. The aliquots were scanned on a Hydroptic ZooScan v.1 using the ZooProcess 7.12 and Vuescan 8.4.57 softwares, or on a Hydroptic ZooScan v.3 using the ZooProcess 7.13 and Vuescan 9.0.51 softwares. The 24 x 15 cm 2400-dpi resolution images (14 150 x 22 640 pixels) were processed with ZooProcess and Plankton Identifier as described in Appendix 1 (p. 161). The categories “badfocus” and ”FishScales” were removed from the analyses, as the images they contained were sampling or scanning artefacts. The “multiple” group, representing about 5.2% of the total number of vignettes per net sample, was removed, as the images in that category contained multiple objects and were non-representative of any given category. The remaining categories were simplified to 7 groups (Table 8), focusing on copepods, the main prey of siphonophores. Abundance was calculated as number of individuals.m⁻³. For copepods, the automatically-measured Equivalent Spherical Diameter was transformed into prosome length using the formulae established by prior calibration analyses, with the category “Other Copepoda” following the regression proposed for combined Calanoida and Poecilostomatoida copepods (*cf.* Appendix 1). Carbon and nitrogen content were estimated for the Poecilostomatoida and all Calanoida except the Eucalanidae following the equation for ‘Total Copepoda’ proposed by Uye (1982):

$$\log_{10}(\text{biomass}(\mu\text{gC})) = 3.07 * \log_{10}(\text{PL}(\mu\text{m})) - 8.37$$

$$\log_{10}(\text{biomass}(\mu\text{gN})) = 3.12 * \log_{10}(\text{PL}(\mu\text{m})) - 9.10$$

For the Eucalanidae, dry weight (DW) was estimated from prosome length using the equation established by Hopcroft *et al.* (2002) for *Eucalanus californicus*:

$$\log_{10}(\text{DW}(\mu\text{g})) = 3.091 * \log_{10}(\text{PL}(\mu\text{m})) - 0.0026$$

Carbon and nitrogen contents were estimated to be 47% and 12% of the dry weight, respectively (Lindsay, 2003; Uye, 1982).

Siphonophore nematocyst studies were carried out by placing a small portion of stem containing nematocyst batteries of a *Clausophyes galeata* polygastric stage from Sagami Bay (MULTI-SPLASH sample) and of a *Dimophyes arctica* eudoxid stage from the Japan Sea (Shinkai 2K1288SS2j (ID#045667)) on a glass slide in a 5% formalin-5% glycerin solution, before observation.

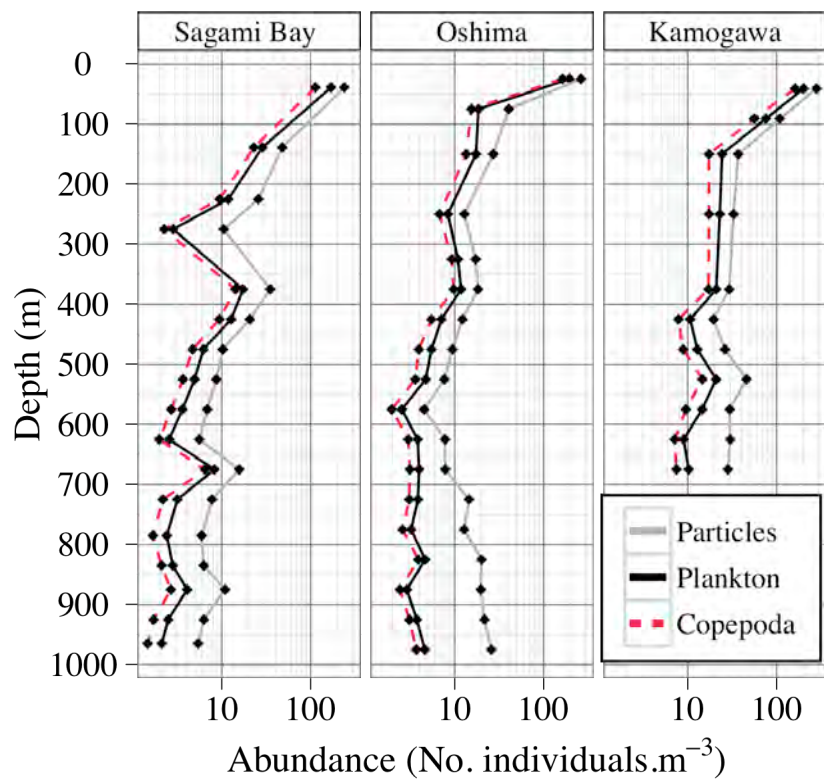


Figure 17: Total particle (grey), plankton (solid black) and copepod (dotted red) abundance (No. individuals.m⁻³) over the water column at night at the 3 stations. Marks represent the mean sampling depth of each net.

Results

1. Abundance

The results of the plankton scanning procedure showed a main peak in total abundance at the surface, with a maximum of 282.1, 351.3 and 239.1 particles.m⁻³ in the shallowest net tow at Kamogawa, Oshima, and Sagami Bay stations, respectively (Fig. 17). There was a small increase in abundance between 300 and 400 m off Oshima and in Sagami Bay, and between 550 and 600 m off Kamogawa. Off Oshima, a third increase in total particle numbers could be seen below 700 m. From the surface to 700 m, living plankton represented, on average, 56% of the total number of particles in each depth stratum, with a maximum, at the surface, of 201.6, 337.9 and 169.5 individuals.m⁻³ at Kamogawa, Oshima and Sagami Bay stations, respectively. Below 700 m, the relative percent of living planktonic organisms dropped to about 30%, with the lowest proportion, 14.7%, between 850 and 900 m at Oshima station. The increase in total particle numbers, and decrease in relative proportion of living plankton between 700 and 1000 m at Oshima could be directly linked to the rough sea conditions on the day of sampling (March 15th), as waves and strong currents increase the physical damage caused to the samples during the retrieval of the net. Indeed, the number of crustacean parts (“deadCope” group) represented around 24.6% of the total number of particles below 700 m at Oshima station, while this group represented only 7%, on average, of the total number of particles in the other net tows and stations.

The total abundance of copepods at the surface was of 165.4, 220.2 and 118.6 individuals.m⁻³ at Kamogawa, Oshima and Sagami Bay stations, respectively (Fig. 17), representing around 83% of the total plankton in abundance at Kamogawa and Oshima, and 70% in Sagami Bay. Copepods then decreased in abundance to 8.6 individuals.m⁻³ on average over the rest of the water column, but the proportion of copepods relative to the total number of planktonic organisms remained relatively high and constant, varying only between 70% (Sagami Bay, 850 to 900 m) and 91.2% (Oshima, 950 to 1000 m).

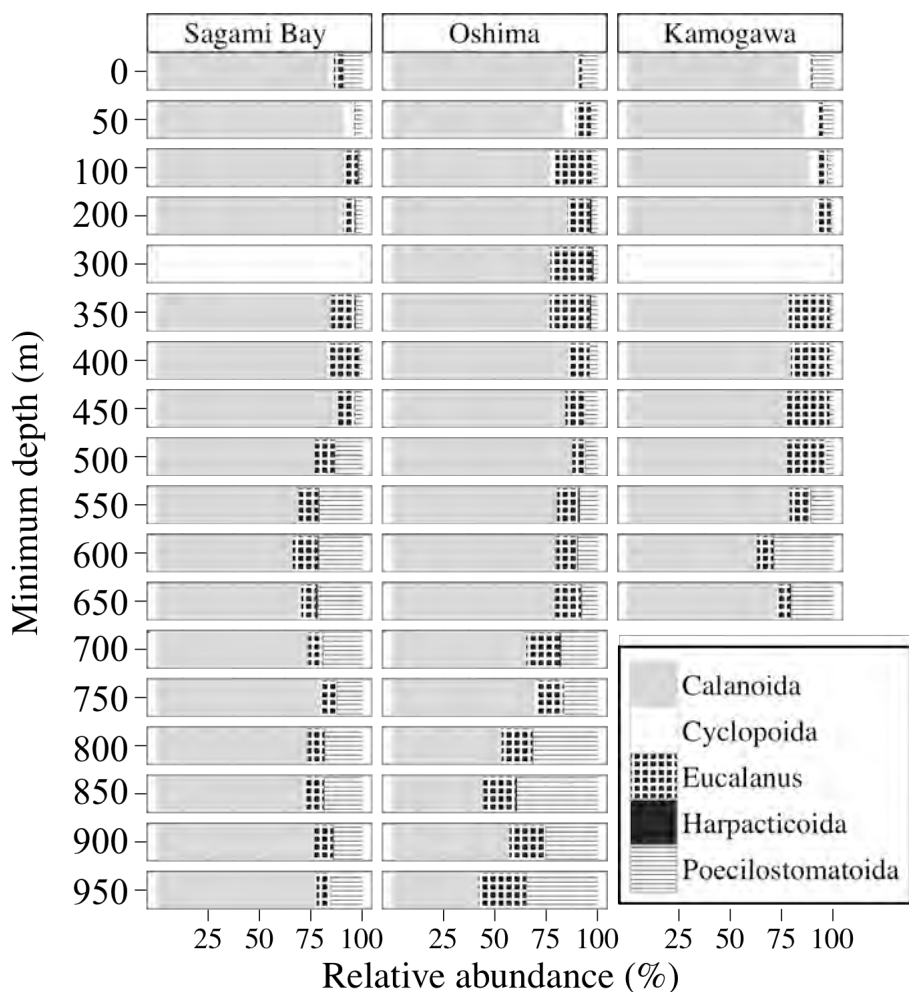


Figure 18: Relative abundance of the 5 considered copepod categories over the water column at the 3 sampling stations. White boxes = missing data.

Amongst the Copepoda, Calanoida dominated at all depths, followed by the Poecilostomatoida, which became abundant below 500 m in Sagami Bay and Kamogawa, and below 700 m off Oshima (Fig. 18). Between 50 and 450 m off Oshima, and between 200 and 550 m off Kamogawa and in Sagami Bay, the family Eucalanidae increased in relative abundance. Cyclopoida copepoda represented up to 7.6% of the total copepod abundance in the upper 200 m of the water column. Harpacticoid copepods were collected from the surface to 1000 m, but these represented 1% or less of the total copepod abundance.

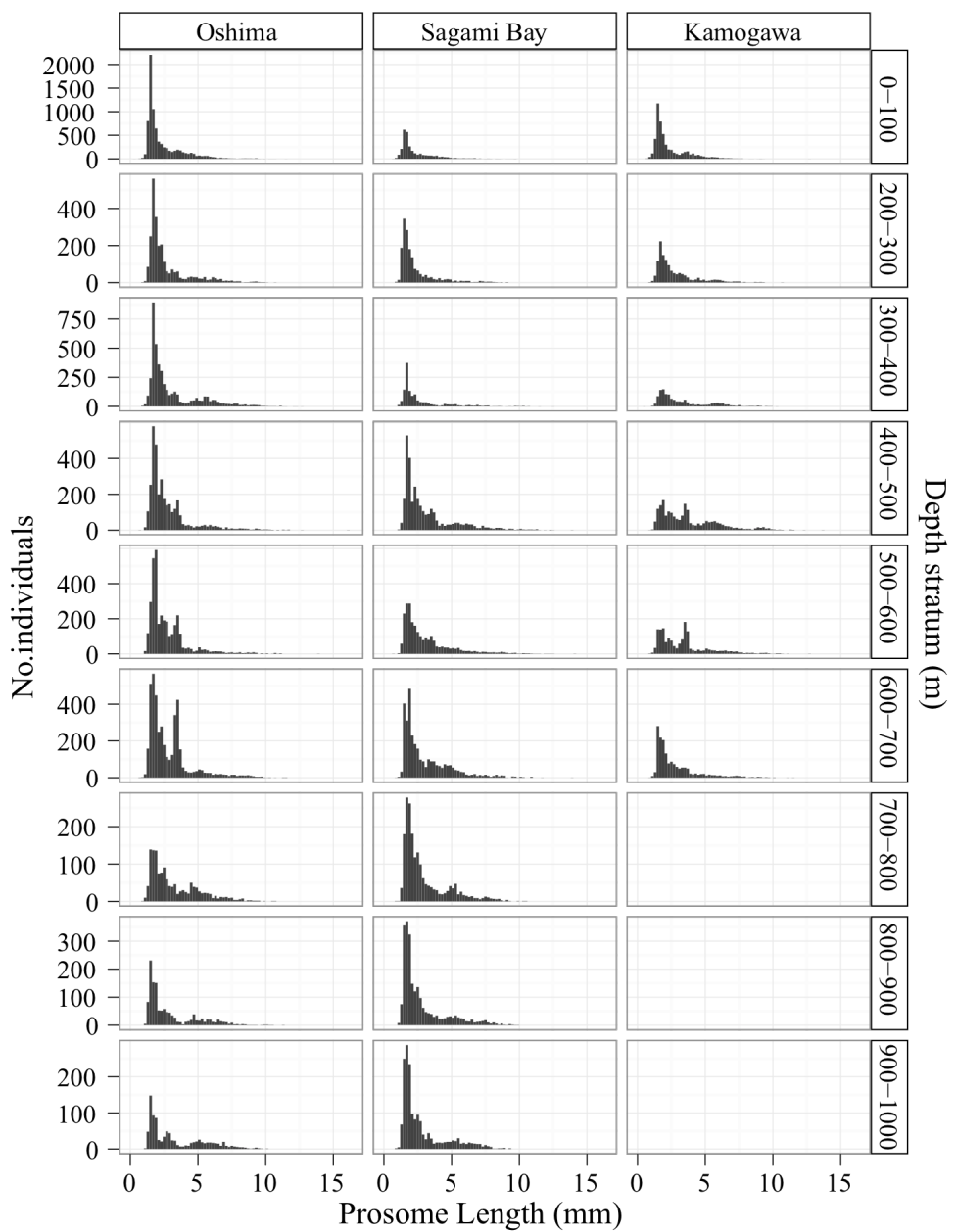


Figure 19: Copepod prosome length (mm) profiles over the water column at night at the 3 sampling stations.

2. Copepoda size spectra

Copepod prosome length (PL), estimated from the automatically measured equivalent spherical diameter (ESD), ranged between 0.75 and 16.12 mm (Fig. 19), the lower size limit being highly influenced by the mesh size of the IONESS net (330 µm). Indeed, copepods are generally of an elongate ovoid shape, and the maximum diameter of the smaller copepods was found to be about half the length of the prosome ($n=48$, PL = 1.09 – 2.07 mm, width = 0.43 – 1.07 mm), and previous studies have shown up to 50% of animals with a diameter equal to the mesh size may escape from the net and not be sampled (Skjoldal *et al.*, 2013). The principal copepod species present in the sampling area having minimum prosome lengths between 0.4 and 0.7 mm (D.J. Lindsay, personal observation; Chihara and Murano, 1997), the studied community was thought to represent a sufficiently good proportion of the copepods present in the sampling area to allow an estimation of predation pressure to be performed.

At the surface, a single, small, and very abundant class of copepods could be found, with a mean prosome length of 1.4 mm off Oshima and 1.45 mm in Sagami Bay and Kamogawa (Fig. 19). Below that, 3 distinct size classes could be observed. The smallest size class was the most abundant over the water column, but an increase in the mean size of this class compared with that observed at the surface (1.8 mm on average at 450 m) seemed to indicate a change in faunal composition. The second size peak corresponded to prosome lengths of 1.9 to 2.2 mm, and were most abundant in the 400- to 700 m depth range. Finally, the largest size class, with prosome lengths of around 2.5 mm in Sagami Bay and larger than 3 mm off Oshima and Kamogawa, primarily represented the Eucalanidae family, and, as with the medium size class, were most abundant in the 400- to 700 m-depth range.

Copepod biomass was, on average, of $26.7 \text{ } \mu\text{gC.copepod}^{-1}$ for Poecilostomatoida, $133.0 \text{ } \mu\text{gC.copepod}^{-1}$ for the Eucalanidae and $78.9 \text{ } \mu\text{gC.copepod}^{-1}$ for the other Canaloida.

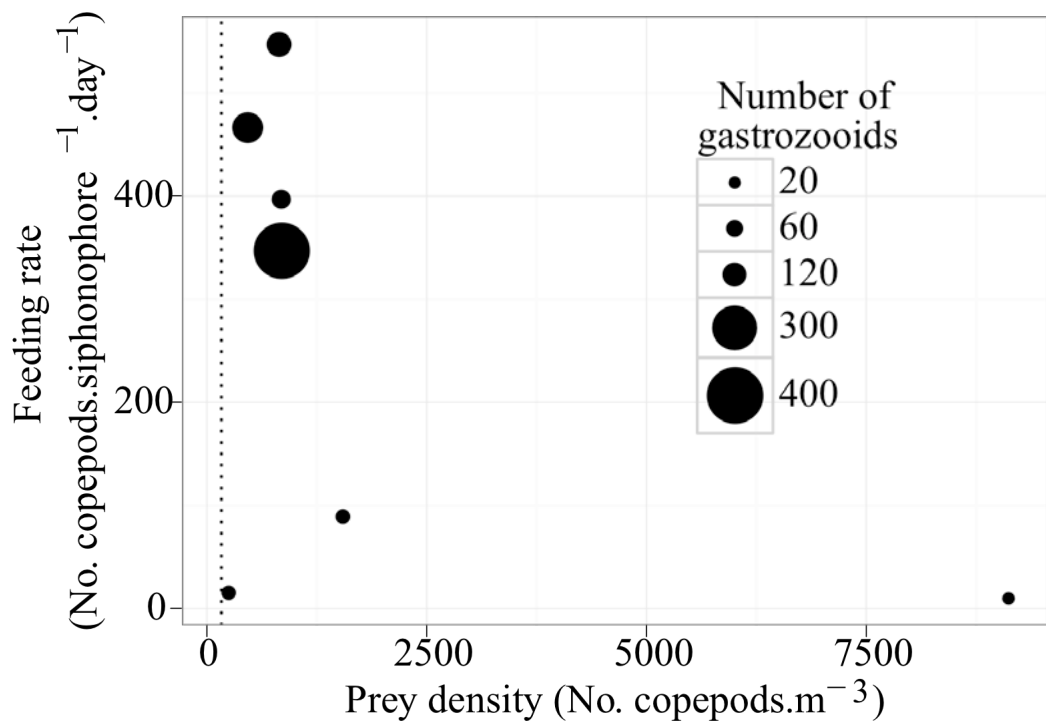


Figure 20: Calycophoran siphonophore feeding rates ($\text{No. copepods.siphonophore}^{-1}.\text{day}^{-1}$), as a function of prey density ($\text{No. copepods.m}^{-3}$) and of number of gastrozooids per siphonophore colony (after Mackie *et al.*, 1987). Vertical dotted line indicates maximum prey density observed during the MULTI-SPLASH cruise ($220.2 \text{ copepods.m}^{-3}$).

3. Predation pressure

Table 15 in the review of siphonophore biology by Mackie *et al.* (1987) showed *Muggiae atlantica* as having the lowest feeding rates of the studied species, between 5.5 and 10.5 copepods.siphonophore⁻¹.day⁻¹ despite a prey density of more than 9000 copepods.m⁻³. The other diphyid siphonophores studied showed feeding rates of between 300 and 550 copepods.siphonophore⁻¹.day⁻¹, at prey densities over an order of magnitude lower than those given for *M. atlantica*. *Sphaeronectes koellikeri* (as *S. gracilis*), the only species whose consumption rates were measured at prey densities similar to those observed in the surface waters during the MULTI-SPLASH cruise (around 250 copepods.m⁻³ for *S. koellikeri*, against a maximum abundance of 220.2 in the MULTI-SPLASH dataset), had feeding rates between 8.1 and 15.5 copepods.siphonophore⁻¹.day⁻¹ (Mackie *et al.*, 1987). No linear correlation could be found between the number of gastrozooids or prey density and feeding rates, however, pointing to a possible influence of swimming behaviour on the efficiency of predation (Fig. 20).

Despite maximum prey concentrations nearly 2 orders of magnitude smaller than the 9000 copepods.m⁻³ at which the *M. atlantica* feeding rates were measured, with the high variety of siphonophore species present in the waters of south-eastern Japan (*cf.* Chapter II), the hypothesis was formed that the feeding rates of *M. atlantica*, between 5.5 and 10.5 copepods.siphonophore⁻¹.day⁻¹, would represent a close estimate of the minimum consumption rate of the total siphonophore community in the present data set, with the possible exception of the uppermost net sampling at night at the Oshima station, as discussed below.

	Kamogawa	Oshima	Sagami bay	Carbon Biomass Intake	Nitrogen Intake
Surface	5.8 – 11.1% (165.4 copepods.m ⁻³)	23.6 – 45.1% (165.08 copepods.m ⁻³)	5.3 – 10% (118.57 copepods.m ⁻³)	245 – 468 µgC siphonophore.day ⁻¹	64.4 – 122.9 µgN siphonophore.day ⁻¹
<i>Dimophyes arctica</i> peak in abundance	11.5 – 22% (8.59 copepods.m ⁻³)	24.9 – 47.7% (9.94 copepods.m ⁻³)	13.3 – 25.5% (14.76 copepods.m ⁻³)	393.8 – 751.8 µgC siphonophore.day ⁻¹	103.4 – 197.4 µgN siphonophore.day ⁻¹

Table 9: Estimated minimum predation pressure of the siphonophore community at the surface and at the depth of maximum abundance of *Dimophyes arctica* at the 3 stations, in percentage of the copepod standing stock, with an estimation of carbon and nitrogen biomass uptake. In parenthesis, total copepod abundance for the considered depth stratum.

The predation pressure was estimated at the depth of maximum siphonophore abundance (uppermost net at all stations except at night in Sagami Bay, where it was in the 78- to 200 m stratum), and at the depth of maximum abundance of *Dimophyes arctica*: between 350 and 400 m off Oshima and Sagami Bay, and between 400 and 450 m at Kamogawa.

At the surface, total siphonophore abundance was of 1.747, 9.458 and 1.248 individuals.m⁻³ at Kamogawa, Oshima and Sagami Bay stations, respectively, with 74, 67 and 48% represented by eudoxid stages (Table 9). *Muggiae atlantica*, the species on which the consumption rates used in the present study were measured, represented 38.3, 92.5 and 35.3% of the total siphonophore abundance at Kamogawa, Oshima and Sagami Bay, respectively. The calculated prey consumption was between 5.8 and 11.1% of the total copepod abundance per day at Kamogawa, between 23.6 and 45.1% at Oshima, and between 5.3 and 10% at Sagami Bay. With a mean biomass of 44.6 µg carbon (C) and 11.7 µg nitrogen (N) per copepod at the surface, this represented an ingestion of between 245 and 468 µgC and between 64.4 and 122.9 µgN.siphonophore.day⁻¹.

At the depths of maximum abundance of *Dimophyes arctica*, total siphonophore abundance was of 0.180, 0.451 and 0.851 individuals.m⁻³ at Kamogawa, Oshima and Sagami Bay stations, respectively, with 30, 24 and 26% represented by eudoxid stages. *Dimophyes arctica* represented 63.9, 70.0 and 80.6% of the total siphonophore abundance at Kamogawa, Oshima and Sagami Bay, respectively. The calculated prey consumption was between 11.5 and 22% of the total copepod abundance per day at Kamogawa, between 24.9 and 47.7% at Oshima, and between 13.3 and 25.5% at Sagami Bay. The mean biomass per copepod was 71.6 µg carbon and 18.8 µg nitrogen at these depths, representing an ingestion of between 393.8 and 751.8 µgC and between 103.4 and 197.4 µgN.siphonophore.day⁻¹.

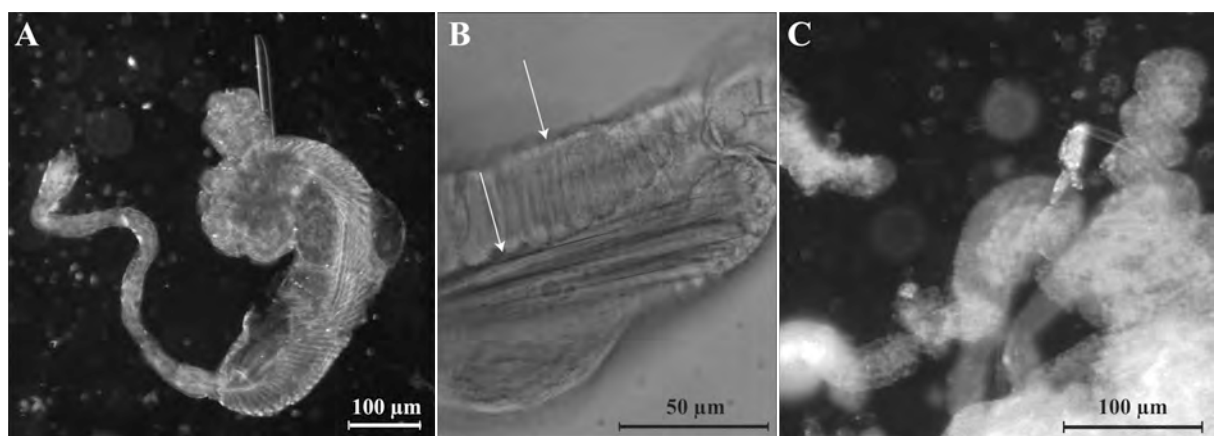


Figure 21: A: Cnidoband of *Dimophyes arctica*; B: Close-up of the same cnidoband showing the 2 types of nematocysts (arrows); C: Cnidoband of *Clausophyes galeata*.

4. Siphonophore nematocysts

To compliment the data on the nematocyst batteries of the calycophore siphonophores of the families Abyla, Sphaeronectes and the diphyid genera *Diphyes* and *Muggiaeae* (Stepanjants, 1967; Purcell, 1984), the nematocyst batteries of one species of the family Clausophyidae, *Clausophyes galeata* Lens and van Riemsdijk, 1908, and of the mesopelagic diphyid species *Dimophyes arctica* were observed. The nematocyst batteries of these two species proved to be of the same kind as those of the Abylidæ, Sphaeronectidae and previously studied Diphyidae, with a long slender cnidoband (Fig. 21). Although no discharged nematocysts could be observed, the size and shape of the capsules could be associated to long thin microbasic mastigophores and smaller, elongate holotrichous isorhizas. The terminal filament was covered in small, spherical nematocysts. In *D. arctica*, the microbasic mastigophores measured 198 µm in length, while the smaller holotrichous isorhizas measured about 30 µm in length. The *C. galeata* sample, having been collected in the IONESS plankton net, had only the most proximal part of the stem remaining, and the entire cnidoband measured 140 by 60 µm.

Discussion

The particle profiles, in March 2006, showed a strong influence of the thermocline and, to a lesser extent, of the midwater Low Salinity Water. Plankton represented between 14.7 and 74.2% and copepods between 12.8 and 62.6% of the total number of particles in each depth stratum, the lowest proportions being found below 700 m off Oshima station and between 250 and 300 m in Sagami Bay.

Contrary to what could be seen in the siphonophore populations, where the surface community at Oshima was nearly 10 times as abundant as that at the two other stations, surface particle numbers were similar at the 3 stations, varying only between 240 and 280 individuals.m⁻³, and with similar proportions of plankton and copepods. This had a direct impact on the calculated potential predation pressure exerted by siphonophores on the surface copepod community. While the siphonophore community at Sagami Bay and Kamogawa stations represented a predation pressure between 5 and 10% of the total copepod standing stock, the calculated predation found at the surface at Oshima station represented between 31.5 and 60% of the copepod standing stock. The copepods being generally large, the carbon biomass intake was well superior to the 2.9 µgC.siphonophore⁻¹.day⁻¹ estimated to be that necessary to maintain a basic metabolism (Mackie *et al.*, 1987). In the period of a spring siphonophore bloom, and considering the probably consequent temporal and spatial patchiness of both the prey and predator communities induced by the complicated hydrography of the sampled area, such predation pressure values are not excessive, and may, indeed, represent the minimum predation pressure exerted by the diverse siphonophore community at the time of sampling.

However, in the surface waters of Oshima stations, a single species, *Muggiaeatlantica*, represented 92.5% of the total siphonophore abundance. The methodological assumption that predation rates of *Muggiaeatlantica* measured at copepod concentrations of over 9000 individuals.m⁻³ would represent the minimum predation pressure of a diverse siphonophore community may not be valid for this net sample, as the feeding rate of a given species will decrease with a decrease in prey abundance. Additionally, Mackie *et al.* (1987) showed *M. atlantica* to feed preferentially on smaller copepods, which may not have been reliably sampled by the 330 µm mesh net. Furthermore, 68% of the *M. atlantica* present were eudoxid stages. Although feeding experiments have been performed exclusively on adult siphonophore polygastric stages, while all adult colonies of a given species can arguably have relatively similar sizes and therefore similar predation rates, this cannot be generalized to the

different life stages of a given species. Indeed, although the morphology of the tentacles and cnidocysts of all life stages at which they are present would appear to be similar, the polygastric stage is, as its name indicates a poly-gastric stage, a stage composed of several stomachs, each stomach having an associated tentacle. The predation pressure of the ‘uni-gastric’ stages (e.g. the eudoxid stage) may therefore be inferior to that of the polygastric stages, limited in the number of prey potentially caught by the digestion time of the single stomach.

In the midwater zone, the dominant siphonophore species was found to be *Dimophyes arctica* (*cf.* Chapter II). A study of their nematocyst batteries showed them to be of similar type and size to those of other Diphyidae or Abylidæ. Their peak in abundance, between 300 and 450 m at Oshima and Sagami Bay, and between 400 and 450 m at Kamogawa, right above the low salinity zone, corresponded to a general increase in abundance and relative abundance of the copepod family Eucalanidae (Fig. 18). These copepods are extremely large and, at these depths, had a mean prosome length of 6.5 mm, or up to 3 times the length of the swimming bells of the majority of the *D. arctica* polygastric stages at these depths (Fig. 10). Although siphonophores are capable of catching and digesting prey that is larger than their gastrozooids (Mackie *et al.*, 1987; Pagès and Madin, 2010), and although *D. arctica*, being primarily a polar species, is likely adapted to the consumption of the larger polar and subpolar copepods, it is possible the small size of the colonies may not allow them to feed on the totality of the prey field available.

In order to test for possible differences in diet between the different sized *Dimophyes arctica* polygastric stages, and between the eudoxid and polygastric stages, the study of the trophic position of these forms, using stable isotope techniques, was employed.

II. Estimation of the trophic niche of eudoxid vs. polygastric stages through stable isotopes: a case study on *Dimophyes arctica* (Chun, 1897)

Introduction

Stable isotope technique

The study of the proportions of the different stable isotopes of nitrogen (^{15}N , ^{14}N) in the different amino acids of plants and animals has proven a useful tool in modelling the trophic position and interactions within the food chain of various ecosystems (McClelland and Montoya, 2002; McClelland *et al.*, 2003; Chikaraishi *et al.*, 2007; 2008; 2009). Indeed, while primary producers biosynthesise amino acids from environmental sources of nitrogen such as dinitrogen (N_2), nitrate (NO_3^-) or ammonia (NH_4^+), secondary producers acquire nitrogen through the food they consume, primarily in the form of free amino acids and proteins. During this process of acquisition, the amino acids present in the food are metabolized following distinct pathways, specific to the amino acid and type of organism considered. Some amino acids, such as glutamic acid (Glu) or isoleucine (Ile), undergo a transamination process during their metabolism, which cleaves the carbon-nitrogen bond of the amino acid. Lighter isotopes being easier to metabolize, the remaining amino acids find themselves enriched in the heavier isotope (^{15}N). This isotopic fractionation occurring at every transfer to a higher trophic position, these amino acids are qualified as ‘trophic’ amino acids (Chikaraishi *et al.*, 2007). For other amino acids, such as phenylalanine (Phe) or methionine (Met), the metabolic pathways involved do not affect the carbon-nitrogen bond of the amino acid: there is no isotopic fractionation. For these amino acids, the proportion of light and heavy nitrogen isotopes ($\delta^{15}\text{N}$) of the consumer is the same as that of the food they consume, the same as that of the primary producers; they are therefore called ‘source’ or ‘baseline’ amino acids.

The baseline value of primary consumers, although remaining unchanged throughout the food chain, is not constant, but varies spatially and temporally, being highly influenced by both biological and environmental factors. Indeed, the specific composition of the autotrophic communities, their ability to perform different types of nitrogen fixation (e.g. the fixation of

N_2 rather than NO_3^-), and the temporal and spatial depletions and enrichments in nutrients in the environment, as observed for example in oligotrophic areas after a spring bloom, or in zones of upwelling, respectively, will all influence the isotopic ratio of the various nitrogen compounds. For example, a depletion of NO_3^- after a bloom will cause an increased intake of heavy $^{15}\text{NO}_3^-$ by some autotrophs, while others will maintain a low concentration of ^{15}N , by preferentially incorporating $^{14}\text{N}_2$, for example. The baseline isotopic enrichment value varying spatially and temporally between autotrophic communities, but remaining constant throughout the food chain, it therefore provides information on the temporal and geographic origins and possible transport of animals of higher trophic levels.

By comparing the relative isotopic enrichment of the trophic amino acids to the enrichment value of the baseline amino acids in any given organism, it is possible to accurately calculate its trophic position (Chikaraishi *et al.*, 2007; 2008; 2009). Additionally, because the results of this calculation are not altered by formalin preservation (Ogawa *et al.*, 2012), this technique could be applied to the formalin-preserved samples collected during the MULTI-SPLASH cruise. The trophic position (TP) of each sample was established as the glutamic acid versus phenylalanine ratio following Chikaraishi *et al.* (2007, 2009): $\text{TP}_{\text{Glu}/\text{Phe}} = (\delta^{15}\text{N}_{\text{Glu}} - \delta^{15}\text{N}_{\text{Phe}} - \beta_{\text{Glu}/\text{Phe}}) / (\Delta_{\text{Glu}} - \Delta_{\text{Phe}}) + 1$, where $\beta_{\text{Glu}/\text{Phe}}$ represents the difference in isotopic composition of the two amino acids in the primary producers, and Δ_{Glu} and Δ_{Phe} represent the specific enrichment factor of each amino acid with each trophic level. The application of this technique to a wide spectrum of terrestrial and marine organisms has shown an increase of 0.4‰ for Δ_{Phe} , and an increase in 8‰ for Δ_{Glu} (Chikaraishi *et al.*, 2007; 2009), thereby giving a $\Delta_{\text{Glu}} - \Delta_{\text{Phe}}$ ratio of 7.6. Phytoautotrophs were found to have a relatively stable value of $\beta_{\text{Glu}/\text{Phe}}$: 3.4. The calculation of trophic position using Glutamic Acid and Phenylalanine thereby follows the formula: $\text{TP}_{\text{Glu}/\text{Phe}} = (\delta^{15}\text{N}_{\text{Glu}} - \delta^{15}\text{N}_{\text{Phe}} - 3.4) / 7.6 + 1$.

This calculation, however, relies on the hypothesis that, in heterotrophic organisms, the metabolic pathways of the trophic amino acids induce isotopic fractionation, and that those of the baseline amino acids cause only a very small amount of isotopic enrichment, leading to a constant $\Delta_{\text{Glu}} - \Delta_{\text{Phe}}$ value of 7.6. This has yet to be tested for any gelatinous plankters, however, as such studies necessitate long-term, controlled cultures of these organisms, and the metabolic pathways of primitive diploblastic animals such as the Cnidaria may differ considerably from those found in higher organisms. It was not possible, therefore, to calculate the exact trophic position of the studied animals. However, the aim of the study was the comparison of the trophic position of the different life stages and size classes of *Dimophyes arctica*, and the $\Delta_{\text{Glu}} - \Delta_{\text{Phe}}$ ratio of isotopic enrichment being a specific characteristic, relative, rather than absolute trophic positions were considered: we calculated

the trophic position of the different groups of polygastric stages relative to the trophic position of the eudoxid stages (called ‘x’).

Origin of *Dimophyes arctica*

Dimophyes arctica was the dominant species in the mesopelagic zone at all stations, both in terms of abundance and in terms of distributional extent, having been collected in all nets sampled between 78 and 1000 m. As described in Chapter II, this species is primarily polar, being most abundant near the surface and in the upper mesopelagic zone in the Arctic and Antarctic (Table 6). Following the transport of polar waters into more temperate oceanic basins, it often finds itself subducted into the deeper mesopelagic zone with the polar waters. In the Southern Ocean, *D. arctica* was found to belong to a siphonophore community abundant in the upper mesopelagic zone near the Antarctic continent, sinking into the lower mesopelagic zone as the Antarctic waters get subducted under the warmer, less saline subantarctic waters (Grossmann, 2010). In the MULTI-SPLASH study, the majority of the occurrences of this species corresponded to the depths of the Low Salinity Water, a water mass formed of a mixture of subducted surface sub-polar waters, primarily of Oyashio origin (Senju *et al.*, 1998; Yang *et al.*, 1993a; 1993b). The study of the potential prey field occurring with this species (Chapter III.1) showed a marked increase of subarctic copepods of the family Eucalanidae concurrent with the increase in *Dimophyes arctica*.

In the subarctic copepod *Neocalanus cristatus*, large numbers of copepodite V stages, originating from the surface subarctic Pacific, get entrained into Sagami Bay by the Oyashio Intermediate Water, at depths of 500 to 600 m. This environment being unsuitable for their development, they then die and sink to the deeper layers of the Bay (Oh *et al.*, 1991). Small numbers of adult *N. cristatus* were also recorded from the Bay, and Oh *et al.* (1991) proposed a deeper pathway of *N. cristatus* into the Bay, around 1000 m, where the environmental and biological parameters would be suitable enough for a small population of adults to survive.

In the case of the present study, the 330 µm IONESS net used for the present sampling was not adapted for the collection of juvenile siphonophore stages. However, of the 82 species identified from the present data set, *D. arctica* was one of the few for which the polygastric stages were of 2 distinct size classes. Large, “adult” polygastric stages, of a size similar to those recorded in the upper-mesopelagic layers in the Canadian Pacific (Mapstone, 2009) or in eastern Antarctica (personal observation), were very rare, and found only between

500 and 750 m (Fig. 10). Extremely small, “young” polygastric stages dominated the water column between 100 and 750 m. It would appear probable these polygastric stages were still too young to have produced a posterior nectophore (*cf.* Chapter II). The presence of a great number of “young” polygastric stages over the whole mesopelagic layer, and of a few isolated “adult” polygastric stages in the deeper depth strata appeared to follow a pattern similar to that observed in *Neocalanus cristatus* (Oh *et al.*, 1991).

It was hoped the study of the baseline isotopic fractionation of the different size classes of *Dimophyes arctica* could help resolve the origin of these different populations.

Trophic position of eudoxid stages

As presented in Chapter III.1, the knowledge of predation and metabolism in siphonophores is extremely limited, both in terms of numbers of species and of developmental stages studied. Indeed, while the production of free eudoxids by polygastric stages is included in the metabolic balance of the polygastric stages (Mackie *et al.*, 1987), the consumption and/or predation of the eudoxid stages once released are often considered negligible (Mackie *et al.*, 1987; Purcell, 1982). However, if the predation of a single eudoxid stage, with its single tentacle, would, indeed, be negligible compared to that of a single polygastric stage with its tens to hundreds of tentacles, the large numbers of eudoxid stages encountered in some depth strata of the present study – up to 83% of all siphonophores, between 600 and 650 m during the day at Oshima station – would have a non-negligible predation pressure at the scale of the siphonophore population. Possessing the same kind and size of nematocysts as the polygastric stages, the eudoxid stages would most likely be capable of feeding on similar prey as the polygastric stages, and it is believed they would have similar digestion rates (J.E. Purcell, personal communication). However, siphonophore predation depends primarily on the type of deployment and spacing of the tentacles (Mackie *et al.*, 1987), and it is possible eudoxid stages may not be capable of catching the same types of prey as the polygastric stages.

The trophic position of the polygastric stages of *Dimophyes arctica*, relative to that of the eudoxid stages, were estimated using the stable isotope method, in order to evaluate a potential prey difference between these two developmental stages.

Material and methods

Dimophyes arctica anterior nectophores and bracts were sorted out of the formalin-preserved IONESS net samples under a dissecting microscope in order to confirm they contained no contaminating particles, and measured. Because the small size of this species prevented the measurement of single-individual isotopic values, each sample contained multiple animals. Although the focus was placed on the Sagami Bay station, following the results in Chapters I and II showing a minimum influence of time of day and sampling station, compared to sampling depth, on the composition of the siphonophore communities, animals collected off Oshima and Kamogawa were also included when the number of animals from Sagami Bay was insufficient. Five samples were prepared: ‘medium’ (> 3 mm but < 5 mm) and ‘small’ (< 2 mm) anterior nectophores collected between 100 and 300 m, ‘big’ (> 5 mm) and ‘small’ (< 2mm) anterior nectophores collected between 400 and 650 m; and eudoxid bracts collected between 400 and 650 m. The samples contained between 7 and 54 individuals (Table 10). Because of the number of individuals needed for each sample, it was not possible to prepare replicate samples. The amino acids were extracted and prepared following the protocol established by Chikaraishi *et al.* (2009). The nitrogen isotopic composition of the amino acids was determined through coupled gas chromatography (GC) / isotope-ratio mass spectrometry (IRMS) analysis using an Argilent 6890N GC with an Argilent HP Ultra-2 column (50 m x 0.32 mm i.d., 0.52 µm filter thickness) column, and a Delta plus XP IRMS. The isotopic enrichment of Glutamic acid versus Phenylalanine in the samples was estimated using the formula established in Chikarashishi *et al.* (2007, 2009) for the study of trophic position (TP): $TP_{Glu/Phe} = (\delta^{15}\text{N}_{\text{Glu}} - \delta^{15}\text{N}_{\text{Phe}} - 3.4) / 7.6 + 1$. As explained above (p. 104), the methodology employed by Chikaraishi *et al.* (2007; 2009) has not been ground-truthed for gelatinous plankton. The “trophic position” values obtained therefore may, or may not correspond to the real trophic position of the studied *D. arctica*, and therefore cannot be directly compared to the trophic position of other organisms obtained by this method. In order not to publish misleading trophic position values, the result obtained for *D. arctica* eudoxid stages was called x, and the results of the different polygastric stage categories established relative to x. Analytical error was estimated to be $\pm 0.5\text{\textperthousand}$ for both $\delta^{15}\text{N}$ and relative trophic position (Chikaraishi *et al.*, 2007; 2009).

Sample	Size range (mm)	Location	n	Depth range (m)	Phe	TP
Polygastric stage	1.5 - 2.5	Sagami Bay	45	200 - 300	1.3	x + 0.13
Polygastric stage	2.8 - 4.5	Sagami Bay	2	200 - 250	1.8	x - 0.09
		Oshima	2	100 - 300		
		Kamogawa	3	200 - 300		
Polygastric stage	0.8 - 2.0	Sagami Bay	34	500 - 650	1.3	x - 1.2
		Oshima	20	500 - 500		
Polygastric stage	5.6 - 11	Sagami Bay	6	500 - 650	2.6	x - 0.61
		Oshima	1	400 - 450		
Eudoxid	3.2 - 4.5	Oshima	29	400 - 550	1.3	x

Table 10: Characteristics of the 5 *Dimophyes arctica* (Chun, 1897) samples, their nitrogen isotopic ratio of phenylalanine (Phe), and relative trophic position (TP) of the polygastric stages to that of the eudoxid stages (x); n: number of animals per sample.

Results

The $\delta^{15}\text{N}$ values of the baseline amino acid phenylalanine (Phe) for each sample are shown in Table 10. The eudoxids and small *Dimophyes arctica* polygastric stages had an isotopic baseline ($\delta^{15}\text{N}$ Phe) of 1.3, while the medium-sized and large polygastric stages had values of 1.8 and 2.6, respectively.

The polygastric stages in the upper-mesopelagic zone had a trophic position similar to that of the eudoxids, followed by the large mesopelagic polygastric stages, 0.61 units lower than the eudoxids. The small, mesopelagic polygastric stages were 1.2 units lower than the eudoxid stages.

Discussion

1. Origin of *Dimophyes arctica*

The eudoxids and small *Dimophyes arctica* polygastric stages had a baseline $\delta^{15}\text{N}$ value of 1.3, despite having been sampled in Sagami Bay (upper-mesopelagic polygastric stages), at the Oshima station (eudoxids), or as a mixture of individuals from both stations. It was therefore hypothesized a $\delta^{15}\text{N}$ value of 1.3 represented the current isotopic ratio present in both Sagami Bay and off Oshima island during the sampling period in March 2006, and that this baseline was relatively stable, the eudoxids and small polygastric stages having the same value.

The large, mesopelagic polygastric stages had a $\delta^{15}\text{N}$ baseline value of 2.6, and the medium-sized upper-mesopelagic ones a value of 1.8. Two hypotheses were established to explain these results. The first was that the large polygastric stages, much older than the small ones, were born in Sagami Bay at a time when the isotopic ratio was much higher, possibly at the end of summer, and their tissue turnover rates have since been extremely slow. Siphonophore nectophores are made up of a gelatinous layer, the mesogloea, primarily composed of collagen and elastin (Mackie, 1965), and of a muscular nectosac. While in some siphonophores, such as the *Hippopodius hippocampus* studied by Mackie (1965), the mesogloea makes up an important proportion of the nectophores, *Dimophyes arctica* nectophores are relatively fragile, without marked ridges, and the muscular nectosac could represent a large

part of the biomass. Therefore, although the turnover rates of collagen are amongst the slowest so far observed, on the order of 6 months to several years half-life (bone collagen $\delta^{13}\text{C}$: Hobson, 1999; MacAvoy *et al.*, 2006; Szpak *et al.*, 2010), turnover rates of muscle usually ranged around 20 days half-life in small vertebrates (MacAvoy *et al.*, 2006), both for carbon and nitrogen. Diapause states having never been recorded in siphonophores, it therefore seems unlikely the large polygastric stages would exhibit, in March, an isotopic signature acquired at the end of summer.

A second hypothesis for the higher proportion of heavy ^{15}N in the large polygastric stages was the different geographic origin of these specimens. Indeed, the waters found between 300 and 600 m were influenced by the Low Salinity Water (LSW), and, the hydrographic characteristics differing from those normally associated with Oyashio Intermediate Water, it was concluded this water mass represented a mixture of waters, some of which were most likely of Oyashio origin, some possibly of Kuroshio origin (*cf.* Chapters I and II). Should the isotopic baseline present in some of the water masses making up the LSW be of 2.6 or higher, the large, mesopelagic polygastric stages would have a similar baseline as the waters they originated from: 2.6. This hypothesis is further strengthened because it also explains the isotopic baseline value found in the medium, upper-mesopelagic polygastric stages. Indeed, measuring between 2.8 and 4.5 mm in length, they were much larger than the “small” polygastric stages, but smaller than the mesopelagic “large” polygastric stages (> 5 mm). Had they arrived into the sampling area at approximately the same time, and from the same place as the large mesopelagic polygastric stages, somatic growth, as well as maintenance metabolism would affect their baseline isotopic signature.

The 1.8 isotopic baseline found in the medium-sized upper-mesopelagic polygastric stages was not significantly different from the 1.3 baseline of the sampling area (analytical error $\pm 0.5\%$), but may represent a mid-point value between the 2.6 value they had in their water mass of origin and the 1.3 baseline found in the sampling area at the time of sampling.

The baseline of a given area depends on many factors, such as the amount of atmospheric nitrogen fixation, and on the limitation in labile nitrogen brought on by intensive spring blooms, for example. Additionally, the baseline value of 1.3 in the sampling area may also reflect a terrestrial influence: anthropogenic nitrogen in the form of fertilizers or industrial wastes often has characteristically low proportions of the heavier ^{15}N isotope (Holtgrieve *et al.*, 2011). The exact geographic origin of the large polygastric stages therefore could not be determined through the present isotopic analyses, though it was possible to infer that they originated outside the present study area.

2. Trophic position

Free eudoxid stages are released from the posterior extremity of the polygastric stage's siphosome. They therefore have the same nematocyst shape and spacing, and the same tentacle length as the oldest, most posterior cormidia of the polygastric stage. The only difference between the two life stages in terms of predation pressure is therefore the number of tentacles, single in the eudoxid stage, and up to several hundreds in large polygastric stages, and, therefore, the fishing posture of the colony.

The study of the trophic position of two sizes of polygastric stages and of the one size of eudoxid stage showed little influence of life stage or colony size on the measured trophic position. Indeed, both the small and medium-sized upper-mesopelagic polygastric stages had similar trophic positions as that of the mesopelagic eudoxids. It would therefore appear that although the different morphology of the two life stages undoubtedly influences the number of prey items consumed, the presence of a single tentacle in the eudoxid stage did not appear to affect the type of prey consumed. The large mesopelagic polygastric stages had a slightly lower trophic position than the eudoxids, which might be linked to their transport from more northern surface waters (*cf.* Chapter II). Indeed, polar and sub-polar trophic chains being usually shorter than temperate and tropical ones (Ainley and DeMaster, 1990) it is possible the calculated trophic position of a *D. arctica* individual in a polar habitat would be lower than that of one living in Sagami Bay, due to the small number of steps connecting the primary producers to the top predators.

The different trophic position of the small, mesopelagic, polygastric stages may be related to the type of prey present at these depths. Indeed, the study of the potential prey field showed an increase in abundance of the medium and large copepod size classes at these depths (Fig. 19), primarily due to the presence of large *Eucalanus* and *Metridia* copepods. These copepods being perhaps too large to be easily caught and immobilized by the small polygastric stages, these may have preyed preferentially on smaller copepod groups such as the poecilostomatoid *Oncaeidae*, which feeds primarily on marine snow and other non-mobile prey items (Turner, 1984), and might have a lower trophic position than the more omnivorous and carnivorous calanoid copepods representing the majority of the copepods in the upper-mesopelagic zone. The small *D. arctica* polygastric stages might also feed on ostracods, rather than copepods, many of which are grazers or detritivores.

III. Genetic divergence

Introduction

The phylogeny of siphonophores has long been of interest to taxonomists because of the complex colonial structure of these animals. The first study of siphonophore phylogeny based on DNA sequencing, performed on the mitochondrial 16S and nuclear 18S genes by Dunn *et al.* (2005), showed the three siphonophore sub-orders Cystonectae, Physonectae and Calycophorae to be genetically distinct groups, with the Cystonectae the most primitive and the Calycophorae the most advanced. Additionally, the Calycophorae were split into two sub-groups: the Prayomorphs, containing the families Prayidae and Hippopodiidae, and the Diphyomorphs, containing the other families. However, the Diphyomorph group was represented by only 10 species, of which five were of the family Diphyidae. In the MULTI-SPLASH data set, the family Diphyidae was by far the most species-rich, with 37 species collected, and many congeneric species within the Diphyidae were shown to have overlapping vertical areas of distribution (*cf.* Chapter II). Additionally, these species all have similar nematocysts and cnidoband structures, and, in the genus *Lensia* for example, many congeneric species found in the same depth stratum had similar colony sizes and might not, as with the very small *Dimophyes arctica* colonies, show clear trophic dissimilarities.

Genetic distance can be used as a proxy for likenesses in physiological and/or life history traits, etc, which would allow niche partitioning in an axis separate to that of the environmental and/or trophic ones.

In order to study the genetic relationships existing between the different diphyid species collected off south-eastern Japan, a more extensive sequence database was established, using the mitochondrial 16S gene, with a focus on the calycophoran siphonophore family Diphyidae.

Species	Sampling depth (m)	Date	Latitude	Longitude	Sampling location	Genbank or ID number
<i>Abyla haekeli</i>	0-1076	8-Jun-2012	27°50.05'N	127°00'E	Izena Hole (Japan)	450106
<i>Abyla haekeli</i>	0-716	8-Jun-2012	27°50.05'N	127°00'E	Izena Hole (Japan)	450133
<i>Abylopsis eschscholtzi</i>	0-679	18-Nov-2011	31°52.3'N	139°59.4'E	Myojin-sho (Japan)	121552
<i>Bassia bassensis</i>	0-400	18-Nov-2011	31°N	132°E	off Kagoshima (Japan)	121430
<i>Bassia bassensis</i>	0-100	18-Nov-2011	31°52.3'N	139°59.4'E	Myojin-sho (Japan)	121512
<i>Ceratocymba leuckartii</i>	0-1076	8-Jun-2012	27°50.05'N	127°00'E	Izena Hole (Japan)	450119
<i>Ceratocymba leuckartii</i>	0-946	7-Jun-2012	27°47.73'N	126°54.11'E	Izena Hole (Japan)	450152
<i>Chelophyes appendiculata</i>	100-200	13-Apr-2006	33°31.5'N	69°57.7'W	north-western Atlantic	DLSI225
<i>Chelophyes appendiculata</i>	0-250	23-Jun-2012	40°58.16'N	02°03.71'E	Mediterranean Sea	Med5
<i>Chelophyes contorta</i>	0-100	18-Nov-2011	31°52.3'N	139°59.4'E	Myojin-sho (Japan)	121513
<i>Chelophyes contorta</i>	0-100	18-Nov-2011	31°52.3'N	139°59.4'E	Myojin-sho (Japan)	121514
<i>Chelophyes contorta</i>	0	16-Oct-2007	37°29.6'N	149°44.5'E	Japan Trench	074828
<i>Chuniphyes moserae</i>	200-500	29-Jan-2008	62°0.63'S	140°0.97'E	eastern Antarctica	DLSI177
<i>Chuniphyes moserae</i>	200-500	29-Jan-2008	62°0.63'S	140°0.97'E	eastern Antarctica	DLSI182
<i>Chuniphyes moserae</i>	700-750	27-Mar-2006	34°42'N	139°50'E	off Oshima (Japan)	DLSI295
<i>Chuniphyes multidentata</i>	400-450	24-Mar-2006	35°0.50'N	139°20'E	Sagami Bay (Japan)	140905b
<i>Chuniphyes multidentata</i>	500-550	23-Mar-2006	35°0.50'N	139°20'E	Sagami Bay (Japan)	DLSI296
<i>Chuniphyes multidentata</i>	600	22-Apr-2009	35°0.50'N	139°20'E	Sagami Bay (Japan)	DLSI336
<i>Chuniphyes multidentata</i>	800	22-Apr-2009	35°0.50'N	139°20'E	Sagami Bay (Japan)	DLSI355
<i>Chuniphyes multidentata</i>	800	22-Apr-2009	35°0.50'N	139°20'E	Sagami Bay (Japan)	DLSI356
<i>Chuniphyes sp.</i>	500-550	24-Mar-2006	35°0.50'N	139°20'E	Sagami Bay (Japan)	141025
<i>Diphyes bojani</i>	0-100	18-Nov-2011	31°N	132°E	off Kagoshima (Japan)	121433
<i>Diphyes bojani</i>	0-400	18-Nov-2011	31°52.3'N	139°59.4'E	Myojin-sho (Japan)	121538
<i>Diphyes bojani</i>	0-70	14-Sep-2011	24°13.9'N	123°47'E	east of Taiwan	121585
<i>Diphyes chamissonis</i>	0-5	10-Oct-2011	4°2.76'N	100°37.28'E	Malaysia	121424
<i>Diphyes chamissonis</i>	0-100	18-Nov-2011	31°N	132°E	off Kagoshima (Japan)	121437
<i>Diphyes dispar</i>	0-1075	25-Apr-2012	34°59.15'N	139°21.05'E	Sagami Bay (Japan)	450065
<i>Eudoxoides mitra</i>	250-495	18-Nov-2011	31°52.3'N	139°59.4'E	Myojin-sho (Japan)	121470
<i>Eudoxoides mitra</i>	0-100	18-Nov-2011	31°52.3'N	139°59.4'E	Myojin-sho (Japan)	121562
<i>Eudoxoides mitra</i>	0-946	7-Jun-2012	27°47.73'N	126°54.11'E	Izena Hole (Japan)	450139
<i>Eudoxoides mitra</i>	0-946	7-Jun-2012	27°47.73'N	126°54.11'E	Izena Hole (Japan)	450140
<i>Eudoxoides spiralis</i>	0-400	18-Nov-2011	31°52.3'N	139°59.4'E	Myojin-sho (Japan)	121546
<i>Eudoxoides spiralis</i>	0-359	25-Apr-2012	35°0.50'N	139°20'E	Sagami Bay (Japan)	450074
<i>Heteropyramis crystallina</i>	0-1076	8-Jun-2012	27°50.05'N	127°00'E	Izena Hole (Japan)	450109
<i>Heteropyramis crystallina</i>	0-1076	8-Jun-2012	27°50.05'N	127°00'E	Izena Hole (Japan)	450126
<i>Heteropyramis crystallina</i>	0-1000	12-Feb-2008	65°41.02'S	143°18.80'E	eastern Antarctica	DLSI097
<i>Heteropyramis crystallina</i>	500-1000	12-Feb-2008	65°30.64'S	143°1.17'E	eastern Antarctica	DLSI147
<i>Heteropyramis crystallina</i>	1000-2000	12-Feb-2008	65°30.64'S	143°1.17'E	eastern Antarctica	DLSI157
<i>Heteropyramis crystallina</i>	200-500	29-Jan-2008	62°0.63'S	140°0.97'E	eastern Antarctica	DLSI176
<i>Heteropyramis crystallina</i>	500-550	24-Mar-2006	34°42'N	139°50'E	off Oshima (Japan)	DLSI293
<i>Kephyses ovata</i>	200-300	19-Mar-2006	35°0.50'N	139°20'E	Sagami Bay (Japan)	151125
<i>Kephyses ovata</i>	450-500	24-Mar-2006	34°42'N	139°50'E	off Oshima (Japan)	151129
<i>Kephyses ovata</i>	0-985	9-Mar-2011	35°0.50'N	139°20'E	Sagami Bay (Japan)	151432
<i>Kephyses ovata</i>	0-985	27-Jun-2010	35°0.50'N	139°20'E	Sagami Bay (Japan)	151522
<i>Kephyses ovata</i>	0-1075	24-Apr-2012	34°59.18'N	139°20.06'E	Sagami Bay (Japan)	450003
<i>Kephyses ovata</i>	400-600	22-Apr-2007	35°0.50'N	139°20'E	Sagami Bay (Japan)	221747
<i>Lensia achilles</i>	750-800	25-Mar-2006	34°59.43'N	140°15.54'E	off Kamogawa (Japan)	161545
<i>Lensia achilles</i>	750-800	19-Mar-2006	35°0.25'N	139°20'E	Sagami Bay (Japan)	KC782553
<i>Lensia achilles</i>	400-600	23-Apr-2009	35°0.25'N	139°20'E	Sagami Bay (Japan)	KC782554
<i>Lensia achilles</i>	1000-2000	11-Jan-2008	65°30.06'S	143°0.05'E	eastern Antarctica	KC782555
<i>Lensia achilles</i>	1000-2000	31-Jan-2008	64°0.62'S	140°0.76'E	eastern Antarctica	KC782556
<i>Lensia achilles</i>	1000-2000	11-Jan-2008	65°30.06'S	143°0.05'E	eastern Antarctica	KC782557
<i>Lensia campanella</i>	0-400	18-Nov-2011	31°N	132°E	off Kagoshima (Japan)	KC782540
<i>Lensia campanella</i>	0-400	18-Nov-2011	31°N	132°E	off Kagoshima (Japan)	KC782541
<i>Lensia conoidea</i>	0-2000	8-Mar-2012	35°0.50'N	139°20'E	Sagami Bay (Japan)	141018
<i>Lensia conoidea</i>	0-500	24-Mar-2009	35°0.50'N	139°20'E	Sagami Bay (Japan)	151516
<i>Lensia conoidea</i>	0-1075	24-Apr-2012	34°59.18'N	139°20.06'E	Sagami Bay (Japan)	450041
<i>Lensia conoidea</i>	0-359	16-May-2012	37°0'N	141°30'E	eastern Japan	450105
<i>Lensia conoidea</i>	400-550	23-Jun-2012	40°58.16'N	02°03.71'E	Mediterranean Sea	Med7

Table 11: Characteristics of the samples sequenced for the present work.

Species	Sampling depth (m)	Date	Latitude	Longitude	Sampling location	Genbank or ID number
<i>Lensia cordata</i>	550-600	23-Mar-2006	35°0.50'N	139°20'E	Sagami Bay	131705
<i>Lensia cordata</i>	600-650	24-Mar-2006	34°42'N	139°50'E	off Oshima (Japan)	141250
<i>Lensia cossack</i>	0-1076	8-Jun-2012	27°50.05'N	127°00'E	Izena Hole (Japan)	KC782543
<i>Lensia cossack</i>	0-946	7-Jun-2012	27°47.73'N	126°54.11'E	Izena Hole (Japan)	KC782544
<i>Lensia cossack</i>	0-946	7-Jun-2012	27°47.73'N	126°54.11'E	Izena Hole (Japan)	KC782545
<i>Lensia cossack</i>	0-946	7-Jun-2012	27°47.73'N	126°54.11'E	Izena Hole (Japan)	KC782546
<i>Lensia cossack*</i>	0-400	18-Nov-2011	31°N	132°E	off Kagoshima (Japan)	KC782542
<i>Lensia cossack*</i>	0-1076	8-Jun-2012	27°50.05'N	127°00'E	Izena Hole (Japan)	KC782547
<i>Lensia cossack*</i>	0-400	15-May-2012	36°40'N	141°50'E	off Fukushima (Japan)	KC782548
<i>Lensia cossack*</i>	0-400	14-May-2012	37°30'N	142°00'E	off Fukushima (Japan)	KC782549
<i>Lensia exeter</i>	767-1100	24 Oct. 2010	27°47.73'N	126°54.11'E	Izena Hole (Japan)	KC782550
<i>Lensia havock</i>	200-500	29-Jan-2008	62°0.45'S	139°58.80'E	eastern Antarctica	KC782532
<i>Lensia havock</i>	500-1000	12-Feb-2008	65°30.64'S	143°1.17'E	eastern Antarctica	KC782533
<i>Lensia havock</i>	600-650	24-Mar-2006	34°59.43'N	140°15.54'E	off Kamogawa (Japan)	KC782534
<i>Lensia havock</i>	700-900	24-Apr-2009	35°0.25'N	139°20'E	Sagami Bay (Japan)	KC782535
<i>Lensia havock</i>	300-600	24-Apr-2009	35°0.25'N	139°20'E	Sagami Bay (Japan)	KC782536
<i>Lensia havock</i>	0-1439	24-Apr-2012	34°59.15'N	139°21.05'E	Sagami Bay (Japan)	450007
<i>Lensia hostile</i>	200-300	19-Mar-2006	35°0.25'N	139°20'E	Sagami Bay (Japan)	KC782551
<i>Lensia hostile</i>	800-850	27-Mar-2006	34°42'N	139°50'E	off Oshima (Japan)	KC782552
<i>Lensia hotspur</i>	0-400	5-Mar-2012	35°0.50'N	139°20'E	Sagami Bay (Japan)	141001
<i>Lensia leloupi</i>	0-2000	5-Mar-2012	35°0.50'N	139°20'E	Sagami Bay (Japan)	141019
<i>Lensia leloupi</i>	0-2000	5-Mar-2012	35°0.50'N	139°20'E	Sagami Bay (Japan)	141020
<i>Lensia leloupi</i>	0-2000	5-Mar-2012	35°0.50'N	139°20'E	Sagami Bay (Japan)	141021
<i>Lensia leloupi</i>	0-1439	25-Apr-2012	34°59.15'N	139°21.05'E	Sagami Bay (Japan)	450011
<i>Lensia leloupi</i>	0-1439	25-Apr-2012	34°59.15'N	139°21.05'E	Sagami Bay (Japan)	450013
<i>Lensia leloupi</i>	0-1357	24-Apr-2012	34°59.18'N	139°20.06'E	Sagami Bay (Japan)	450045
<i>Lensia leloupi</i>	0-400	16-May-2012	36°28'N	141°43'E	eastern Japan	450129
<i>Lensia leloupi</i>	n/a	22-Apr-2009	35°0.50'N	139°20'E	Sagami Bay (Japan)	DLSI344
<i>Lensia multicristata</i>	0-200	27-Jan-2008	53°8.19'S	130°8.19'E	eastern Antarctica	KC782537
<i>Lensia multicristata</i>	300-600	24-Apr-2009	35°0.25'N	139°20'E	Sagami Bay (Japan)	KC782538
<i>Lensia multicristata</i>	300-600	24-Apr-2009	35°0.25'N	139°20'E	Sagami Bay (Japan)	KC782539
<i>Lensia panikkari</i>	0-400	18-Nov-2011	31°52.3'N	139°59.4'E	Myojin-sho (Japan)	121549
<i>Lensia panikkari</i>	0-1076	8-Jun-2012	27°50.05'N	127°00'E	Izena Hole (Japan)	450130
<i>Lensia</i> sp. A	0-100	18-Nov-2011	31°52.3'N	139°59.4'E	Myojin-sho (Japan)	121500
<i>Lensia</i> sp. A	0-946	7-Jun-2012	27°47.73'N	126°54.11'E	Izena Hole (Japan)	450143
<i>Lensia</i> sp. A	0-946	7-Jun-2012	27°47.73'N	126°54.11'E	Izena Hole (Japan)	450144
<i>Lensia subtiloides</i>	0-400	18-Nov-2011	31°N	132°E	off Kagoshima (Japan)	121451
<i>Lensia subtiloides</i>	0-946	7-Jun-2012	27°47.73'N	126°54.11'E	Izena Hole (Japan)	450141
<i>Lensia subtiloides</i>	0-100	18-Nov-2011	31°N	132°E	off Kagoshima (Japan)	121452
<i>Lensia subtiloides</i>	0-100	18-Nov-2011	31°N	132°E	off Kagoshima (Japan)	121453
<i>Lensia subtiloides</i>	0-100	18-Nov-2011	31°N	132°E	off Kagoshima (Japan)	121456
<i>Muggiae atlantica</i>	0-439	3-May-2001	36°39.60'N	142°0.6'E	Japan Trench	048790
<i>Muggiae atlantica</i>	0-180	27-Jun-2010	34°30'N	140°0'E	south-eastern Japan	151509
<i>Muggiae atlantica</i>	0-20	n/a	35°0.50'N	139°20'E	Sagami Bay (Japan)	DLSI189
<i>Muggiae kochi</i>	0-250	19-Jun-2012	41°04.16'N	01°24.36'E	Mediterranean Sea	Med2
<i>Muggiae kochi</i>	0-250	19-Jun-2012	41°04.16'N	01°24.36'E	Mediterranean Sea	Med3
<i>Muggiae kochi</i>	0-80	14-Jun-2012	43°41.10'N	7°18.94'E	Mediterranean Sea	Vlfr6
<i>Sphaeronectes haddocki</i>	0-500	8-Mar-2012	24.4°N	142°28.7'E	eastern Japan	230019
<i>Sphaeronectes koellikeri</i>	0-400	18-Nov-2011	31°N	132°E	off Kagoshima (Japan)	121530
<i>Sphaeronectes koellikeri</i>	0-200	25-Jan-2008	42°47.91'S	121°4.21'E	eastern Antarctica	DLSI088
<i>Sphaeronectes koellikeri</i>	0-80	14-Jun-2012	43°41.10'N	7°18.94'E	Mediterranean Sea	Vlfr28
<i>Sphaeronectes pagesi</i>	0-800	10-Mar-2012	42°17.6'N	139°28.3'E	Japan Sea	230003
<i>Sphaeronectes pagesi</i>	0-800	10-Mar-2012	42°17.6'N	139°28.3'E	Japan Sea	230011
<i>Sulculeolaria chuni</i>	0-400	18-Nov-2011	31°N	132°E	off Kagoshima (Japan)	121460
<i>Sulculeolaria chuni</i>	0-400	18-Nov-2011	31°N	132°E	off Kagoshima (Japan)	121461
<i>Sulculeolaria turgida</i>	0-1357	24-Apr-2012	34°59.18'N	139°20.06'E	Sagami Bay (Japan)	450008
<i>Sulculeolaria turgida</i>	0-1076	8-Jun-2012	27°50.05'N	127°00'E	Izena Hole (Japan)	450121

Table 11 (cont.): Characteristics of the samples sequenced for the present work. *:GenBank submission under the appellation *Eudoxia macra* Totton, 1954 (cf. Appendix II.2.1)

Genbank accession			
Species	number	Location	Reference
<i>Abylopsis tetragona</i>	AY935303	north Atlantic	Dunn <i>et al.</i> , 2005
<i>Chelophyes contorta</i>	AY935304	north Atlantic	Dunn <i>et al.</i> , 2005
<i>Chuniphyes multidentata</i>	AY935293	eastern Pacific	Dunn <i>et al.</i> , 2005
<i>Clausophyid</i> sp.	AY935293	eastern Pacific	Dunn <i>et al.</i> , 2005 He, J.R., Zheng, L.M., Lin, Y.S., Zhang,
<i>Diphyes chamissonis</i>	JQ715939	China Seas	W.J., Cao,W.Q. (unpublished) He, J.R., Zheng, L.M., Lin, Y.S., Zhang,
<i>Diphyes chamissonis</i>	JQ715940	China Seas	W.J., Cao,W.Q. (unpublished) He, J.R., Zheng, L.M., Lin, Y.S., Zhang,
<i>Diphyes chamissonis</i>	JQ715941	China Seas	W.J., Cao,W.Q. (unpublished) He, J.R., Zheng, L.M., Lin, Y.S., Zhang,
<i>Diphyes chamissonis</i>	JQ715942	China Seas	W.J., Cao,W.Q. (unpublished)
<i>Diphyes dispar</i>	AY935276	north Atlantic	Dunn <i>et al.</i> , 2005
<i>Kephyes ovata</i>	AY935294	eastern Pacific	Dunn <i>et al.</i> , 2005
<i>Lensia conoidea</i>	AY935318	eastern Pacific	Dunn <i>et al.</i> , 2005
<i>Muggiae atlantica</i>	AY935295	north Atlantic	Dunn <i>et al.</i> , 2005
<i>Muggiae atlantica</i>	HM053548	China Seas	Wang, R., Sun, S., Li, C. (unpublished)
<i>Muggiae atlantica</i>	EU999225	north Atlantic	Licandro <i>et al.</i> , 2010
<i>Muggiae kochi</i>	EU999226	north Atlantic	Licandro <i>et al.</i> , 2010
<i>Sphaeronectes koellikeri</i>	AY935301	north Atlantic	Dunn <i>et al.</i> , 2005
<i>Sulculeolaria quadrivalvis</i>	AY935288	north Atlantic	Dunn <i>et al.</i> , 2005
<i>Sulculeolaria quadrivalvis</i>	AY935276	eastern Pacific	Dunn <i>et al.</i> , 2005

Table 12: Calycophoran sequences obtained from GenBank.

Material and Methods

The study was performed on 115 specimens from locations around the world, including the tropical western Atlantic Ocean, the Mediterranean Sea, the Southern Ocean, Malaysia, and Japanese waters. These were collected using plankton nets (IKMT, IONESS, MOCNESS, ORI) or by the submersible Kaiko 7000. Eighty samples were of the family Diphyidae, 7 of the family Abylidiae, 22 of the family Clausophyidae and 6 of the family Sphaeronectidae (Table 11). The specimens were preserved in 99.5% ethanol or frozen at -20°C onboard after identification to species level. Frozen specimens were transferred to 99.5% ethanol before DNA extraction. For 88 specimens (GenBank accession numbers KC78253434, 40-53 and non 'DLSI' ID numbers), total DNA was extracted using the Qiagen DNEasy Blood & Tissue kit, and a 625 bp segment of the mitochondrial 16S gene amplified and sequenced using 'primer 1' and 'primer 2' from Cunningham and Buss (1993) with the TaKaRa ExTaq and BigDye kits. Sequencing was performed on an ABI 3130xl sequencer. For the other 27 samples, DNA extraction, amplification and sequencing were performed following the protocol established in Collins *et al.* (2008). Eighteen sequences, available on Genbank, were added to the analysis (Table 12). Sequence alignment was performed manually using the Se-Al v.2.0a11 software (Rambaut, 2002). The sequence portion found between the areas annotated H2077 and H2246 in figure 4.b of Dunn *et al.* (2005) was excluded from the analyses, as extremely variable in length. Intra- and inter-specific genetic variation was calculated as the Kimura 2 parameter (K2P) genetic distance using MEGA ver. 5.05 (Tamura *et al.*, 2011). A Bayesian analysis was performed on MrBayes ver. 3.2.1 (Huelsenbeck and Ronquist, 2001; Ronquist and Huelsenbeck, 2003) under a General Time Reversible (GTR) model, with 1 million generations, a sampling every 1000 generations, and a burn-in period of 5000 generations. The convergence of the data was verified using Tracer v. 1.5 (Rambaut and Drummond, 2003). The consensus tree was analyzed in FigTree v. 1.4.0 (Rambaut, 2007). Neighbour-Joining and Maximum Likelihood analyses were performed using MEGA ver. 5.05 (Tamura *et al.*, 2011), with complete gap deletion. A Maximum Parsimony analysis was performed using SeaView v. 4.3.0 (Gouy *et al.*, 2010), with complete gap deletion and 5 randomizations. Bootstrap support was estimated over 1000 replicates.

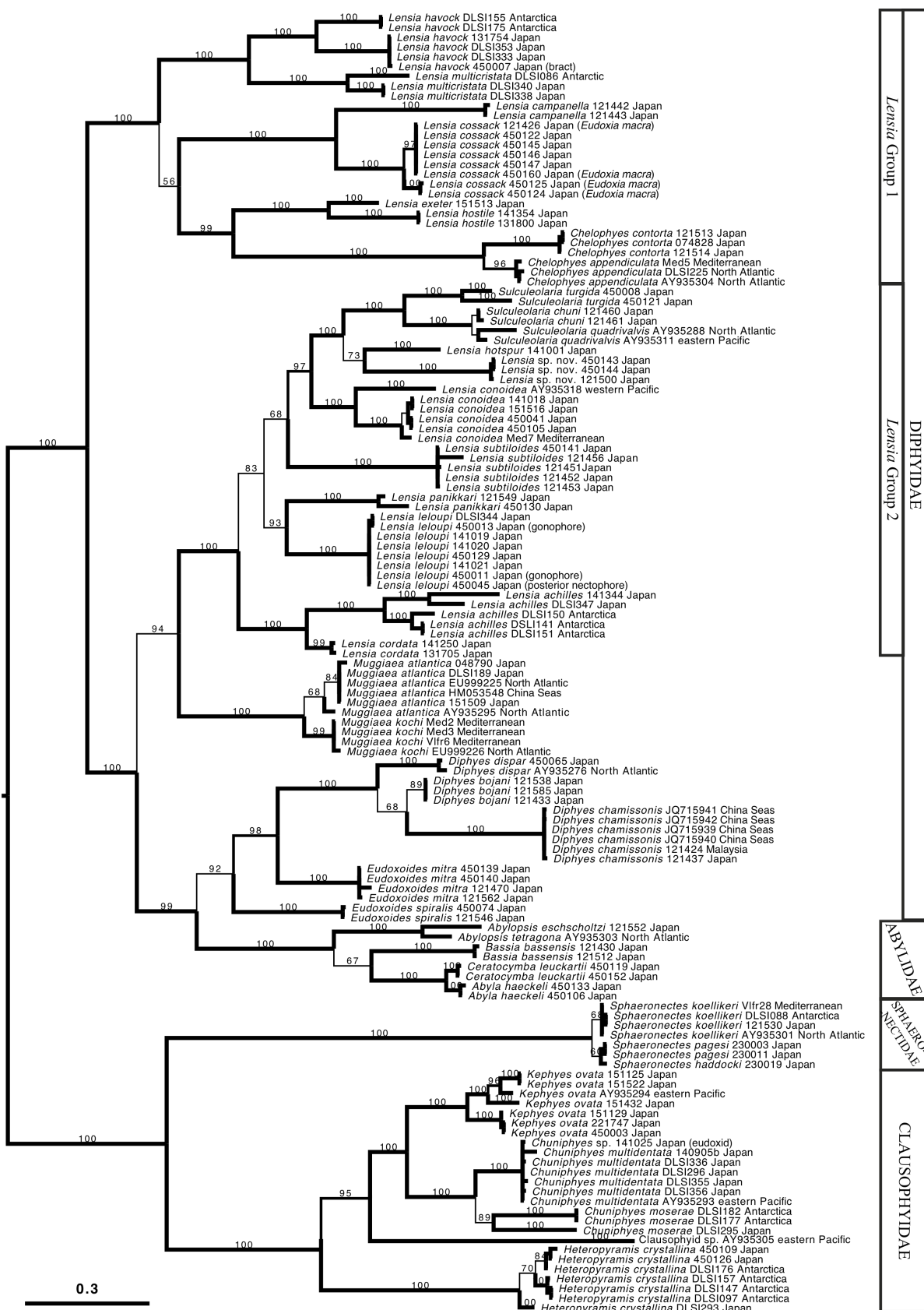


Figure 22: Bayesian consensus tree based on the mitochondrial 16S gene. Bayesian posterior probabilities in percent. Terminal posterior probabilities, and those inferior to 95% not shown.

Results

A total of 115 sequences were obtained, to which were added 18 database sequences, to obtain a dataset representing a total of 38 species: 5 species of the family Abylididae, 25 Diphyidae, 5 Clausophyidae and 3 Sphaeronectidae.

In the Bayesian analysis, all individuals of the same species clustered together in a monophyletic group (Fig. 22), and 31 out of the 38 studied species could be reliably identified (posterior probabilities $\geq 99\%$) using the mitochondrial 16S gene. Additionally, the genera *Chelophyes*, *Diphyes*, *Muggiaeae*, *Sulculeolaria* and the families Abylididae, Clausophyidae and Sphaeronectidae were well supported, although their positioning in the tree did not follow traditional taxonomy. Indeed, the present study could confirm what had been hinted at in previous studies of the mitochondrial CO1 (Ortman *et al.*, 2010) and 16S and 18S genes (Dunn *et al.*, 2005): the family Diphyidae was non-monophyletic, the family Abylididae being nested within it. Additionally, the genera *Eodoxoides* and *Lensia* did not form monophyletic groups. Indeed, the node containing both *Eodoxoides* species also contained the genus *Diphyes*, species that show morphological similitude to *Eodoxoides*, and particularly to *E. mitra*: the species of both these genera have much more robust mesogloea than that found in species of *Lensia* or *Muggiaeae*, the hydroecial cavity usually extends at least 1/3 of the nectophore in height, and the 5 complete ridges are particularly well marked, often with posterior cusps or teeth on the nectophores and gonophores. The genus *Lensia* was split into 2 main clusters, the first, containing all 7-ridged and multi-ridged species, as well as *L. campanella* and *L. cossack*, with 5 vestigial ridges, also contained the genus *Chelophyes*, which was found to be most closely related to the multi-ridged *Lensia*. These groups of species do not, superficially, share many morphological traits. However, it is interesting to note that in neither of the two *Chelophyes* species do all 5 ridges reach the apex of the anterior nectophore, a character not normally found with 5-ridged diphyids, but which has also been reported by Claude Carré (1968) for *L. campanella* (*cf.* Fig. 26, p. 126). The ridges on *L. cossack* were very unpronounced, and it was not possible to determine their course in the studied material. The second cluster, containing all other 5-ridged *Lensia*, also contained the genus *Sulculeolaria* (presently placed in its own diphyid sub-family, the Sulculeolariinae), as a sister group to that containing *Lensia hostpur* and to an undescribed *Lensia* species showing some morphological similarities with *L. hostpur* (*cf.* Appendix 2.4, p. 209).



Figure 23: Neighbour-Joining (NJ) tree based on the mitochondrial 16S gene. NJ, Maximum Likelihood (ML) and Maximum Parsimony (MP) bootstrap values in percent. Terminal values, and those inferior to 95% not shown. Scale represents 0.05 substitutions per site.

The present study also hinted at the existence of species complexes within the 5-ridged *Lensia*, corresponding to common morphological traits: *L. campanella* and *L. cossack*, with 5 vestigial ridges that do not join at the nectophore apex, were found to belong to *Lensia* group 1; *L. achilles* and *L. cordata*, which both have upward-curving lateral ridges and orange-pigmented somatocysts, formed a distinct clade with 100% posterior probabilities, and *L. leloupi* and *L. panikkari*, with incomplete lateral ridges, also clustered together, but with only 93% posterior probabilities.

Chuniphyes moserae, *Lensia achilles*, *L. havock* and *L. multicristata* showed distinct separation of the samples from the Southern Ocean and from Japanese waters. High genetic divergence amongst inter-geographic groups may hide the presence of cryptic species, a point discussed for the 3 *Lensia* species in Appendix 2.1 (p. 185).

In the Neighbour-Joining (NJ), Maximum Likelihood (ML) and Maximum Parsimony (MP) analyses, the global topology of the tree was similar to that found in the Bayesian analysis (Fig. 23), but only 19, 11 and 9 species, respectively, could be reliably identified (bootstrap $\geq 99\%$). Additionally, the majority of the deeper nodes of these trees showed very low bootstrap values, often inferior to 50%, and the exact positioning of some nodes, such as the species *Lensia multicristata*, *L. subtiloides*, or the genus *Muggiaeae*, were variable. Additionally, while *Sulculeolaria chuni* and *S. quadriculata* formed monophyletic, if unsupported, nodes in the Bayesian analysis, these two species could not be distinguished in the NJ, ML and MP analyses, and *Sphaeronectes haddocki* and *S. pagesi* could not be distinguished in the Maximum Parsimony tree.

The present study was composed of a large number of taxa, for which a single gene (mitochondrial 16S) was sequenced, and for which no specific evolutionary models exist. Additionally, siphonophores being fragile, gelatinous animals, there are no fossil records for these animals on which to calibrate the phylogenetic tree. The amount of genetic information available to the models was therefore extremely low. In these conditions, the Bayesian posterior probabilities observed would tend to be excessively high, while the NJ, ML and MP bootstrap values may show excessively low support on some of the deeper nodes (Simmons *et al.*, 2004; Suzuki *et al.*, 2002; Taylor and Piel, 2004).

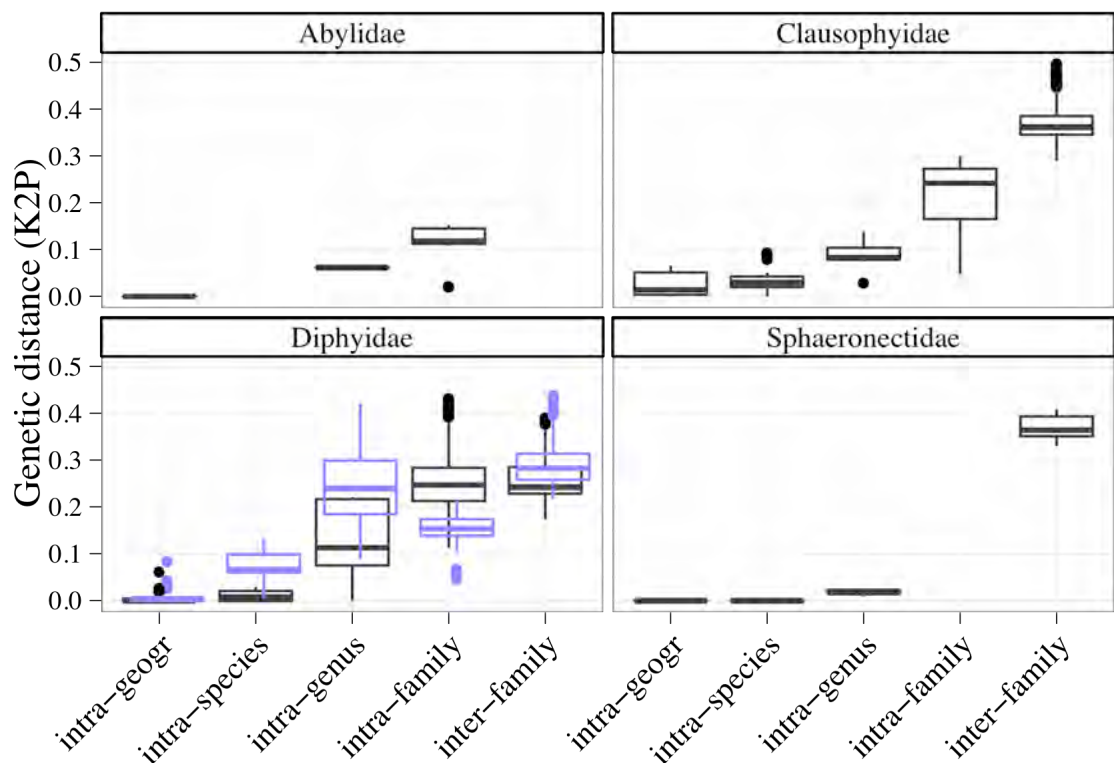


Figure 24: Quantile boxplot of the genetic distance (Kimura-2 Parameter) between families (“inter-family”), genera (“intra-family”) and species (“intra-genus”); between individuals of the same species from different geographic locations (intra-specific, inter-geographic: “intra-species”); and between individuals of the same species from the same geographic location (intra-specific, intra-geographic: “intra-geogr.”), for the 4 studied calycophoran families. For the Diphyidae: in light blue, genetic distances between species of the genus *Lensia*; in black, genetic distances between species of all other Diphyid genera.

The presence or absence of a ‘barcoding gap’ was a characteristic specific to each family (Fig. 24): the Clausophyidae showed no significant variations between intra and inter-geographic distances, but significantly different genetic distances between intra-species, intra-genus, intra-family and inter-family categories (Mann-Whitney-Wilcoxon test, $p < 0.01$). The same could be observed in the family Sphaeronectidae, but while the intra-generic distances were significantly higher than the intra-specific ones (Mann-Whitney-Wilcoxon test, $p = 0.01$), the K2P distances were extremely small, varying only between 0.004 and 0.022. This represented a difference in nucleotides of only between 0.4 and 2%, while in the family Clausophyidae, inter-species distances represented between 3 and 12.7% nucleotide differences. The present work did not represent a wide enough coverage of the species and genera of the family Abylididae to conclude about the presence of a barcoding gap in this family.

Amongst the Diphyidae genera, the genetic distance profiles resembled that of the family Clausophyidae, when not considering the genus *Lensia* (Fig. 24, in black), but because of the positioning of the family Abylididae, there were no significant differences between intra- and inter-family distances. Because of the polyphyly found in the genus *Lensia* and of the positioning of the genus *Sulculeolaria*, for example (Fig. 22), the inter-specific genetic distances within the *Lensia* were equivalent to those found between the other diphyid genera (0.23 and 0.25 average K2P distance between *Lensia* species, and between other diphyid genera, respectively), and the inter-genus distances were, on average, smaller than those observed between the different species of *Lensia* (Fig. 24, in blue). Additionally, some *Lensia* species, such as *L. achilles*, *L. havock* or *L. multicristata* showed extremely high inter-geographic intra-specific distances, similar or greater to those observed between other diphyid genera (K2P distances between 0.067 and 0.13). However, this difference was not consistent over all the tested *Lensia* species: *L. conoidea* samples from the Mediterranean Sea differed from Japanese samples by only one nucleotide, or a K2P distance of 0.004, similar to inter-geographic intra-species distances found between *Chelophyses appendiculata*, *Diphyes dipar*, *Muggiae atlantica*, and between some of the *Chuniphyses multidentata* specimens.

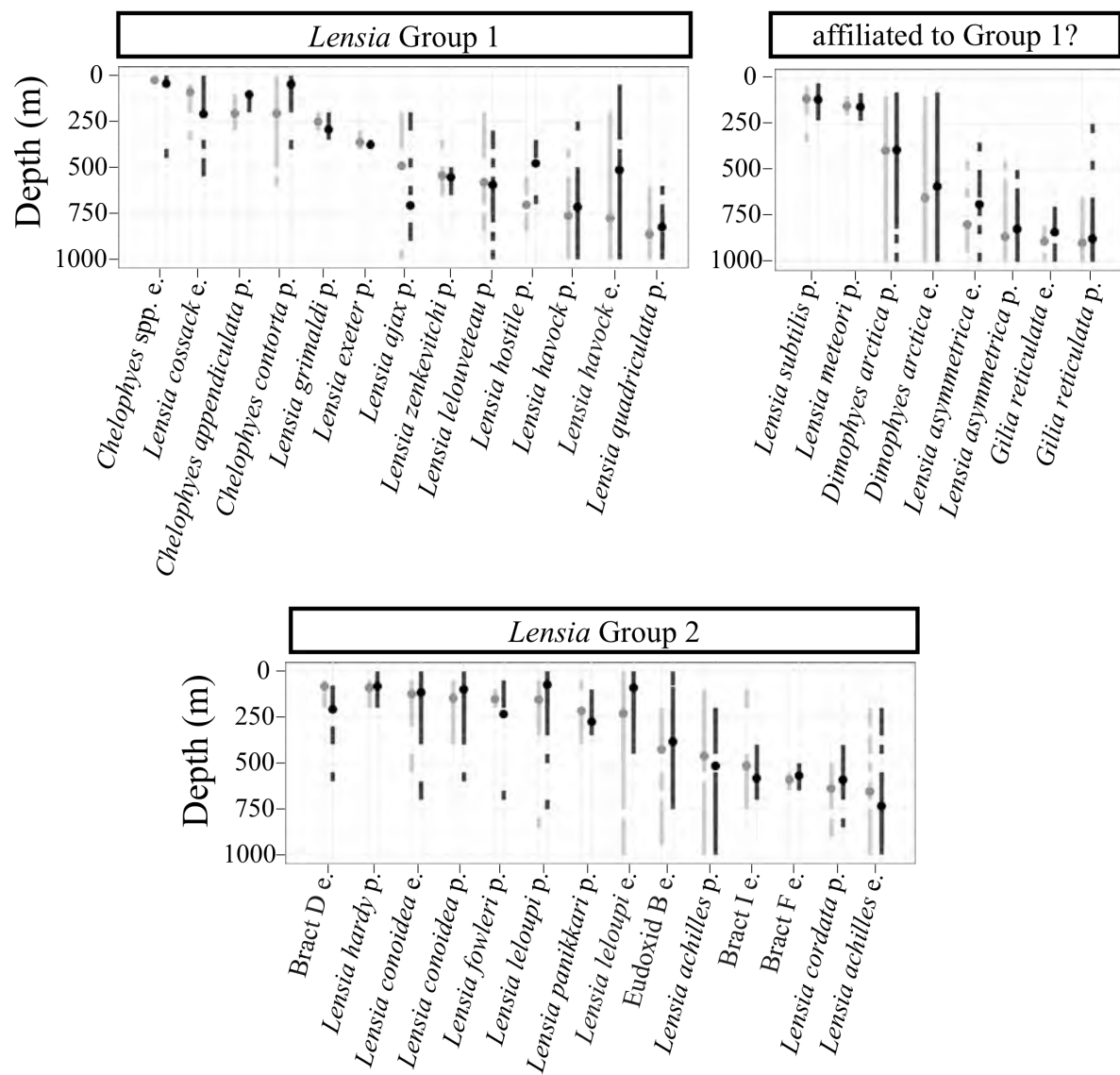


Figure 25: Maximum vertical range and mean depth (weighted by abundance) during the day (grey) and night (black) of diphid forms belonging to the 2 genetically defined *Lensia* groups, and those tentatively assigned to group 1. e: eudoxid, p: polygastric stage.

Discussion

Dunn *et al.* (2005) showed, using the mitochondrial 16S and nuclear 18S genes, that the order Siphonophora and the 3 sub-orders it contains are monophyletic. However, this could not be shown at family levels. Indeed, within the Calycophorae, 2 groups could be distinguished, the Prayomorphs, containing the families Prayidae and Hippopodiidae, and the Diphyomorphs, containing the Abylidiae, Clausophyidae, Diphyidae and Sphaeronectidae families. Globally, families, represented by 1 to 4 specimens only, did not show clear statistical support. A database of ribosomal 16S sequences was therefore established, containing the most diverse species assemblage of Abylid, Clausophyid, Diphyid, and Sphaeronectid species to date, and this gene proved useful for the discrimination of 82% of the included species, with all species forming monophyletic groups in the Bayesian analysis.

The extensive sequencing of the mitochondrial 16S gene in species of the family Diphyidae allowed us to confirm, using a Bayesian approach, what had been hinted at by previous studies of the mitochondrial CO1 (Ortman, 2010) and 16S genes (Dunn *et al.*, 2005) and nuclear 18S gene (Dunn *et al.*, 2005): the family Diphyidae was non-monophyletic, the family Abylidiae being nested within it. The Abylidiae have, by many authors (e.g. Bigelow, 1911; Moser, 1925; Sears, 1953), been considered a sub-family of the Diphyidae, the characteristic atrophy of the anterior nectophore and particular bract shapes not being considered sufficiently different characters from those observable in the family Diphyidae to warrant their own family. Such a positioning would appear justified with regard to the present data. No genetic support was found for the sub-family Sulculeolariinae as it appeared, in all 3 phylogenetic trees, as a sub-group of the 5-ridged *Lensia*. Additionally, the genera *Eudoxoides* and *Lensia* were found to be non-monophyletic. This latter was split into 2 main groups: one containing all 5-ridged *Lensia* with vestigial ridges, 7-ridged and multi-ridged *Lensia*, and the genus *Chelophyses*, and the other containing all other 5-ridged *Lensia*. These different *Lensia* groups corresponded not only to clear morphological characteristics, but also decreased the amount of overlap in the vertical distributions of closely-related species (Fig. 25). Diel vertical migration patterns did not appear correlated to the phylogenetic position of the considered species, and were present in some species of both these *Lensia* sub-groups, as well as in other diphyid genera such as *Eudoxoides*.

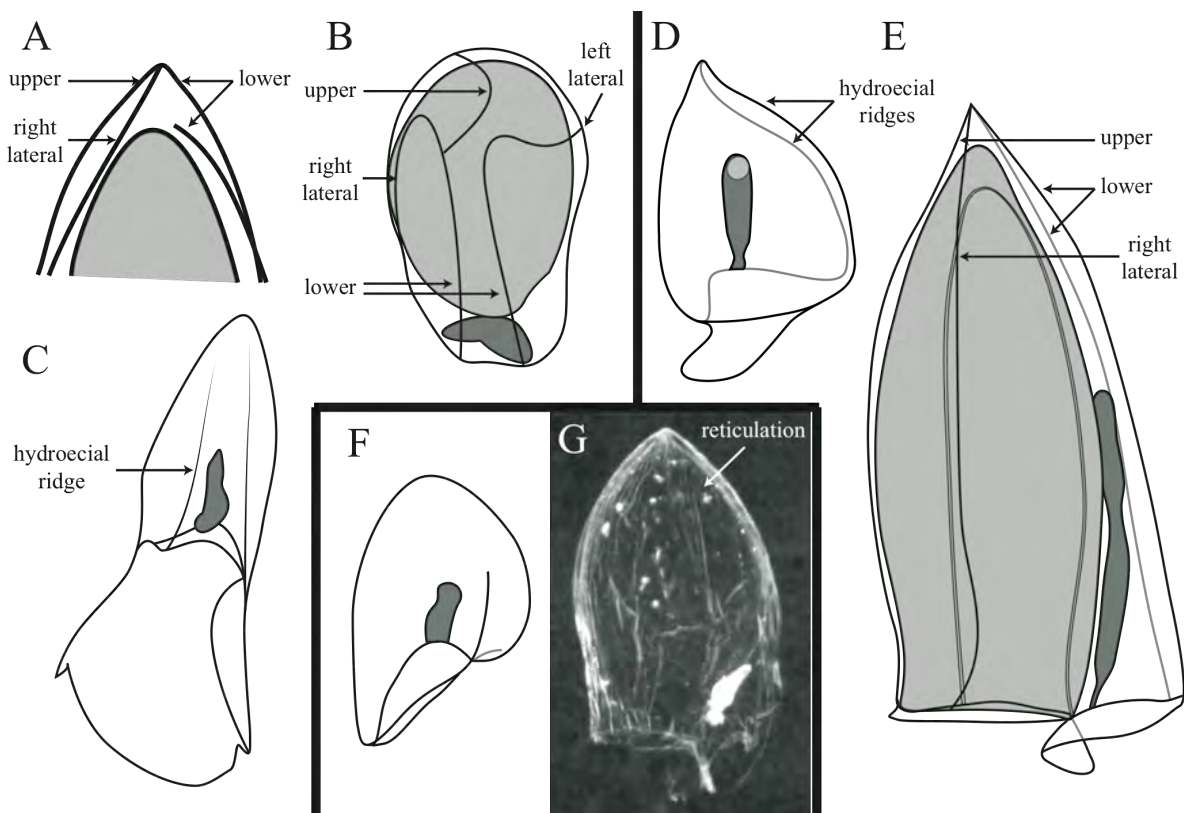


Figure 26: Illustration of the morphological characteristics associated with the two *Lensia* groups: Group 1: A: right lateral view of anterior part of *Chelophyses contorta* anterior nectophore showing incomplete lower ridge, B: apical view of *Lensia campanella* anterior nectophore (redrawn after Carré, 1968, Fig. 1.B), C: lower view of *Lensia havock* bract; Group 2: D: right lateral view of *Lensia conoidea* bract, E: right lateral view of *Lensia achilles* (*sensu* Patriti, 1970) anterior nectophore; species tentatively affiliated to group 1: F: right lateral view of *Lensia subtilis* bract (redrawn after Totton, 1954, Fig. 59), G: right lateral view of *Lensia asymmetrica* anterior nectophore showing reticulated patterns. Images not to scale.

It is, unfortunately, not known to which of these *Lensia* sub-groups the non-ridged *Lensia* belong to, no sequences having been obtained for these species. It is suspected, however, that they will be part of the first group. Indeed, in the 5-ridged *Lensia* group (group 2), not only do all polygastric stages have 5 ridges, complete in their anterior part, but all known eudoxid bracts have marked ridges (Fig. 26 D, E). In non-ridged *Lensia* however, as in those with 5 vestigial ridges and with 7 ridges, as well as in the genus *Chelophyses*, the bracts are devoid of marked ridges – low ridges border the hydroecial groove, but these do not extend to the apex of the bract (Fig. 26 C). Additionally, it is interesting to note nearly all of the *L. asymmetrica* samples (non-ridged *Lensia*) collected during the MULTI-SPLASH cruise were covered in a network of poorly-defined ridges (Fig. 26 G), as described and illustrated by Stepanjants (1970). Although we entirely agree with Pugh and Pagès (1997) that the visibility of this network is most likely a preservation artefact, a couple of well-preserved specimens from the MULTI-SPLASH cruise being devoid of them, it may be interesting to study the phylogenetic relationships between this species and the multi-ridged *Lensia*, or *Gilia reticulata*, a species presently in a different diphyid sub-family, the Giliinae, and for which there are as yet no sequences available, but which may prove a key species in the future rearrangement of the family Diphyidae. *Dimophyes arctica* may also belong in or near to this *Lensia* group, as it has no ridges on the polygastric and eudoxid stages.

Most species within the 5-ridged *Lensia* subgroup (group 2) were mesopelagic, but showed some differences in depth distribution or differed in migratory behaviour (Fig. 25). Additionally, several genetically distinct sub-groups could be differentiated, corresponding to specific morphologies of the lateral ridge. It is hypothesized the shape of the lateral ridge may influence the swimming behaviour of the colony, but the effect of the morphology of the nectophores on the swimming patterns of diphyomorphs is not yet well understood.

Because of the lack of support of many of the nodes making up the 5-ridged *Lensia* sub-group, of the low bootstrap values found in the deeper nodes of the NJ, ML and MP analyses, and of the lack of genetic information on some key Diphyid species such as *Dimophyes arctica* (Chun, 1897), *Gilia reticulata* (Totton, 1941) or *Lensia asymmetrica* Stepanjants, 1970 and the other non-ridged *Lensia*, *L. meteori* (Leloup, 1934) and *L. subtilis* (Chun, 1886), the present genetic information was not considered sufficiently robust to erect new families and genera for the taxa presently in the families Abylidæ and Diphyidae. A multi-gene approach, based on both nuclear and mitochondrial genes, and including a wide taxonomic and geographic range of species, will be necessary to finally resolve the phylogeny of calycophoran diphyomorphs.

Chapter III Summary

Siphonophores, contrary to the copepods or amphipods used for previous studies on niche partitioning in the open ocean (Kuriyama and Nishida, 2006; McGowan and Walker, 1979; 1985; 1993; Shulenberger, 1979), are exclusively carnivorous, and consume preferentially crustacean copepods (Mackie *et al.*, 1987). It was found that at the time of sampling, siphonophores, and especially the community present at the surface, represented a very important predation pressure on the copepod community. Additionally, we were able to confirm, for one of the most abundant diphyid species, *Dimophyes arctica*, that the sexual eudoxid stages appeared to have a similar trophic position as the polygastric stages. Unfortunately, no studies have yet been made on the exact predation pressure of these ‘single stomach’ stages relative to that of the polygastric ones.

Additionally, although siphonophores are known to catch and ingest prey larger than their stomach size (Mackie *et al.*, 1987; Pagès and Madin, 2010), the analysis of the trophic position of different sized *D. arctica* polygastric stages showed that, at mesopelagic depths dominated by extremely large copepods, these might have induced a trophic shift in the smallest polygastric stages, towards a consumption of the smaller, less abundant copepods, such as herbivore and detritivore Poecilostomatoida, or of ostracods. Therefore, despite having similar nematocysts and cnidoband organisations, two individuals of the same species may have different trophic niches if they are of different sizes.

The siphonophore phylogeny established for the most abundant families in the present study to test how congeneric species could, and did, coexist showed the most species-rich calycophoran family, the Diphyidae, was polyphyletic, as were the diphyid genera *Lensia* and *Eudoxoides*. The two main *Lensia* subgroups observed in the phylogeny corresponded to distinct morphological characteristics and specific depth distributions. Thus, within genetically related species assemblages, vertical distributional ranges were more unique, and morphological differences, which might induce differences in swimming behaviour and prey capture ability, could be observed between those species found in the same depth strata. Unfortunately, the phylogenetic information obtained from the mitochondrial 16S gene was not robust enough to allow for a revision of the diphyomorph families and genera.

General Discussion

The cnidarian order Siphonophora was chosen as a biological model for the study of biodiversity and niche partitioning off south-eastern Japan, in order to provide information on a group of planktonic organisms that differed in several regards from the previous biological models: the Copepoda and Amphipoda (Kuriyama and Nishida, 2006; McGowan and Walker, 1979; 1985; 1993; Shulenberger, 1979). Siphonophores have been found to be the second most abundant group of planktonic predators after crustaceans in many systems and, each individual being composed of a multitude of stomachs, their predation pressure is non negligible.

Siphonophore biodiversity off south-eastern Japan was found to be exceptionally high, with 43% of all valid siphonophore species collected during the MULTI-SPLASH cruise, and more than 60% of the world biodiversity in siphonophores having been recorded in Sagami Bay since the first studies were performed in this area in the early 20th century (e.g. Bigelow 1913; Moser 1925). With specific abundances on the scale of tens of individuals per 1000 m³, the siphonophore population was found to have a consequent predation pressure on the copepod population present in the sampling area, not only at the surface but also in the mesopelagic zone.

Most of the siphonophore species studied showed distinct vertical distribution patterns. However, for the community associated with the lateral transport of cold sub-polar waters into the sampling area, the vertical ranges of the species were variable, being much shallower in polar and sub-polar waters than in temperate ones, and therefore the observed vertical niche of these species is dependent on the latitude at which sampling is performed. Additionally, the modification of the path of the Kuroshio Current caused a marked modification of the surface community at Oshima station at the end of the sampling period, and thereby modified the vertical range of migrating mesopelagic species found at the surface at night at the other stations. The lateral transport of organisms, absent or minimal in the large Oceanic Gyres where the previous studies of niche partitioning amongst copepods and amphipods (McGowan and Walker, 1979; 1985; Shulenberger, 1979) were performed, therefore appeared to play an important role in the vertical and horizontal delimitation of siphonophore niches off south-eastern Japan.

However, contrary to most copepod and amphipod species, very few siphonophore species show distinctive geographic distributions. Indeed, while each species appeared to have specific depth preferences, their horizontal niches often extend through several oceanic realms and basins (Longhurst, 1995; 2006), in contrast, for example, to the distinct specific composition of the copepod communities found within the North Pacific Gyre and along the

California Current (McGowan and Walker, 1985). Physico-chemical water characteristics such as temperature, salinity, oxygen, or nutrient concentrations do not seem to greatly affect siphonophore distribution. Notable exceptions are three siphonophore species, apparently endemic to the Southern Ocean: *Pyrostethos vanhoeffeni* Moser, 1925, and its probable post-larval stage *Mica micula* Margulis, 1982 (Grossmann *et al.*, 2013b), *Diphyes antarctica* Moser, 1925, and *Marrus antarcticus* Totton, 1954, with all records confined within the Antarctic Convergence (50 to 60°S). However, the lack of studies performed in the subantarctic zones north of the Antarctic Convergence means the siphonophore populations of these waters are still relatively unknown, and new species are still to be described. For example *Sphaeronectes pughi* Grossmann, Lindsay and Fuentes, 2012 was described from subantarctic waters north of the French Antarctic base Dumont d'Urville (Grossmann *et al.*, 2012), one of the most studied areas of the Southern Ocean. Similarly, an intensive, multi-annual study of the fjords of southern Chili by Palma *et al.* (Palma and Rosales, 1997; Palma *et al.*, 1999; Palma and Aravena, 2001), showed the presence of *Pyrostethos vanhoeffeni* as far north as 41°50'S. Considering the lack of knowledge of most waters surrounding the Antarctic region, and of the extent and faunal composition of the Antarctic-derived water masses flowing northwards at depth through the Atlantic, Indian and Pacific Oceans (e.g. Antarctic Bottom Water (AABW), Antarctic Intermediate Water (AAIW), etc...) it is possible that in the future species considered Antarctic endemics may turn out to inhabit all colder waters of the Southern hemisphere, or be bipolar. On the other hand, recent applications of genetic analyses to the order Siphonophora uncovered geographically-distinct cryptic species within the genus *Physalia* Lamarck, 1801, of the siphonophore sub-order Cystonectae (Pontin and Cruickshank, 2011), and, within the present study, several diphyid calycophoran species with worldwide distributions showed a clear genetic distinction between samples from Japanese waters and those from the Southern Ocean, and appeared to be complexes of cryptic species. An exact estimation of the biodiversity of the Siphonophora will therefore necessitate much more intensive sampling and study of these still relatively unknown animals, and genetic techniques such as DNA barcoding may be necessary to assess the extent of crypticity in what are now considered species with worldwide or bipolar distributional ranges. The genetic analyses of the mitochondrial 16S gene showed all tested calycophoran species from within a given geographic area to have a good genetic coherence, and this gene shows promise for the identification of siphonophores to species level through DNA barcoding alone, to be used by non-experts or when morphological identification is difficult (Continuous Plankton Recorder, sediment samples, high throughput plankton pumps, etc...).

Diel vertical migration was a character associated with certain genetically similar groups (Abylidae, *Chuniphyes* spp., *Eudoxoides* spp., etc...) but, based on the phylogenetic tree obtained from the mitochondrial 16S gene, seemed to be a character having appeared several times during evolutionary history. After their identity could be confirmed through DNA barcoding when necessary, eudoxid stages were commonly found to have similar vertical niches and migratory patterns as the polygastric stages of the same species. Additionally, the eudoxids of *Dimophyes arctica* were found, using stable isotope techniques, to have the same trophic level as the polygastric stages. However, the study of stable isotopes provides information only on the type of food consumed (herbivorous, detritivorous, carnivorous, etc...), and more precise studies of the predation of eudoxid stages would be needed, in order to determine whether they consume the same size and the same species of prey as the polygastric stages. Indeed, if they are found to consume similar prey, the shape and fishing posture of the colony, thought to be a determining factor in siphonophore feeding (Mackie *et al.*, 1987), may play a less important role than the shape and spacing of the cnidobands along the tentacles, for example.

Within a group of morphologically and genetically similar species, differences in mean nectophore size were often important (e.g. *Chelophyes appendiculata* > *C. contorta*, *Eudoxoides mitra* > *E. spiralis*), associated with sometimes small, but distinct morphological differences affecting the pattern of ridges or the size and shape of the somatocyst. Unfortunately, because of the difficulty in maintaining siphonophores under laboratory conditions, or in observing their natural swimming behaviours *in-situ*, the impact these morphological characters may have on the swimming and feeding of the animals is not well understood. However, although little is known of the diets and feeding patterns of oceanic or deep-water siphonophore species, the isotopic analyses performed during this study revealed a possible trophic shift occurring between different sized *Dimophyes arctica* anterior nectophores. Potentially, therefore, predation pressure, and competition between species, may be influenced by the generational cycles of the considered species.

Additionally, it has been hypothesized for boreal *Neocalanus cristatus* copepods swept into Sagami Bay with Oyashio waters, that the physico-chemical parameters of the waters of Sagami Bay are unsuited for the survival and reproduction of this species (Oh *et al.*, 1991). For a certain proportion of the mesopelagic siphonophore community originating from northern waters, therefore, their presence and sometimes high abundances in the Bay may not represent a reproducing stock of these species, but rather a community which, unsuited for its

environment, will be out-competed by the more temperate mesopelagic species present in the Bay.

The community structure and niche partitioning amongst Siphonophora are therefore determined by complex mechanisms, controlled by a variety of physical, chemical and biological parameters. It is hoped the recent models on the effect of landscape and population connectivity on the competition and community structure of benthic organisms having pelagic larval stages (e.g. Berkley *et al.*, 2010; Selkoe *et al.*, 2010) might be extrapolated to entirely pelagic animals such as siphonophores in order to help resolve the importance of lateral transport and temporal variations on the stability and robustness of the siphonophore communities found off south-eastern Japan.

General Conclusion

The focus of this study was to assess the biodiversity of the Siphonophora off south-eastern Japan, one of the most species-rich areas of Japanese waters, and review the temporal, distributional and physiological processes helping to maintain this high biodiversity.

1. Study location and hydrography

The study location showed a complex hydrographic structure. During the sampling period, the Kuroshio Current did not directly flow into the sampling area. However, the run of the current and the position of its meanders clearly influenced the structure of the water column. A mixture of water masses could be found in the mesopelagic zone, with marked sub-polar influences, associated with low salinities. High temperatures and salinities, linked to Kuroshio influences, could be found both at the surface and at mesopelagic depths, and, at night off Oshima station, a warm but less saline water mass, possibly originating in Tokyo Bay or the coastal areas of Sagami Bay was present.

The sampling, performed in 50- to 100 m-depth intervals with an IONESS net system allowed environmental parameters such as water temperature and salinity to be measured concurrently with the sampling. A flow-meter attached to the net allowed for an estimation of abundance of the observed animals, which could then be compared with results obtained in different locations or using different sampling systems.

2. Diversity, distribution and spatio-temporal niche partitioning of the Siphonophora

Thanks to the intensive sampling carried out during the MULTI-SPLASH cruise, an extremely high siphonophore biodiversity was recorded from the 3 stations, with the collection of 82 siphonophore species, including 16 first-time records from Japanese waters, and 3 first-time records from not only Japanese waters, but from the whole Pacific Ocean. The first-time records of 11 species from Sagami Bay showed we have yet to fully understand the biodiversity of even the most well-studied areas around Japan.

The Siphonophora could be split into seven communities, characterized by the vertical distribution, geographic origin, and physiological characteristics (such as diel vertical migration) of the species they contained. Hydrographically driven lateral transport of the

planktonic organisms played a dominant role in both the community composition and in the specific vertical distribution of the species found in the present study.

Two species, *Dimophyes arctica* and *Muggiae atlantica* dominated the water column in terms of abundance and, at their maximum peak in abundance, caused a drastic decrease in the overall diversity and evenness (H' and J' indices, respectively) of the siphonophore community. The size ratios of eudoxids to polygastric stages in these species indicated they were in a period of spring bloom.

3. Trophic partitioning and taxonomic spread

The presence of these abundant, and possibly fast-growing siphonophore communities was found to have a potentially large trophic impact on the ecosystem, consuming up to 60% of the copepod standing stock present at the time of sampling. Additionally, the use of stable isotopes did not indicate a marked difference in trophic position between the sexual and asexual stages of a species, although the overall size of the colonies may affect the trophic position of these, the smaller animals being unable to feed on the largest copepods.

Furthermore, although many congeneric siphonophore species had similar depth distribution patterns, these species did not necessarily show high levels of genetic relatedness as present-day siphonophore taxonomy, based on morphological similarities of the polygastric stages, was found to inaccurately represent the phylogenetic evolution within the more evolved calycophoran siphonophores. Indeed, the most species-rich genera and families present in waters off south-eastern Japan were found to form polyphyletic groups.

4. Conclusions

The waters off south-eastern Japan house an amazing siphonophore diversity, with records of more than 43% valid siphonophore species (WoRMS). This can be explained by the hydrographic complexity of this zone, allowing for a mixing and coexistence of tropical, temperate, sub-polar and coastal species.

The sheer abundance and species richness of the Siphonophora in this zone made them an ideal community on which to test whether specific niche partitioning could explain the Paradox of the Plankton, with the added advantage of showing distinct physiological differences with the Copepoda and Amphipoda employed by previous studies: they are gelatinous, colonial and entirely pelagic animals, have one of the largest size ranges of the animal kingdom, and are believed to be exclusively carnivorous. Shulenberger (1979) established seven criteria that influence niche partitioning: vertical range, diel vertical migration patterns, feeding periodicity, reproductive habits, diet, patchiness and co-occurrence with other species.

Our studies showed the importance of vertical range, diel vertical migration, co-occurrence with other species and possibly diet, were factors that could help maintain a high siphonophore biodiversity. Because of their fragility and the difficulty in sampling intact colonies and maintaining them in laboratory conditions, little is known of feeding periodicity and reproductive habits of the majority of the species studied. Additionally, it is extremely difficult to estimate spatial and temporal scales for planktonic organisms. Therefore, it seems very likely all seven of the aforementioned criteria influence niche partitioning of the Siphonophora. However, one of the most important factors influencing the observed niche partitioning of the Siphonophora in the present study was lateral transport. Indeed, as well as creating temporal and spatial variability within the sampling area, it also influenced the vertical distribution of some siphonophores: species with worldwide distributions, such as *Chuniphyes* spp. and *Dimophyes arctica*, have variable depth distributions at different latitudes, according to the depth at which their preferred water mass is found. Therefore, niche partitioning in the Siphonophora depends not only on the biology and physiology of the siphonophores themselves, represented as Shulenberger's seven criteria (1979), but also on the physico-chemical, abiotic parameters of the environment.

5. Further Research

The study of Siphonophora is constantly limited by the lack of knowledge of the basic biological and physiological functions of these animals. Indeed, without a clear understanding of the physiology or development of the considered species, it is difficult to assess whether the siphonophore communities observed are thriving, or whether the individuals present have been transported into waters that do not allow reproduction, but merely survival of the species.

The colonial, gelatinous structure of siphonophores makes them difficult to maintain in laboratory conditions, yet they are also sensitive to the physical and photic stress of underwater survey vehicles. It is hoped the development of untethered underwater vehicles, inducing less intense disturbance waves as those attached to the mother ship by a cable, and of sessile observation platforms equipped with video recording systems, may be useful for the study of swimming and feeding behaviours in the Siphonophora. The latter, recording at a fixed peridocity over a long period of time, may also be useful for the study of the spatial and temporal patchiness that may affect the Siphonophora. Indeed, spatial and temporal disturbances in the ocean have been shown to function along a log-log scale (Haury *et al.*, 1978), disturbances in the order of seconds having effects in the micrometre to milimetre scale, while disturbances on the daily scale, such as diel vertical migrations, affect several tens or hundreds of meters. Siphonophores having such a wide size range, even at the scale of the different life stages of a single species, the study of temporal and spatial patchiness may provide important insights into their intra- and inter-specific interactions.

Finally, it is hoped recently developed computer models aiming at explaining and predicting the effect of landscape and population connectivity on niche partitioning and community structure of benthic organisms having pelagic larval stages (e.g. Berkley *et al.*, 2010; Selkoe *et al.*, 2010) might be extrapolated to entirely pelagic animals in order to provide a global answer to the Paradox of the Plankton.

References

- Ainley, D.G., DeMaster, D.P. (1990) The upper trophic levels in polar marine ecosystems. In: Smith, W.O. (Ed.) *Polar oceanography*. Academic Press, San Diego, CA, USA, pp. 599–630.
- Alvariño A. (1971) Siphonophores of the Pacific with a review of the world distribution. *Bull. Scripps Inst. Oceanogr. Univ. Calif. Tech. Ser.* 16:1–432.
- Alvariño, A. (1980) The relation between the distribution of zooplankton predators and anchovy larvae. *CalCOFI Reports* 21: 150–160.
- Alvariño, A. (1981) Siphonophorae. In: Boltovskiy, D., Ed., *Atlas del zooplankton del Atlántico Sudoccidental y métodos de trabajo con zooplankton marino*. Publicación especial del Instituto Nacional de Investigación y Desarollo Pesquero (INIDEP), Mar del Plata, Argentina, pp. 383–441.
- Alvariño, A., Wojtan, J.M. & Martinez, M.R. (1990) Antarctic siphonophores from plankton samples of the United States Antarctic Research Program. In: Kornicker, L.S., Ed., *Biology of the Antarctic Seas XX*. 49, pp. 1–436.
- Berkley, H.A., Kendall, B.E., Mitarai, S., Siegel, D.A. (2010) Turbulent dispersal promotes species coexistence. *Ecol. Lett.* 13: 360–371.
- BISMaL (Biological Information System for Marine Life) data portal, *Order Siphonophora*: <http://www.godac.jamstec.go.jp/bismal/view/0000187>. Accessed 20 November, 2012.
- Bigelow, H. (1913) Medusae and Siphonophorae collected by the U.S. Fisheries steamer "Albatross" in the northwestern Pacific, 1906. *Proc. U.S. Natl. Mus.* 44(1946): 1–119.
- Bouillon, J., Medel, M.D., Pagès, F., Gili, J-M., Boero, F., Gravili, C. (2004) Fauna of the Mediterranean Hydrozoa. *Sci. Mar.* 68(Suppl. 2): 5–449.
- Breiman, L. (2001) Random forests. *Machine Learning* 45(1): 5–32.
- Carré, C. (1968) L'eudoxie de *Lensia campanella* Moser, 1925, avec des précisions sur le stade polygastrique (siphonophore calycophore Diphyidae). *Bulletin du Museum d'Histoire Naturelle* 50(2): 438–445. (in French)
- Carré, C. (1979) Sur le genre *Sulculeolaria* Blainville, 1834 (Siphonophora, Calycophorae, Diphyidae). *Ann. I. Oceanogr. Paris* 55(1), 27-48. (in French)
- Carré, C., Carré, D. (1995) Ordre des siphonophores. In: Doumenc (Ed.) *Traité de zoologie*, tome III. Anatomie, systématique, biologie. Fascicule II Cnidaires, Cténaires. Masson, Paris. pp. 523–596. (in French)
- Carré, D. (1972) Etude du développement des cnidocytes dans le gastrozoïde de *Muggiae kochi* (Will, 1844) (siphonophore calycophore). *Comptes Rendus de l'Académie des Sciences de Paris* 275(D), 1263-1266. (in French)

- Chihara, M., Murano, M. (1997) *An illustrated guide to marine plankton in Japan*. Tokai University Press, Tokyo, Japan.
- Chikaraishi, Y., Kashiyama, Y., Ogawa, N.O., Kitazato, H., Ohkouchi, N. (2007) Metabolic control of nitrogen isotope composition of amino acids in macroalgae and gastropods: implications for aquatic food web studies. *Mar. Ecol. Prog. Ser.* **342**: 85–90.
- Chikaraishi, Y., Kashiyama, Y., Ogawa, N.O., Kitazato, H., Satoh, M., Nomota, S., Ohkouchi, N. (2008) A compound-specific isotope method for measuring the stable nitrogen isotopic composition of tetrapyrroles. *Org. Geochem.* **39**: 510–520.
- Chikaraishi, Y., Ogawa, N.O., Kashiyama, Y., Takano, Y., Suga, H., Tomitani, A., Miyashita, H., Kitazato, H., Ohkouchi, N. (2009) Determination of aquatic food-web structure based on compound-specific nitrogen isotopic composition of amino acids. *Limnol. Oceanogr.: Methods* **7**: 740–750.
- Clarke, K.R., Warwick, R.M. (2001) *Change in marine communities: an approach to statistical analysis and interpolation*, 2nd edition. Primer-E Ltd, Plymouth, UK.
- Collins, A.G., Bentlage, B., Lindner, A., Lindsay, D., Haddock, S.H.D., Jarms, G., Noremburg, J.L., Jankowski, T., Cartwright, P. (2008) Phylogenetics of Trachylina (Cnidaria: Hydrozoa) with new insights on the evolution of some problematical taxa. *J. Mar. Biol. Ass. U.K.* **88**(8): 1673–1685.
- Cunningham, C., Buss, L. 1993. Molecular evidence for multiple episodes of Paedomorphosis in the family Hydractiniidae. *Biochemical Systematics and Ecology* **21**: 57–69.
- Daniel, R. (1970) Some new species of Siphonophora (Coelenterata) from the Indian Ocean. *J. Zool. Soc. India* **22**(1 & 2): 147–156.
- Daniel, R. (1985) *Coelenterata: Hydrozoa, Siphonophora*. In: Tikader, B.K. (ed.) The fauna of India and the adjacent countries. Zoological Survey of India, Calcutta, India, pp. 1–440.
- Dunn, C.W., Pugh, P.R., Haddock, S.H.D. (2005) Molecular phylogenetics of the Siphonophora (Cnidaria), with implications for the evolution of functional specialization. *Syst. Evol.* **54**(6): 916–935.
- Fishbase: <http://www.fishbase.org/search.php>
- Fisher, J., Lindenmayer, D.B., Manning, A.D. (2006) Biodiversity, ecosystem function, and resilience: ten guiding principles for commodity production landscapes. *Front Ecol. Environ.* **4**(2): 80–86.
- Fujikura, K., Lindsay, D.J., Kitazato, H., Nishida, S., Shirayama, Y. (2012) Marine biodiversity in Japanese waters. *PloS One* **5**(8): e11836. doi:10.1371/journal.pone.0011836

- Gamulin, T. (1966) Contribution to the knowledge of *Lensia fowleri* (Bigelow) (Siphonophora, Calycophorae). *Pubblicazioni della Stazione Zoologica di Napoli* **35**(1): 1–6.
- Gamulin, T., Kršinić, F. (2000) Calycophores (Siphonophora, Calycophorae) of the Adriatic and Mediterranean Seas. *Fauna Natura Croatica* **9**(2): 1–198.
- Gao, S., Hong, H., Zhang, S. (2002) *Phylum Cnidaria, class Hydrozoa, subclass Siphonophora*. In: Gao S, Hong H, Zhang S (eds.) *Fauna Sinica (Invertebrata)* 27, Science Press, Beijing, China, pp. 1–177.
- Gasca, R. (2009) Diversity of Siphonophora (Cnidaria: Hydrozoa) in the western Caribbean Sea: new records from deep-water trawls. *Zootaxa* **2095**: 60–68.
- Gasparini, S. (2007) *PLANKTON IDENTIFIER: a software for automatic recognition of planktonic organisms*. http://www.obs-vlfr.fr/~gaspari/Plankton_Identifier/index.php
- Gause, G.F. (1935) *The struggle for existence*. Williams and Wilkins, Baltimore, USA, pp. 1–129.
- Gibbons, M.J., Thibault-Botha, D. (2002) The match between ocean circulation and zoogeography of epipelagic siphonophores around southern Africa. *J. Mar. Biol. Ass. U.K.* **82**(5): 801–810.
- Gorsky, G., Ohman, M.D., Picheral, M., Gasparini, S., Stemman, L., Romagnan, J-B., Cawood, A., Pesant, S., García-Comas, C., Prejer, F. (2010) Digital zooplankton image analysis using the ZooScan integrated system. *J. Plankt. Res.* **32**: 285–303.
- Grossmann, M.M. (2010) *A study of the gelatinous mesozooplankton (Cnidaria and Ctenophora) of Eastern Antarctica, summer 2008*. M. Sc. dissertation, Université Pierre et Marie Curie, Paris, France.
- Grossmann, M.M., Lindsay, D.J. (2013a) Diversity and distribution of the Siphonophora (Cnidaria) in Sagami Bay, Japan, and their association with tropical and subarctic water masses. In: Lindsay, D.J.: *Multiple Sampling Platform Survey of Whole Ecosystem Database* (MULTI-SPLASH Database): Biological Information System for Marine Life (BISMAL): http://www.godac.jamstec.go.jp/bismal/e/JAMSTEC_MULTISPLASH2006_SagamiBay_Siphonophora
- Grossmann, M.M., Lindsay, D.J. (2013b) Diversity and distribution of the Siphonophora (Cnidaria) in Sagami Bay, Japan, and their association with tropical and subarctic water masses. *J. Oceanogr.* **69**(4): 395–411.

- Grossmann, M.M., Lindsay, D.J., Fuentes, V. (2012) *Sphaeronectes pughi* sp. nov., a new species of sphaeronectid calycophoran siphonophore from the subantarctic zone. *Polar Sci.* **6**(2): 196–199.
- Grossmann, M.M., Lindsay, D.J., Collins, A.G. (2013a) The end of an enigmatic taxon: *Eudoxia macra* is the eudoxid stage of *Lensia cossack* (Siphonophora, Cnidaria). *Syst. Biodiv.* **11**(3): 381–387.
- Grossmann, M.M., Lindsay, D.J., Fuentes, V. (2013b) A redescription of the post-larval physonect siphonophore stage known as *Mica micula* Margulis 1982, from Antarctica, with notes on its distribution and identity. *Marine Ecology* **34**(suppl.1): 63–70.
- Gouy, M., Guindon, S., Gascuel, O. (2010) SeaView version 4 : a multiplatform graphical user interface for sequence alignment and phylogenetic tree building. *Molecular Biology and Evolution* **27**(2): 221–224.
- Haddock, S.H.D., Dunn, C.W., Pugh, P.R. (2005) A re-examination of siphonophore terminology and morphology, applied to the description of two new prayine species with remarkable bio-optical properties. *J. Mar. Biol. Ass. U.K.* **85**: 695–707.
- Haury, L.R., McGowan, J.A., Weibe, P.H. (1978) Patterns and processes in the time-space scales of plankton distributions. In: Steele, J.H. (Ed.) *Spatial pattern in plankton communities*. Plenum press, New York, USA; pp. 277–327.
- Hidaka, K. (2008) Species composition and horizontal distribution of the appendicularian community in waters adjacent to the Kuroshio in winter-early spring. *Plankton Benthos Res.* **3**(3): 152–164.
- Hobson, K.A. (1999) Tracing diets and origins of migratory birds using stable isotope techniques. In: *Biology and conservation of forest birds*. Soc. of Can. Ornith. Special Publication 1. pp. 21–41.
- Holtgrieve, G.W., Schindler, D.E., Hobbs, W.E., Leavitt, P.R., Ward, E.J., Bunting, L., Chen, G., Finney, B.P., Gregory-Eaves, I., Holmgren, S., Lisac, M.J., Lisi, P.J., Nydick, K., Rogers, L.A., Saros, J.E., Selbie, D.T., Shapley, M.D., Walsh, P.B., Wolfe, A.P. (2011) A coherent signature of anthropogenic nitrogen deposition to remote watersheds of the northern hemisphere. *Science* **344**: 1545–1548.
- Hopcroft, R.R., Clarke, C., Chavez, F.P. (2002) Copepod communities in Monterey Bay during the 1997-1999 El Niño and La Niña. *Prog. Oceanogr.* **54**: 251–264.
- Hosia, A., Båmstedt, U. (2008) Seasonal abundance and vertical distribution of siphonophores in western Norwegian fjords. *J. Plankton Res.* **30**(8): 951–962.

- Hosia, A., Stemmann, L., Youngbluth, M. (2008) Distribution of net-collected planktonic cnidarians along the northern Mid-Atlantic Ridge and their associations with the main water masses. *Deep-Sea Res. Pt. II* **55**(2008): 106–118.
- Huelsenbeck, J.P., Ronquist, F. (2001) MrBayes, Bayesian inference of phylogenetic trees. *Bioinformatics* **17**, 754-755.
- Hunt, J.C., Lindsay, D.J. (1999) Methodology for creating an observational database of midwater fauna using submersibles: Results from Sagami Bay, Japan. *Plankton Biol. Ecol.* **46**(1): 75–87.
- Hutchinson, G.E. (1941) Ecological aspects of succession in natural populations. *Am. Nat.* **75**: 406–418.
- Hutchinson, G.E. (1961) The paradox of the plankton. *Am. Nat.* **95**(882): 137–145.
- Japan Coast Guard, *Marine Information Service, Oceanographic Data Information Division*, 14-21 March 2006: <http://www1.kaiho.mlit.go.jp/KANKYO/KAIYO/qboc/2006/qboc200611cu0.pdf>. Accessed 20 January 2013.
- Kâ, S., Hwang, J-S. (2011) Mesozooplankton distribution and composition on the northeastern coast of Taiwan during autumn: effects of the Kuroshio current and hydrothermal vents. *Zool. Stud.* **50**(2): 155–163.
- Kawabe, M. (1995) Variations of current path, velocity, and volume transport of the Kuroshio in relation with the large meander. *J. Phys. Oceanogr.* **25**: 3103–3117.
- Kawamura, T. (1954) A report on Japanese siphonophores with special references to new and rare species. *J. Shiga. Prefect. Jnr. Coll. Ser. A* **2**(4): 99–129.
- Kidachi, T., Ito, H. (1979) Distribution and structure of macroplankton communities in the Kuroshio and coastal region, South of Honshu, during spring season. *Bull. Tokai Reg. Fish. Res. Lab.* **97**: 1–119. (in Japanese with English abstract)
- Kindt, R. (2013) GUI for biodiversity, suitability and community ecology analysis: <http://cran.r-project.org/web/packages/BiodiversityR/index.html>
- Kitamura, M. (1997) *Taxonomic study and seasonal occurrence of jellyfish in Sagami Bay*. M. Sc. Dissertation, Tokyo University of Fisheries, Tokyo, Japan.
- Kitamura, M. (2000) *Taxonomy and distribution of planktonic Cnidaria around Japan*. Ph. D. Dissertation, Tokyo University of Fisheries, Tokyo, Japan. (in Japanese)
- Kitamura, M. (2009) Vertical distribution of planktonic Cnidaria in three sites of northwestern Pacific. *Kaiyo monthly*, **41**: 382–392. (in Japanese)

- Kitamura, M., Tanaka, Y., Ishimaru, T., Mine, Y., Noda, A., Hamada, H. (2001) Sagami Bay research report: Improvement of multiple opening/closing net, IONESS (Intelligent Operative Net Sampling System). *J. Tokyo Univ. Fish.* **10**: 149–58. (in Japanese)
- Kitamura, M., Tanaka, Y., Ishimaru, T. (2003) Coarse scale distributions and community structure of hydromedusae related to water mass structures in two locations of Japanese waters in early summer. *Plankton Biol. Ecol.* **50**(2): 43–54.
- Kobari, T., Moku, M., Takahashi, K. (2008) Seasonal appearance of expatriated boreal copepods in the Oyashio-Kuroshio mixed region. *ICES J. Mar. Sci.* **65**: 469–476.
- Kuriyama, M., Nishida, S. (2006) Species diversity and niche-partitioning in the pelagic copepods of the family Scolecitrichidae (Calanoida). *Crustaceana* **79**(3): 293–317.
- Leloup, von E., Hentschel, E. (1935) Die Verbreitung der calycophoran Siphonophoren in Südatlantischen Ozean. *Wiss. ergebn. Dtsch. Atl. Exped. "Meteor"* **12**(1): 474–475. (in German)
- Levin, S.A. (1970) Community equilibria and stability, and an extension of the Competitive Exclusion Principle. *Am. Nat.* **104** (939): 413–423.
- Licandro, P., Conway, D.V.P., Daly Yahia, M.N., Fernandez de Puelles, M.L., Gasparini, S., Hecq, J.H., Tranter, P., Kirby, R.R. (2010) A blooming jellyfish in the northeast Atlantic and Mediterranean. *Biol. Lett.* **6**: 688–691.
- Lindsay, D.J. (2003) Carbon and nitrogen contents of mesopelagic organisms: Results from Sagami Bay, Japan. *JAMSTEC Deep Sea Res.* **22**: 1–13.
- Lindsay, D.J., Grossmann, M.M., Minemizu, R. (2011) *Sphaeronectes pagesi* sp. nov., a new species of sphaeronectid calycophoran siphonophore from Japan, with the first record of *S. fragilis* Carré, 1968 from the North Pacific Ocean and observations on related species. *Plankt. Benthos Res.* **6**(2): 101–107.
- Lindsay, D.J., Hunt, J.C. (2005) Biodiversity in midwater cnidarians and ctenophores: submersible-based results from deep-water bays in the Japan Sea and north-western Pacific. *J. Mar. Biol. Ass. U.K.* **85**(2): 503–517.
- Lindsay, D.J., Hunt, J.C., Hashimoto, J., Fujikura, K., Fujiwara, Y., Tsuchida, S., Itoh, K. (1998) The benthopelagic community of Sagami Bay. *JAMSTEC J. Deep Sea Res.* **14**: 493–499.
- Lindsay, D.J., Miyake, H. (2009) A checklist of midwater cnidarians and ctenophores from Japanese waters: species sampled during submersible surveys from 1993–2008 with notes on their taxonomy. *Kaiyo Monthly* **41**: 417–438. (in Japanese with English abstract)
- Longhurst, A. (1995) Seasonal cycles of pelagic production and consumption. *Prog. Oceanogr.* **36**: 77–167.

- Longhurst, A. (2006) *Ecological geography of the sea*. Academic Press, San Diego, USA. pp. 560.
- MacAvoy, S.E., Arneson, L.S., Bassett, E. (2006) Correlation of metabolism with tissue carbon and nitrogen turnover rate in small mammals. *Oecologia* **150**: 190–201.
- Mackie, G.O. (1965) Conduction in the nerve-free epithelia of siphonophores. *Am. Zool.* **5**: 439–455.
- Mackie, G.O., Pugh, P.R., Purcell, J.E. (1987) Siphonophore Biology. *Adv. Mar. Biol.* **24**: 97–262.
- Mapstone, G.M. (2001) Siphonophora. In: Costello MJ, Emblow C, White R (Eds.) *European register of marine species. A check-list of the marine species in Europe and a bibliography of guides to their identification*. Publ. Sci. Mus. Hist. Nat, Paris, France. 120–122.
- Mapstone, G.M. (2009) *Siphonophora (Cnidaria: Hydrozoa) of Canadian Pacific waters*. NRC Research Press, Ottawa, Canada, pp. 302.
- Margulis, R.Ya. (1970) A new species of siphonophore *Lensia zenkevitchi* sp. n. (Siphonanthae, Calycophorae) from the Atlantic Ocean. *Zool. Zh.* **49**: 148–149.
- Margulis, R.Ya. (1971) Distribution of siphonophores of the genus *Lensia* (suborder Calycophorae) in the Atlantic. *Okeanologiya* **11**: 80-84.
- Margulis, R.Ya. (1978) The distribution of siphonophores in the western North Atlantic in summer of 1974. *Vestn. Mosk. Univ. Ser. XVI Biol.* **3**: 1–11. (in Russian with English abstract)
- Margulis, R.Ya. (1980) On the vertical distribution of siphonophores in the world's oceans. In: Naumov DV, Stepanjants SD (Eds.) *The theoretical and practical importance of coelenterates*. Zoological Institute, Russian Academy of Sciences, Leningrad, URSS, pp. 60–65. (in Russian)
- Margulis, R.Ya., Alekseev, D.O. (1985) On the genus *Lensia* Totton, 1932 (Siphonophora: Calycophorae). *Zool. Zh.* **64**(1): 5–15. (In Russian with English abstract)
- McClelland, J.W., Holl, C.M., Montoya, J.P. (2003) Relating low $\delta^{15}\text{N}$ values of zooplankton to N_2 -fixation in the tropical North Atlantic: insights provided by stable isotope ratios of amino acids. *Deep-Sea Res. I* **50**: 849–861.
- McCleland, J.W., Montoya, J.P. (2002) Trophic relationships and the nitrogen isotopic composition of amino acids in plankton. *Ecology* **83**(8): 2173–2180.
- McGowan, J.A., Walker, P.W. (1979) Structure in the copepod community of the North Pacific Central Gyre. *Ecol. Monogr.* **49**(2): 195–226.

- McGowan, J.A., Walker, P.W. (1985) Dominance and diversity maintenance in an oceanic ecosystem. *Ecol. monogr.* **55**(1): 103–118.
- McGowan, J.A., Walker, P.W (1993) Pelagic diversity patterns. In Ricklefs, R.E., Schluter, D. (Eds.) *Species diversity in ecological communities: historical and geographical perspectives*. Chicago University Press, Chicago, Illinois, USA, pp. 203–214.
- Mills, C.E. (1982) *Patterns and mechanisms of vertical distribution of medusae and ctenophores*. PhD Dissertation, University of Victoria, Victoria, B.C., Canada.
- Miranda, L.S., Collins, A.G., Marques, A.C. (2010) Molecules clarify a cnidarian life cycle – the “hydrozoan” *Microhydrula limopsicola* is an early life stage of the staurozoan *Haliclystus antarcticus*. *PLoS One* **5**(4): e10182.
- Miyamoto, H., Nishida, S., Kuroda, K., Tanaka, Y. (2012) Vertical distribution and seasonal variation of chaetognaths in Sagami Bay, central Japan. *Plankton Benthos Res.* **7**(2): 41–54.
- Moser, F. (1913) Zur geographischen Verbreitung der Siphonophoren nebst andern Bemerkungen. In: Korschelt, E. (Ed.) *Zoologischer Anzeiger, Wissenschaftliche Mitteilungen*. Deutschen Zoologischen Gesellschaft **61**(4): 145–49.
- Moser, F. (1925) Die Siphonophoren der Deutsche Südpolar-Expedition 1901-1903. In: Drygalski, von E. (Ed.), *Dtsch. Südpol.-Exped. 1901-1903 (Zoologie)*, Vol. 17. Walter de Gruyter and co., Berlin and Leipzig, pp. 1–541
- Moura, C.J., Cunha, M.R., Porteiro, F.M., Rogers, A.D. (2011) The use of the DNA barcode gene 16S mRNA for the clarification of taxonomic problems within the family Sertulariidae (Cnidaria, Hydrozoa). *Zoologica Scripta* **40**(5): 520–537.
- Nishikawa, J., Matsuura, H., Castillo, L.V., Campos, W.L., Nishida, S. (2007) Biomass, vertical distribution and community structure of mesozooplankton in the Sulu Sea and its adjacent waters. *Deep Sea Research II* **54**: 114–130.
- Ogawa, N.O., Chikaraishi, Y., Ohkouchi, N. (2012) Trophic position estimates of formalin-fixed samples with nitrogen isotopic compositions of amino acids: an application to gobiid fish (Isaza) in Lake Biwa, Japan. *Ecol. Res.* DOI 10.1007/s11284-012-0967-z
- Oh, B-C., Terazaki, M., Nemoto, T. (1991) Some aspects of the life history of the subarctic copepod *Neocalanus cristatus* (Calanoida) in Sagami Bay, central Japan. *Mar. Biol.* **111**: 207–212.
- Ohshima, K.I., Wakatsuchi, M., Saitoh, S. (2005) Velocity field of the Oyashio region observed with satellite-tracked surface drifters during 1999-2000. *J. Oceanogr.* **61**: 845–855.

- Oksanen, J., Blanchet, F.G., Kindt, R., Legendre, P., Minchin, P.R., O'Hara, R.B., Simpson, G.L., Solymos, P., Steven, M.H., Wagner, H. (2013) Community ecology package: <http://cran.r-project.org>, <http://vegan.r-forge.r-project.org/>
- Okutani, T. (2005) *Cuttlefishes and squids of the world*. National Cooperative Association of Squid Processors, Tokyo, Japan.
- Ortman, B.D, Bucklin, A., Pagès, F., Youngbluth, M. (2010) DNA barcoding the Medusozoa using mtCOI. *Deep-Sea Res. II* **59**: 2148–2156.
- Pagès, F., Flood, P., Youngbluth, M. (2006) Gelatinous zooplankton net-collected in the Gulf of Maine and adjacent submarine canyons: new species, new family (Jeanbouillonidae), taxonomic remarks and some parasites. *Sci. Mar.* **70**(3): 363–379.
- Pagès, F., Kurbjewitz, F. (1994) Vertical distribution and abundance of mesoplanktonic medusae and siphonophores from the Weddell Sea, Antarctica. *Polar Biol.* **14**: 243–251.
- Pagès, F., Madin, L.P. (2010) Siphonophores eat fish larger than their stomachs. *Deep-Sea Res.* **57**: 2248–2250.
- Pagès, F., Pugh, P.R. (2002) Fuseudoxid: the elusive sexual stage of the calycophoran siphonophore *Crystallophyes amygdalina* (Clausophyidae: Crystallophyinae). *Acta Zool. Stockholm* **83**: 329–336.
- Pagès, F., Schnack-Schiel, S.B. (1996) Distribution patterns of the mesozooplankton, principally siphonophores and medusae, in the vicinity of the Antarctic Slope Front (eastern Weddell Sea). *J. Marine. Syst.* **9**: 231–248.
- Palma, S.G., Aravena, G. (2001) Distribution of chaetognaths, euphausiids and siphonophores in the Magellan region. *Cienc. Tecnol. Mar.* **24**: 47–59.
- Palma, S.G., Rosales, S.G. (1997) Epipelagic siphonophores from southern Chilean inlets ($41^{\circ}30'$ – $46^{\circ}40'$ S). *Cienc. Tecnol. Mar.* **20**: 125–145.
- Palma, S.G., Ulloa, R., Linacre, L. (1999) Siphonophores, chaetognaths and euphausiids from southern Chilean inlets between Gulf of Penas and Magellan Strait. *Cienc. Tecnol. Mar.* **22**: 111–142.
- Park, J.H., Won, J.H. (2004) Three new records of marine Hydromedusae (Cnidaria: Hydrozoa) in Korea. *Korean J. Syst. Zool.* **20**(2): 179–184.
- Patriti, G. (1964) Les siphonophores calycophores du Golfe de Marseille. *Rec. Trav. Stn. Mar. Endoume Fac. Sci. Mars.* **35**(51): 185–258. (in French)
- Patriti, G. (1970). Aperçu systématique de la faune de siphonophores des zones superficielles des eaux du large de Tuléar (S.W. de l'Océan Indien, Madagascar). *Recueil de Travaux de la Station Marine d'Endoume. Suppl.* **10**: 285–303. (in French)

- Pontin, D.R., and Cruickshank, R.H. (2011) Molecular phylogenetics f the genus *Physalia* (Cnidaria: Siphonophora) in New Zealand coastal waters reveals cryptic diversity. *Hydrobiologia* **686**: 91–105.
- Pugh, P.R. (1984) The diel migrations and distributions within a mesopelagic community in the North East Atlantic, Siphonophores. *Prog. Oceanog.* **13**: 461–489
- Pugh, P.R. (1992) A revision of the sub-family Nectopyramininae (Siphonophora, Prayidae). *Phil. Trans. R. Soc. Lond. B* **335**: 281–322.
- Pugh, P.R. (1999a) A review of the genus *Bargmannia* Totton, 1954 (Siphonophora, Physonecta, Pyrostephidae). *Bull. Nat. Hist. Mus. Lond. (Zool.)* **65**(1): 51–72.
- Pugh, P.R. (1999b) Siphonophorae. In: Boltovskoy, D. (Ed) *South Atlantic Zooplankton*. Backhuys publishers, Leiden, The Netherlands, pp. 467–511.
- Pugh, P.R. (2001) A review of the genus *Erenna* Bedot, 1904 (Siphonophora, Physonectae). *Bull. Nat. Hist. Mus. Lond. (Zool.)* **67**(2): 169–182.
- Pugh, P.R. (2003) A revision of the family Forskaliidae (Siphonophora, Physonectae). *J. Nat. Hist.* **37**: 1281–1327.
- Pugh, P.R. (2005) A new species of *Physophora* (Siphonophora: Physonectae: Physophoridae) from the North Atlantic, with comments on related species. *Syst. Biodivers.* **2**(3): 251–270.
- Pugh, P.R. (2006) Reclassification of the clausophyid siphonophore *Clausophyes ovata* into the genus *Kephyes* gen. nov. *J. Mar. Biol. Ass. U.K.* **86**: 997–1004.
- Pugh, P.R., Pagès, F. (1997) A re-description of *Lensia asymmetrica* Stepanjants, 1970 (Siphonophorae, Diphyidae). *Sci. Mar.* **61**(2): 153–161.
- Pugh, P.R., Youngbluth, M.J. (1988) A new species of *Halistemma* (Siphonophora: Physonectae: Agalmatidae) collected by submersible. *J. Mar. Biol. Ass. U.K.* **68**: 1–14.
- Purcell, J.E. (1982) Feeding and growth of the siphonophore *Muggiae a atlantica* (Cunningham 1893). *J. ExP. Mar. Biol. Ecol.* **62**: 39–54.
- Purcell, J.E. (1984) The functions of nematocysts in prey capture by epipelagic siphonophores (Coelenterata, Hydrozoa). *Biol. Bull.* **166**: 310–327.
- Rambaut, A. (2002) *Se-Al, sequence alignment editor*: <http://tree.bio.ed.ac.uk/software/seal/>
- Rambaut, A. (2007) *FigTree, a graphical viewer of phylogenetic trees*: <http://tree.bio.ed.ac.uk/software/figtree/>
- Rambaut, A., Drummond, A. (2003) *Tracer 1.5*: <http://tree.bio.ed.ac.uk/software/tracer/>
- Rengarajan, K. (1973) Siphonophores obtained during the cruises of R.V. *Varuna* from the west coast of India and the Laccadive Sea. *J. Mar. Biol. Ass. India* **15**(1): 125–159.

- Ronquist, F., Huelsenbeck, J.P. (2003) MrBayes, Bayesian phylogenetic inference under mixed models. *Bioinformatics* **19**: 1572–1574.
- Russel, F.S. (1938) On the development of *Muggiae atlantica* Cunningham. *J. Mar. Biol. Ass. U.K.* **19**(1): 73–81.
- Sears, M. (1953) Notes on siphonophores: A revision of the Abylinae. *Bull. Mus. Comp. Zool.* **109**(1): 1–119.
- Sekine, Y, Uchiyama K (2002) Outflow of the Intermediate Oyashio Water from Sagami Bay to the Shikoku Basin. *J. Oceanogr.* **58**: 531–537
- Selkoe, K.A., Watson, J.R., White, C., Horin, T.B., Iacchei, M., Mitarai, S., Siegel, D.A., Gainess, S.D., Toonen, R.J. (2010) Taking the chaos out of genetic patchiness: seascape genetics reveals ecological and oceanographic drivers of genetic patterns in three temperate reef species. *Mol. Ecol.* **19**: 3708–3726.
- Senju, T., Asano, N., Matsuyama, M., Ishimaru, T. (1998) Intrusion events of the Intermediate Oyashio Water into Sagami Bay, Japan. *J. Oceanogr.* **54**: 29–44.
- Shimode, S., Toda, T., Kikuchi, T. (2006) Spatio-temporal changes in diversity and community structure of planktonic copepods in Sagami Bay, Japan. *Mar. Biol.* **148**: 581–597.
- Shulenberger, E. (1979) Distributional pattern and niche separation among North Pacific hyperiid amphipods. *Deep-Sea Res.* **26**(A): 293–315.
- Simmons, M.P., Pickett, K.M., Miya, M. (2004) How meaningful are Bayesian support values? *Mol. Biol. Evol.* **21**(1): 188–199.
- Skjodlal, H.R., Wiebe, P.H., Postel, L., Knutsen, T., Kaartvedt, S., Sameoto, D.D. (2013) Intercomparison of zooplankton (net) sampling systems: Results from the ICES/GLOBEC sea-going workshop. *Prog. Oceanogr.* **108**: 1–42.
- Stepanjants, S.D (1967) Siphonophores of the seas of the USSR and the northern part of the Pacific Ocean. *Opred. Faune Akad. Nauk. SSSR* **96**: 234–249. (in Russian)
- Stepanjants, S.D. (1970) Siphonophora of the southern part of the Kurile-Kamchatka Trench and adjacent marine areas. *Trudy Inst. Okeanol.* **86**: 222–236. (in Russian)
- Stepanjants, S.D., Cortese, G., Kruglikova, S.B., Bjørklund, K.R. (2006) A review of bipolarity concepts: History and examples from Radiolaria and Medusozoa (Cnidaria). *Mar. Biol. Res.* **2**: 200–241.
- Suzuki, Y., Glazko, G.V., Nei, M. (2002) Overcredibility of molecular phylogenies obtained by Bayesian phylogenetics. *PNAS* **99**(25): 16138–16143.

- Szpak, P., Gröcke, D.R., Debruyne R., MacPhee, R.D.E., Gunthrie, R., Froese, D., Zazula, G.D., Patterson, W.P., Poinar, H.N. (2010) Regional differences in bone collagen $\delta^{13}\text{C}$ and $\delta^{15}\text{N}$ of Pleistocene mammoths: Implications for paleoecology of the mammoth steppe. *Palaeogeogr. Palaeocl.* **286**: 88–96.
- Talley, L.D. (1993) Distribution and formation of North Pacific Intermediate Water. *J. Phys. Oceanogr.* **23**: 33–47.
- Tamura, K., Peterson, D., Peterson, N., Stecher, G., Nei, M. & Kumar, S. (2011) MEGA5, Molecular Evolutionary Genetics Analysis using Maximum Likelihood, Evolutionary Distance, and Maximum Parsimony methods. *Molecular Biology and Evolution* **28**(10): 2731–2739.
- Taylor, D.J., Piel, W.H. (2004) An assessment of accuracy, error, and conflict with support values from genome-scale phylogenetic data. *Mol. Biol. Evol.* **21** (8): 1534–1537.
- Thibault-Botha, D., Gibbons, M.J. (2005) Epipelagic siphonophores off the east coast of South Africa. *Afr. J. Mar. Sci.* **27**(1): 129–139.
- Totton, A.K. (1932) Siphonophora. *Scientific Reports of the Great Barrier Reef Expedition* **4**(10): 317–374.
- Totton, A.K. (1941) New species of the siphonophoran genus *Lensia* Totton, 1932. *Ann. Mag. Nat. Hist. Ser. 11* **8**: 145–168.
- Totton, A.K. (1954) Siphonophora of the Indian Ocean together with systematic and biological notes on related specimens from other oceans. *Discovery Reports* **27**: 145–168.
- Totton, A.K. (1965a) *A synopsis of the Siphonophora*. British Museum (Natural History), London, U.K, pp. 230
- Totton, A.K. (1965b) A new species of *Lensia* (Siphonophora: Diphyidae) from the coastal waters of Vancouver, B.C; and its comparison with *Lensia achilles* Totton and another new species *Lensia cordata*. *Ann. Mag. Nat. Hist., Ser. 13* **8**(85-86): 71–76.
- Toyokawa, M., Terasaki, M. (1994) Seasonal variation of medusae and ctenophores in the innermost part of Tokyo Bay. *Bull. Plankt. Soc. Jap.* **41**(1): 71–75.
- Toyokawa, M., Toda, T., Kikuchi, T., Nishida, S. (1998) Cnidarians and ctenophores observed from the manned submersible *Shinkai 2000* in the midwater of Sagami Bay, Pacific coast of Japan. *Plankton Biol. Ecol.* **45**(1): 61–74.
- Turner, J.T. (1985) The feeding ecology of some zooplankters that are important prey items of larval fish. NOAA Technical report NMFS **7**: 1–28.
- Uye, S. (1982) Length-weight relationships of important zooplankton from the Inland Sea of Japan. *J. Oceanogr. Soc. Jap.* **38**: 149–158.

- Vogt, C. (1854) Recherches sur les animaux inférieurs de la Méditerranée. 1. Sur les Siphonophores de la mer de Nice. *Mémoires de l'Institut National Genèvois* **1**: 1–164. (in French)
- Warembois, C. (2005) *Analyse temporelle du mészooplancton dans la rade de Villefranche-sur-Mer à l'aide d'un nouveau système automatique d'imagerie numérique: le ZOOSCAN – Influence des apports particulaires, de la production primaire et des facteurs environnementaux*. PhD thesis, Université Paris VI, France. (in French)
- Wickham, H. (2009) *ggplot2: elegant graphics for data analysis*. Springer, New York, USA: <http://ggplot2.org/>
- Wiebe, P.H., Morton, A.W., Bradley, A.M., Backus, R.H., Craddock, J.E., Barber, V., Cowles, T.J., Flierl, G.R. (1985) New development in the MOCNESS, an apparatus for sampling zooplankton and micronekton. *Marine Biology* **87**: 313–323.
- World Register of Marine Species (WoRMS) portal, *Order Siphonophora*: <http://www.marinespecies.org/aphia.php?p=taxdetails&id=1371>. Accessed 20 January 2013
- Xu, Z., Lin, M., Gao, Q. (2008) Causal analysis of the diversity of medusae in the East China Sea. *Frontiers of Biology in China* **3**(3): 300–307.
- Yang, S-K., Nagata, Y., Taira, K., Kawabe, M. (1993a) Southward intrusion of the Intermediate Oyashio Water along the east coast of the Boso peninsula. I. Coastal salinity-minimum-layer water off the Boso peninsula. *J. Oceanogr.* **49**: 89–114.
- Yang, S-K., Nagata, Y., Taira, K., Kawabe, M. (1993b) Southward intrusion of the Intermediate Oyashio Water along the east coast of the Boso peninsula. II. Intrusion events into Sagami Bay. *J. Oceanogr.* **49**: 173–191.
- Zhang, J.B. (1984) The Calycophorae (Siphonophora) from tropical waters of the western Pacific Ocean. In: *Proceedings on Plankton from the Tropical Region of the Western Pacific Ocean*. China Ocean Press, Beijing, China, pp. 52-85. (in Chinese with English abstract)
- Zhang, J.B. (2005) *Pelagic Siphonophora in China Seas*. China Ocean Press, Beijing, China, pp. 151
- Zhang, J.B., Lin, M. (1997) Study on the ecogeography of Siphonophora in the South China Sea. *Acta Oceanol. Sin.* **19**(4): 121–131. (in Chinese)
- Zhang, J.B., Lin, M. (2001) Vertical distribution of the Hydromedusae and Siphonophora in western waters of Taiwan Strait. *J. Oceanogr. Taiwan* **20**(1): 1–8. (in Chinese with English abstract)

Zhang, J.B., Xu, Z. (1980) On the geographical distribution of the siphonophores in the China Sea. *Acta Sci. Nat. Univ. Amoiensis* **19**(3): 121–125. (In Chinese with English abstract)

Acknowledgements

I would like to thank the great many people who provided help and guidance invaluable to the completion of this thesis.

I cannot express enough thanks to my supervising Professor Dhugal Lindsay, who got me interested in, and taught me all I know about siphonophores, and guided me through the intricacies of the graduate life. I also thank Professor Yasuhiro Ozeki for his help in navigating university bureaucracy, Drs. Tadashi Maruyama and Katsunori Fujikura for having accepted me within the BioGeos team at JAMSTEC, and Mikiko Tagomori, Atsuko Watanabe and Yu Haraoka for having ironed out the administrative side of things. I also thank the jury of Yokohama City University for their constructive comments.

I also thank Professor Miwa, Drs. Hiromi Watanabe, Minoru Kitamura, James Reimer, Frederic Sinniger, Julien Lorion, Kiyotaka Takishita and the rest of the BioGeos team for their constructive comments without which this thesis could not have seen the light of day, and Asuka Yamaki for her introduction to the Adobe Illustrator software. Thanks are also due to the past and present students of seitaitō, especially Nanae Fukumoto and Tomomi Ogura, and of course to the ‘dream team’ Karine Heerah, Laura Turon-Lacarrieu and Lucie Buttay, and the other OEM students for their eternal support though this endeavour, to Nozomi Kawai, Mie Tachi, Mieko Ishida and Erika Kamimachi for all the fun times and total misunderstandings, and of course to my parents for letting me fly away to the other side of the world and for providing me with an invaluable crash-course in English grammar.

Thanks are due to Captains Inoue and Yoshida and the crew of the R/V *Tansei-maru*, and to professors Jun Nishikawa and Shuhei Nishida of the Atmosphere and Ocean Research Institute of Tokyo University and the onboard research teams for their help with sampling; to Captain Stanislas Zamora and crew of the M/V *L'Astrolabe* and the onboard ICO²TA team; to the captain and crew of the R/V *García del Cid* and to Ana Sabates and the FISHJELLY

team; and especially to Verónica Fuentes of the Institut de Ciències del Mar for her invitation to participate in these cruises.

I must thank the captain and crew of the R/V *Kaiyo* during the MULTI-SPLASH cruise KY06-03, the onboard team of Drs. Minoru Kitamura, Yasuo Furushima, Francesc Pagès (deceased), Satoshi Konishi, Sumihiro Koyama, Jun Nishikawa, Mikiko Kuriyama, Hiroyuki Matsuura, Jun Kita, Haruko Kurihara, Satoko Iguchi, Hiroshi Miyake, Tomohiko Kikuchi, Satoshi Katoh, Takenori Kawabata and Mr. Jun Tanada, Mitsugu Kitada, Toshishige Itoh, Masaru Satoh, Sayaka Matsumura, Teruki Tanaka, Satoshi Okada, Maiko Kimino, Naotaka Togashi, Akira Soh, Tamami Ueno, Hiroyuki Hayashi, Yūko Sagawa, Yasushi Hashimoto, Hirokatsu Uno and Shinsuke Toyoda for their help with sampling; Dr. Hiroshi Itoh and staff at Suidosha Inc. for help in sorting the cnidarians from the bulk IONESS samples, and Tomohiko Kikuchi for the nutrient analyses. I also thank Dr. Hiroyuki Yamamoto of JAMSTEC for mentorship and logistical support.

Thanks also go to Sanae Chiba of JAMSTEC and to Toru Kobari of Kagoshima University, for the loan of their respective ZooScan machines, and to Kazuko Nishikawa for her welcome help with the not-so-automatic vignette sorting; to Yoshito Chikaraishi, Masashi Tsuchiya, Nao Ohkouchi and Yoko Sasaki of JAMSTEC for the stable isotope analyses; and to Allen Collins of the National Museum of Natural History, Washington and Nanae Fukumoto of JAMSTEC for their help with sequencing.

I gratefully acknowledge programmatic support from the Alfred P. Sloan Foundation. This work was partially funded by the Japan Society for the Promotion of Science (JSPS) KAKENHI – grant number 24248032. This study is a contribution to the Census of Marine Zooplankton (CMarZ), an ocean realm field project of the Census of Marine Life (CoML), the Japan National Regional Implementation Committee of the Census of Marine Life, and the International Network for Scientific Investigations of Deep-Sea Ecosystems (INDEEP).

Appendices

Appendix 1

First application to Japanese waters of automated plankton identification using the ZooScan-ZooProcess-Plankton Identifier system: methodological overview

Introduction

As technological advances have allowed faster and better quality data acquisition from more and more extreme environments, automated data analysis has become a necessity in order to deal with the quantity of information provided daily by physical and chemical remote sensors, or by in-situ camera and video platforms. However, more traditional data acquisition methods such as plankton net towing may also, when performed on a daily or weekly basis, yield quantities of information that are not practical to analyze manually. It was in this context that the first ZooScan was built and the ZooProcess and Plankton Identifier softwares developed, in order to create a virtual library of the contents of plankton nets towed daily at the long-term monitoring station Point B in the Mediterranean Sea near Villefranche sur Mer, France (Gorsky *et al.*, 2010; Warembourg, 2005).

This system is composed of 3 main steps: sample scanning, image analysis, and automatic identification. In the present study, these steps were performed as follows:

1. Scanning was performed at 2400 dpi using a Hydroptic ZooScan v.1 with the Vuescan 8.4.57 and ZooProcess 7.12 softwares, or a Hydroptic ZooScan v.3, set in a backlighting mode, with the Vuescan 9.0.51 and ZooProcess 7.13 softwares.

2. Image analysis was performed using the default parameters of the ZooProcess softwares, with a gamma value of 1.0.

3. Automatic identification of plankton was conducted using the Plankton Identifier software (Gasparini, 2007), in which a pre-established algorithm sorts images based on a user-defined template called the learning set. For the present analysis, the Random Forest (Breiman, 2001) algorithm was chosen.

It is at this 3rd step that problems inherent to the automation of image analysis appear: the best of models can, and will, predict only those characters for which they were programmed. The automated sorting of images relies on digital, computer-generated characters of images, measured in pixels or in various colour or gray-scale values. Additionally, for the models presently applied to automatic image sorting, all images of a given data set will be sorted into the categories contained in the template. Therefore, the adequacy of the output of the automated image sorting relies highly on the adequacy of the template on which it was based. The template must therefore be carefully constructed, in order to best represent the goals of the study (number, biological meaning of the categories chosen), while keeping with the mechanical and computational limitations of the software.

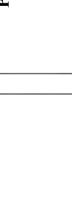
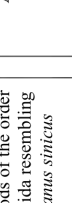
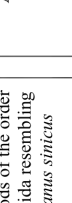
Calanoida1 (525)		Copepods of the order Calanoida resembling <i>Calanus sinicus</i>	Annelida (156)		Pisces (23)		Fish and non-euphausiid adult crustaceans
Calanoida2 (532)		Copepods of the order Calanoida resembling <i>Calanus sinicus</i>	Appendicularia (62)		Protista (172)		
Calanoida3 (536)		Copepods of the order Calanoida resembling <i>Calanus sinicus</i>	Chaetognatha (240)		Salpa (9)		Salps and doliolids
Cyclopoida (104)		Copepods of the order Cyclopoida	Echinodermata (22)		deadCope (517)		Crustacean body parts (Copepoda, Ostracoda, Euphausia, ...)
Eucalanidae (533)		Copepods of the Calanoida family Eucalanidae	Egg (240)		Particles : ‘Fiber’ ⁽⁵⁰³⁾ ‘ParticleBig’ ⁽⁵⁴²⁾ ‘ParticleSmall’ ⁽⁵⁰⁹⁾		Non-living organic and inorganic particles (different shapes)
Harpacticoida (17)		Copepods of the order Harpacticoida	Other Crustacea (47)		Calyptophora (14)		Siphonophore cnidarians
Heterorhabdidae (138)		Copepods of the Calanoida family Heterorhabdidae	Mollusca (26)		badfocus (352)		Scanning artifacts and air bubbles
Poecilostomatoida (423)		Copepods of the order Poecilostomatoida	Nauplius (382)		FishScales (185)		Loose fish scales
			Ostracoda (529)		multiple (567)		Images containing multiple organisms

Table 13: Composition of the learning set; in parentheses, the number of images making up each category.

1. Establishment and validation of a learning set adapted to the waters off south-eastern Japan

The IONESS net system used during the MULTI-SPLASH cruise was composed of 7 nets, the first, open during the descent, and the following 6 nets sampling successively on the upward tow. The first net of the midwater nighttime IONESS tow performed on March 24th therefore sampled from the surface down to 700 m (I060324d0). This unsplit sample, containing all size classes sampled by the IONESS, was used as a base for the learning set created for the present study. To this were added images from the nighttime IONESS samples processed for the study of the potential prey field (*cf.* Chapter III.1), in order to improve the efficiency of the automatic sorting.

The learning set created for the identification of the IONESS samples contained 29 categories (Table 13), each category containing between 9 and 567 images. The images defining each category covered the widest possible range of sizes, shapes and shades, a fact discussed below. This learning set was then used, in conjunction with the decision tree algorithm Random Forest (Breiman, 2001), to automatically sort the scanned IONESS samples into the predefined categories.

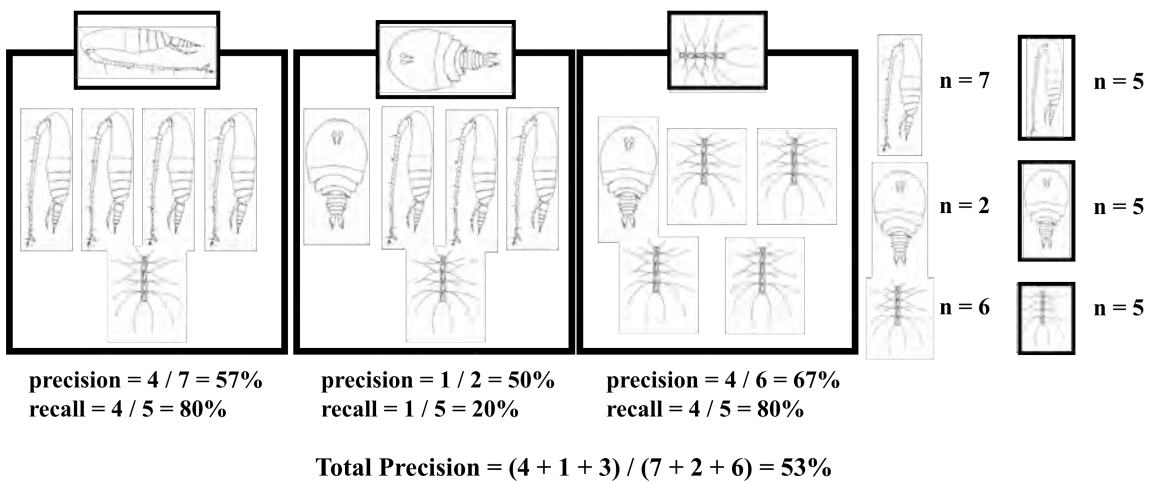


Figure 27: Graphical representation of the three parameters used to test the efficiency of automatic recognition: total precision (total proportion of correctly sorted images), precision (proportion of the images of a given category correctly sorted) and recall (proportion of correct images sorted into a given category). Animals represent individual images, boxes represent image categories.

The automatic sorting was verified manually, and the efficiency of the automatic sorting was tested using 3 parameters (Fig. 27):

- Total precision: total proportion of correctly sorted images
- Precision: proportion of the images of a given category correctly sorted
- Recall: proportion of correct images sorted into a given category

The more efficient the data set, the higher these 3 parameters become, on a 0 to 100% scale. However, as seen in figure 27, the Precision and Recall parameters are influenced both by the efficiency of the sorting, and by the total number of animals in a given category. Indeed, these two parameters will show more extreme variations (precision values of 0 or 100%) in rare categories than in those containing numerous organisms, and the interpretation of extremely high (or low) values of precision and recall parameters in these categories must be done with care.

Total Precision = 62%

	precision (%)	recall (%)	n
<i>Calanoida1</i>	74.11	67.73	1062
<i>Calanoida2</i>	41.51	27.33	212
<i>Calanoida3</i>	35.40	75.32	2526
<i>Cyclopoida</i>	81.82	12.86	11
<i>Eucalanidae</i>	88.50	68.87	766
<i>Harpacticoida</i>	0.00	n/a	11
<i>Heterorhabdidae</i>	27.49	61.70	211
<i>Poecilostomatoidea</i>	38.26	34.85	563
<i>Annelida</i>	12.20	50.00	82
<i>Appendicularia</i>	0.00	0.00	1
<i>Chaetognatha</i>	87.62	38.98	106
<i>Echinodermata</i>	0.00	n/a	5
<i>Egg</i>	18.08	22.00	426
<i>Krill</i>	38.10	18.18	12
<i>Mollusca</i>	30.00	25.00	10
<i>multiple</i>	49.13	29.04	345
<i>Nauplius</i>	17.65	0.84	17
<i>Ostracoda</i>	87.51	28.35	865
<i>Phytoplankton</i>	77.14	3.63	35
<i>Pisces</i>	33.33	6.67	4
<i>Protista</i>	50.00	0.56	4
<i>Salpa</i>	33.33	50.00	3
<i>deadCope</i>	34.77	61.57	935
<i>Fiber</i>	83.06	100.00	2126
<i>ParticleBig</i>	57.67	73.51	2303
<i>ParticleSmall</i>	81.38	92.49	3872
<i>Calycophora</i>	0.00	0.00	3
<i>badfocus</i>	55.23	87.48	2189
<i>FishScales</i>	70.00	90.24	370

Table 14: Efficiency of the automatic identification of the Kamogawa 700 to 400 m plankton samples: total precision (total proportion of correctly sorted images), precision (proportion of the images of a given category correctly sorted) and recall (proportion of correct images sorted into a given category); n: number of images of each category; n/a: value cannot be calculated with null divisor.

The learning set established for the present study showed automatic image recognition to be a promising method for the study of planktonic communitites off south-eastern Japan. Automatic plankton identification using the established learning set showed a global precision of between 52 and 62%, the highest precision being for the automatic sorting of the 700- to 400 m stratum (Table 14), followed by the 400- to 0 m stratum, and finally the 1000- to 700 m one. This could be directly linked to the learning set having been established using a majority of samples collected above 700 m. The identification efficiency of the different categories varied, the categories “Calanoida 1”, “Chaeognatha” and “Eucalanidae” showing high efficiency throughout all samples, and categories such as “Calanoida 2” and “Nauplius” having a low automatic sorting efficiency. Rare categories, for which the learning set contained only a couple of dozen images, generally had a lower identification efficiency, except for the categories “Cyclopoida” and “Salpa”, for example, as the specific morphology and patterns of these organisms allowed them to be easily distinguishable.

Indeed, a category is characterized by the images it contains: for each category characteristic (size, grey scale value, etc...), a Gaussian bell-curve is established from the combination of the characters of each image in that category, and the probabilities associated with this curve are used by the sorting algorithms to determine whether an unidentified image is, or is not, of that category. In a category containing an insufficient number of images, the characters associated with a given category may not correctly represent the images it should contain. However, because these categories are rare, they do not greatly influence the total sorting efficiency and, indeed, Gorsky *et al.* (2010) found that once all categories contained a sufficient number of images to characterize them (200 – 300 images), total precision increased little with the addition of images to the learning set.

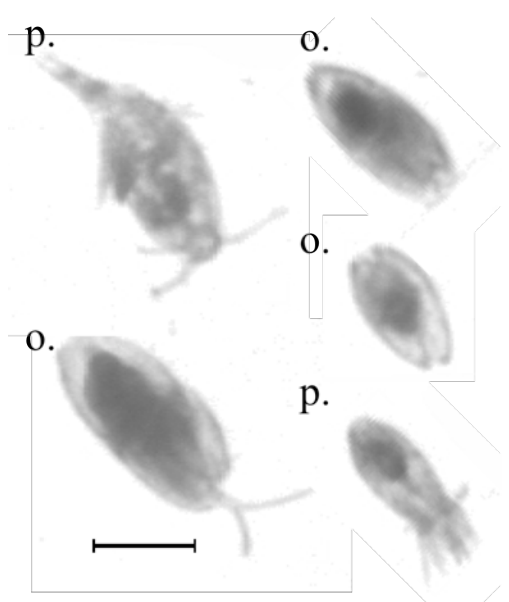


Figure 28: Examples of images of the categories “Ostracoda” (o.) and “Poecilostomatoida” (p.) that showed low automatic recognition efficiency. Scale bar = 1 mm.

The category “Ostracoda”, which had amongst the highest precision rates ($> 80\%$), often had very low recall values. This was because, when oriented in a certain manner during scanning, some Poecilostomatoida copepods greatly resemble ostracods, by their general shape and shade of grey (Fig. 28). To resolve this kind of problem, hardware modifications such as the modification of the light intensity during scanning, or the implementation of some kind of polarization filter may be necessary.

Although up to half the scanned images had to be manually resorted into the correct categories (a total precision of 52% indicates 48% of images are incorrectly sorted), the quality of the images obtained usually allowed a rapid manual identification, and the automatic measurements of the different parameters, scanning and automatic image recognition was found to be a time-gaining procedure, compared to the manual identification and especially to the manual measurement of organisms under the microscope. As the quality of the learning set improves, the amount of time involved in manually verifying the automatic sorting should decrease. Additionally, the Zooscan-ZooProcess system allowing the imaging of between 1000 and 2000 particles per scan, this method should give a better estimate of the rare planktonic categories, which tend to be underestimated by the amount of splitting the sample requires to allow rapid manual identification.

2. Estimation of copepod prosome length from pixel-based measurements derived from the ZooScan and ZooProcess systems.

After **Mary M. Grossmann** and Dhugal J. Lindsay: Estimation of calanoid copepod prosome length from pixel-based measurements derived from the ZooScan and ZooProcess systems. *Bull. Plankton Soc. Jpn.* (accepted)

Introduction

Recent technological advances have seen computer-automated image capture and analysis techniques applied to the study of plankton, in a bid for faster and less labour-intensive, if somewhat less reliable, results. The present study focuses on the ZooScan (Hydroptic Inc.), a system that allows high quality greyscale imaging of plankton in the lab, and the associated image processing software, ZooProcess.

A certain number of measurements, such as organism size or weight, are often important parameters in a range of biological studies. However, the dimensions used for the measurement of an organism's size or weight are often phylum-specific. Indeed, many animals possess appendages of variable length and fragility. Because of the fragility and morphological variability of these appendages, they are not usually taken into account when measuring the length of animals. Examples of this include the standard length in fish (from most anterior point of jaw to the end of the vertebral column), mantle length in squid, and carapace length in shrimp (Chihara and Murano, 1997; Fishbase.org; Okutani, 2005).

The length of the prosome is, for most copepod orders, the most-used size measurement, and is also, therefore, the basis of many studies on the mathematical relationships between the length of an animal and other biologically important characters such as body weight or carbon and nitrogen content. Unfortunately, because the automatic image processing software recognizes only numbers of pixels and grey scale values, although a great many parameters are automatically measured on each image (including area, perimeter,

average level of grey, etc...), these do not directly equate to variables that appear in the biological literature.

In order to allow for an easier and more accurate analysis of the data obtained through the ZooScan and ZooProcess analysis, we studied the relationship between automatically-measured image parameters and prosome length in two of the most abundant copepod orders off south-eastern Japan: the Calanoida and Poecilostomatoida.

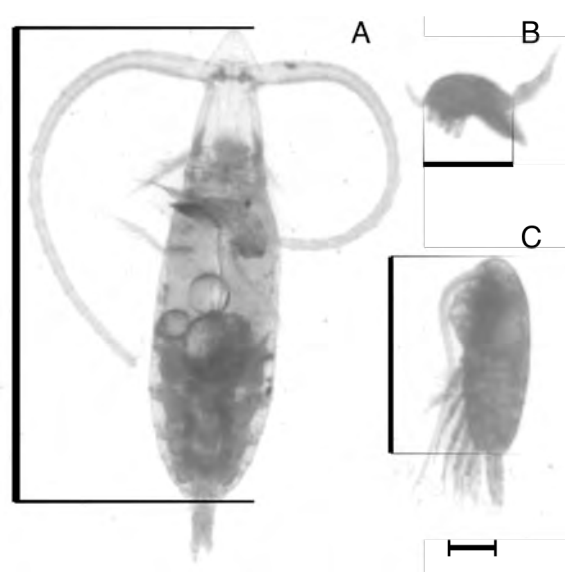


Figure 29: Illustration of the prosome length measurement applied to the calanoid family Eucalanidae (A), the order Poecilostomatoidea (B), and all other calanoid copepods (C). Scale bar = 1 mm.

Materials and Methods

As part of the MULTI-SPLASH cruise that took place aboard the *R/V Kaiyo* (KY06-03), plankton samples were collected, at nighttime, east of Oshima Island ($34^{\circ}42'N$, $139^{\circ}50'E$) on the 24th of March 2006 using a 330 μm -meshed IONESS (Intelligent Operated Net Environmental Sampling System) net (Kitamura *et al.*, 2001). Previous studies on the copepod populations of Sagami Bay having shown the highest species richness to be between 300 and 500 m-depth (Shimode *et al.*, 2006), the 400 to 500 m IONESS depth stratum was therefore studied, in order to analyse the largest taxonomic breadth possible. The bulk samples were preserved in 5% seawater-buffered formalin. After removal of all gelatinous plankton and after being filtered through a 5 mm mesh, the remaining sample was split using a Motoda Box Splitter, in order to obtain aliquots containing about 4000 individuals. The aliquots were scanned on a Hydroptic ZooSCAN v.1 using the ZooProcess 7.12 and Vuescan 8.4.57 software. The 24 x 15 cm 2400-dpi resolution scans (14150 x 22640 pixels) were processed with ZooProcess using the default parameters and a gamma value of 1.0. This produced a data set composed of ‘vignettes’, single-animal images with which are associated a certain number of parameters, automatically measured by the ZooProcess software, describing the size (in pixels), and shade (in levels of greyscale) of the object in the vignette (Gorsky *et al.*, 2010).

Vignettes containing copepods were identified to order or family level using the *Illustrated Guide to Marine Plankton In Japan* (Chihara and Murano, 1997). The prosome length of copepods was measured manually on random vignettes, using Adobe Illustrator v.5.1 (Fig. 29). The images were chosen for the cleanliness of the animal they contained (no overlapping particles or animals), in order to assure correct automatic size calculations, and the certitude of its identification, but no discrimination was performed on the basis of size or animal orientation.

Plots were performed with the R package ggplot2 (Wickham, 2009), and linear regressions were calculated using the linear model function ‘lm’.

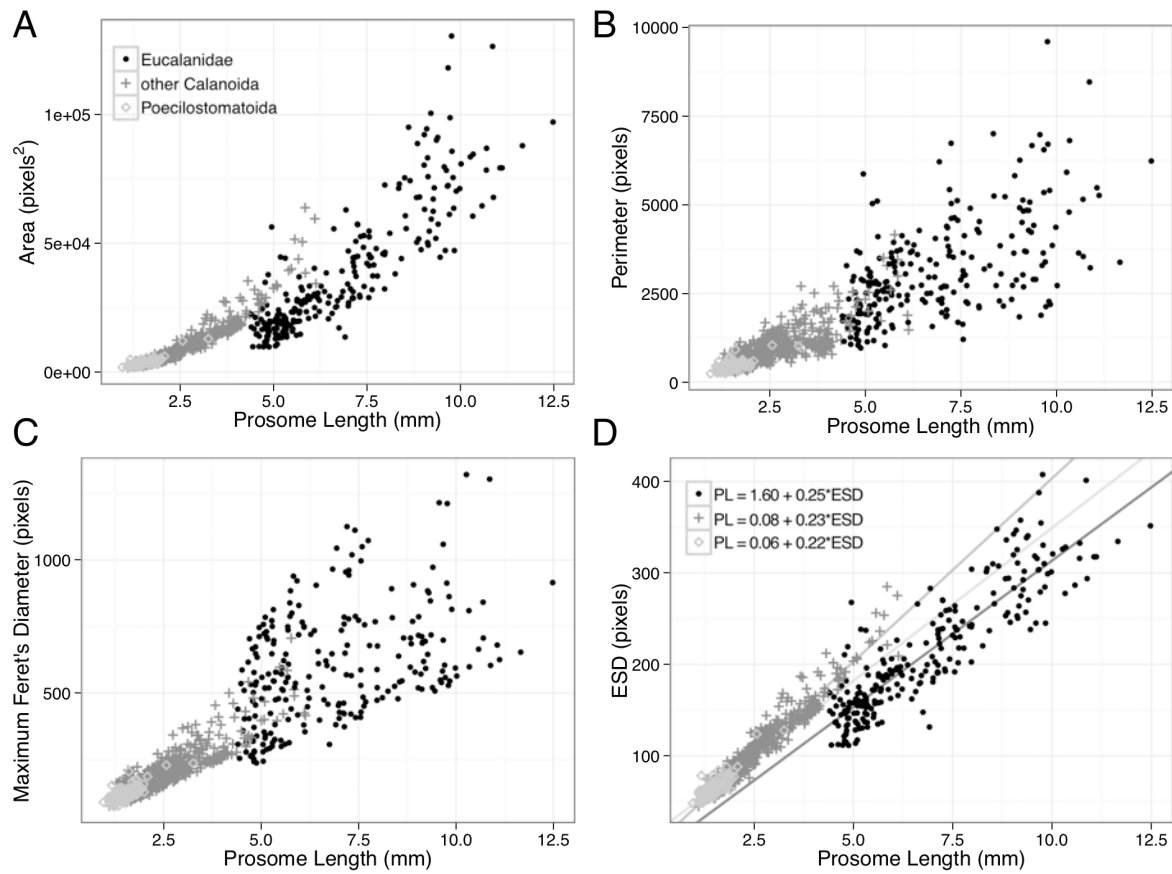


Figure 30: Relationships between prosome length and area (A), diameter (B), maximum Feret's diameter (C) and equivalent spherical diameter (ESD) (D). In D, the linear regressions and their equations are shown. Prosome length in mm, area in pixels², maximum Feret's diameter, perimeter and ESD in pixels.

Results

The prosome lengths of 1166 copepods were measured. These corresponded to 1018 copepods of the order Calanoida (of which 242 were of the family Eucalanidae), and 148 copepods of the order Poecilostomatoida. These two orders represented 89.93 and 4.82% of the total copepod abundance in the samples, respectively (not shown).

The prosome length measurements were plotted as a function of some of the image parameters automatically measured by the ZooProcess software: Area (the surface of the object), Perimeter (length of the outside boundary of the object), maximum Feret's diameter (the longest distance between any two points on the object boundary), and Equivalent Spherical Diameter (ESD: $2\sqrt{\text{Area}/\pi}$) (Fig. 30). The calanoid family Eucalanidae formed a distinct group from the other calanoid families, and was therefore considered separately to improve the estimation of the rest of the calanoid copepods. The ESD was found to have the best linear correlation with prosome length (Table 15), and a global equation could be established (regression coefficient $r^2 = 0.943$) for all Calanoida excepting those of the family Eucalanidae:

$$\text{PL (mm)} = 0.08 + 0.023 * \text{ESD (pixels)}$$

The regression coefficients being lower for the calanoid Eucalanidae family and the Poecilostomatoida order, the estimated prosome lengths will be slightly erroneous at either end of the size spectrum.

Additionally, there was found to be no statistical difference in the automatically-measured ESD depending on the orientation of the animal in the image (ventro-dorsal versus lateral orientations) for the family Eucalanidae (Mann-Whitney-Wilcoxon test, $n= 50$, $p = 0.23$), the rest of the order Calanoida excepting the family Eucalanidae (Mann-Whitney-Wilcoxon test, $n= 296$, $p = 0.78$) or the Poecilostomatoida (Mann-Whitney-Wilcoxon test, $n= 96$, $p = 0.34$).

Taxon	Equation	Regression Coefficient (r^2)	Prosome Length Range
Calanoida	$PL = -0.57 + 0.032*ESD$	0.911	1.10 - 12.48 mm
Eucalanidae	$PL = 1.60 + 0.025*ESD$	0.793	4.21 - 12.48 mm
Calanoida minus Eucalanidae	$PL = 0.08 + 0.023*ESD$	0.943	1.10 - 6.13 mm
Poecilostomatoidea	$PL = 0.06 + 0.022*ESD$	0.739	0.95 - 3.25 mm
Calanoida + Poecilostomatoidea	$PL = -0.575 + 0.032*ESD$	0.919	0.95 - 12.48mm

Table 15: Regression equation of copepod prosome length (PL) against equivalent spherical diameter (ESD), for common copepod orders and families collected between 400 and 500 m, east of Oshima Island, in south-eastern Japan on March 24th, 2006. PL in mm; ESD in pixels.

Discussion

The sampling location, in the midwater zone east of Oshima island, was chosen as, due to the dynamism of the flow path of the Kuroshio current, this zone is influenced by many different water masses, with Kuroshio, Oyashio, Sagami Bay, and Tokyo Bay signatures (Grossmann and Lindsay, 2013b; Senju *et al.*, 1993; Shimode *et al.*, 2006). The copepod population on which the present study was performed was therefore hopefully general enough in taxonomic breadth that the regressions obtained may be applicable to all waters off southern, and along the eastern coast of Japan.

The Equivalent Spherical Diameter (ESD (pixels) = $2*\sqrt{(\text{Area}/\pi)}$), automatically measured by the image analysis software, showed a good linear relationship with the manually-measured prosome length of two of the most abundant copepod orders. This relationship was not influenced by the orientation of the copepods in the scanned images. With the exception of copepods of the family Eucalanidae, the prosome length of all calanoid copepods could be estimated by a single regression equation. Copepods of the family Eucalanidae have a distinct morphology and image texture that makes them easily recognisable by the imaging software. In the present data set, the family Eucalanidae was accurately identified 88% of the time (unpublished data) using the Random Forest algorithm (Breiman, 2001) in the Plankton Identifier software (Gasparini, 2007), and they are therefore relatively easy to remove from the total copepod image dataset. For the order Poecilostomatoida, the lower regression coefficient means prosome sizes will be slightly erroneous at both ends of the size spectrum.

These regressions provide a rapid and efficient way of analysing copepods from the automatically generated data obtained from the ZooProcess image analysis process. The obtained information on prosome length allows an easy comparison with literature results, such as those available for long-term monitoring stations. Additionally, copepod biomass in terms of carbon and nitrogen may be estimated following previous studies based on samples from Japanese waters providing regression equations based on prosome length (e.g. Uye, 1982). In this manner, the automated analysis of copepods may help provide large amounts of information for the study or modelling of matter transport and marine trophic webs.

Appendix 2

Application of DNA barcoding to the identification of Siphonophora

In part to be included in: **Mary M. Grossmann**, Dhugal J. Lindsay and Allen G. Collins: Use of the mitochondrial 16S gene for barcoding in the calycophoran siphonophore family Diphyidae, and its' application to the redescription of *Lensia leloupi* Totton, 1954. (*in preparation*)

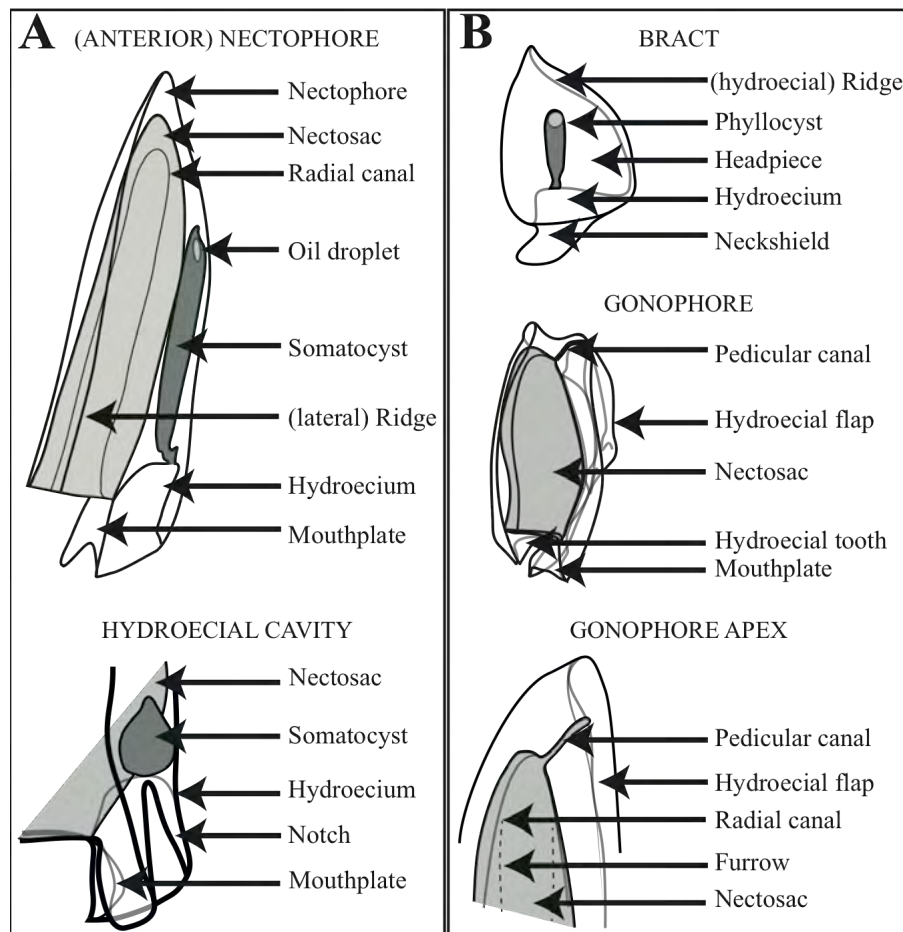


Figure 31: Guide to the taxonomic terms employed for the description of A: polygastric stages (example of anterior nectophore); and B: eudoxid stages of diphyid-type calycophoran siphonophores. Schematic diagrams not representative of any given species; not to scale.

Introduction

Most invertebrate taxa have complex life styles, composed of a succession of different life stages that do not necessarily share any common morphological traits. Regrouping all life stages of an organism under the same species name is therefore challenging when using morphology alone, and the identification of different life stages of species under different names is not uncommon in the history of binomial taxonomy. Within the Cnidaria, the Anthomedusae and Athecata orders, and the Leptomedusae and Thecata orders separated the medusoid and polypoid forms, respectively, of species presently regrouped into the Anthoathecata and Leptotheccata. In the order Siphonophora, species are usually established based on the morphology of at least one swimming bell of the polygastric stage, and eudoxid stages whose polygastric stages have yet to be determined have traditionally been placed in the genus *Eudoxia*. No other life stages have been described unless they could be linked to a known polygastric stage (e.g. Russell, 1938; C. Carré, 1979; D. Carré, 1972), except for the small post-larval physonect stage *Mica micula* Margulis, 1982, which may well be conspecific with *Pyrostephos vanhoeffeni* Moser, 1925 (Grossmann *et al.*, 2013b).

DNA barcoding is a technique in which a small but variable portion of nuclear or mitochondrial DNA, usually 500 to 900 base pairs in length, is used as a ‘barcode’ for specific identification. The sequences will usually show relatively little intra-specific variation, but sometimes considerable inter-specific variations. A certain number of genes, such as the mitochondrial Cytochrome Oxydase I (COI), or ribosomal 16S genes, or the nuclear Internal Transcribed Spacer (ITS) provide areas that can be relatively easily amplified in all organisms using universal or phylum-specific primers, and which can be sequenced at good cost-efficiency using first-generation sequencing techniques.

DNA Barcoding techniques have been shown to be useful in linking the morphologically differing medusae stages and their sessile polyps (e.g. Miranda *et al.*, 2010). However, they have yet to be applied to the identification of the different life stages of siphonophores. DNA barcoding was first tested in the cnidarian sub-phylum Medusozoa by Ortman *et al.* (2010), using the mitochondrial Cytochrome Oxydase 1 (COI) gene. This gene proved to be a powerful tool applicable to a large number of tested species and genera. However, only 15 out of the 54 valid species of the family Diphyidae were included in the study and, of those, only 3 out of the 9 species of the genus *Lensia* included showed bootstrap support $\geq 99\%$. Plankton net studies have shown that off south-eastern Japan, Diphyidae was by far the most species-rich and abundant cnidarian family, at nearly all depths from the surface to 1000 m (Kitamura, 2000; Kitamura *et al.*, 2009; present study), of which up to 64% were of the genus *Lensia*. However, this family, and more specifically the genus *Lensia* are relatively little-known taxonomically: of the 26 valid *Lensia* species (World Register of Marine Species), less than half have had their posterior nectophores and/or eudoxid stage described. The present study, presenting the most comprehensive collection of mitochondrial 16S sequences of the calycophoran families Abylidae, Clausophyidae, Diphyidae, and Sphaeronectidae presently available (*cf.* Chapter III.3), allowed DNA barcoding techniques to complement the knowledge of several siphonophore species. The enigmatic eudoxid stage *Eodoxia macra* Totton, 1954 could be successfully linked to its polygastric stage, *Lensia cossack* Totton, 1941; the eudoxid stage and posterior nectophore of the polygastric stage of *Lensia leloupi* Totton, 1941 could be described; the eudoxid stage of *Lensia havock* Totton, 1941 could be identified; and the genetic distinctness of a new species of the genus *Lensia* could be confirmed.

A guide to the taxonomic terms employed is given in Figure 31.

1. *Eudoxia macra* Totton, 1954, is the eudoxid stage of *Lensia cossack* Totton, 1941 (Siphonophora, Cnidaria).

After: **Mary M. Grossmann**, Dhugal J. Lindsay and Allen G. Collins (2013a): The end of an enigmatic taxon: *Eudoxia macra* is the eudoxid stage of *Lensia cossack* (Siphonophora, Cnidaria). *Syst. Biodivers.* **11**(3): 381–387.

Introduction

The genus *Eudoxia* (and its precursor *Ersaea*), extensively used until the early 20th century, has progressively been emptied and, at the present day, contains only one completely enigmatic form: *Eudoxia macra* Totton, 1954. The association of eudoxid and polygastric stages of siphonophores is primarily done through morphological and distributional similarities. Indeed, the phyllocyst of the bract of many eudoxid stages resembles, in shape, the somatocyst of the anterior nectophore of the polygastric stage (Mapstone, 2009; Totton, 1965); and polygastric stages having nectophores with marked ridges tend to have eudoxid stages with ridged bracts (personal observation: e.g. 5-ridged *Lensia*, genera *Diphyes*, *Eudoxoides*, *Muggiaeae*, etc...). Although this identification of eudoxid stages has been performed successfully many times in the Mediterranean Sea (e.g. Gamulin, 1966; Gamulin and Kršinić, 2000; Totton, 1932), where the diversity of Siphonophora is relatively low, the extremely high biodiversity of Japanese waters (Fujikura *et al.*, 2012) would not normally lend itself to this type of enterprise.

Applying DNA barcoding techniques to the cnidarian order Siphonophora, the position of *Eudoxia macra* within the family Diphyidae Quoy and Gaimard, 1827 and, more specifically, amongst *Lensia* species with 5 vestigial ridges is discussed, using both morphological and genetic data from specimens caught in south-east Asian and Antarctic waters.

Species	GenBank accession No.	Depth (m)	Date	Sampling location		
				Lat.	Long.	Location
<i>Eudoxia macra</i>	KC782542	0-400	18-Nov-2011	31°N	132°E	off Kagoshima (Japan)
<i>E. macra</i>	KC782547	0-1076	8-Jun-2012	27°50.05'N	127°00'E	Izena Hole (Japan)
<i>E. macra</i>	KC782548	0-400	15-May-2012	36°40'N	141°50'E	off Fukushima (Japan)
<i>E. macra</i>	KC782549	0-400	14-May-2012	37°30'N	142°00'E	off Fukushima (Japan)
<i>Lensia achilles</i>	KC782553	750-800	19-Mar-2006	35°0.25'N	139°20'E	Sagami Bay (Japan)
<i>L. achilles</i>	KC782554	400-600	23-Apr-2009	35°0.25'N	139°20'E	Sagami Bay (Japan)
<i>L. achilles</i>	KC782555	1000-2000	11-Jan-2008	65°30.06'S	143°0.05'E	eastern Antarctica
<i>L. achilles</i>	KC782556	1000-2000	31-Jan-2008	64°0.62'S	140°0.76'E	eastern Antarctica
<i>L. achilles</i>	KC782557	1000-2000	11-Jan-2008	65°30.06'S	143°0.05'E	eastern Antarctica
<i>Lensia campanella</i>	KC782540	0-400	18-Nov-2011	31°N	132°E	off Kagoshima (Japan)
<i>L. campanella</i>	KC782541	0-400	18-Nov-2011	31°N	132°E	off Kagoshima (Japan)
<i>Lensia cossack</i>	KC782543	0-1076	8-Jun-2012	27°50.05'N	127°00'E	Izena Hole (Japan)
<i>L. cossack</i>	KC782544	0-946	7-Jun-2012	27°47.73'N	126°54.11'E	Izena Hole (Japan)
<i>L. cossack</i>	KC782545	0-946	7-Jun-2012	27°47.73'N	126°54.11'E	Izena Hole (Japan)
<i>L. cossack</i>	KC782546	0-946	7-Jun-2012	27°47.73'N	126°54.11'E	Izena Hole (Japan)
<i>Lensia exeter</i>	KC782550	767-1100	24 Oct. 2010	27°47.73'N	126°54.11'E	Izena Hole (Japan)
<i>Lensia havock</i>	KC782532	200-500	29-Jan-2008	62°0.45'S	139°58.80'E	eastern Antarctica
<i>L. havock</i>	KC782533	500-1000	12-Feb-2008	65°30.64'S	143°1.17'E	eastern Antarctica
<i>L. havock</i>	KC782534	600-650	24-Mar-2006	34°59.43'N	140°15.54'E	off Kamogawa (Japan)
<i>L. havock</i>	KC782535	700-900	24-Apr-2009	35°0.25'N	139°20'E	Sagami Bay (Japan)
<i>L. havock</i>	KC782536	300-600	24-Apr-2009	35°0.25'N	139°20'E	Sagami Bay (Japan)
<i>Lensia hostile</i>	KC782551	200-300	19-Mar-2006	35°0.25'N	139°20'E	Sagami Bay (Japan)
<i>L. hostile</i>	KC782552	800-850	27-Mar-2006	34°42'N	139°50'E	off Oshima (Japan)
<i>Lensia multicristata</i>	KC782537	0-200	27-Jan-2008	53°8.19'S	130°8.19'E	eastern Antarctica
<i>L. multicristata</i>	KC782538	300-600	24-Apr-2009	35°0.25'N	139°20'E	Sagami Bay (Japan)
<i>L. multicristata</i>	KC782539	300-600	24-Apr-2009	35°0.25'N	139°20'E	Sagami Bay (Japan)

Table 16: Characteristics of the samples sequenced for the present work.

Material and Methods

The formalin-seawater preserved material included 4 complete *Eudoxia macra* eudoxids, 9 bracts and 14 gonophores collected in 330 µm-mesh IONESS (Kitamura *et al.*, 2001) tows in March 2006 off south-eastern Japan; 7 gonophores collected with a 1.13 m-diameter fry net (330 µm mesh) between October and December 2010 off the north-eastern coast of Japan; 8 gonophores collected by MOCNESS (Wiebe *et al.*, 1985) from the Sulu Sea in November 2002 (Nishikawa *et al.*, 2007); and 2 bracts and 4 gonophores from MOCNESS tows in the Celebes Sea, November 2002 (Nishikawa *et al.*, 2007). Specimens of 23 species of *Lensia*, from the collections of the Japan Agency of Marine-Earth Science and Technology, were also examined.

Twenty-two specimens of 7 species of the genus *Lensia*, and 4 *Eudoxia macra* gonophores were collected using plankton nets and preserved in 99.5% ethanol or frozen at -20°C onboard after identification to species level (Table 16). Frozen specimens were transferred to 99.5% ethanol before DNA extraction. For 15 specimens (GenBank accession numbers KC78253434, 40-53), total DNA was extracted using the Qiagen DNEasy Blood & Tissue kit, and a 623 bp segment of the mitochondrial 16S gene amplified and sequenced using ‘primer 1’ and ‘primer 2’ from Cunningham and Buss (1993) with the TaKaRa ExTaq and BigDye kits. Sequencing was performed on an ABI 3130xl sequencer. For the other eleven samples, DNA extraction, amplification and sequencing were performed following the protocol established in Collins *et al.* (2008). Sequence alignment was performed manually using the Se-Al v.2.0a11 software (Rambaut, 2002). Intra- and inter-specific genetic variation was calculated as the Kimura 2 parameter (K2P) genetic distance using MEGA ver. 5.05 (Tamura *et al.*, 2011). A Bayesian analysis was performed on MrBayes ver. 3.2.1 (Huelsenbeck and Ronquist, 2001; Ronquist and Huelsenbeck, 2003) under a General Time Reversible (GTR) model, with 1 million generations, a sampling every 1000 generations, and a burn-in period of 5000 generations. The convergence of the data was verified using Tracer v. 1.5 (Rambaut and Drummond, 2003). The consensus tree was analyzed in FigTree v. 1.4.0 (Rambaut, 2007). A Neighbour-Joining analysis was performed using MEGA ver. 5.05 (Tamura *et al.*, 2011), with complete gap deletion. Bootstrap support was estimated over 1000 replicates.

Artwork was created from photographs of formalin-preserved specimens using Adobe Illustrator CS5.1.

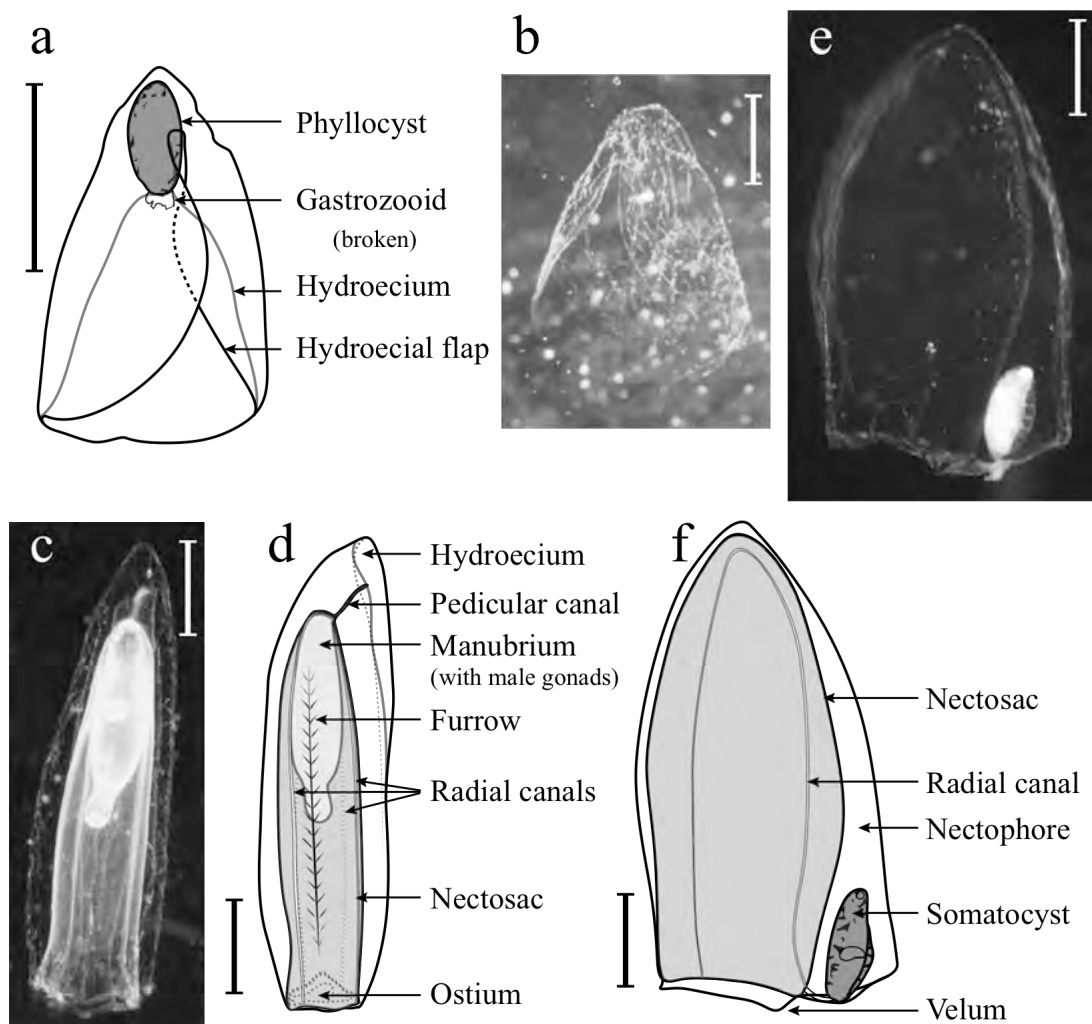


Figure 32: *Eudoxia macra* (a, b: lower view of bract, c: right lateral view of gonophore, d: upper view of gonophore); and *Lensia cossack* (e, f: right lateral view), collected in Japanese waters (south of Kamogawa (a), east of Oshima Island (b), off north-eastern Japan (c, d), and North of Okinawa (e,f)). Scale bar = 1 mm.

Results

The *Eudoxia macra* material conformed with that described and illustrated by Totton (1954), being elongate, without any marked teeth or ridges. The bracts (Fig. 32 a-b) were conical, with a smooth transition between headpiece and neck shield, about 2 mm tall. The distal margin showed a small, shallow central notch in some specimens. The hydroecium, reaching to 80% of the bract height (from distal edge of the neck shield), was enclosed by large lateral flaps of the neck shield. The phyllocyst, of variable size, was ovoid, extending from the roof of the hydroecium nearly to the apex of the bract. The gonophores (Fig. 32 c-d) were elongate, 5 mm tall on average, without ridges or mouthplate but with large longitudinal furrows, and a large bluntly pointed proximal projection directed towards the lower side. Small hydroecial flaps bordered the flat hydroecial surface of the gonophore, at the proximal end, but were undeveloped at the distal (ostial) end. The pedicular canal extended from the gonophore surface to one side of the apex of the nectosac, as shown in Fig. 32 (c); it gave rise to four radial canals which each passed distally down the nectosac to the ostial region of the gonophore. The nectosac was 40% thinner and 15% shorter than the nectophore.

Due to the morphology of *Eudoxia macra*, we considered *Lensia* species without marked ridges to be a possible polygastric stage of it. However, because the eudoxids of multistriate *Lensia* species have yet to be described, a couple of representatives of this group were also included in the study. Following the results of a study using the mitochondrial COI gene (Ortman *et al.*, 2010), 7-ridged *Lensia* species were expected to be the closest related species, and *L. achilles* Totton, 1941 was chosen to represent the 5-ridged *Lensia*, and placed as outgroup.

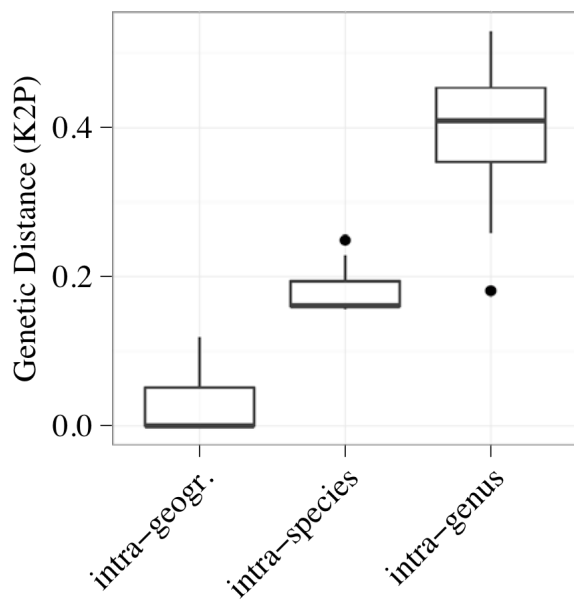


Figure 33: Quantile boxplot of the genetic distance (Kimura-2-Parameter) between species (“intra-genus”); between individuals of the same species from different geographic locations (intra-specific, inter-geographic; “intra-species”); and between individuals of the same species from the same geographic location (intra-specific, intra-geographic; “intra-geogr.”).

A total of 26 mitochondrial 16S sequences were obtained, of which four belonged to *E. macra*. All sequence data has been deposited on GenBank (Table 16). The presence of a barcoding gap between all but the multistriate *Lensia* species was verified (Fig. 33). The phylogenetic tree (Fig. 34) showed a perfect discrimination between the seven considered species (Bayesian posterior probabilities = 100%, Neighbour-Joining bootstrap \geq 99%). Three main morphologically dissimilar *Lensia* subgroups could be discerned, with the 5-ridged *L. achilles* placed as outgroup: the 7-ridged group containing *L. havock* Totton, 1941 and *L. multicristata* (Moser, 1925); the multistriate group with *L. exeter* Totton, 1941 and *L. grimaldi* Leloup, 1933, and, finally, *Lensia* without marked ridges: *L. campanella* (Moser, 1925) and *L. cossack* Totton, 1941. Additionally, for the three species for which specimens from the Southern Ocean could be obtained, the sequences formed distinct clades according to their geographic origin, and the intra-specific variation between samples from different geographic areas (intra-specific, inter-geographic) was on average six times higher than that between specimens from the same geographic area (intra-specific, intra-geographic) (Fig. 33). Nucleotide differences between sequences varied from 9.5 to 21% for inter-species comparisons, from 8 to 12.2% for inter-geographic intra-specific comparisons, and from 0 to 6.6% for intra-geographic intra-specific comparisons.

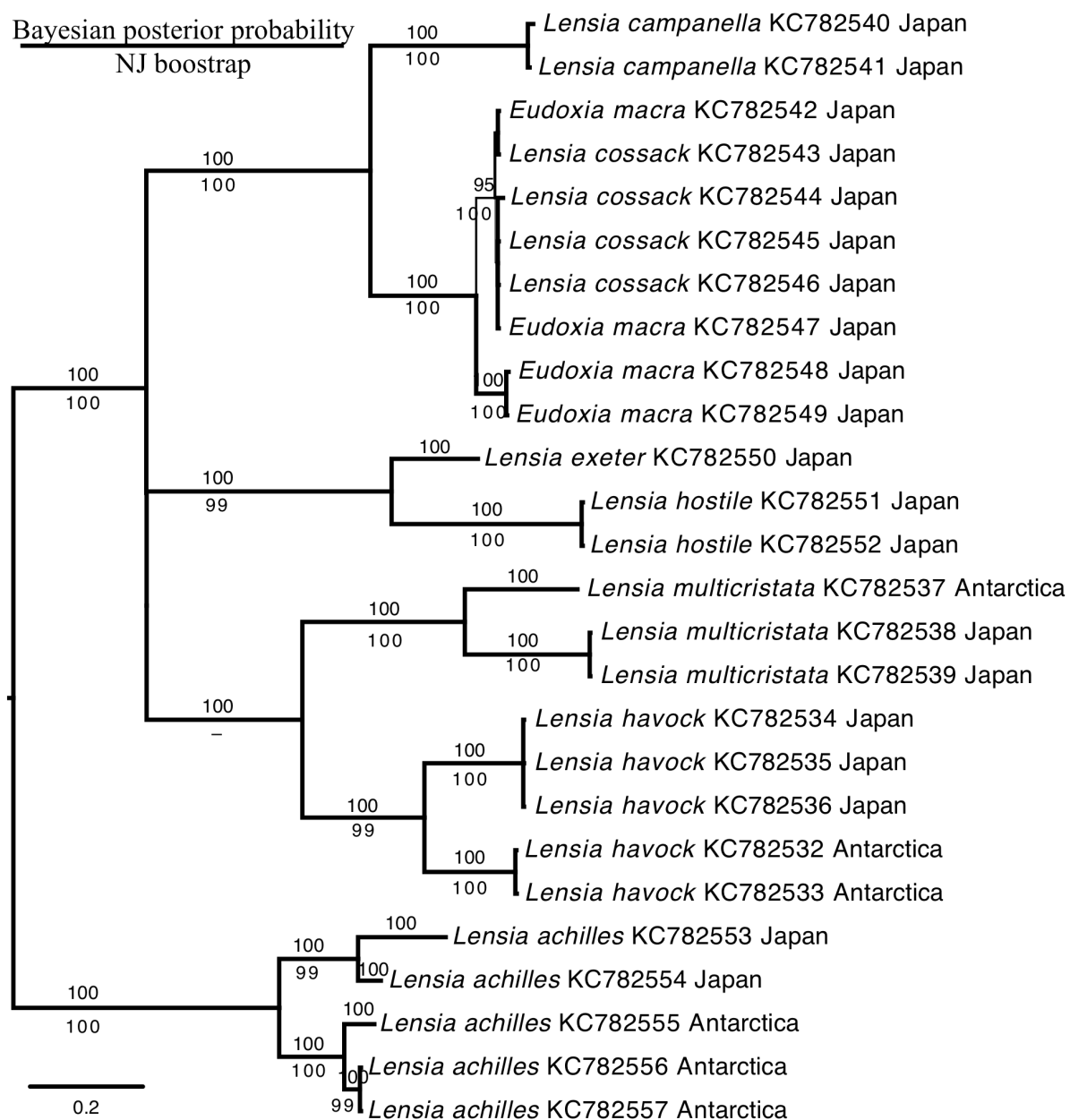


Figure 34: Bayesian consensus tree based on the mitochondrial 16S gene. Bayesian posterior probabilities (top) and Neighbour-Joining bootstrap values (bottom) in percent. Terminal posterior values, and those inferior to 95% not shown. Scale represents 0.2 substitutions per site.

All *Eudoxia macra* sequences formed a statistically supported clade containing all four *Lensia cossack* polygastric stage specimens (Fig. 34). This clade was subdivided into two sub-groups, with lower posterior probability values, only one of which contained the *L. cossack* samples. These two groups corresponded to small-scale geographic variations, the group containing the *L. cossack* samples being from waters south of mainland Japan, while the two *E. macra* samples forming the second group were from off the north-eastern shores of the main island of Japan. The genetic distances between sequences from these two groups were of 0.061 at their highest, well below the average inter-species distances observed for this group (Fig. 33). Microscope observations of the sequenced *E. macra* samples did not uncover sufficient morphological differences to discriminate two distinct species.

Discussion

First described from the Indian and Atlantic Oceans (Totton, 1954), *Eudoxia macra* has since been found in all tropical and temperate waters (Alvariño, 1980; 1981; Alvariño *et al.*, 1990; Daniel, 1985; Kitamura, 2000; 2009; Gao *et al.*, 2001; Grossmann and Lindsay, 2013b; Patriti, 1970; Totton, 1965; Xu *et al.*, 2008; Zhang, 1984; 2005; Zhang and Lin, 1997). In the present material from along the north-eastern and south-eastern shores of Japan, the bracts and gonophores, of similar size to those reported from the western Pacific (Zhang, 1984), were up to twice as long as those described by Totton (1954) from the Indian ocean, or the ones collected in the Sulu and Celebes Seas for the present study. The samples collected south of Japan during the March MULTI-SPLASH cruise had undeveloped gonads, while samples collected in May and June from similar locations possessed mature or spent gonads. No pigmentation was observed in any of the live material from Japanese waters. This could possibly represent a geographical variation from the specimens from the Atlantic and eastern coast of Africa described by Totton (1954), which were stated to have a manubrium with a “deeply pigmented tip”.

Based on the sequences of a fragment of the 16S ribosomal RNA gene, *Eudoxia macra* formed a well-supported clade with *Lensia cossack*. These latter were about 4.5mm tall, without marked ridges (Fig. 32 e-f), and without the characteristic apical twist observed in some preserved *L. campanella*. The somatocysts of the anterior nectophores were of the same general shape as the phyllocysts of *E. macra* bracts. Both *E. macra* and *L. cossack* are present in all oceans, if not very common in the Pacific, mostly in the tropical to subtropical zone, and primarily in the upper 500 m of the water column (Margulis, 1971; Zhang, 2005).

Although only two *Lensia* without marked ridges were successfully sequenced, *Lensia campanella* and the remaining three non-ridged *Lensia* species, *L. asymmetrica* Stepanjants, 1970, *L. meteori* (Leloup, 1934b) and *L. subtilis* (Chun, 1886) all have known eudoxid stages, described by Carré (1968), Pugh and Pagès (1997), Gamulin and Kršinić (2000), and Totton (1932), respectively. A eudoxid stage associated with *L. cossack* was briefly described and illustrated by Daniel (1985), but the illustration does not resemble *Eudoxia macra*, and, as the listed characters are insufficient to assign it to another species, this record is considered a *nomen nudum*.

Daniel (1985) tentatively assigned *Eudoxia macra* to *Sulculeolaria chuni* (Lens and van Riemsdijk, 1908). However, rearing experiments of the latter by Claude Carré (1979) showed this species released only the gonophores of the cormidia, the bracts and gastrozooids and tentacles remaining attached to the stem. Additionally, *Sulculeolaria* cormidia differ morphologically from *Eudoxia macra*, the bracts being flattened as in *Chuniphyes*, curled around the stem so as to form a cone, with marked basal teeth. No phyllocyst has so far been described in *Sulculeolaria* bracts, while Figure 4 in Carré (1979) shows two lateral bracteal canals. The gonophores display clear ostial teeth (Vogt, 1854; Carré, 1979).

The three genetically and morphologically dissimilar groups found within the genus *Lensia* corresponded to those previously observed using the mitochondrial COI gene (Ortmann *et al.*, 2010), and may, once a sufficiently representative genetic database is established, serve as a solid base for a splitting of the genus *Lensia* in order to obtain new, monophyletic genera. Another important result from the present study was the quantification of intra-specific distances observed amongst taxa from different geographic regions, and the separation of the sequences of a given species into distinct clades according to their geographic origin, and this even at a regional scale. Small-scale geographical differences may also explain the higher genetic distance (0.12) found between the two Japanese *L. achilles* samples. Indeed, although both sampled in Sagami Bay, KC782554 was collected between 400 and 600 m, a depth at which waters of northern origin such as the Oyashio Intermediate Water (Senju *et al.*, 1998) periodically intrude into the Bay, while KC782553 was collected between 750 and 800 m, a more hydrographically stable layer. The depth of the inter-geographic divergences observed in *L. achilles*, *L. havock* and *L. multicristata*, with K2P genetic distances between 0.16 and 0.25, and between 8.0 and 12.2% nucleotide differences, were similar to the inter-specific variations found between the multistriate *Lensia*, and those between *L. campanella* and *L. cossack*, and may reflect the existence of cryptic species rather than intra-specific variations. More diverse and detailed sampling would be needed to study the extent of regional, water-mass specific and large-scale inter-geographic genetic variation, and the existence of cryptic species complexes within the genus *Lensia*. For DNA barcoding to be a useful tool for the reliable identification of Siphonophora by non-experts, not only do a representative number of species need to be present in the databases, these should also cover the widest geographic ranges possible, in order to allow the highest matching probabilities.

Within medusozoan Cnidaria, the mitochondrial 16S gene shows promise in linking different life stages *via* genetic barcoding. For instance, this approach has been used to show that the minute, putative hydrozoan, *Microhydrula limopsicola* Jarms & Tiemann, 1996, is really a distinct life stage of the stauromedusa *Haliclystus antarcticus* Pfeffer, 1889 (Miranda *et al.* 2010), and an intensive study of the Leptothecata family Sertulariidae using this gene allowed both cryptic species complexes and potential synonymies to be identified (Moura *et al.*, 2011). For the first time, DNA barcoding using the mitochondrial 16S gene was successfully applied to the taxonomic identification of cnidarians of the order Siphonophora. This technique allowed the eudoxid stage known as *Eudoxia macra* to finally be linked with its polygastric stage, *Lensia cossack*. As the database of well-characterized medusozoan samples associated with the mitochondrial 16S gene grows, we expect further improvement in this group's systematics.

2. Re-description of *Lensia leloupi* Totton, 1954

Despite representing only 14 species of *Lensia* of the 24 recorded from Japanese waters (Bigelow, 1913; Grossmann and Lindsay, 2013b; Kawamura, 1954; Kitamura, 1997; 2000; 2009; Kitamura *et al.*, 2003; Lindsay and Miyake, 2009; Pagès *et al.*, 2006), the present data set (*cf.* Chapter III.3) allowed the identification of the posterior nectophore and gonophore of *Lensia leloupi* Totton, 1954 through DNA barcoding. Because this species shows great morphological similarities with another tropical diphyid species – *Lensia subtiloides* (Lens and van Riemsdijk, 1908) – a redescription is given here. For the present, as discussed in Chapter III.3, no attempt has been made to modify the taxonomic position of this species.

Lensia leloupi Totton, 1954

Lensia leloupi Totton, 1965a (*non Lensia* sp. aff. *leloupi* = *Lensia achilles*); Patriti, 1970; Zhang and Xu, 1980; Alvariño, 1981 (?Fig. 174 49); Zhang, 1984; Daniel, 1985 (Fig. 58 a; *non* Fig. 58 b (see Discussion below)); Margulis and Alekseev, 1985 (Fig. 1 A); Kitamura, 1997 (Fig. 27); Alvariño *et al.*, 1990; Pugh, 1999b (Fig. 3.96); Zhang 2005 (Fig. 59); Gasca, 2009

?*Lensia nagabushanami* Daniel, 1970

?Bract C (Grossmann and Lindsay, 2013b)

Diagnosis:

Polygastric stage:

Anterior nectophore with 5 ridges joining at apex, the laterals incomplete in their posterior part; nectosac extensive; hydroecium extending slightly anterior of ostial level; mouthplate medium-sized; posterior border of the lower facet with small central notch; somatocyst elongate, globular in anterior part, 25% the height of the nectophore.

Posterior nectophore with 5 complete ridges; nectosac extensive; pedicular canal arising near apex of nectosac; articulate surface truncate; mouthplate short, slightly bilobed, hydroecial flaps thick, asymmetrical.

Eudoxid stage:

Bract tentatively assigned to this species: bluntly conical, with marked bracteal ridges; neckshield 1/3 the height of the headpiece, without marked notches; hydroecial cavity flattened; phyllocyst elongate, without terminal swelling, about 50% of the headpiece in height.

Gonophore conical, with 4 marked, complete ridges; nectosac the height of the nectophore; mouthplate short, hydroecial flaps thin, more developed in anterior part.

Material examined: *Lensia leloupi* Holotype (BMNH 1952.11.19.1) and 123 additional anterior nectophores from the Discovery collections (BMNH 1958.4.29.106 – 1958.4.29.108), collected at Discovery station 277 in the equatorial Atlantic (01°44'S, 08°38'E), between 88 m and the surface; 239 anterior nectophores and 143 posterior nectophores from Sagami Bay (35°N, 139°20'E), 79 anterior nectophores, 49 posterior nectophores and 46 gonophores collected east of Oshima Island (34°42'N, 139°50'E), 322 anterior nectophores, 43 posterior nectophores and 45 gonophores from off Kamogawa (34°59.43'N, 140°02.97'E), 2 anterior nectophores from the off the north-eastern coast of Japan (36°28'N, 141°43'E), and one very small anterior nectophore from near Rosslyn Bay, Australia (23°10'S, 150°48'E). Additionally, one *Lensia subtiloides* (Lens and van Riemsdijk, 1908) anterior nectophore collected north of Okinawa, Japan (27°47.73'N, 126°54.11'E), 5 anterior nectophores collected near Kagoshima, on the south-western coast of Japan (34°59.43'N, 140°02.97'E), and 19 anterior nectophores from the Sulu Sea (8°N, 120°E) were examined. One *Lensia subtiloides* eudoxid and 4 gonophores collected in Malaysia (2°27.64'N, 101°51.06'E) were observed. A total of 1171 bracts tentatively assigned to *Lensia leloupi* were collected in Sagami Bay (35°N, 139°20'E), east of Oshima Island (34°42'N, 139°50'E) and off of Kamogawa (34°59.43'N, 140°02.97'E).

DNA sequences obtained (Table 11, pp.114) included 4 anterior nectophores (DLSI344, 141020, 141021 and 141019), 1 posterior nectophore (450045), and 2 gonophores (450011, 450013) from Sagami Bay, and one anterior nectophore from north-eastern Japan (450129).

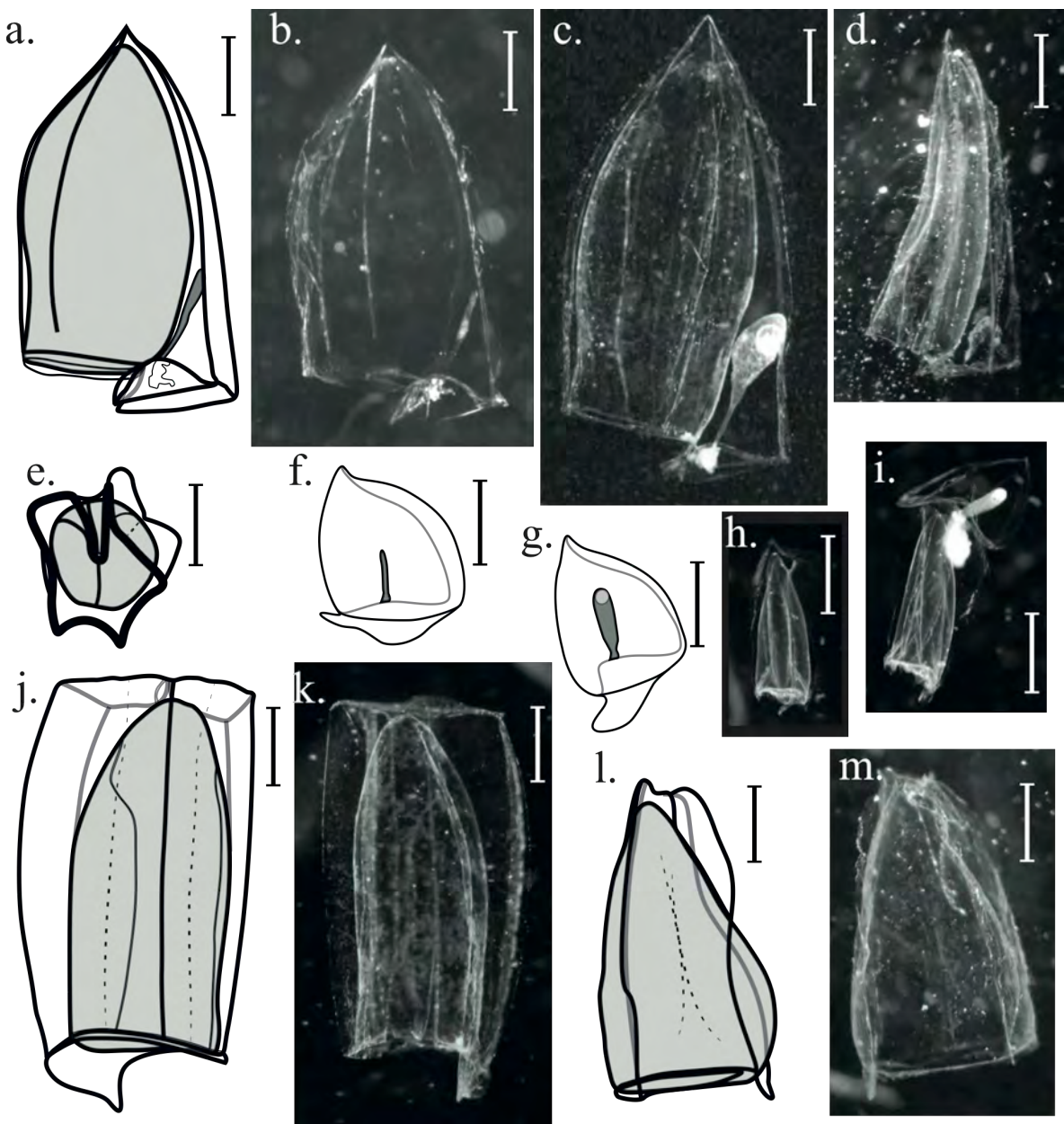


Figure 35: Polygastric and eudoxid stages of *Lensia leloupi* Totton, 1954 and some related species: a., b.: *L. leloupi* Holotype, anterior nectophore, right lateral view; c.: *L. leloupi* anterior nectophore from Japanese waters, right lateral view; d.: *Lensia subtiloides* (Lens and van Riemsdijk, 1908) anterior nectophore, right lateral view; e.: *L. leloupi* posterior nectophore, anterior view (hydroecium towards top of page); f.: *L. leloupi* bract, right lateral view; g.: *Lensia conoidea* (Keferstein and Ehlers, 1860) bract, right lateral view; h.: *L. subtiloides* gonophore, right lateral view; i.: *L. subtiloides* eudoxid stage, right lateral view; j.: *L. leloupi* posterior nectophore, upper-left-lateral view; k.: *L. leloupi* posterior nectophore, right lateral view; l.: *L. leloupi* gonophore, right lateral view; m.: *L. leloupi* gonophore, left lateral view. Dotted lines indicate furrows. Scale bar = 1 mm. (f., g. from Grossmann and Lindsay, 2013b)

Description of Material (Fig. 35)

Polygastric stage

Anterior nectophore: Holotype 4.3 mm tall by 2.4 mm wide (Fig. 35 a, b). Five longitudinal ridges, joining in a point at the apex of the nectophore, the lateral ridges incomplete in their posterior part, the left lateral ridge extending further towards the ostium than the right lateral one; nectosac extensive, occupying 90% of the nectophore in height, musculature causing a central bulge; hydroecium extending slightly above ostial level in its central part, mouthplate 10% the length of the nectophore, with overlapping, rounded flaps; posterior border of the lower facet with small, rounded central notch; somatocyst globular, without pedicle but thinner in its posterior part, 25% the height of the nectophore, in contact with, or ending near the lower border of the nectophore in its anterior part.

Posterior nectophore (Fig. 35 e, j, k): up to 5 mm long by 2.5 mm wide, with 5 marked, complete ridges; nectosac with blunt conical apex, same height as nectophore, pedicular canal straight, following the antero-posterior axis, originating at 5% nectosac height from the apex, radial canals following a normal diphyine course; articulate surface truncate; mouthplate short, slightly bilobed, 20% the length of the nectophore in length; hydroecial flaps well developed in their anterior part, asymmetrical, the left slightly shorter and with thicker mesogloea, the right slender and pointed.

Eudoxid stage

Bract (Fig. 35 f): up to 3 mm tall, bluntly conical with marked bracteal ridges; neckshield 1/3 the height of the headpiece, without marked notches; hydroecial cavity flattened; phyllocyst elongate, without terminal swelling, about 50% of the headpiece in height.

Gonophore (Fig. 35 l, m): up to 5 mm long by 2.4 mm at the widest point, with 4 marked, complete ridges; conical in shape, distal portion up to twice as wide as articulate surface; nectosac the height of the nectophore, course of the radial canals unknown, mouthplate 10% nectophore in length, without rounded edges, hydroecial flaps thin, more developed in anterior part.

Comments

The anterior nectophores of *Lensia leloupi* labelled with Discovery collection numbers 1958.4.29.106 to 1958.4.29.108 and those collected in Japanese waters (Fig. 35 c) were generally larger than the holotype, measuring up to 7.5 mm in height, the posterior nectophores thereby being markedly shorter than the anterior ones. The *L. leloupi* anterior nectophores collected in eastern Australia, although measuring only 2.75 mm in height, showed all the morphological characters of the larger specimens. Not visible in the holotype specimen, the radial canals followed a typical diphyine course. While possibly a preservation artefact, most *L. leloupi* specimens showed a general shape described by Daniel (1970) for *Lensia nagabhushanami* as “a pointed tip, bulged middle region and a broad ostium”. Many of the more poorly preserved specimens also showed large lateral folds on either side of the lateral ridge. Although slightly larger than the specimens from Japanese waters, the specific characteristics of *L. nagabhushanami* Daniel, 1970 are not sufficient to differentiate it from *L. leloupi* Totton, 1954, and it is therefore synonymized with the latter.

The main characters differentiating the anterior nectophores of *Lensia leloupi* from those of *L. subtiloides* (Fig. 35 d) were the length of the mouthplate and lateral wall of the hydroecium, as well as the height of the hydroecium, larger in the former species, and the presence of a rounded notch in the posterior margin in *L. leloupi*. The somatocyst, while usually taller in *L. leloupi* (25 to 30% of nectophore length, against 15 to 20% in *L. subtiloides*), showed a great amount of variation in size and shape, depending on the number of oil droplets it contained. When preserved in formalin, *L. leloupi* specimens displayed a smaller width/height ratio than *L. subtiloides*, but these characters may not apply to live material. Genetically, these two species were found to be quite distinct, *L. leloupi*, a well-defined clade, most closely related to *L. panikkari*, another 5-ridged *Lensia* species with lateral ridges incomplete in their posterior part, while *L. subtiloides* formed a separate clade (Fig. 22, p. 118).

Very similar in shape to those of *L. achilles*, the posterior nectophores of *L. leloupi* could be differentiated by the more conical shape of the apex of the nectosac. The nectophores were also much smaller (up to 5 mm in length), than the 13 mm reported as maximum size for *L. achilles* posterior nectophores (Mapstone, 2009). However, the *L. achilles* anterior nectophores found in Japanese waters were also smaller than the 18 mm stated (Mapstone, 2009), with a maximum length of 15.4 mm, and a mean length of about 8

mm. The posterior nectophores of *L. leloupi* were shorter and wider than those of *Lensia conoidea*, and without a clearly bilobed mouthplate, and could be differentiated from the posterior nectophores of *L. fowleri* and *L. subtiloides* by the extent of the nectosac anterior to the insertion point of the pedicular canal. All posterior nectophores observed and sequenced had 5 straight, complete ridges. This is contrary to the characters of a posterior nectophore Daniel (1985) associated with *L. leloupi* and briefly described as being the same height as the anterior nectophore, with incomplete lateral ridges. The illustration provided (Fig. 58 b) does not show any lateral ridges, and the height of the posterior nectophore is only about half that of the anterior.

The bracts tentatively associated with *Lensia leloupi* were the most common bract of unknown parentage in the upper 200 m of the water column in March 2006 (*cf.* Chapter II) and their phyllocyst showed some resemblance to the somatocyst of *L. leloupi* anterior nectophores. However, this identification will need to be confirmed through DNA barcoding. Most similar in size and shape to the bracts of *Lensia conoidea* (Keferstein and Ehlers, 1860) these former can be differentiated by the less pronounced teardrop shape, their flattened hydroecial cavity and their shorter, thinner phyllocyst (Fig. 35 f, g). The bracts of *L. subtiloides* (Fig. 35 i), generally smaller than those of *L. leloupi*, could be differentiated by the shape of the neckshield that, on the right lateral side, possessed a large notch, similar to that found in the bracts of *L. achilles*.

The gonophores of *L. leloupi* (Fig. 35 l,m) differed from other described *Lensia* gonophores by their conical shape, marked ridges and untwisted apex. The hydroecial flaps were less developed than in *L. subtiloides* gonophores (Fig. 35 h) and, although conical in shape, the apex of the nectosac of *L. leloupi* gonophore was more rounded than in *L. subtiloides*. These characters, however, may be altered during preservation, and a review of all the known *Lensia* eudoxid stages may be necessary in order to establish species-specific characteristics.

3. Description of the eudoxid stage of *Lensia havock* Totton, 1941

The study of the Siphonophora collected by IONESS nets during the March 2006 MULTI-SPLASH cruise revealed the presence of several previously undescribed but very abundant eudoxid stages. One of these, the most abundant stage in many of the net samples collected between 600 and 1000 m in Sagami Bay (Grossmann and Lindsay, 2013b), and equally abundant in the deeper strata of Kamogawa and Oshima stations, was the eudoxid form referred to as “Eudoxid A”. The collection of live specimens of this eudoxid stage in ORI nets aboard the R/V *Tansei maru* showed them to have orange-coloured phyllocysts. The colouration and shape of the eudoxid stage bract is believed to be similar to that of the somatocyst of the anterior nectophore of the polygastric stage. However, three species of *Lensia*, known to have globular, orange-coloured somatocysts, were collected in the lower mesopelagic zone during the MULTI-SPLASH cruise: *L. achilles* Totton, 1941, *L. cordata* Totton, 1965b and *L. havock* Totton, 1941. DNA barcoding techniques, using the mitochondrial 16S gene, were performed in order to definitively assign the eudoxid stage “Eudoxid A” (Grossmann and Lindsay, 2013b) to its polygastric stage: *Lensia havock* Totton, 1941.

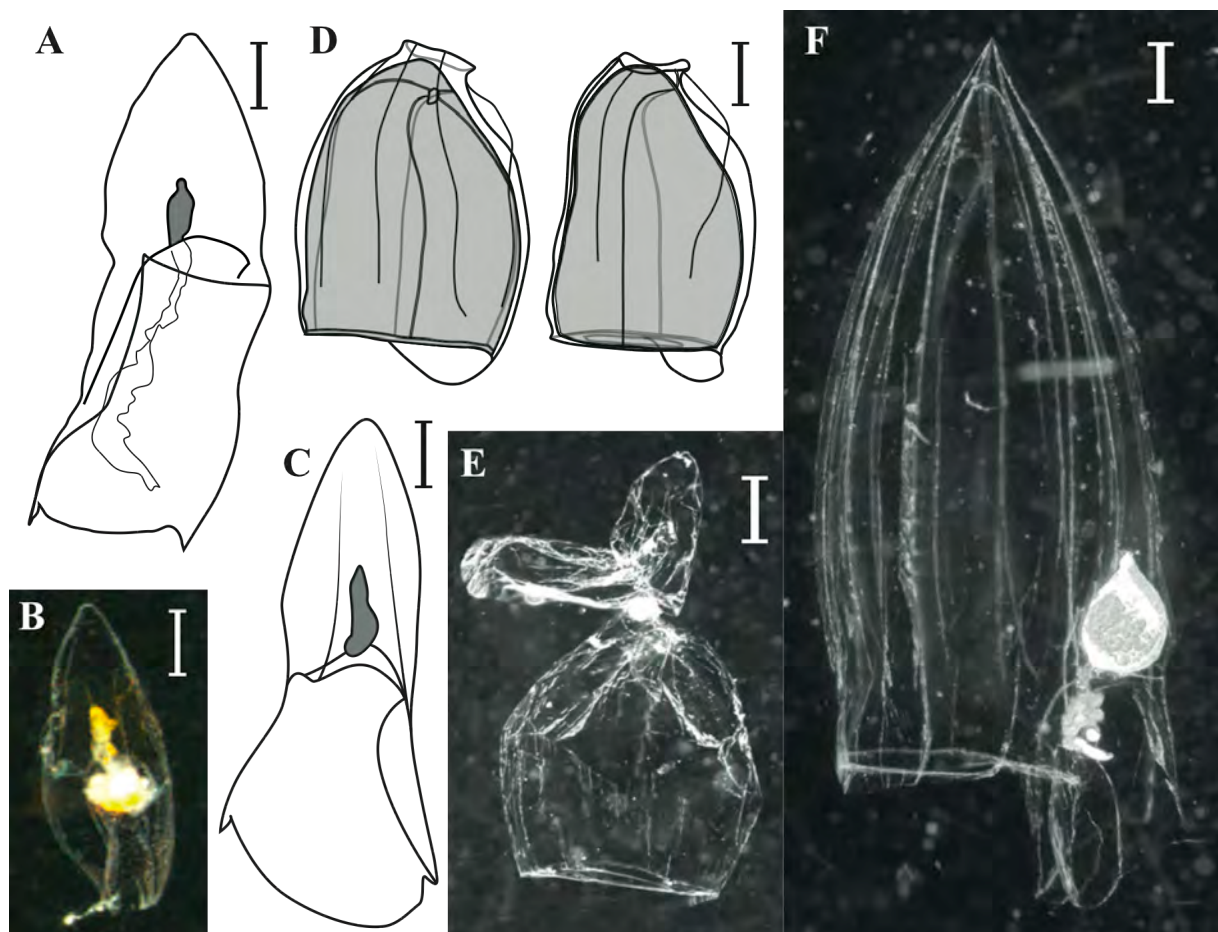


Figure 36: Eudoxid stage of *Lensia havock* Totton, 1941, A, B, C: bract in upper view (B: photograph the living specimen from Sagami Bay from which the DNA sequence 450007 was obtained); D: gonophore, upper-right and right lateral views from left to right; E: complete eudoxid stage, photograph of preserved specimen; F: *L. havock* polygastric stage in right lateral view (photograph of preserved specimen). Scale bar = 1 mm. (*modified after* Grossmann and Lindsay, 2013b (as 'Eudoxid A')).

Lensia havock Totton, 1941

Eudoxid A (Grossmann and Lindsay, 2013b)

Diagnosis:

Polygastric stage:

Anterior nectophore: seven complete ridges, upper lateral bending towards upper surface at ostial level, lower laterals bending towards lower side to run onto the mouthplate; hydroecium extending anterior of ostial level, lower facet with extensive triangular posterior notch; somatocyst spindle-shaped, with orange pigmentation.

Posterior nectophore: unknown

Eudoxid stage:

Bract: conical headpiece without marked ridges; neckshield at least as long as headpiece, with tooth-like projections on baso-lateral corners; hydroecial cavity flattened; phyllocyst globular, with orange pigmentation.

Gonophore: 6 ridges, incomplete in posterior part except for lower, running onto large rounded mouthplate; hydroecium shallow; articulate surface concave; nectosac wide, with rounded, conical apex.

Material examined: One hundred and eighty five complete eudoxid stages, 299 bracts, and 921 gonophores, as well as 262 anterior nectophores were collected during the MULTISPLASH cruise and preserved in 5% seawater-buffered formalin; four bracts and one gonophore, collected in Sagami Bay ($34^{\circ}59.18'N$, $139^{\circ}20.06'E$) in April 2012, and 2 bracts collected north of Okinawa ($27^{\circ}47.73'N$, $127^{\circ}E$) in June 2012 were preserved in 99.5% ethanol and stored at $-20^{\circ}C$ for genetic analyses. The *Lensia havock* sequence 450007 (Table 11, p. 114) corresponds to one of these later.

Description of eudoxid stage (Fig. 36)

Bract: up to 6.4 mm long, by 1.7 mm wide; conical headpiece without marked ridges; neckshield at least as long as headpiece, wider at posterior margin, with 2 tooth-like projections, one on each baso-lateral corner; hydroecial cavity flattened; phyllocyst about half the length of the headpiece, asymmetrical in shape, containing oil droplets, orange in colour in living animals.

Gonophore: 5.7 mm long by 3.2 mm wide; 6 incomplete ridges extending to 1/5 gonophore length from ostium, except for lower pair, extending onto large rounded mouthplate; hydroecium shallow; articulate surface concave; nectosac as wide as gonophore, with rounded conical apex, radial canals straight, joining on ventral facet at about 1/5th nectosac length from its apex.

Comments

The large size of this eudoxid, its lower mesopelagic distribution, as well as the bright orange pigmentation of the phyllocyst when alive (Fig. 36), made this a likely eudoxid stage of *Lensia achilles*, *L. cordata* or *L. havock*, all present in the sampling zone and having orange-pigmented somatocysts of a similar globular shape as the phyllocyst of “Eudoxid A”. However, a gonophore having been collected in the Southern Ocean north-east of the Dumont d’Urville Antarctic base (CEAMARC campaign, station UM8 (65°30’S, 143°E), 500 – 1000 m, Grossmann unpublished data), this eudoxid was unlikely to be associated with a tropical mesopelagic species such as *L. cordata*.

The sequencing of a bract collected in Sagami Bay confirmed this eudoxid stage to be that of *Lensia havock* Totton, 1941 (Fig. 22, 23, p. 118, 120 –*Lensia havock* 450007), and clustered with the polygastric stages collected in Japanese waters, *L. havock* showing important inter-geographic intra-specific genetic distances. As seen above, such large genetic distances may correspond to the presence of cryptic species, and further sampling in the Southern Ocean may be necessary to determine whether the Japanese and Antarctic eudoxid types present distinct morphological characteristics.

4. *Lensia* sp. A, a new species of five-ridged *Lensia*.

The diphyid siphonophore genus *Lensia* is a catch-all genus that contains a great many species, many of which have rarely, or never, been recorded since their description (e.g. *Lensia gnanamuthui* Daniel and Daniel, 1963; *L. landrumae* Alvariño and Wojtan, 1984; *L. minuta* Patriti, 1970; etc...). However, with no information on the life cycle of these species, or on possible geographic morphological differences, it is often difficult to establish the validity or synonymy of *Lensia* species, and more particularly of the 5-ridged species. The present species, absent from the MULTI-SPLASH samples, appeared to be an undescribed type of siphonophore, morphologically similar to other 5-ridged *Lensia* with complete lateral ridges. However, as seen in Chapter III.3, the genus *Lensia* is, genetically, a non-monophyletic genus, and the taxonomic position of this species will undoubtedly be changing in the next few years.

Lensia sp. A

Diagnosis:

Polygastric stage:

Anterior nectophore with 5 marked, complete ridges; nectosac extensive; hydroecium at ostial level; mouthplate triangular; posterior border of the lower facet with small central notch; somatocyst vertical, ovoid, 12% the height of the nectophore.

Posterior nectophore undescribed.

Eudoxid stage: unknown

Material examined: Three anterior nectophores collected in an oblique 0.33 mm-mesh ORI net north of Okinawa, Japan ($27^{\circ}47.73'N$, $126^{\circ}54.11'E$), between 0 and 946 m, on June 7th, 2012. One nectophore was preserved in 5% seawater-buffered formalin, the other 2 were preserved in 99.5% ethanol, and stored at -20°C (sequences 450143 and 450144, Table 11, p. 114). One posterior nectophore was collected in the central part of the Izu archipelago (Myojin-sho: $31^{\circ}39.6'N$, $142^{\circ}0.6'E$) and preserved in 99.5% ethanol, before being stored at -20°C (sequence 121500, Table 11, p. 114). The ethanol-preserved specimens were sequenced following the procedure established in Chapter III.3. Additionally, 6 *Lensia hotspur* anterior nectophores collected north of Okinawa ($27^{\circ}47.73'N$, $126^{\circ}54.11'E$), one collected east of Kagoshima ($31^{\circ}N$, $132^{\circ}E$), one collected in Sagami Bay ($35^{\circ}0.25'N$, $139^{\circ}20'E$), and one collected at Myojin-sho ($31^{\circ}39.6'N$, $142^{\circ}0.6'E$), were observed and preserved in 99.5% ethanol or 5% formalin-seawater.

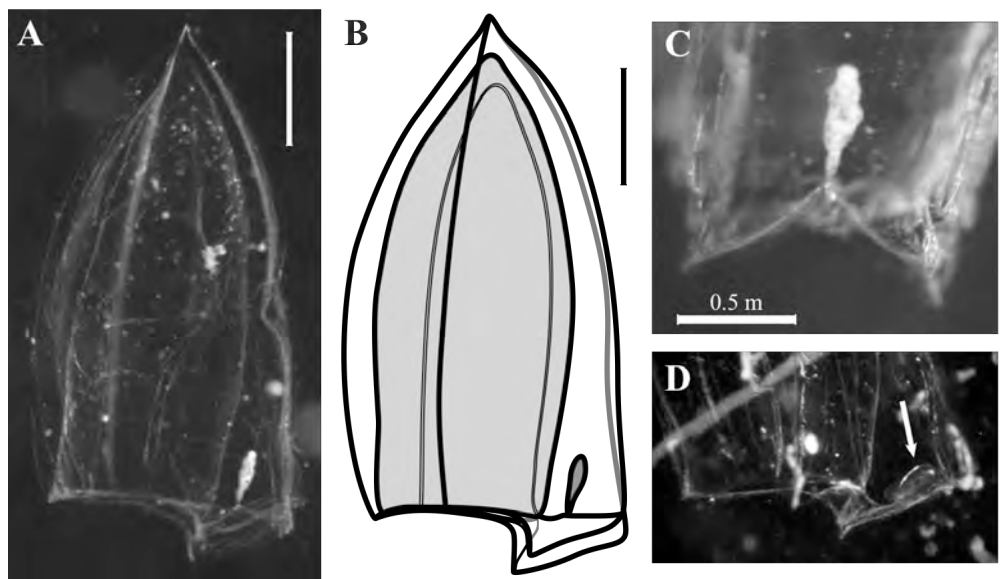


Figure 37: *Lensia* sp. A: right lateral view of anterior nectophore (A, B); C: upper view of mouthplate and somatocyst; D: right lateral view of the posterior margin of *Lensia hotspur* Totton, 1941. Photographs and drawing of formalin-preserved specimens collected north of Okinawa. Scale bars = 1 mm unless indicated.

Description of material:

Polygastric stage:

Anterior nectophore (Fig. 37): Up to 4.2 mm tall by 2.3 mm wide; 5 marked, complete longitudinal ridges, upper ridge forming a small tooth at ostial level; nectosac extensive, occupying 93% of the nectophore in height; radial canals following a normal diphyine course; hydroecium horizontal, at ostial level, extending to lower facet, lateral hydroecial flaps triangular, mouthplate 11% the length of the nectophore, with short, triangular flaps, overlapping only in their most central part; somatocyst vertical, ovoid, 12% the height of the nectophore, originating from center of hydroecium.

Posterior nectophore: similar to that of *Lensia conoidea* as illustrated by Mapstone (2009).

Eudoxid stage: unknown

Comments

The anterior nectophores collected off southern Japan most closely resembled *Lensia hotspur* Totton, 1941, in the triangular shape of the mouthplate, but differed from this latter in the vertical axis of the somatocyst and the horizontal hydroecial cavity extending to the lower facet (Fig. 37). It formed a genetically distinct clade in the phylogenetic trees (Fig. 22, 23, p. 118, 120), as a sister group to *L. hotspur*.

The posterior nectophore, similar to those of *Lensia conoidea*, was not recorded photographically before being preserved in ethanol, and its size and distinctive characteristics could not be observed on the ethanol-preserved specimen.

Collected only in the most southern sampling locations, in zones highly influenced by the Kuroshio Current and counter-current (Ryukyus and Izu archipelagos), this species may be restricted to tropical waters.

Summary

Within medusozoan Cnidaria, the mitochondrial 16S gene shows promise in linking the different life stages of a species *via* genetic barcoding. For instance, this approach has been used to show that the minute, putative hydrozoan, *Microhydrula limopsicola* Jarms and Tiemann, 1996 is really a distinct life stage of the stauromedusa *Haliclystus antarcticus* Pfeffer, 1889 (Miranda *et al.*, 2010), and for the first time, DNA barcoding using the mitochondrial 16S gene was successfully applied to the taxonomic identification of cnidarians of the order Siphonophora. This technique allowed the eudoxid stage known as *Eudoxia macra* Totton, 1954 to finally be linked with its polygastric stage *Lensia cossack* Totton, 1941, the description of the eudoxid stage and posterior nectophore of the polygastric stage of *Lensia leloupi* Totton, 1941, and of the eudoxid stage of *Lensia havock* Totton, 1941, and the identification of a new species of five-ridged *Lensia*.

However, due to the fragility of the gelatinous animals, and the difficulty in collecting samples in good condition, the taxonomy of species of the order Siphonophora is still, in many cases, a matter of expert opinion, especially when considering life stages other than the polygastric one. Indeed, although DNA barcoding techniques could be successfully used to link different life stages of a species, and identify a new *Lensia* species, this kind of endeavour relies on the correct identification of the sequences contained in the genetic databases. Well behind other cnidarian groups such as the scleractinian corals, or the universal laboratory guinea pig *Hydra magnipapillata*, siphonophore sequence information is still scarce, and more intensive and wide-spread sampling and sequencing would be required before DNA barcoding techniques can be reliably applied to the identification of siphonophores.

Appendix 3

**Taxonomic notes on some forms collected during the MULTI-SPLASH
cruise.**

Introduction

In the MULTI-SPLASH data set, several eudoxid stages of unknown parentage were found to contribute greatly to both the total siphonophore abundance, and to the coherence of the different siphonophore communities observed. Three of these were successfully linked to their polygastric stages using DNA barcoding techniques, after supplementary material could be collected in 2012 and identified onboard before being preserved in ethanol (*cf.* Appendix 2.1 – 2.3). However, because of the structure of the mesogloea, and its high water content, the preservation of Siphonophora in ethanol, suitable for genetic analyses, will usually cause intensive shrinkage and bleaching of the animals, which prevents the observation of internal structures such as the nectosac's radial canals, or the clear distinction of the number and extent of the ridges, rendering post-preservation identification of animals difficult if not impossible. The aims of the MULTI-SPLASH cruise being the study and comparison of planktonic communities off south-eastern Japan, only a small number of siphonophores, identified onboard, were preserved in ethanol, whilst the rest of the plankton samples were preserved in 5% seawater-buffered formalin. Formalin preservation, however, which allows the most reliable taxonomic identification, does not allow an efficient extraction and sequencing of genomic DNA.

Unable to be associated with any known polygastric stage through the use of DNA barcoding, a short description of these eudoxid stages of unknown parentage is provided, as well as some taxonomic notes on some of the multistriate *Lensia* species collected during the MULTI-SPLASH cruise. Considering the great diversity of diphyid siphonophores in Japanese waters, the application of DNA barcoding techniques may be necessary to definitively assign these eudoxids to known polygastric stages, and to determine the taxonomic level of the multistriate *Lensia* considered.

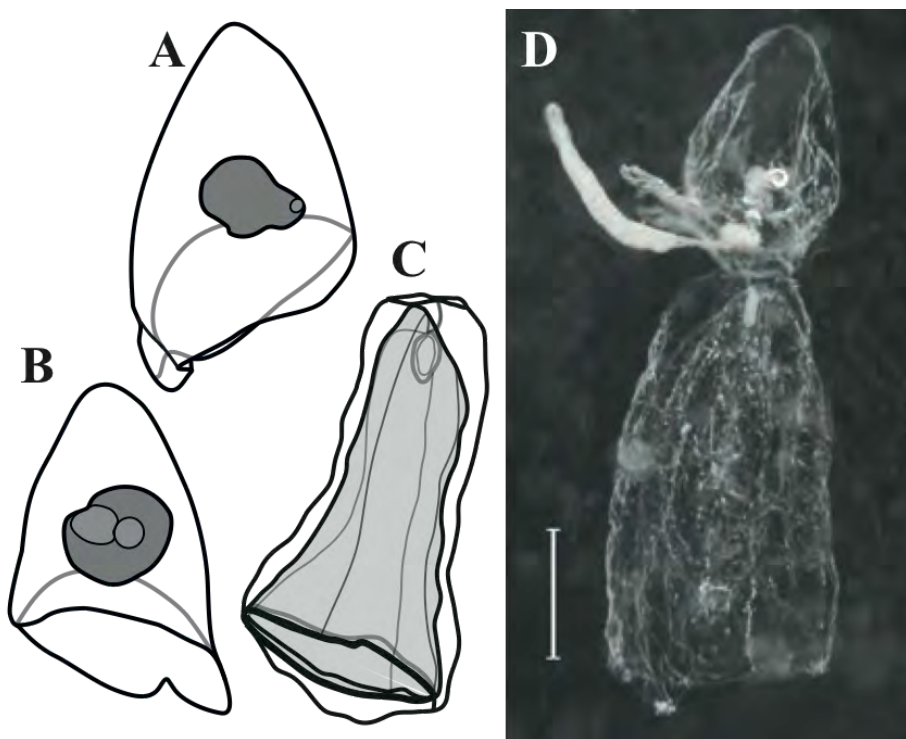


Figure 38: *Eudoxia cf. galathea* Moser, 1925: A: right lateral view, B: upper view of bract; C: right lateral view of gonophore; D: complete eudoxid stage, all from Sagami Bay, all at the same scale. Scale bar = 1 mm. (modified after Grossmann and Lindsay, 2013b, Fig.8)

1. Description of eudoxid stages

Eudoxia cf. galathea Moser, 1925 (Fig. 38)

Diagnosis:

Bract: up to 2.92 mm tall and 1.6 mm wide; headpiece conical, without ridges; neckshield usually half the headpiece height in length, posterior margin bilobed due to wide central notch of varying height; hydroecium deep, evenly rounded; phyllocyst globular and asymmetrical, without pedicle, varying greatly in size depending on the number of oil droplets contained.

Gonophore: up to 3.8 mm tall by 1.4 mm wide, without marked ridges; short rounded mouthplate; articulate surface flat; nectosac conical at apex, radial canals originating on upper side of nectosac, near the apex, running straight to the ostial canal; pedicular canal short, curving to the apex of the gonophore.

Comments:

The length of the bract's neckshield, usually only half the headpiece in length, and the presence of a large posterior notch in it; as well as the shape of the gonophores, clearly differentiate this eudoxid from that of *Lensia asymmetrica* Stepanjants, 1970, the only other small, unridged Diphyid-type bract to have an asymmetrical phyllocyst. The eodoxids described by Moser (1925) under the name *Eudoxia galathea*, had an average size of 3 to 4 mm, and the overall shape of the bract and somatocyst led us to tentatively assign our samples to this species. The original description does not mention a posterior notch or bilobed neckshield, however the illustrations on plate IV (Moser, 1925) show an undulating posterior margin to the bracts, perhaps an interpretation of a shallow posterior notch. As described in Chapter II.1, the bracts of these eodoxids also bear some resemblance to those of *Muggiaeabargmannae* as illustrated by Stepanjants (1967) and Zhang and Lin (2001). However, *E. cf. galathea* was one of the most abundant eudoxid stages in the lower mesopelagic zone, while *M. bargmannae*, an exclusively bipolar species, is found only rarely outside polar regions, and, indeed, only 2 polygastric stages were collected during the MULTI-SPLASH cruise, at night, in Sagami Bay.

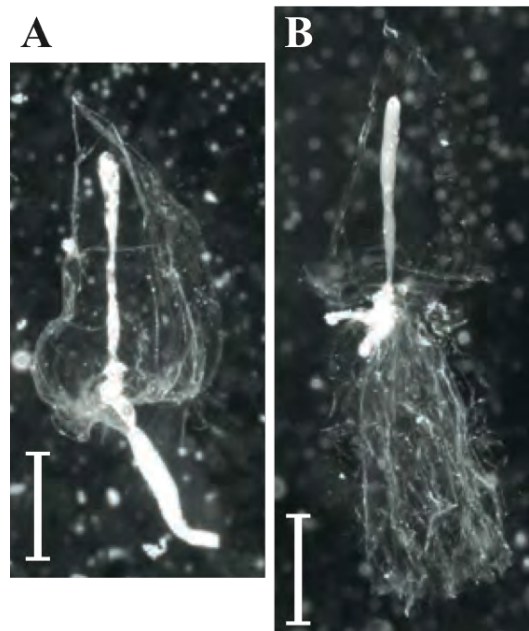


Figure 39: Eudoxid B: A: right lateral view of bract; B: complete eudoxid (photographs of formalin preserved specimens collected off Kamogawa). Scale bar = 1 mm. (*modified after* Grossmann and Lindsay, 2013b, Fig.8)

Eudoxid B (Fig. 39)

Diagnosis:

Bract: up to 3.19 mm tall and 1.35 mm wide; headpiece conical, with 2 marked bracteal ridges extending to the apex of the headpiece; neckshield greatly reduced; hydroecium shallow; phyllocyst long and thin, without pedicle, occupying 80% of the headpiece in height.

Gonophore: up to 2.9 mm tall by 1.24 mm wide; 4 well developed, complete ridges, the lower merging into the mouthplate; mouthplate short, square.

Comments:

Abundant, and influential in the community structure analyses, the vertical distribution of this eudoxid stage most closely resembled that of *Lensia multicristata*. However, the present eudoxids did not resemble *Eudoxia dohrni* Gamulin, 1966, or *E. tenuis* Patriti, 1965, two eudoxid stages tentatively associated with *L. multicristata* by Mapstone (2009) and Gamulin and Kršinić (2000), respectively. Additionally, in their study of the mitochondrial CO1 gene, Ortman *et al.* (2010) reported the presence of two cryptic *L. multicristata* types from the Sargasso Sea, in the central Atlantic, and, in the present study, the *L. multicristata* samples from Japan and Antarctica also appeared to form a cryptic species complex.

Given the high diversity of mesopelagic species, and the as-yet unfathomable number of cryptic species complexes, DNA barcoding will be the most reliable way of linking this eudoxid to its polygastric stage.

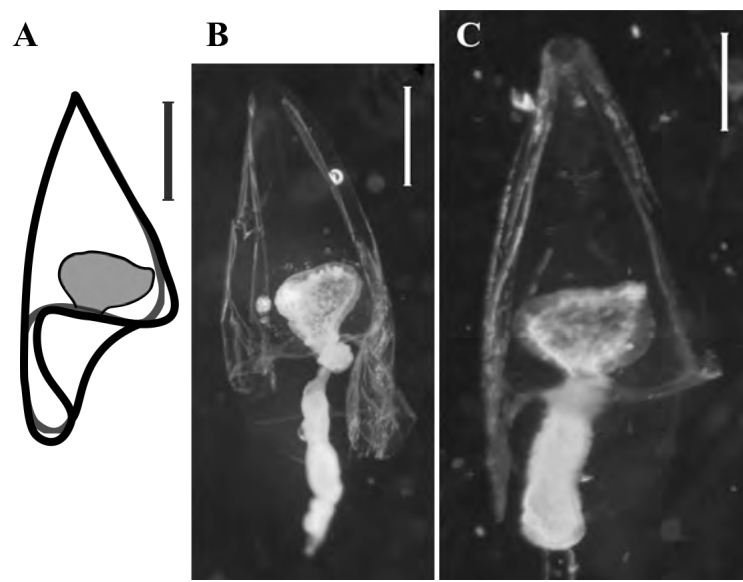


Figure 40: Bract I: A: right lateral view of bract collected in Sagami Bay; B: lower view of bract, photograph of a preserved specimen from Oshima; C: right lateral view of bract, photograph of preserved specimen from the Weddell Sea, Antarctica (ANT IX/2 station 67; '*Lensia* sp. e' in Pagès and Kurbjewitz, 1994). Scale bar = 1 mm.

Bract I (Fig 40)

Lensia sp. e. Pagès and Kurbjewit, 1994

Eudoxia X Pagès and Schnack-Schiel, 1996 in part (*non* Eudoxia X in Pugh and Pagès, 2002 and references therein)

Diagnosis:

Bract: up to 4 mm tall; headpiece conical, with 2 marked bracteal ridges extending to the apex of the headpiece; neckshield up to half the headpiece in length, marked notch near the junction with the headpiece on right side, similar to that found in *Lensia achilles* bracts, well-marked central posterior notch in the neckshield; hydroecial cavity flattened; phyllocyst short and globular, containing oil droplets, orange-pigmented in life.

Gonophore: unknown.

Comments

Collected primarily around 500 m during the MULTI-SPLASH cruise, the orange pigmentation and globular shape of the phyllocyst, as well as the particular sheen of the bract mesogloea made this form a likely eudoxid stage of the little-known mesopelagic species *Lensia cordata* Totton, 1965b. However, several bracts appearing to be of the same species were also collected during ANTARKTIS cruises to the Weddell Sea in Antarctica (ANT IX/2 station 067: 66.5°S, 27°W; ANT X/3 station 373: 68°S, 7.5°W) by the German R/V *Polarstern* (Pagès and Kurbjewit, 1994, as '*Lensia* sp. e.'; Pagès and Schnack-Schiel, 1996, as 'Eudoxia X'). The maximum water temperature at the latter sampling points being lower than 1°C, it seems unlikely this eudoxid stage could be that of *L. cordata*. Indeed, the present study represented the most northerly record for this tropical species, all other records being from the tropical Indian and eastern Pacific Oceans.

Further sampling, and possibly genetic analyses will be necessary to determine whether the Japanese and Southern Ocean samples truly represent the same form, and to allow these eudoxids to be linked to their polygastric stage.

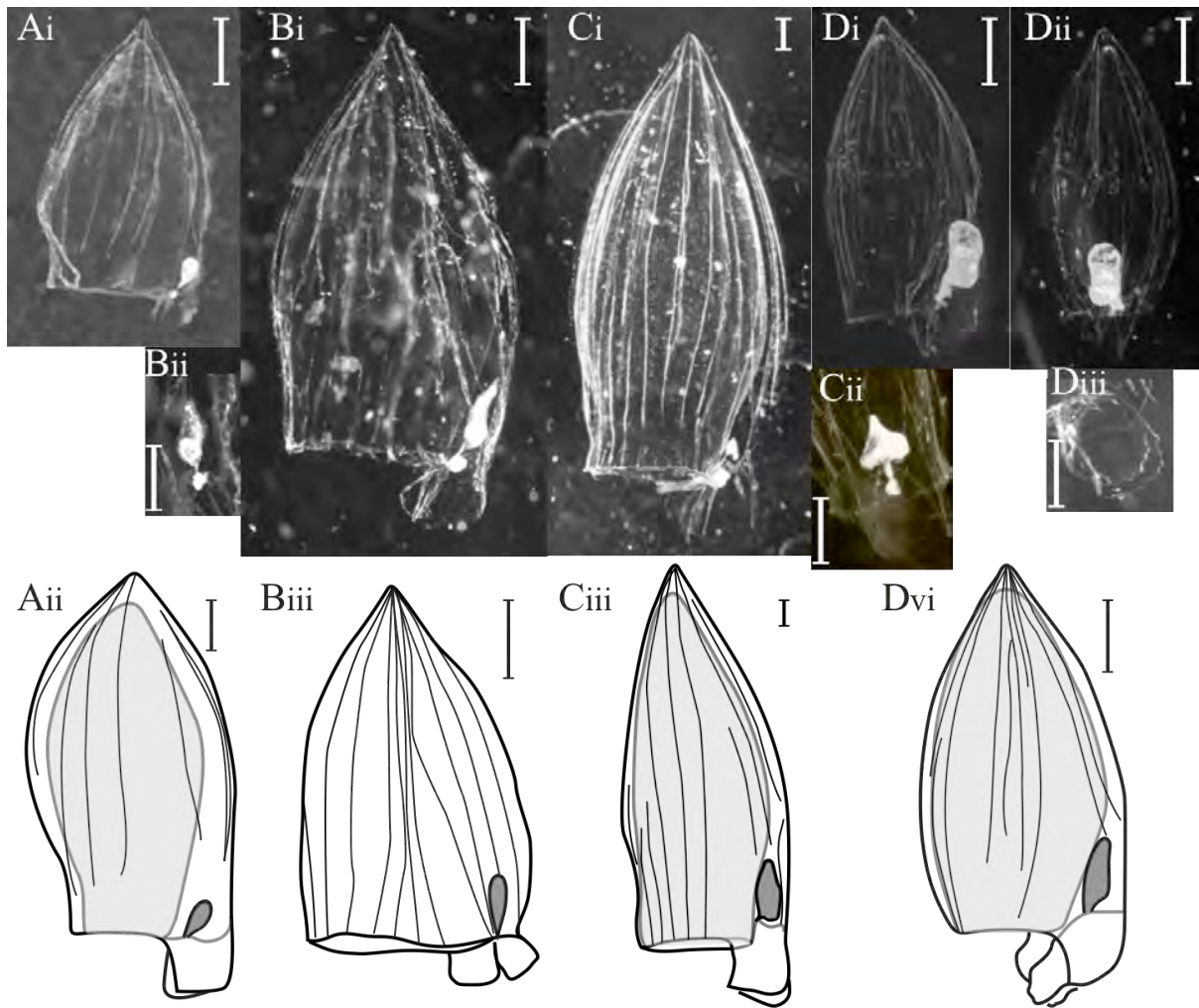


Figure 41: A: *Lensia ajax* Totton, 1941 anterior nectophore, i: photograph of preserved nectophore from Sagami Bay in right lateral view, ii: Holotype in right lateral view (redrawn after Totton, 1941); B: *L. ajax* sensu Margulis and Alekseev, 1985, i: photograph of preserved nectophore from Sagami Bay in right lateral view; ii: lower view of somatocyst of same individual, iii: right lateral view of anterior nectophore (redrawn after Margulis and Alekseev, 1985); C: *L. hostile* Totton, 1941, i: photograph of preserved nectophore from Oshima in right lateral view, ii: lower view of somatocyst of preserved nectophore from Kamogawa, iii: Holotype in right lateral view (redrawn after Totton, 1941); D: *L. zenkevitchi* Margulis, 1970, i: photograph of preserved nectophore from Oshima in right lateral view, ii: lower view of same individual, iii: right lateral view of mouthplate of a preserved specimen from the Caribbean Sea, vi: Holotype in right lateral view (redrawn after Margulis, 1970). All photographs at the same scale except Ci, half as small as others. All scale bars = 1 mm.

2. Taxonomic notes on some multistriate *Lensia* species

The calycophore *Lensia ajax* Totton, 1941 was recorded from the first time from Japanese waters in the present study. It was noted, however, that the ridge pattern of the anterior nectophores came in two distinct types. The first resembled that described by Totton (1941) from the southern Atlantic (Fig. 41 A). The second ridge pattern observed was similar to that described and illustrated by Margulis and Alekseev (1985), with seemingly complete ridges disposed at equal distances over the nectophore surface, except on the lower side, where the ridges did not extend beyond the ostial level (Fig. 41 B). These anterior nectophores measured 5 mm in length on average, while the ones similar to Totton's 1941 illustration measured about 3 mm in length. In fact, a close examination of the second type of nectophore showed several of the upper-lateral ridges to be incomplete in their anterior part, and several ridges were very weak, or totally absent, in an area level with the upper half of the somatocyst. The ridge pattern on this latter type of *L. ajax* would appear to more closely resemble that of another multi-striate species, *L. hostile* Totton, 1941.

However, although the somatocysts on all *L. ajax* specimens measured more than 1/10th the nectophore height, the other characters Mapstone (2009) stated to distinguish *L. ajax* from *L. hostile* were verified: the somatocysts were globular and not heart-shaped (Fig. 41 Bii, Cii), and the hydroecium stopped at, or just above ostial level. *L. hostile* specimens, also present in the MULTI-SPLASH samples, confirmed the validity of these characters (Fig. 41 C). The *L. hostile* specimens from south-eastern Japan, as those described by Mapstone (2009), measured 7 mm in length, on average, while those described by Totton (1941) measured up to 15 mm in length.

The animals described by Margulis and Alekseev (1985) as *Lensia ajax* may therefore represent a new species of multi-ridged *Lensia*. However, for the present study, and because of the lack of genetic information for either type of *L. ajax*, the two morphologies were maintained as a single species. A re-examination of the *L. ajax* syntype material, and of the samples described by Margulis and Alekseev (1985), as well as the acquisition of genetic information on the two *L. ajax* types would be necessary to establish the true taxonomic position of these observed phenotypes.

Lensia zenkevitchi, a species synonymised with *L. hostile* by Mapstone (2009) was considered a valid species in this study, following Pugh (1999b), as the shape of the somatocyst, the ridge pattern, and characteristic serration of the inner mouthplate borders were sufficient characters to reliably indentify it by (Fig. 41 D). Although the MULTI-SPLASH samples represent the first official record of this species from the Pacific Ocean, the animal collected in Canadian waters and figured by Mapstone (2009, Fig. 51) as *L. hostile* would appear to be of this species.

Summary

The use of multiple opening-closing nets allowed the collection of a large number of siphonophore forms. The good quality of the preserved material made identification to species level possible for the great majority of the material sampled, and several species were recorded for the first time from the sampling area, and several previously undescribed life stages were identified. However, because of the important diversity of siphonophores found in the sampling area, the association of these new life stages to known polygastric stages, and the description of new species were extremely difficult. For these reasons, a series of supplementary cruises were undertaken off the southern and eastern coasts of Japan, in order to collect, identify onboard and preserve in ethanol the greatest number of siphonophores species possible, in order to establish a data set with which unknown siphonophore parts could be linked to known species using DNA barcoding techniques (*cf.* Appendix 2).

Unfortunately, the ethanol-preserved samples obtained, collected in non-closing oblique net tows, did not cover the whole range of diversity found during the MULTISPLASH cruise. For some abundant eudoxid stages of unknown parentage, and some multi-ridged *Lensia* polygastric stages, a short description is given in the hope further sampling may provide taxonomic clarification.

